NILU OR: 19/97

NILU : OR 19/97
REFERENCE : O-1900
DATE : APRIL 1997
ISBN : 82-425-0866-6

Atmospheric Research in Ny-Ålesund

Proceedings from the Third NySMAC meeting

NILU, Kjeller, Norway

9.-11. April 1997

Edited by Inga Fløisand, Hartwig Gernandt, Elisabeth Stoltz Larsen, Frode Stordal, Makoto Wada

Preface

The Ny-Ålesund Seminar Series was conceived by NySMAC (Ny-Ålesund Science Managers Committee) as a means of bringing together research scientists involved in programmes running at Ny-Ålesund or having an interest in that area. The first Seminar was held in Potsdam in Germany in May 1995, and included talks which covered all current research disciplines; physical, atmospheric, earth and biological sciences. The Second Seminar was devoted to biological science and particularly to ecology. It was held in Cambridge in UK in February 1996.

The subject of this Third Seminar, held in Kjeller in Norway in April 1997, is atmospheric research in Ny-Ålesund. Since the early 1980s a wide range of projects have been carried out on Svalbard and particularly at Ny-Ålesund. Prominent in this research have been several international research programmes with emphasis on topics of e.g. Arctic (Arctic Monitoring and Assessment Programme, AMAP), European (European Monitoring and Evaluation Programme, EMEP) or global (International Geosphere-Biosphere Programme, IGBP; World Climate Research Programme, WCRP) scales.

Atmospheric observations have been carried out in Ny-Ålesund in Svalbard for several years. From the early 1980s, the long range transport of sulphur dioxide and sulphate aerosols leading to Arctic Haze, has been studied. As a consequence, EMEP included Ny-Ålesund in their network. In the following years the transport of ozone and chemical precursors were observed, and recently the naturally occurring phenomenon of rapid surface ozone loss has been given particular attention.

From the late 1980s observations of the stratospheric ozone layer and related chemical species were undertaken, and the efforts have increased considerably since. Ny-Ålesund is now one of the primary Arctic sites of the NDSC (Network for Detection of Stratospheric Change) network. Important efforts have been undertaken to participate in the European campaigns as the European Stratospheric Ozone Experiment (EASOE) and the Second European Stratospheric Arctic and Mid-latitude Experiment (SESAME) which were focused on the changing ozone layer. Observations are now also directed towards the climate change issue, with measurements of CO_2 and other climate gases as a key activity.

Ny-Ålesund is a remote background atmospheric research station, with only minor influences from local sources. Several institutions are now present in Ny-Ålesund with long term measurement programmes, including groups from Germany, Japan, Sweden, Italy and Norway. The observations are connected to several international research projects and programmes, as e.g. IGBP and WCRP programmes. Ny-Ålesund is also included in the WMO network, Global Atmospheric Watch (GAW).

The increasing activity in atmospheric observations in Ny-Ålesund calls for extended exchange of information between scientists in order to stimulate the scientific discussion and interaction. Therefore, presentation of scientific results obtained in Ny-Ålesund, which can stimulate further scientific development, is the main objective of the seminar. There is a wealth of information and results available from atmospheric research in Ny-Ålesund.

A second objective is to bring this to the attention of the scientific community, so that observations in Ny-Ålesund can be used in new contexts, e.g. in comparative studies involving observations from other locations or in modelling studies. Furthermore, the seminar will enable discussions to strengthen the collaboration between researchers which is also necessary in order to avoid duplication of efforts.
The Third Seminar therefore provides an opportunity for those who have been working in the field of atmospheric research at Ny-Ålesund and in other areas of Svalbard to summarise their research and findings and to identify their achievements. During the discussions we also hope that participants will identify what they consider the new challenges to be, so that we can set out ideas from which new programmes can be developed. However, if we are to propose new programmes these need to fit into both a national and international context. Besides meeting national criteria, research programmes have to fit into the international context. Arctic science is by its nature international both in concept and in practice.

On behalf of the organising committee:

Inga Fløisand
Hartwig Gernandt
Elisabeth Stoltz Larsen
Frode Stordal
Makoto Wada

Contents

Page

Oral presentations

Poster presentations

Abstracts from oral presentations

The Nature and History of Arctic Air Pollution

Leonard A. Barrie
Atmospheric Environment Service
4905 Dufferin St., Downsview, ON M3H 5T4, Canada

The Arctic has been influenced significantly by atmospheric long range transport of pollution since at least the middle of the 19th century. In the 1950's, military pilots reported reduced visibility in the arctic troposphere calling it "Arctic haze". However, it was not until the 1970's that the science community began to appreciate the origin of Arctic haze. That was when G. Shaw and K. Rahn linked visibility reduction to sulphur pollution released at mid-latitudes from smelting and fossil fuel combustion on surrounding continents. After 25 years of research, we are now aware of the nature and extent of pollution. A variety of contaminants and attendant environmental impacts that are present in what was once thought to be a pristine remote environment are listed in Table 1.

Norwegian scientists and the Ny-Ålesund station at Spitsbergen have played a key role in advancing our understanding of Arctic air pollution. Dr. B. Ottar of NILU was instrumental in the establishment of the Arctic air chemistry monitoring network in the early 1980's. The network included sites in Alaska, the Canadian Arctic, Greenland and Spitsbergen. In addition he hosted the first international symposium where an Arctic air chemistry research community was formed. In the 1980s, not only routine measurements but also shorter term field campaigns, glacial ice coring and chemical transport modelling were used to understand the history, nature and occurrence of pollution. To illustrate the importance of Ny-Ålesund geographically, consider the schematic in Figure 1. It is unique in its proximity to Eurasia and the open waters of the North Atlantic. Together with Alert and Barrow, it forms the backbone of the Arctic network. It has the longest record of sulphate and sulphur dioxide observations and a lengthy set of observations for many of the compound classes in Table 1.

In this presentation, highlights of the insight into Arctic air pollution gained from atmospheric chemistry research will be presented for each class of contaminant represented in Table 1. In order to appreciate, the impact of anthropogenic substances in the Arctic, one needs a good understanding of the occurrence of atmospheric constituents of natural origin. These include soil dust, sea salt and marine biogenic sulphur. These will also be discussed.

Table 1 Groups of gaseous and particulate trace constituents in the Arctic troposphere that are of regional, hemispheric or global interest.

Contaminant Group	**Environmental Significance in the Arctic**
Sulphur Compounds	Climate Change, Visibility, Acidification of Ecosystems, Biogenic Marine Tracer
Black Carbon	Climate Change, Fossil Fuel Combustion Tracer of sources
Metals	Toxicity, Tracers of sources
Nitrogen oxide	Atmospheric Oxidant Chemistry, Ecosystem Acidification and Fertilization
Reactive Hydrocarbons	Atmospheric Oxidant Chemistry, Tracers of Natural and Anthropogenic Sources, Indicator of Chemical Reactions
Ozone	Climate Change, Atmospheric Chemical Stability
Halogens(Br, I)	Ozone depletion, Biogenic Marine Tracers
PAHs	Tracers of sources, Toxicity
Industrial Organics(PCBs)	Toxicity, Tracers of sources
Agricultural Pesticides	Toxicity, Tracers of sources
Greenhouse Gases	Climate Change

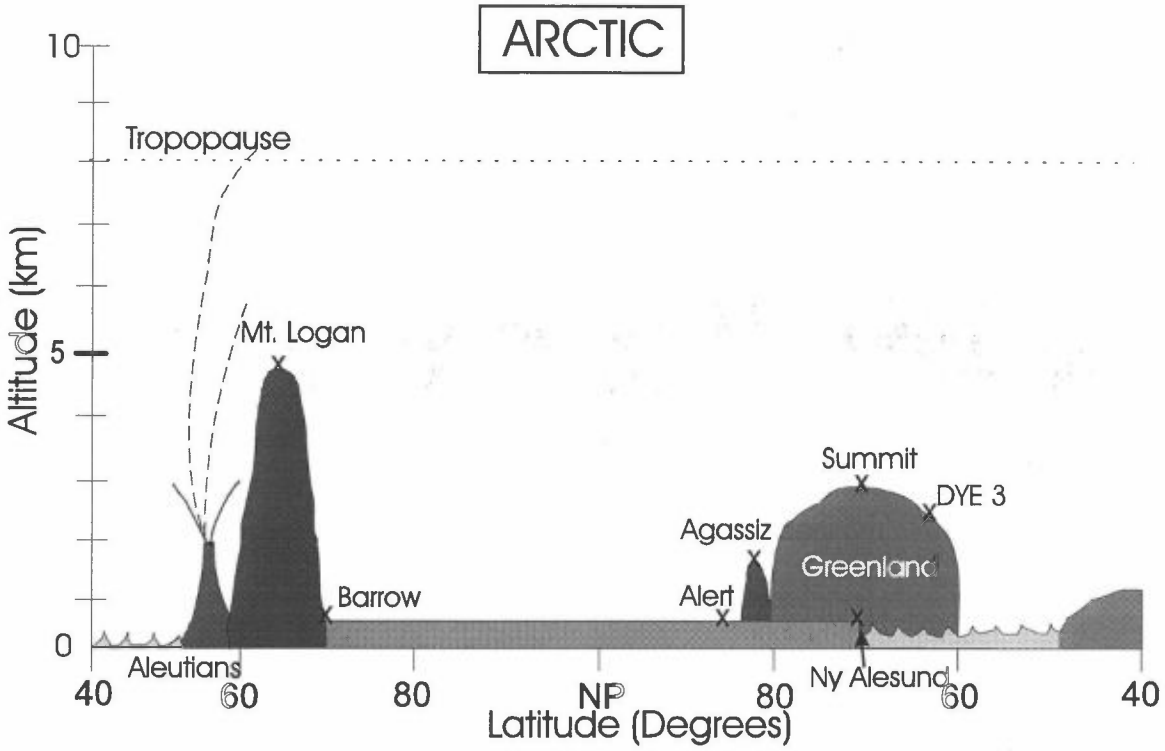

Figure 1 A schematic cross section of the Arctic troposphere from Europe to Alaska showing the location of major long-term baseline air chemistry observatories, major ice core chemistry sites and the major topographic features of the northern region. Elevated sites on Greenland, Agassiz and Mt. Logan glaciers have had only intermittent atmospheric composition measurements while the ground level observations at Ny Alesund, Barrow and Alert offer continuous multi-year data.

NILU's Atmospheric Measurements in Ny-Ålesund

Frode Stordal and Harry Beine,
Norwegian Institute for Air Research (NILU)
P.O.Box 100, 2007 Kjeller, Norway

1 Introduction

Much of NILU's research in the Arctic is today centered at the Zeppelin station near Ny-Ålesund, Svalbard (78°54'29"N, 11°52'53"E, 474 m. a. s. l.). The operation of the NILU sampling site 'Badehuset' had increasingly revealed problems with local pollution, especially during periods of low winds and/or inversion. In October 1989 a new atmospheric research station on the Zeppelin mountain, Svalbard was put into operation. The station was planned and built for measurements of background air in the high Arctic troposphere [*Braathen et al.*, 1990]. It was located on top of the Zeppelin mountain to minimize impacts from the nearby village of Ny-Ålesund, and to permit sampling of free tropospheric. Access to the station is possible via a dedicated electric cablecar. No combustion sources are located at the mountain top. Local contamination at the station is rarely seen [*Beine et al.*, 1996].

2 Recent advances in knowledge

The main purpose of this paper is to highlight some results that were published in recent years based on the measurements made at Zeppelin. A unique long term record of the Arctic aerosol shows that non-sea-salt sulfate is correlated with anthropogenically derived heavy metals, such as arsenic [*Maenhaut et al.*, 1997]. During the summer months a strong biogenic source for MSA can be detected in the fine particles [*Heintzenberg and Leck*, 1994]. The sources, composition, transport, and cycling of aerosols are today fairly well understood [*Pacyna*, 1995]. Aerosol measurements are the main verification for our understanding of transport in the Arctic [*Djupström et al.*, 1993], which often can be described by isentropic trajectories [*Iversen*, 1989a; b]. Aerosols currently partly offset a warming in the atmosphere. CO_2 has increased at Zeppelin in recent years by up to 4 ppmv/year. It has a clear annual cycle, with a summer minimum and a winter maximum [*Holmén et al.*, 1995]. Other greenhouse gases such as CFCs show a trend which is more slowly increasing in the 90's than in the 80's, reflecting reduced emissions. Transported both in the gas-phase and adsorbed on aerosols, POPs are enriched in the Arctic with significant consequences for Arctic biota [*Oehme et al.*, 1996a; b; 1995a; b]. NILU's main scientific focus has been on Arctic photochemistry in recent years. As explained above, troposphere chemistry is strongly connected to ozone, which has been measured for many years in Ny-Ålesund. The interaction of ozone, VOC, NO_x, and other species in the Arctic atmosphere are well described in a number of publications.

3 Atmospheric aerosol composition

Unlike the measurement programs at other sites NILU in collaboration with the University of Gent carries out a long term program to characterize the chemical composition of the Arctic atmospheric aerosol. High volume filter samples and samples from impactors are analyzed for SO_4^{2-}, methanesulfonate (MSA), NO_3^-, Cl^-, Br^-, and a number of cations by ion chromatography, as well as for 40 elements by neutron activation and particle induced X-ray emission (PIXE) [*Maenhaut et al.*, 1997]. It was found for example that both sulfate and MSA are connected to fine particles (< 2.5 μm), and that this fine sulfate was virtually all nss-

sulfate. Correlating those with episodes of high concentrations of anthropogenically produced metals, e.g. As, the anthropogenic origin of sulfate is visible. MSA on the other hand shows no correlation with As, its seasonal cycle is almost opposite to that of sulfate, which is expected since MSA is entirely generated from DMS emissions by phytoplankton.

4 Aerosol

Pacyna [1995] has recently reviewed many aspects of Arctic air pollution. Pollution in the lower layers of the Arctic troposphere during winter originates from Eurasian sources. During summer European sources are more important. In altitudes of 4 - 5 km a mixture of pollution from a multitude of sources - both natural and anthropogenic - can be found. Less than 10% of the emitted pollution seems to be deposited within the Arctic, however, many sink processes are not fully understood. During the 1980's the concentrations of major pollutants such as sulfur species stayed constant, while a decrease, particularly in lead and fine particle concentration has been observed in the 1990's, and is probably a reflection of a decrease of emissions in some source regions.

The fine particle fraction of the Arctic aerosol is of particular significance for Arctic haze and pollution. The fine particles are mainly composed of anthropogenic pollutants during winter, mostly sulfuric acid. They also contain high concentrations of anthropogenic heavy metals and persistent organic pollutants (POPs). Coarse particles on the other hand are not connected to anthropogenic pollution and consist of clay minerals, soil, and sea salt. The introduction of fine particles into the Arctic has also climatological consequences.

5 Tropospheric photochemistry

Ozone

Ozone has an annual cycle with a summer minimum and a spring maximum. Ozone is lower during summer and higher during winter than at a midlatitude station, for example Birkenes in the south of Norway. This shows that there is a pool of excess ozone in Europe during summer, and a deficit during winter, which reaches the south part of Norway, but not Svalbard. Due to episodic ozone depletion events the spring maximum is not as pronounced as at continental northern hemispheric sites.

NO_x

Accurate measurements of NO and NO_2 in the Arctic during winter and spring were not made until 1994 in a collaboration between the Geophysical Institute, University of Alaska, and NILU [*Beine et al.*, 1996]. These measurements, concurrently taken with measurements of ozone, PAN, and $J(NO_2)$ provided insight into the Arctic spring-time photochemistry [*Beine et al.*, 1997]. During the Arctic winter-spring transition, light and temperatures change dramatically the concentration of many NO_y species, which accumulate in the Arctic during winter and are thermally or photochemically processed to yield NO_x, which in turn can produce ozone.

NO_y and PAN

PAN was identified as the major NO_y component during spring, reaching mixing ratios as high as 800 pptv during individual episodes [*Solberg et al.*, 1997]. The annual PAN cycle reaches a maximum during spring. PAN is mostly transported into the Arctic over long distances, model results show however, that local photochemistry may produce up to 1 - 2 pptv/h PAN during April - May, arising mainly from acetaldehyde.

Tropospheric ozone depletion

Based on NILU's ozone, VOC, sulfate, and meteorology data *Solberg et al.* [1996b] analyzed ozone depletion events in the atmsopheric boundary layer since 1989 on a climatological basis. The first measurements of NO_x during ozone depletion events taken with a high sensitivity instrument during the spring of 1994 were discussed by *Beine et al.* [1996]. These studies showed that tropospheric ozone depletion at Ny-Ålesund occurred within a cold boundary layer up to about one km height, which was capped by a thermally stable layer. The airflow arrived from north-westerly directions. Several individual hydrocarbons were reduced concurrently with ozone and it was shown that the depletion of these hydrocarbons must have occurred via reaction with halogen radicals rather than with OH. NO_x during the ozone depletion events was low.

VOC: NMHCs and Carbonyls

Within EMEP VOC are measured regularly at the Zeppelin station [e.g. *Solberg et al.*, 1996a]. It was shown that hydrocarbons originating from natural gas become well mixed in the Arctic, while fuel evaporation and combustion products show a latitudinal gradient, with lower concentrations at Zeppelin than further south. The sum of C_2 - C_5 NMHC shows an annual cycle with a summer minimum and a winter maximum of about 4 and 20 ppbC by volume, respectively.

Oxidized hydrocarbons contribute about 10 % to the sum of VOC at Zeppelin in winter. This fraction rises to 50% during the summer, consistent with the oxidation of NMHCs. Ethane and propane are the most abundant NMHCs, consistent with their OH reactivity [*Hov et al.*, 1989]. The annual cycle of hydrocarbons in the Arctic was already established following measurements in 1982/83 [*Hov et al.*, 1984].

6 Greenhouse gases

NILU has measured CFCs at Zeppelin since 1990. Compared with measurements made in 1982 these species showed an average annual trend between 1982 and 1990 of 10.7 pptv/yr. The trend in the nineties is smaller, 7.3 pptv/yr. [*Hermansen and Solberg*, 1994], which reflects the success of curbing the emissions of these species. Since 1991 N_2O has been measured at Zeppelin. Although the data show some scatter, a trend of +2.7 ppbv/year is visible.

7 POPs

Persistent organic pollutants (POP) have been measured at various times during the last 15 years at Ny-Ålesund. Identified species include pesticides, polychlorinated biphenyls, polyaromatic biphenyls, and, since 1995 toxaphens and dioxins [e.g. *Oehme et al.*, 1995a; b; 1996a;b]. POPs are brought into the Arctic via long range transport, due to their long life time

volatile organochlorines show similar mixing ratios in the Arctic as in the mid-latitudes where the sources are found. Due to the physical properties of POPs they are enriched in the Arctic, with significant consequences for Arctic biota such as seals and polar bears.

8 Stratospheric ozone

Since 1990 a UV-visible spectrometer (SAOZ) measures the total column ozone and NO_2 routinely. Ozone measurements were made daily in peiods in 1994 and 1995 and NO_2. Readings cannot be made during the summer because of the high latitude of the station [*Høiskar et al.*, 1997]. Total ozone is also measured at various locations in Norway, including Ny-Ålesund, with multi-channel UV-filter instruments [*Dahlback et al.*, 1996].

9 Models

Tropospheric modeling:

Modeling efforts over the previous years have proceeded along two different paths. During the ARCTOC campaign a chemical box model was developed to interpret measurements of halogen species and low ozone events made during the campaigns in 1995 and 1996 [*Flatøy et al.*, 1996]. This particular model includes gas phase as well as some heterogeneous chemistry. The work is in progress, so far only the sensitivity studies have been published. A second strand is the work with transport models on a larger scale. A lagrangian numerical model was applied recently to simulate VOC concentrations and compare them to measurements taken at a number of sites, including Zeppelin [*Hov et al.*, 1997].

Stratospheric modeling

Stratospheric ozone is influenced by both dynamical and chemical processes, and this is reflected in stratospheric models. Ozone sonde data from Ny-Ålesund have been compared with chemical trajectory model calculations done at NILU [*Fløisand et al.*, 1995]. In particular heterogeneous reactions of Cl species on Polar Stratospheric cloud surfaces have been studied [*De Haan et al.*, 1997] in a stratospheric chemical transport model.

10 Radioactivity

Since 1986 Ny-Ålesund is part of an alert-network to measure radioactivity in Norway [*Berg*, 1996].

11 Final comments

Arctic research at Ny-Ålesund has stimulated scientific questions and contributed to our understanding of the atmosphere on both the regional and global scale. NILU's work in Ny-Ålesund and specifically at the Zeppelin station on the many aspects of atmospheric chemistry is important with respect to the national and international research and environmental policy agenda.

More details on NILU's measurement programmes in Ny-Ålesund are available in Beine (1997) along with information on data dissemination. The Zeppelin station is open for international collaboration.

12 References

Beine, H. J, NILU's atmospheric research at Ny-Ålesund, *NILU*, OR 20/97, 1997.

Beine, H. J., D. A. Jaffe, J. A. Herring, J. A. Kelley, T. Krognes, F. Stordal, High latitude springtime photochemisty part 1: NOx, PAN, and ozone relationships. *J. Atm. Chemistry*, accepted for publication, March 1997.

Beine, H. J., M. Engardt, D. A. Jaffe, Ø. Hov, K. Holmén, F. Stordal, Measurements of NOx and aerosol particles at the Ny-Ålesund Zeppelin mountain-station on Svalbard: Influence of regional and local pollution sources. *Atmospheric Environment,* 30(7), 1067-1079, 1996.

Berg. T. C., Overvåkning av radioaktivitet i Norge. Årsrapport 1995. Kjeller (Statlig program for forurensningsovervåkning. Rapport 666/96), *NILU*, OR 46/96, 1996.

Braathen, G. O., Ø. Hov, F. Stordal, Arctic atmospheric research station on the Zeppelin mountain (474 m a.s.l.) near Ny-Ålesund on Svalbard (78°54'29"N, 11°52'53"E). *NILU*, OR 85/90, 1990.

Dahlback, A., G. Hansen, T. Svenøe, L. Opedal, F. Tønnessen, Monitoring of total ozone by means of multi-channel filter instruments. *XVIII Quadrennial Ozone Symposium*, L'Aquila, Italy, 1996.

De Haan, D. O., I. Fløisand, F. Stordal, Modeling studies of the effects of the heterogeneous reaction ClOOCl + HCl $\rightarrow$ Cl_2 + HOOCl on stratospheric chlorine activation and ozone depletion. *J. Geophys. Res.*, 102(D1), 1251-1258, 1997.

Djupström, M., J. M. Pacyna, W. Maenhaut, J. W. Winchester, S.-M. Li, G. E. Shaw, Contamination of Arctic air during a haze event in late winter 1986. *Atmospheric Environment*, 27A, 2999-3010, 1993.

Flatøy, F., Ø. Hov, S. Solberg, F. Stordal, A chemical box model for studies of Arctic tropospheric ozone chemistry. In U. Platt, E. Lehrer (Eds.), *ARCTOC, Final report of the EU project*, Heidelberg, November 1996.

Fløisand, I., F. Stordal, N. Larsen, B. Knudsen, G. O. Braathen, Trajectory model calculations compared with ozonesonde data, 1994-95. In: J. A. Pyle et al. (Eds.) *Polar Stratospheric ozone*, Proceedings of the third European workshop, 1995.

Heintzenberg, J., C. Leck, Seasonal variation of the atmospheric aerosol near the top of the marine boundary layer over Spitsbergen related to the Arctic sulphur cycle. *Tellus*, 46B, 52-67, 1994.

Hermansen, O., S. Solberg, CFC-11 trends ar Spitsbergen. *NILU*, OR 20/94, 119-121, 1994.

Holmén, K., M. Engardt, S.-Å. Odh, The carbon dioxide measurement program at the Department of Meteorology at Stockholm university. International Meteorological Institute in Stockholm, *Report*, CM-84, 1995.

Hov, Ø., A. Sorteberg, N. Schmidbauer, S. Solberg, F. Stordal, D. Simpson, A. Lindskog, H. Areskoug, P. Oyola, H. Lättilä, N. Z. Heidam, European VOC emission estimates evaluated by measurements and model calculations. *J. Atm. Chem.*, Accepted for publication, January 1997.

Hov, Ø., N. Schmidbauer, M. Oehme, Light hydrocarbons in the Norwegian Arctic. *Atmospheric Environment*, 23(11), 2471-2482, 1989.

Hov, Ø., S. A. Penkett, I. S. A. Isaksen, A. Semb, Organic gases in the Norwegian Arctic. *Geophys. Res. Lett.*, 11(5), 425-428, 1984.

Høiskar, B. A. K., A. Dahlback, G. Vaughan, G. O. Braathen, F. Goutail, J.-P. Pommereau, R. Kivi, Interpretation of ozone measurements by ground based visible spectroscopy - a study of the seasonal dependence of airmass factors for ozone based on climatology data. *J. Quant. Spectroscopy Rad. Transfer*, 57(4), 569-579, 1997.

Iversen, T. Some statistical properties of ground level and air pollution at Norwegian Arctic stations and their relation to large scale atmospheric flow systems, *Atmos. Environ.*, 23, 2451-2462, 1989a

Iversen. T., Numerical modelling of the long range atmosperic transport of sulphur dioxide and particulate sulphate to the Arctic, *Atmos. Environ.*, 23, 2571-2595, 1989b.

Maenhaut, W., K. Beyaert, G. Ducastel, V. Havránek, R. Salomonovic, J. E. Hanssen, Long-term measurements of the atmospheric aerosol composition at Ny-Ålesund, Spitsbergen. *Proceedings of EUROTRAC Symposium '96*, Editors: P. M. Borrell, P. Borrell, T. Cvitaš, K. Kelly, W. Seiler, Computational Mechanics Publications, Southampton, 273-276, 1997.

Oehme, M., J.-E. Haugen, M. Schlabach, Seasonal changes and relations between levels of organochlorines in the Arctic ambient air: First results of an all-year-round monitoring program at Ny-Ålesund, Svalbard, Norway. *Environmental Science and Technology*, 30(7), 2294-2304, 1996a.

Oehme, M., M. Schlabach, R. Kallenborn, J.-E. Haugen, Sources and pathways of persistent polychlorinated pollutants to remote areas of the North Atlantic and levels in the marine food chain: A research update. *The Science of the Total Environment*, 186, 13-24, 1996b.

Oehme, M., J.-E. Haugen, M. Schlabach, Ambient air levels of persistent organochlorines in spring 1992 at Spitsbergen and the Norwegian mainland: Comparison with 1984 results and quality control measures. *The Science of the Total Environment*, 160/161, 139-152, 1995a.

Oehme, M., A. Biseth, M. Schlabach, Ø, Wiig, Concentrations of polychlorinated dibenzo-p-dioxins, dibenzofurans, and non-ortho substituted biphenyls in polar bear milk from Svalbard (Norway). *Env. Poll.*, 90(3), 401-407, 1995b.

Pacyna, J. M., The origin of Arctic air pollutants: Lessons learned and future research. *The Science of the Total Environment*, 160/161, 39-53, 1995.

Solberg, S., T. Krognes, F. Stordal, Ø. Hov, H. J. Beine, D. A. Jaffe, K. Clemitshaw, S. A. Penkett, Reactive nitrogen compounds at Spitsbergen in the Norwegian Arctic. *J. Atmos. Chem.*, accepted for publication 1997.

Solberg, S., C. Dye, N. Schmidbauer, A. Herzog, R. Gehrig, Carbonyls and nonmethane hydrocarbons at rural European sites from the Mediterranean to the Arctic. *J. Atm. Chem.*, 25, 33-66, 1996a.

Solberg, S., N. Schmidbauer, A. Semb, F. Stordal, Ø. Hov, Boundary-layer ozone depletion as seen in the Norwegian Arctic. *J. Atm. Chemistry*, 23, 301-332, 1996b.

The Koldewey-Station in Ny-Ålesund
Contributions to atmospheric studies in the Arctic

Hartwig Gernandt
Alfred Wegener Institute of Polar and Marine Research
Research Department Potsdam

1. Introduction

The Koldewey-Station (78.9°N; 11.9°E) is located within the Norwegian settlement Ny-Ålesund at Svalbard. It is the Arctic observatory of AWI for regular observations as well as biological and geoscientific field activities. A major part is focused to atmospheric research. First studies began in 1988 by lidar and balloon-borne observations. Since then the observations of atmospheric parameters have been extended by installing new remote sensing techniques. So the observatory became an important tool for AWI's polar atmospheric research. Since 1991 the station has been permanently operated by a station leader and a station engineer. In 1995 a new laboratory, called the NDSC observatory, was established. The station is equipped with a local computer network and connected via Internet for data transmissions.

Beside the AWI national contributors to arctic atmospheric research are the University of Bremen and the Free University Berlin participating in regular observations and performing data analysis.

The Koldewey-Station is participating in international campaigns and global networks. These activities are focused to the Network for Detection of Stratospheric Change (NDSC) with qualified ground-based remote sensing and balloon-borne instruments as well as to the global Baseline Radiation Network (BSRN) with qualified radiation instruments for long-term record of the short-wave and long-wave surface radiation budget. Both the NDSC and BSRN observations are performed in German-Norwegian cooperation.

Since 1991 the participation in international campaigns as EASOE in winter 1991/92, SESAME focused on winters 1993/94 and 1994/95, and recently OSDOC has been a major part of stratospheric studies. In spring 1994 and 1995 the ARTOC campaign was supported by tropospheric ozone sonde observations.

2. Objectives of AWI's atmospheric research in the Arctic

The main focus is addressed on modelling the climate of the arctic atmosphere. So a tight connection between model applications and observations is considered for getting convenient results on dynamical and chemical processes in the Arctic atmosphere, to understand the natural variability and long-term changes of the system as well as the impact by global atmospheric processes and by the ocean.

The tools are the regional climate model HIRHAM, the permanent atmospheric observations at the Koldewey-Station in the Arctic and at Neumayer Station in the Antarctic. These regular measurements were completed by observations on board of the research vessel "Polarstern".

The regional climate model is the basic tool to study in detail climatic processes, to generate consistent climate data in remote areas, and to investigate in more detail the chemical and dynamical processes. The Arctic observatory is the main experimental site of AWI to measure meteorological and chemical processes in the atmosphere, to detect long-term changes in atmospheric composition, and to provide data for validation of model runs and satellite observations (Tab. 1).

Tab. 1: AWI's ARCTIC OBSERVATORY AT (79°N; 12°E)

OBJECTIVES: vertical column; stratospheric and tropospheric processes
long-term variability (anthropogeneous impact and natural variability)
validation (methods, satellites, models), instrument intercomparisons

---

PARAMETERS: T, W, O_3, trace gases, aerosols, PSCs, radiation, samples

Profiles (Lidar, Radiometer, Balloon):
temperature, wind, humidity, aerosols, PSCs (formation, variability, properties), O_3, ClO.

Total column measurements (Spectrometer, Photometer):
reactive (NO_x and ClO_x) and inert trace gases in the stratosphere.
anthropogeneous trace gases in the troposphere.
spectral optical depth (350 - 1050 nm) of aerosols (Arctic Haze).

Surface:
short and longwave radiation balance, high resolution UV-B (280-320 nm).
precipitation and snow deposition sampling (long-range transport, aerosols, heavy metals)

METHODS: **Active and passive remote sensing up to 50 km**

Multiwavelength-Lidar: upper troposphere, stratosphere (DIAL, backscatter, Raman)
UV-VIS-Lidar: boundary layer, free troposphere (DIAL, 250-300 nm, 375-450 nm)
Fourier-Spectrometer (IR, UV/vis / Sun, Moon as light sources, scattered light, emission).
Two channel-microwave radiometer (110-280 GHz)
Photometer (350 - 1050 nm, Sun and Moon light sources).
Telescope-Photometer (350 - 1050 nm, cold stars as light sources).
UV-B Multi channel-Radiometer (280-320 nm, high spectral resolution).
DOAS - Differential Optical Absorption Spectrometer (340-500 nm / scattered light)

In-situ balloon measurements

Radiosonde station DigiCORA for standard observations up to 35 km:
Radiosonde RS 80, Ozone sensor (ECC), backscatter sonde

Radiosonde station GK 90, high altitude balloon (BT-5) for special experiments up to 45 km:
digital radiosonde DFM 90 (7 additional channels) with differential GPS:
recent options: optical ozone sensor, optical particle counter (aerosols and PSCs)

Automatic ground stations

Radiation and synoptical station, precipitation and snow deposition samplers

---

GLOBAL NETWORKS:
NDSC (Network for Detection of Stratospheric Change): arctic primary station.
BSRN (Baseline Surface Radiation Network) radiation components
GAW (Global Atmospheric Watch) trace gases and aerosols - recently proposed

3. Summary of scientific results

First model runs of the regional climate model HIRHAM and their validation including Ny-Ålesund observations have shown the potential for realistic simulations of climatic processes in the Arctic. Validation experiments are recently focused to GOME satellite data.

A quantitative Lagrangian approach has been successfully used to assess the degree of chemically-induced ozone loss in the Arctic lower stratosphere by a coordinated network of ozone soundings. The main advantage of this method (Match) is that chemical and dynamical effects can be separated to a high degree. Chemical ozone destruction rates were achieved in temporal and coarse spatial resolution.

Since 1985 in the Antarctic at Georg Forster and Neumayer and since 1988 at Ny-Ålesund ozone and temperature profiles were measured by balloon-borne sensors. As Ny-Ålesund and both Antarctic stations are mainly located within the polar vortex most of the winter time they are prime locations for continuous and long-term observations for detection of stratospheric change the major aim of the NDSC network.

Special attention was paid for polar stratospheric cloud studies and the occurrence of volcanic aerosols in the Arctic stratosphere after the eruption of Mt. Pinatubo in June 1991. The formation and development of PSC events can be shown in detail by the multiwavelength lidar backscatter ratio R, the aerosol depolarisation d (both at the 532 nm wavelength), and the colour ratio calculated from the backscatter signals at 353 and 532 nm. during the observations.

The mean seasonal variation of two species, HCl and $ClONO_2$, in the ozone depletion cycles was recorded by ground-based Fourier spectrometer and modelled by a one dimensional chemical model. Furthermore the high resolution spectroscopy by the Fourier spectrometer made it possibly to identify the column densities of the ozone isotopes O_3 (16-16-18) and O_3 (16-18-16). During sunlit seasons the enrichment of both isotopes is significantly different.

In the Arctic tropospheric ozone concentrations are elevated during spring while high aerosol concentrations were detected in the boundary layer. The optical depths of tropospheric aerosols could be retrieved from combined ground-based photometer measurements and SAGE II satellite data.

Strong ozone depletion events were detected in ozone sonde data within the boundary layer. The intercomparison with Antarctic observations has shown that similar ozone minima appear at both polar stations during polar spring.

4. Data quality and new instruments

Intercomparisons for NDSC qualified instruments took place for Fourier spectrometers in 1995 and for microwave radiometers in 1997. Lidar instruments will be parallel operated in 1998. In order to improve the quality as well as the temporal and vertical resolution of observations new instruments has been recently tested and partially included in the regular research programme:

During winter 1995/96 a new Fourier Spectrometer (IFS 120 HR) was installed for high resolution measurements (0.0025 cm^{-1}) in the spectral range from UV to IR (300 nm - 16m).

During winter 1996/97 first test measurements were performed with a newly developed telescope photometer for measurements of the spectral optical depths by using cold stars as the light sources.

Since March 1996 a new UV-B spectroradiomter type for solar irradiance measurements was installed. A complete spectrum from 280 to 320 nm (290 to 330 nm resp.) is taken each second in 32 parallel channels with 1.3 nm resolution.

In spring 1966 a tropospheric Differential absorption lidar (DIAL) was firstly operated to measure fast variations of the vertical distributions of ozone and aerosols in the lower troposphere.

In September 1997 the digital radiosonde DFM 90 with differential GPS will be tested for balloon-borne measurements up to the upper stratosphere with the high altitude balloon (BT-5).

5. International management and future projects

The Koldewey-Station and its NDSC laboratory are part of the Ny-Ålesund International Arctic Research and Monitoring Facility, the scientific activities of which are coordinated by an international advisory board (Ny-Ålesund Scientific Managers Committee - NySMAC). Access to the Koldewey-Station for researchers from EU countries is supported by the EU framework on Training and Mobility (TRM).

The Koldewey-Station is continuing the contributions to global networks. It will participate in THESEO and other projects as ARCTOC II. The participation in SAGE III validation as a primary site has been suggested.

6. Relevant references

Beyerle, G., A. Herber, R. Neuber, and H. Gernandt: Temporal development of Mt. Pinatubo aerosols as observed by lidar and sun photometer at Ny-Ålesund, Spitsbergen. Geophys. Res. Lett., 22, 2497-2500, 1995.

Dethloff, K., A. Rinke, R. Lehmann, J.H. Christensen, M. Botzet, and B. Machenhauer: Regional climate model of the Arctic atmosphere. J. Geophys. Res., 101, 23,401-23,422, 1996.

Ladstaetter-Weissenmayer, A., J.P. Burrows, A. Richter, F. Wittrock, M. Buchwitz, M. Weber, M. Eisinger, and R. Neuber: Validation of GOME O3 and NO2 measurements in Bremen, Ny-Alesund, and Neumayer. In: GOME Geophysical Validation Campaign: Final Results, ESA WPP-108, 153-160, 1996.

Gernandt, H., P. von der Gathen, and A. Herber: Ozone change in the polar atmosphere. NATO ASI Series I, Vol. 53, 75-102, 1997.

Herber, A., K. Dethloff, L.W. Thomason, P. Viterbo, V.F. Radionov, U. Leiterer: Volcanic Perturbation of the Atmosphere in both Polar regions: 1991-1994. J. Geophys. Res., 101, 3921-3928, 1996.

Meier, A., and J. Notholt: Determination of the isotopic abundances of heavy O3 as observed in arctic ground-based FTIR spectra. Geophys. Res. Let., Vol. 23, 551-554, 1996.

Stebel, K., O. Schrems, R. Neuber, G. Beyerle, J. Biele, I. Beninga, P. Scheuch, H. Schuett, and P. von der Gathen: Polar stratospheric clouds above Spitsbergen. Proceedings XVIII Quad. Ozone Symposium, L'Aquilla, Italy, submitted, 1996.

Notholt, J., G. Toon, F. Stordal, S. Solberg, N. Schmidbauer, E. Becker, A. Meier, B. Sen: Seasonal variation of atmospheric trace gases in the high Arctic at 79°N. J. Geophys. Res., in press, 1997.

Rex, M. et al.: Chemical ozone loss in the Arctic winters 1991/92 and 1994/95 (Match). In Air pollution research report 56, Polar stratospheric ozone 1995, Proceedings of the third European workshop, Schliersee, Bavaria, Germany, ISBN 92-827-5722-6, pp 586-589, 1996.

von der Gathen, P., M. Rex, N.R.P. Harris, D. Lucic, B.M. Knudsen, G.O. Braathen, H. De Backer, R. Fabian, H. Fast, M. Gil, E. Kyr, I.S. Mikkelsen, M. Rummukainen, M., J. Staehelin, and C. Varotsos: Observational evicence for chemical ozone depletion over the Arctic in winter 1991-92, NATURE, Vol. 375, 131-134, 1995.

Wessel, S., S. Aoki, R. Weller, A. Herber, H. Gernandt, and O. Schrems: Aerosol and ozone variations in the polar troposphere at Spitzbergen in spring 1994. Special Issue Atmospheric Research, in press, 1997.

Climatically Active Species in Ny-Ålesund; a Synopsis of the MISU Activities

Kim Holmén
Department of Meteorology (MISU), Arrhenius Laboratory, Stockholm University
S-106 91 Stockholm, Sweden

Abstract

We summarize the work performed by the Department of Meteorology at Stockholm University (MISU) at the air chemistry station on Zeppelinfjellet near Ny-Ålesund, Spitsbergen (78°54'N, 11°53'E, 474 m). Baseline measurements have been operational since the spring of 1990. The measured atmospheric parameters are carbon dioxide (CO_2) mixing ratios, particle concentrations in two size ranges, light scattering coefficient at 0.55 mm wavelength and aerosol composition, (elemental carbon, major anions and cations). As complementary meteorological data we also monitor air pressure and temperature and the horizontal wind components and local cloudiness. Highlights of the results are presented elsewhere in this volume.

Project Background

Since the spring of 1990 regular Swedish atmospheric baseline measurements are ongoing at the monitoring station on Zeppelinfjellet near Ny-Ålesund, Spitsbergen. The Swedish program is focused on climatically active species and has two main thrusts. The first aim is to provide the first continuous atmospheric CO_2 measurements in the European Arctic and gain an understanding of the regional aspects of the carbon cycle. The second part of the monitoring program focuses on physical and chemical properties of aerosols. The baseline station has been described in detail in Heintzenberg et al. 199la. A first summary of the measurements from 1979 until 1990 has been published in Heintzenberg et al. 1991b. The data for 1991 and 1992 can be found in Heintzenberg et al. (1992 and 1993 respectively) and for 1993 in Holmén et al. (1995). Monthly average sulfur components for the first two years have been compared to the output of a global sulfur model by (Langner et al., 1993). A first assessment of the biological sulfur components of the regional aerosol and of the cloud processing of Arctic aerosol has been deduced by (Heintzenberg and Leck, 1994) from the baseline records. An analysis of CO_2 variability during the first years of mountain top operation has been completed (Engardt et al., 1995, Engardt 1997a). Characteristics of the large-scale circulations influence on the transport of pollutants to the Arctic has recently been completed (Lejenäs and Holmén, 1996). Both the particle data and modeling efforts regarding the CO_2 record are presented in this volume by Leck and Engardt respectively.

Flask samples have been collected on Zeppelinfjellet at least once a week since early 1994. The flasks are shipped via diplomatic pouch to NOAA/CMDL in Boulder, Colorado, USA where the analysis for ^{13}C, ^{18}O and CO_2 are performed.

Intercalibrations with the international CO_2 community is achieved by exchanging cylinders that have been calibrated at a central laboratory and recalibrating them at the individual laboratories. At Zeppelinfjellet there is an additional intercalibration possibility through the parallel programs of NOAA/CMDL flask sampling and the MISU continuous instrument. The flask intercomparison is performed continuously as the data become available.

The interpretive work is concentrated on developing regional transport models to identify sources and sinks. The regional modeling component of the MISU effort has developed into utilizing an off-line transport model based on output meteorological data from ECMWF and high resolution regional meteorological models (the HIRLAM weather

prediction model). The model is driven by observed meteorology, with a parameterized boundary layer, and utilizes a mass conserving advection scheme with only small phase and amplitude errors. The model has been tested with ^{222}Rn simulations (Robertson et al., 1996). The model is applied to the Zeppelinfjellet record to determine regional sources and sinks (see Engardt and Holmén, this volume).

The development of the high-resolution regional transport model (MATCH) was completed during 1996 (Robertson et al., 1996). The first studies have been conducted with input data from ECMWF, thus not utilizing the full flexibility power of the MATCH modeling system. The results to date are encouraging and have been presented in the Ph.D thesis "Climate Change and Carbon Dioxide Fluxes in the High Latitude Northern Hemisphere" defended by Mr. Magnuz Engardt in January 1997. The thesis contains several articles (Robertson et al., 1996; Engardt and Holmén, 1997; Engardt, 1997) based on the MATCH model and its utilization to study the Zeppelinfjellet CO_2 record. Two results that potentially are very important for our understanding of the carbon cycle in and near Europe have emerged from the MATCH studies. The first result is that the scaling of anthropogenic CO_2 emissions over Russia should not be based on population density as has frequently been done to date but should be evaluated based on the distribution of heavy industry. The second result is that the pollution plumes (often called "Arctic haze") seen in the Arctic region during winter to a large proportion emanate from the emissions created by flaring and other activities with connection to the very large gas fields in Northern Russia. The present model is unable to simulate this episode unless the CO_2 emissions occur in Northern Russia. Verification of these results is an important component of the work planned for 1997.

Data Summaries

Carbon dioxide

The continuous CO_2 data are available in preliminary form up to and including March 18, 1997. The data through the first half of 1996 have also been reported to the WMO greenhouse gas data center in Japan. Figure 1 displays the complete record from Zeppelinfjellet including March 18, 1997. The amplitude of the seasonal cycle as determined by fitting a harmonic function through the data is 15.7 ppm(v) and the trend through the entire data set gives an average increase rate of 0.98 ppm(v)/year. The flask program is equally successful and data are available for all of 1996. The comparison of data between the continuous record and the flask samples show a correspondence within 0.15 ppm(v) (Holmén et al., 1995).

As reported in the literature (Sarmiento, 1993; Conway et al., 1994; Keeling et al., 1995) there has been an unusual behavior of atmospheric CO_2 concentrations during the past years. Following the time of the Pinatubo eruption on the Philippines in 1991 there has been little increase in atmospheric CO_2. Fitting a harmonic function (as was done in Figure 1 through the entire data-set) through only the 5-day mean CO_2 from January 1992 through December 1993 data from Zeppelinfjellet gives a yearly increase rate of only 0.01 ppm(v). This is substantially lower than the average increase calculated above but consistent with other monitoring stations around the world. The reasons for this anomaly (compared to the trend during previous decades) is not understood at this time. There is no clear mechanism that could tie the anomaly to the Pinatubo eruption; the common timing can be entirely coincidental. During 1994 a sudden increase in CO_2 occurred in July. The higher level has prevailed ever since. This sudden increase is probably a result of some response from the terrestrial biosphere to climatic changes created by the Pinatubo eruption. These features are currently being explored in Stockholm with the aid of a global GCM coupled to a terrestrial biosphere model.

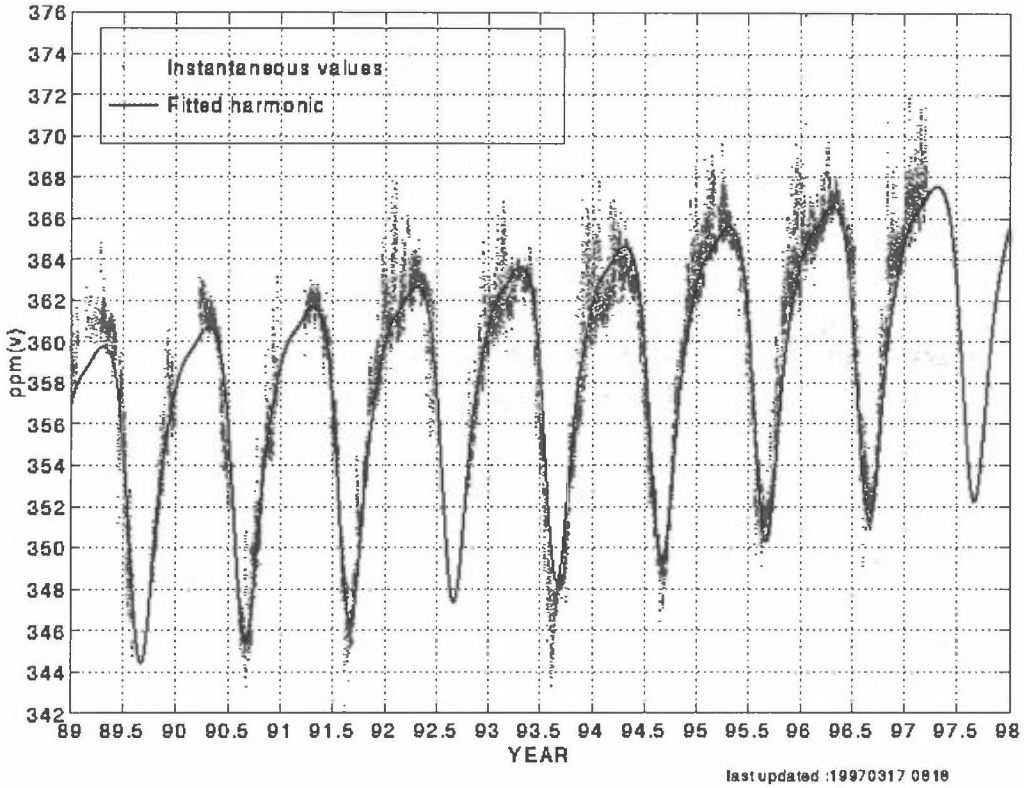

Figure 1 Atmospheric CO_2 mixing ratios (ppm(v) vs. decimal year) every third hour directly following a calibration from the continuous recording instrument in Ny-Ålesund January 1, 1989 to March 17, 1997. Data prior to Mars 1990 (decimal year 90.21) is collected at "Gruvbadet", (ca. 50 m asl). Thereafter all monitoring was performed at the baseline station on Zeppelinfjellet (ca. 474 m). The average annual increase for the period is 0.98 ppm(v)/year and the average seasonal amplitude is 15.66 ppm(v).

Synoptic time-scale anomalies in CO_2 are visible in all years: positive anomalies, on the order of several ppm(v), during winter when Svalbard was affected by the Arctic front and polluted air was advected from Siberia; negative deviations, on the order of a few ppm(v) in spring, caused by air advected to Svalbard from the then highly undersaturated waters of the northern North Atlantic. These features have been explored in several manuscripts (Engardt et al., 1995; Lejenäs and Holmén, 1996; Engardt, 1997a). As of 1994 flask samples have been collected for ^{13}C measurements during the spring episodes to gain further understanding of the origins of the variability. The interpretation of these data is ongoing.

In order to understand these excursions better it would be most valuable to monitor ^{222}Rn at Ny-Ålesund. Since the only significant source for atmospheric ^{222}Rn is the exhalation from soils and ^{222}Rn has a well known short decay time, (half life about 3.8 days), it is often used as a tracer to calculate the time spent by the air since its last contact with land. The possibility of ^{222}Rn monitoring has been evaluated further and is today considered to be an important complement to the current program that should be pursued.

Particle Counters, nephelometer and filter samples

After several years of baseline monitoring a seasonal variation of the Arctic aerosol is evolving with number maxima in the summer and light-scattering maxima in the winter season. A distinct summer maximum in fine particles is clearly seen and the wintertime maximum in light scattering is also obvious. The data set are still too short to explore trends due to the very high variability of these quantities. Important to point out is, however, that

these climatically important species are inherently difficult to monitor and the record is extremely sensitive to local contamination.

The nephelometer, nss-SO_4^{2-}, NH_4^+ and EC data show the typical Arctic haze seasonality, based on a strong import of polluted mid-latitude air during November-April. The situation changes thereafter when the main air mass origin moves farther north into the Arctic basin. During summer a dramatic change in atmospheric circulation is experienced, with advection of air masses originating over the North Atlantic dominating over shorter periods of air being either advected from the continents at lower latitudes or subsiding from the free troposphere. The annual minimum pollution import is reached during June-August. We note that calcium and magnesium show similar seasonal patterns consistent with the interpretation that there is stronger transport of continental air to the Arctic in winter. The seasonal variation of particulate MSA are fundamentally different from those of the former compounds. MSA concentrations began to increase in May with largest concentrations, coinciding with the summer maxima in aerosol number concentration, taking place in May-August. Low winter concentrations of MSA are reached in October. For a thorough discussion of the particle samples and in particular the MSA data see Leck in this volume.

Future developments by MISU on Zeppelinfjellet

The model studies will be developed further by incorporating isotopes in the MATCH model. During 1997 experiments will also be performed with higher resolution meteorological data from the HIRLAM weather prediction system. The further quantification of the role of the Russian gas and oil fields for Arctic pollution will be pursued with these refined models.

During 1997 all instruments will be replaced; as of April there will be an entirely new particle counter system including size segregated statistics and a three wave-length nephelometer. The carbon cycle studies will be expanded to include higher temporal resolution in the isotopic sampling.

Of paramount importance for this work is, however, the continued maintenance of a clean background in the Ny-Ålesund area. The time-series is jeopardized by every increase in activities that create emissions to the atmosphere.

Collaborative efforts with other Ny-Ålesund scientists are eagerly sought; request for data should be directed to KH.

Acknowledgements

This project is supported by the Swedish Environmental Protection Board. We thank Mrs. Astrid Jacobsson who did most of the tedious work of preparing and processing of the particle samples. We appreciate the help from the Norwegian Institute for Air Research and from the Norwegian Polar Research Institute.

References

Conway, T. J., Tans, P. P., Waterman, L. S., Thoning, K. W., Kitzis, D. R., Masarie, K. A. and Zhang, N., 1994, *Evidence for interannual variability of the carbon cycle from the National Oceanic and Atmospheric Administration/Climate Monitoring and Diagnostics Laboratory Global Air Sampling Network.* Journal of Geophysical Research **99,** 22831-22855.

Engardt, M. 1997a, *Climate Change and Carbon Dioxide Fluxes in the High Latitude Northern Hemisphere.* Department of Meteorology, Stockholm University, **Ph.D. thesis**, 104pp.

Engardt, M. 1997b, *Atmospheric transport of anthropogenic CO_2 to an Arctic monitoring station in winter,* manuscript, 22pp (in Engardt, 1997a).

Engardt, M. and Holmén, K. 1996, *Towards deducing regional sources and sinks from atmospheric CO_2 measurements at Spitsbergen.* **Physics and Chemistry of the Earth**. in press.

Engardt, M., K. Holmén, and J. Heintzenberg, 1996, *Short-term variations in atmospheric CO_2 at Ny-Ålesund, Svalbard during spring*, Tellus, 48B, 33-43.

Heintzenberg, J., J. Ogren, S.-Å. Odh, L. Bäcklin, T. Danielsen, 1991a, *The MISU baseline station*, Department of Meteorology, Stockholm University, Report AA-2, 42 pp.

Heintzenberg, J., K. Holmén, S.-Å. Odh, J. Ogren, 1991b, *Air Monitoring in the Arctic: 1980-90*, Swedish Environmental Protection Agency, Rapport 3945, 46 pp.

Heintzenberg, J., K. Holmén, S.-Å. Odh, M. Engardt, 1992, *Air Monitoring in the Arctic*, Swedish Environmental Protection Agency, Rapport 4094, 62 pp.

Heintzenberg, J., M. Engardt, K. Holmén, C. Leck, S.-Å. Odh, 1993, *Air Monitoring in the Arctic*, Swedish Environmental Protection Agency, Rapport 4217, 47 pp.

Heintzenberg, J. and C. Leck, 1994, *Seasonal variation of the atmospheric aerosol near the top of the marine boundary layer over Spitsbergen related to the Arctic sulphur cycle*, Tellus, 46 B, 52-67.

Holmén, K., Engardt, M. and Odh, S.-Å. 1995, *The carbon dioxide measurement program at the Department of Meteorology at Stockholm university.* International Meteorological Institute in Stockholm, **Report CM-84,** 38 pp.

Holmén, K., C. Leck, M. Engardt, S.-Å. Odh, 1995, *Air Monitoring in the Arctic 1993*, Swedish Environmental Protection Agency, Report 4404, 27 pp.

Keeling, C. D., T. P. Whorf, M. Wahlen, J. van der Plicht, 1995, *Interannual extremes in the rate of rise of atmospheric carbon dioxide since 1980*, Nature, 375, 666-670.

Langner, J., T. S. Bates, R. J. Charlson, A. D. Clarke, P. A. Durkee, J. Gras, J. Heintzenberg, B. Huebert, C. Leck, J. Lelieveld, J. A. Ogren, J. Prospero, P. K. Quinn, H. Rodhe, A. G. Ryaboshapko, 1993, *The global atmospheric sulfur cycle: an evaluation of model predictions and observations*, Department of Meteorology, Stockholm University, Report CM-81, 28 pp.

Lejenäs, H. and K. Holmén, 1996, *Characteristics of the large-scale circulation during episodes with high and low concentrations of carbon dioxide and air pollutants at an Arctic monitoring site*, Atmospheric Environment,, 30, 3045-3057.

Robertson, L., Langner, J. and Engardt, M. 1996. *MATCH - Meso-scale Atmospheric Transport and Chemistry Model. Basic model description and control experiments with ^{222}Rn.* Swedish Meteorological and Hydrological Institute, **Report RMK-70**, 37pp.

Sarmiento, J., 1993, *Atmospheric CO_2 stalled*, Nature, 365, 697-698.

Overview of our observations for clouds and precipitation and atmospheric minor constituents at Japanese Ny-Ålesund Observatory

Makoto Wada, Gen Hashida, Shinji Morimoto, Shuhji Aoki, Masataka Shiobara and Takashi Yamanouchi
National Institute of Polar Research
9-10, Kaga 1-chome, Itabashi-ku, Tokyo 173 Japan

1. Introduction

Our observations on atmospheric sciences in Ny-Ålesund were started in 1991 at Japanese Ny-Ålesund Observatory, in order to clarify the global atmospheric change in the Arctic. The main house is called "Rabben". The monitoring items of atmospheric components are greenhouse gases including surface ozone, clouds and precipitation. Intensive observations were carried out twice for a few months in winters of 1993/1994 and 1994/1995 for the purpose of studying the interaction of precipitation and aerosols in the atmosphere.

2. Instrumentation

Air is collected once a week using flask for measuring the concentrations of carbon dioxide, methane and carbon 13 isotope ratio of carbon dioxide through the air intake which is mounted on the roof of the house "Rabben". Surface ozone concentration is measured continuously using ultraviolet absorption technique by "Dashibi Ozone Monitor", introducing air from another intake on the roof. Monitoring instruments of clouds and precipitation are a vertically pointing X-band radar and a 37 GHz microwave radiometer. Snowfall/rainfall intensities can be calculated continuously using an experimental equation between radar reflectivity intensity and rainfall rate. Variations of column liquid water can be measured continuously using brightness temperature data of microwave radiometer on the assumption that water vapor amount varies slowly.

3. Observation periods by the monitoring instruments.

No permanent staff has stayed at the Observatory through a year for maintaining the instruments. Most of the air sampling and the minimum maintenance of the instruments, e.g. changing chart and floppy diskette, etc., are supported by the staff of the Norwegian Polar Institute. Figure 1 shows the observation periods in which we have got the data using each instrument. Some started in autumn, 1991 and some in autumn, 1992. Observations of clouds and precipitation were halted from April 1995 to January 1997, because of failure of instruments. Radar observation, however, were started again in February 1997.

4. Results

We summarize the results here which were reported in detail by Yamanouchi et al. (1997) and Wada et al. (1997). Figure 2 shows variations of carbon dioxide, methane and carbon 13 isotope ratio from 1991. Figure 3 shows a variation of surface ozone and Figure 4 shows a variation of precipitation calculated from radar data.

- Large seasonal variation with peak to peak amplitude of about 18 ppmv can be seen and the annual mean of 1994 is 360.6 ppmv in carbon dioxide concentration.
- The amplitude of seasonal variation is more than 100 ppbv and annual average in 1994 is 1828 ppbv in methane concentration.
- The amplitude of seasonal variation is about 1.2 % in carbon 13 isotope ratio of carbon dioxide. The seasonal variations of carbon 13 isotope ratio and carbon dioxide correlate well.
- Surface ozone shows a rough seasonal variation, with high values in March to may and low values in June to July, and a peak to peak seasonal amplitude of about 20 to 25 ppbv. Extremely low values are found during April to May.
- Two remarkable minimum peaks in a year are found in the variation of monthly precipitation. The peaks are January and July.

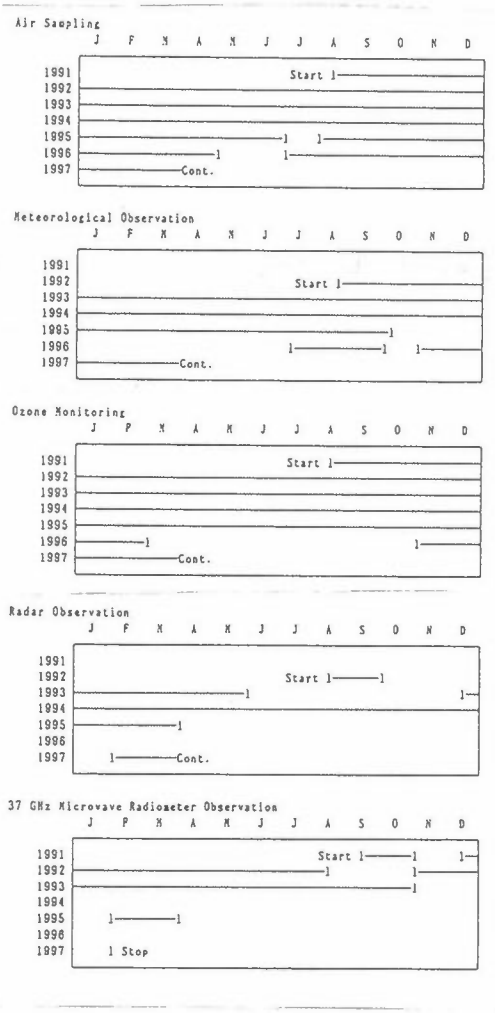

Figure 1: Observation periods in which we have got the data using each instrument. Air sampling, Meteorological observation, Ozone monitoring, Radar observation and microwave radiometer observation (from top to bottom).

5. Future plan

New instruments will be set in Ny-Ålesund in order for the research of aerosol-cloud-radiation studies around coming autumn. The instruments are an aureolemeter, a star photometer, a micropulse lidar and conventional flux radiometers. Aureolemeter is used to acquire spectral optical thickness and size distribution of aerosols from the solar aureole measurements. Micropulse lidar

can acquire long-term data sets of back-scatter profiles of aerosol and clouds. Star photometer can measure spectral attenuation of star light to obtain optical thickness and size distribution of aerosols. Flux radiometers are also used to obtain surface albedo and radiation budget from downward/upward facing pyranometer/pyrgeometer measurements.

A new dual frequency microwave radiometer, a precipitation occurrence sensor system are planed. Dual frequency microwave radiometer can measure column liquid water content in the atmosphere. Precipitation occurrence sensor system can get information of precipitation occurrence, precipitation type and precipitation intensity stronger than 0.01 mm/ hr. A three-color integrating nepelometer, a submicrometer particle sizer, a optical counter, two particle samplers will be prepared. Integrating nephelometer can get total light extinction by aerosols. The particle sizer and the optical counter can measure a particle size distribution in 0.007 to 5 um of aerosols. Aerosols obtained from the particle samplers will be analyzed at the home institutions for aerosol chemistry.

Since some of them are difficult for maintain without person, intensive observations for a few months should be needed. We would like to have observations for comparing with the instruments of other institutions, because some of our new instruments are similar type in their instruments.

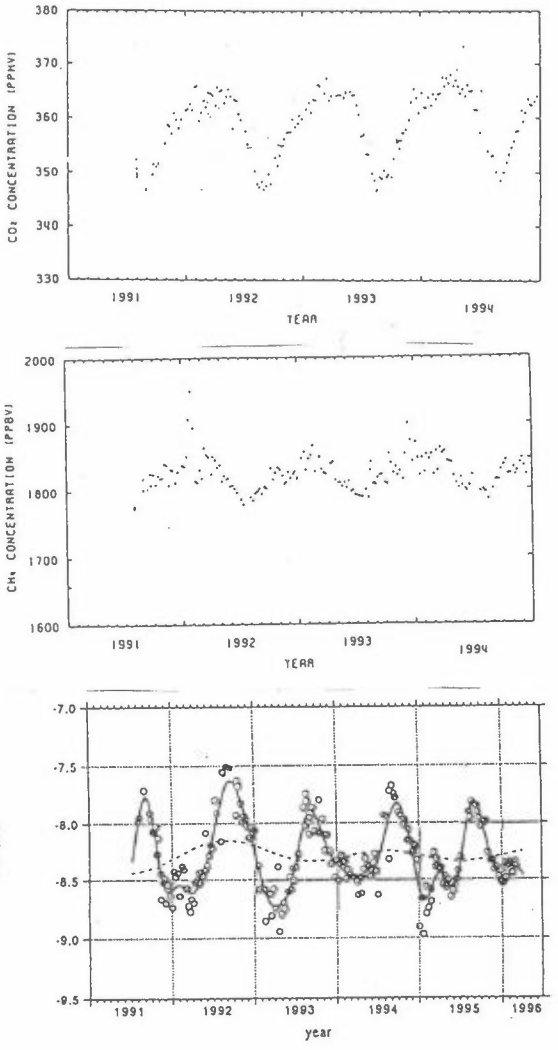

Figure 2: Variation of Carbon dioxide, methane and carbon 13 isotope ratio (from top to bottom).

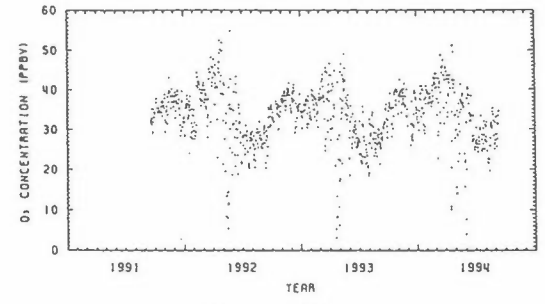

Figure 3: Variation of ozone concentration.

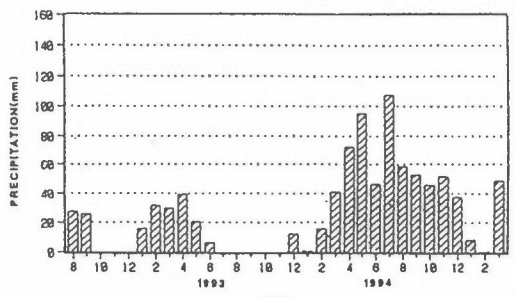

Figure 4: Variation of monthly mean precipitation obtained from radar. The logarithmic amplifier in the radar receiver was changed between February and March 1994.

Acknowledgments

The authors wish to express their sincere thanks to the staff of the Norwegian Polar Institute for their support in the observation. We also have to say to express our sincere thanks to the Norwegian Meteorological Institute and Alfred Wegener Institute for polar and marine research for serving their data.

References

Wada, M., Konishi, H. and Yamanouchi, T., 1997: Variation of monthly precipitation and frequency of radar echo existence at some altitudes in Ny-Ålesund, Svalbard. Mem. Natl. Inst. Polar Res., Spec. Issue, 51, 241-248.

Yamanouchi, T., Aoki, S., Morimoto, S. and Wada, M., 1997: Report on atmospheric science observations at Ny-Ålesund, Svalbard. Mem. Natl. Inst. Polar Res., Spec. Issue, 51, 155-166.

Lidar and Balloon Measurements of Polar Stratospheric Aerosols at Ny-Ålesund

Yasu-Nobu Iwasaka
Solar-Terrestrial Environment Laboratory, Nagoya University

Italian Research in Tropospheric Chemistry at Ny-Ålesund

Ivo Allegrini
CNR - Institute for Atmospheric Pollution, Monterotondo S. (Rome), Italy

Preface

Arctic troposphere is characterised by phenomena which are nowadays under intensive investigation by the scientific community. It includes the so called "Arctic fog", depletion of tropospheric ozone and the formation, especially in springtime, of ozone. In addition, recent observations show that a tropospheric denitrification is occurring during the transfer of air masses from the continent (mid latitudes) to polar regions. Such a loss of nitrogen containing species seems to be a persistent effect in the Arctic. Even though all these phenomena are very peculiar for the Arctic troposphere, their occurrence is clearly related to atmospheric chemistry, related in turn to radicals and ozone chemistry [Niki H. and Becker K.H., 1992]. Thus, the study of such phenomena would be an important step to understand the formation of ozone and other photo oxidants or to understand the processes related to the formation or to the deposition of nitrogen containing compounds in different sites, such as those at middle or low latitudes. The European dimension of these research activities was the main reason for a dedicated research activity in the Arctic by Italian scientific institutions.

Inorganic species

Preliminary measurements in the Arctic (Zeppelin station at Ny-Ålesund) have been carried out with the aim to test instrumentation and methods for the characterisation of relevant compounds in gas phase and in particulate matter. Inorganic species were collected by using a proper combination of diffusion denuders and filter packs [Possanzini M. et al., 1983; Possanzini et al., 1992]. After sampling, the denuders and the filters were extracted with water and analysed according to their ionic content. The technique is very suitable for the collection of acid species such as nitric and nitrous acid, as well as for many other species. Nitrous acid is an extremely important species because it easy photolises to yield OH radicals, thus affecting the chemical properties of polar troposphere. In addition, size distribution measurements were carried out using a multistage impactor [Hillamo R., 1991] for the sampling of aerosols and determining the ionic content by ion chromatography. Since the denuder/filter pack sampling line is also equipped with a cyclone having a nominal cut size of 2.5 μm, data on the large aerosol size region fraction may also be obtained.

Experimental evidences show that nitrites are present in particulate matter as the result of nitrous acid absorption [Li S.-M., 1993; Li S.-M., 1994]. Under particular thermodynamic conditions, such species may be desorbed in gas phase taking place to a variety of reactions in atmosphere. Fine particulate nitrate and nitrite, although detected in the denuder line, were not found in the impactor stages. These is not surprising since losses of fine nitrates were also reported in other sites, thus the denuder measurements ensure good reliability though they are limited in size resolution. In fact, after the cyclone, the filter pack will collect all particulate matter having aerodynamic size below 2.5 μm. Sulphates show a well defined size distribution which appears to be trimodal as shown in Figure 1. The accumulation mode, which was located always around 0.5 μm, comprises 85 to 99 % of total sulphate mass. Most of the sulphate was obviously in the form of sulphuric acid from which gaseous species could be desorbed. In fact it was also observed that sulphur dioxide and nitrous acid also evaporated from particulate matter.

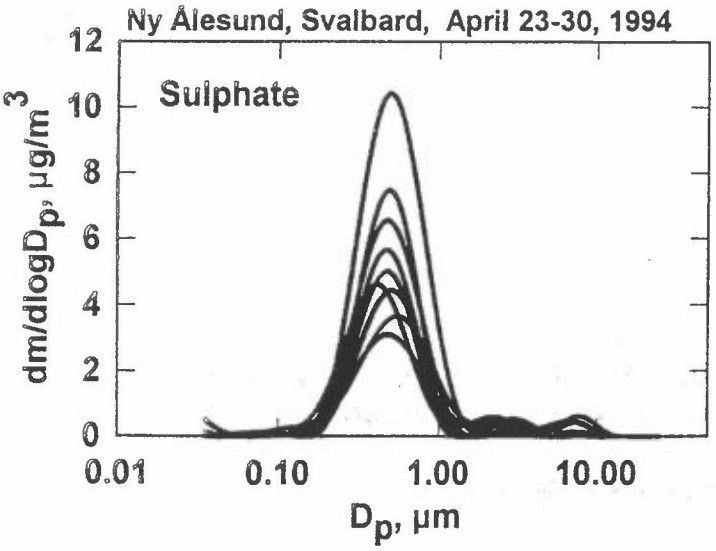

Figure 1: Size distributions of particulate sulphate, Ny-Ålesund.

Data on nitric acid, which are shown in Figure 2, demonstrate that this component can be easily analysed with a reasonable time basis. The observed concentrations are in the order of parts per trillions and it is not clear if they are resulting directly from the oxidation of nitrogen dioxide in gas phase or, from heterogeneous reactions occurring on particulate matter. Also, Figure 2 reports the observed concentrations of nitrous acid in gas phase. This component is present at concentration levels much lower than those of nitric acid. The sources of nitrous acid in gas phase is still unknown, although this species may be formed on surfaces through the heterogeneous reaction of nitrogen dioxide with water, followed by HONO evaporation in the gas phase. The occurrence of these species, as well as its distribution in gas phase or in particulate matter is still largely unknown. Therefore, more measurement have been devised in order to clear the specific problem of nitrous acid.

It is therefore essential that more measurements are carried out in the nitrogen containing compounds field. In fact, future activities, in addition to the continuation of the work done in past, are specifically addressed to the analysis of environmentally significant species related to nitrogen chemistry. The important links between nitrogen species and chlorides make the measurement of HCl and fine and coarse particulate Cl^- essential to fully understand the behaviour of nitric acid, nitrate, ammonia and ammonium in troposphere [Masia P. et al., 1993]. Moreover, as the chemical and/or physical form of the nitrogen species changes, also the nitrogen deposition velocity may be greatly changed. Thus measurements of nitrogen dioxide, PAN and alkyl nitrates are also devised. The recent development of carbon coated denuders [De Santis F. et al., 1996] will be an important step toward these goals. In fact, these denuders ensure the measurements of nitrogen dioxide at concentration levels below 0.01 $\mu g/m^3$. The technique is also very useful for PAN and Alkyl nitrates, even though it is not able to discriminate between the different organic nitrated species.

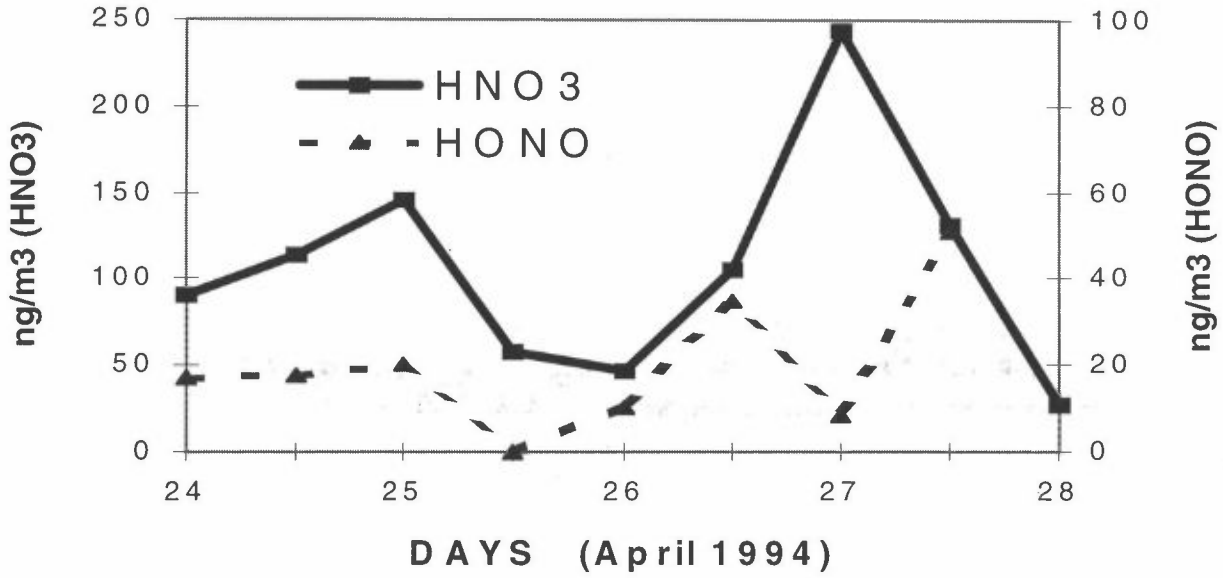

Figure 2: Typical measurements of Nitric and Nitrous Acid in gas phase, Ny-Ålesund.

As far as sulphur chemistry is concerned, research is planned in order to continue the measurements on the aerosol size distribution to elucidate the mechanism of interaction between nitrogen compounds and acidic particulate matter, as well as the reactivity of sulphur dioxide on particulate matter in either fine and coarse fractions.

Organic species

Data collected in the Arctic region [Penkett, 1993] have clearly shown a seasonal trend in the concentration of man-made organic compounds present in the troposphere. Trends which were recorded, showed high concentrations during winter season, while low levels are typical of summertime. This is due to the photochemical activity which is easily to occur in summer when ozone and hydroxyradicals are able to degrade organic compounds. In addition, experimental evidences shows [Lindskog, 1997] that a relatively small south-north gradient for volatile organic compounds (VOC) is observed. This suggests that accumulation of pollutants in the Northern regions are easily to occur and that, at sunrise, a noticeable amount of ozone is expected.

These speculations are based on the assumption that the main source of VOC in polar regions is transport from areas where man-made emissions are significant. Recent observations in Antarctica and at the Svalbard Islands, carried out by the Institute, showed the presence of compounds for which a clear origin cannot be assessed. The presence in air of oxygenated components [Ciccioli et al., 1996] have been explained by the possible presence of biogenic sources, clearly very active during polar summertime. In particular, it was postulated that emissions of semi-volatile carbonyls and aldehydes can take place from biogenic sources. The high concentrations which were observed might be due, rather than to the source strength, to the poor atmospheric mixing. However, it is possible that a major role in ozone formation can be played by biogenically oxygenated components. This is the reason why the systematic study of such components in polar regions and the assessment of the different sources is considered very important.

The experimental plan will include a novel micro-meteorological technique (Conditional sampling based on trap enrichment-relaxed-eddy accumulation, TREA) which was exploited and successfully used for the measurement of emissions of monoterpene from Mediterranean vegetation.

Other activities related to organic components include the measurement of source strength of DMS (Dimethyl sulphide) as a source of condensation nuclei and, as source of sulphur components which will be evaluated by means of denuders.

References

Ciccioli P., Cecinato A., Brancaleoni E., Frattoni M., Bruner F. and Maione M., (1996) Occurrence of oxygenated volatile organic compounds (VOC) in Antartica. Intern. J. Environ. Anal. Chem., 62, 245-253.

De Santis F., Allegrini I., Di Filippo P. and Pasella D. (1996) Simultaneous determination of nitrogen dioxide and peroxyacetil nitrate in ambient atmosphere by carbon-coated annular diffusion denuder. Atm. Envir., 30, pp. 2637-2645.

Hillamo R.E. and Kauppinen E.I. (1991) On the performance of the Berner low pressure impactor. Aerosol Science and Technology, 14, 33-47.

Li S.-M. (1993) Particulate and snow nitrite in the spring Arctic troposphere. Atmos. Environ., 27(A), 2959-2967.

Li S.-M. (1994) Equilibrium of particle nitrite with gas phase HONO: Tropospheric measurements in the high Arctic during polar sunrise. J. Geoph. Res., 99, 25;469-25;478.

Lindskog A., (1997) The influence of the biosphere on the budget of VOC: Ethane, propane, n-butane and i-butane. "*Biogenic Volatile Compounds in the Atmosphere*" Edited by G. Helas, J. Slanina and R. Steinbrecher. SPB Academic Publishing Bv, Amsterdam, The Netherlands, pp. 45-52.

Masia P., Allegrini I., Possanzini M. and Angelici L. (1993) Measurement of HCl, HNO3 and their Ammonium Salts for the Study of Atmospheric Acid Deposition. Proceedings of the Sixth European Symposium, Physico-chemical behaviour of atmospheric pollutants, Varese 18-22 October, pp. 699 - 705.

Niki H. and Becker K.H. (1992) "*The tropospheric chemistry of ozone in the Polar Regions*". NATO ASI Series, Series 1: Global Environmental Change, Vol. 7, Springer-Verlag, Heidelberg.

Penkett S.A., (1992) Measurements of hydrocarbons in polar marittime air masses. "*The tropospheric chemistry of ozone in the Polar Regions*" Edited by H. Niki and K.H. Becher, NATO ASI Series, Series 1: Global Environmental Change, Vol. 7, Springer-Verlag, Heidelberg, pp. 131-153.

Possanzini P., Di Palo V. and Masia P. (1992) Evaluation of a denuder method for ambient NO_2 measurements at ppb levels. Intern. J. Anal. Chem., 49, 139-147.

Possanzini P., Febo A. and Liberti A. (1983) New design of a high-performance denuder for the sampling of atmospheric pollutants. Atmospheric Environment, 17, 2605-2610.

Abstract to the Scientific Seminar "Atmospheric Research in Ny-Ålesund" at NILU, Norway, April 9-11, 1997

Overview of Research Activities performed by the Norwegian Polar Institute in Ny-Ålesund within Atmospheric Sciences

by
Jon Børre Ørbæk
Norwegian Polar Institute, P.Box 5072 Majorstua, 0301 Oslo

Introduction

The Norwegian Polar Institute was established in Ny-Ålesund in 1968 when the European Space Research Organization (ESRO) opened its satellite telemetry station in Ny-Ålesund. Regular meteorological observations started at the ESRO station in 1969. After the ESRO-activity closed down in 1974, the small NP research station (2 engineers) continued together with 3-4 maintenance people form KBKC, and a permanent surface radiation station was established at the station. The meteorological station was moved to the present locality downtown. Ionospheric research connected to optical observation of the Aurora as well as measurements of the earth magnetic field and ELV/VLF-emissions were among the first research activities to be supported at the station, and is still an important part of the atmospheric research activities there. The station moved into new localities in 1982. In 1990, an atmospheric monitoring station on the Zeppelin mountain was constructed, for the purpose of long term monitoring of greenhouse gases and transport of pollutants.
The NP research station serve as an observatory for long and short term variations in the physical and biotic environment, as well as a field station for visiting scientists. The station hosts a large number of different research projects and operates as Auroral Observatory, Radiation observatory, Meteorological observatory, and Air-monitoring Observatory.

Monitoring of the Surface Radiation Budget

Surface radiation budget (SRB) measurements have been performed by NP on a permanent basis in Ny-Ålesund during the past 20 years since 1974. The main objective of the activity is the continuation of a long term environmental monitoring program for the investigation of the long and short term variations in the Arctic radiation climate as related to different atmospherical, glaciological and oceanographical factors. The activity is a basis for multidisciplinary programs studying the interaction between the changing environmental conditions and Arctic ecosystems, as well as giving the possibility to detect global change signals as early as possible, for the purpose of giving the environmental management high quality scientific information as basis for their decisions. GCM-models show that the Arctic is very sensitive to climate perturbations, and that radiation processes and feedback mechanisms are very important for the Arctic climate and energy balance. The radiation and energy budget parameters may therefore be used as diagnostics for possible climate warming in the Arctic.

The measurements of solar shortwave and atmospheric longwave radiation is performed on the roof platform of NP, on the tundra and on the Zeppelin mountain. Measurements include:

- Global
- Diffuse
- Direct
- Reflected shortwave radiation
- Albedo
- UV
- UVB
- Longwave downward
- Longwave upward radiation

Calibrations are performed on site with the sun as a source and a self-calibrating absolute cavity pyrheliometer (AHF) tracable to the WWR. The data-acquisition is Pc-based with Internet connection for routine transfer of data.

Since 1994 the surface radiation budget measurements are performed within the framework of the BSRN-network (Baseline Surface Radiation Network) in co-operation with AWI. The main objective of this activity is to evaluate high quality, high time resolution SRB-data, in order to provide data for calibration of satellite-based estimates of the surface radiation fluxes, as well as to provide data for validation of the model flux computation.

Spectral Reflective Characteristics of Snow and Sea Ice

This project investigates the radiative characteristics of arctic sea ice and snow, i.e. how shortwave radiation is reflected at the snow/sea ice surface, how it penetrates through the snow and ice, and how it is absorbed in the tundra below or in the upper parts of the under ice water masses. This involves the studies of albedo variations on different types of snow, sea ice, melt ponds, etc..

The overall objective of the project is to study the variability of the spectral characteristics of snow and sea ice with the use of advanced spectroradiometers, in order to determine the amount of solar radiation that is available for biological production. The field studies will be carried out in three different types of areas, i) terrestric - snow covered ground on the Brøggerhalvøya peninsula close to Ny-Ålesund, ii) coastal - sea ice on the Kongsfjorden close to Ny-Ålesund and iii) marine - sea ice in the Barents sea.

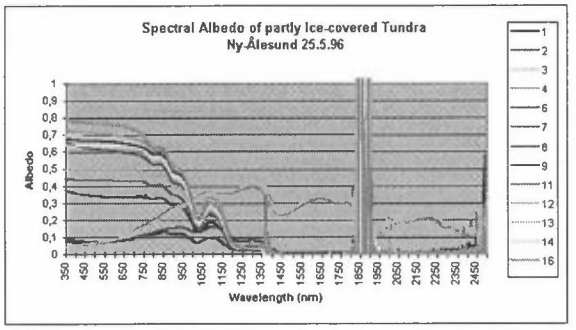

Fig. 1: Plot of the spectral reflectance of partly snow and ice-covered tundra, illustrating the large difference in reflecting properties within small spatial areas. Ny-Ålesund 1996

During the melting season, large changes in reflective characteristics take place both in snow and sea ice, due to the formation of liquid water, crystal growth, thinning of the snow/ice cover, development of melt ponds and changes in surface albedo. The amount of radiation that penetrates through the snow and sea ice varies considerably within a few weeks in the spring and is an important parameter determining the onset of biological production, both terrestrial and marine. Figure 1 illustrates the large difference in surface reflectance properties within small spatial areas in the melting period, especially the transition from vegetated ground to snow/ice-cover. The project studies the optical and physical properties of Arctic sea ice and snow and their variability in the melting season, i.e. during May to July.

The following investigations are important for the overall goal:

- To determine the variation of spectral surface albedo at different types of snow and sea ice at the arctic tundra, in arctic fjords and in the arctic ocean.
- To determine the natural variation of spectral solar radiation under snow and sea ice, i.e. under the snow cover on the tundra and within the upper layer of the water beneath the ice.
- To determine the physical factors responsible for the spectral attenuation of shortwave radiation in snow and sea ice.
- To determine the physical parameters controlling the spectral attenuation of shortwave radiation in arctic water columns.
- To investigate the natural variability of relevant meteorological, oceanographical and sea ice data controlling the amount of radiation at the surface, radiation that penetrates through the ice, and finally into the water masses below

- To investigate the climatology of extreme meteorological, oceanographical and sea ice-related events, influencing the conditions for biological production.

Monitoring of Broadband and Spectral UV-radiation

This activity supports the increased interest from the international society to quantify the changing UV-environment in the Arctic and to assess the effects of possible increased levels of UV/UVB-radiation on DNA and biological ecosystems as a result of antropogenic ozone-depletion. Broadband measurements of solar UV-radiation (Eppley TUVR 295-385 nm) has been performed in Ny-Ålesund since 1981 by NP (Hisdal et al., 1992). Broadband UVB measurements have been performed since 1992 by means of RB-meters (Solar Light Company model SL501), measuring biologically effective UV-doses by simulating the McKinley-Diffey Erythema Action Spectrum (CIE). A high resolution UV-spectroradiometer type Bentham DM150 will come into operation in Ny-Ålesund during 1997. The current measurement program includes the following instruments:

- Bentham DM150 UV-spectroradiometer measuring high res. UV-spectra from 200-600nm.
- Solar Light Company SL501 UV-Biometers measuring Erythemal UV-doses
- Eppley TUVR UV-radiometers measuring broadband UVB+UVA.
- Licor 1800UW Underwater spectroradiometer measuring low res. spectra at 300-800 nm.

The main objective of the activities is the investigation of the natural intensity and variability of arctic UV-radiation and biological effective UV-doses at different time-scales, including surface and underwater measurements and use of radiation transfer modelling. The geophysical measurements support biological effect studies on marine, terrestrial and freshwater ecosystems. This includes the following goals:

- The determination of the daily and seasonal surface UV/UVB-climatology by means of spectral and broadband measurements in Ny-Ålesund,
- The determination of the physical parameters controlling the attenuation of UV/UVB-radiation in arctic water columns,
- Provide high time resolution biological effective UV-doses for a variety of action spectra such as Erythema Dose rates, DNA-effective radiation, etc., on different timescales and at different sites around Ny-Ålesund,
- The evaluation of the relative intensity of biological effective UV-doses to other parts of the radiation spectrum, such as UVB/UVA, UVB/PAR, etc.., in support to the biological effect studies on terrestrial, marine and freshwater ecosystems.
- Investigation of the influence of atmospheric ozone, clouds and albedo on the spectral distribution of the surface UV radiation in the Arctic, as well as the relation between the surface UVB-radiation and short- and longwave radiation and meteorological parameters such as humidity and temperature,

NP now runs side by side at the research station in Ny-Ålesund the UV-spectroradiometer, a DOBSON-spectrophotometer (for Univ. of Oslo), a broadband UV-Biometer and a multichannel UV filter instrument (for NILU). This extensive instrument park gives very good opportunities for quality check and to meet the different biological and geophysical needs.

Passive Broadband Infrasonic Sodar in Ny-Ålesund

The Passive Broadband Infrasonic Sodar (PBIS) system estimates the directionality of the local atmospheric low-frequency noise field by performing frequency/phase analysis of the acoustical wavefield, as measured in space by a right angled three-partite array of infrasound microphones. By estimating the direction-of-arrival (DOA) of possible coherent

acoustical signals, the system performs a passive acoustical remote sensing of distant infrasonic noise-generators.

Some part of the measured wavefield may have been generated by sources several 100 km away, as for example weather fronts. During periods of low local wind induced turbulence noise, these sources may be detectable by the PBIS system. Since it is likely that Polar Lows generate strong infrasound, the objective of this project is to detect low frequency signatures from Polar Lows in the Norwegian, Greenland and Barents Seas.

The PBIS system consists of three infrasound microphones placed in the corners of a right angled triangle array, protected from local turbulence noise by "bird-cages" filled with polyetylen foam, as well as by perforated aluminium wind-shields. The system performs 3 channel FFT-analysis and Phase discrimination for the evaluation of DOA-spectra. Statistically averaged DOA-spectra are stored on the local PC with Internet connection for routine transfer of data.

Other atmospheric research and monitoring programs supported by NP in Ny-Ålesund

Standard meteorological observations has been performed on a regular basis in Ny-Ålesund since 1969. The station was moved to the current position in 1974. Up till now the synop-observations have been performed 3 times a day. However, the manual observations are now complemented by a new automatic weather station, generating regular 3 hour synop during the whole day. This will to a large extent improve the conditions for getting basic environmental data for the different research campaigns in Ny-Ålesund

Total ozone is monitored with Dobson spectrophotometer nb. 8, belonging to the Univ. of Oslo, and is operated once a day by the station engineers for the careful measurements of total ozone conditions. The instrument is operated from the roof of the NP station and stored in a temperature stabilised room between the measurements.

NP owns and operates the reference station for atmospheric air-research at mount Zeppelin. The major part of the scientific programs there are run by NILU and is connected to the monitoring of greenhouse gases and long range transport of pollutants. The NILU activities downtown also include UV-filter and -spectral measurements.

NP also give engineering and observational support to the research campaigns within ionospheric and auroral researh, including optical observations of the aurora, observation of the earth magnetic field, ionospheric absorption, etc..

Conclusions

As central institution for scientific and environmental investigations in the Arctic and Antarctic, NP gives important scientific input and recommendations to the environmental management for the polar areas. The atmospheric research at NP therefore aims at improving our abilities to detect climate change signals as early as possible, for the purpose of giving the environmental management high quality scientific information as basis for their decisions. The research is mainly directed towards multidisciplinary programs studying the interaction between changing environmental conditions and Arctic ecosystems, or is related to other geophysical fields such as glaciology and hydrology through the climatically important surface radiation processes.

NP also function as a service institution in Ny-Ålesund for other Norwegian research institutions and foreign collaborators, and operates and maintain a number of atmospheric research programs on longer and shorter time-scales.

Aurora, Ozone, and Dust: Atmospheric Research on Svalbard by UNIS

Birgit Heese, Ove Havnes[1], Jøran Moen

The University courses on Svalbard, Longyearbyen, Norway.
[1] also at IMR, University of Tromsø, Norway.

Abstract - Investigations in atmospheric research by UNIS has so far been in the field of northern lights, which has a tradition on Svalbard, and in ozone and trace gas measurements during polar night using starlight, which has been implemented during winter 1996/97. A new project is planned to start in autumn 1997 is the investigation of subvisual dust at the mesopause by small, cheap rockets launched from Ny-Ålesund.

The University Courses on Svalbard

The University Courses on Svalbard (UNIS) is a private foundation established by the Norwegian government and owned by Norway's four universities. The objecive of the foundation is to offer university-level courses and to perform research relevant to Svalbard's geographical location in the high arctic. This location gives the archipelago a number of advantages as a laboratory and arena for observations and for gathering and analysing data. The courses are intended to complement the teaching given by the mainland universities, and they form part of standard courses of study that lead to examinations and degrees at intermediate, advanced and doctoral level. UNIS is located in Longyearbyen. It came into operation in autumn 1993, when its first 23 students started courses in Arctic Geology and Arctic Geophysics. In autumn 1994, the range of subjects offered were expanded to include Arctic Biology, and a total of 33 students were admitted. The Arctic Technology program was initially introduced in the autumn of 1996. UNIS reached its intended size of some 100 students and about 35 different courses during 1996. The study programs will gradually be given an international profile, and up to half of our students will be recruited from abroad. The instruction will therefore be in English. In the longer term, UNIS will form the core of the Svalbard Science Centre (SSC), an international Arctic centre of expertise in research and education on Svalbard, which will also incorporate a large number of professional and scientific institutions on the archipelago.

Auroral Dynamics and Plasma Convection in the Polar Ionosphere

The dayside boundary layers at the solar wind-magnetosphere interface are key areas of research on electrodynamic processes of magnetized, collision-free plasma. Solar wind-magnetosphere coupling mechanisms such as reconnection of solar and terrestrial magnetic field lines represent great challenges to experimental as well as theoretical plasma physics at present.

The ionospheric signatures of magnetospheric boundary layer mechanisms are essential for understandig solar wind-magnetosphere-ionosphere-interactions. Ground-based remote sensing of the ionosphere provides a necessary supplement to satellite/rocket in-situ observations. The spatial and temporal evolution of solar wind-magnetospheric

coupling events can be studied by continuous ground-based observations when the ionospheric signatures have been identified.

Svalbard is one of the most suitable sites for remote sensing of plasma processes in the dayside magnetospheric boundary layers. Two of the most relevant parameters in this connection are optical aurora and ionospheric plasma convection since they are most sensitive to the transfer of plasma and momentum from the solar wind. Different aspects of the polar cusp/cleft aurora have been studied by the Universities of Oslo and Tromsø over the last 15 years based on winter-campaigns in Longyearbyen and Ny-Ålesund, and UNIS were immediately after its birth in 1993 incorporated in the Norwegian cusp programme on Svalbard.

UNIS is actively taking part in the daily run and the upkeep of instruments at Nordlysstasjonen (The Auroral Station) in Adventdalen. The station serves as a platform for both research and teaching activities. UNIS is responsible for the Internet connection and for the facilitation of a PC-network to drain data from the individual instrument PC to the www-server. Quick-looks of assembled data from a selection of instruments are available on the internet address: http://haldde.unis.no.

During the 1997/98 polar winter UNIS will be participate in providing ground-based optical and EISCAT support to three rocket campaigns. In November/December 2 cusp rockets, HUGIN and MUNIN, are scheduled from Ny-Ålesund, and in January 1997 the CAPER rocket (Cleft Accelerated Plasma Experiment Rocket) will be launched from Andøya.

Ozone, NO_2, and OClO measurements by a Star-pointing Spectrometer

During polar night, spectroscopic measurements of ozone and other relevant trace gases involved in heterogeneous ozone chemistry could only be taken using the moon as a light source during relativly short periods each month. The coupling of a telecope to a spectrometer allows the use of stars for this purpose, which provide a light source available every clear day. Such a system has been set up on Svalbard in Adventdalen near Longyearbyen in winter 1996/97. Similar systems have earlier been used by *Roscoe* et al. (1994) and *Oikarinen* et al. (1996) in northern Sweden and Finland and another is under operation at Halley Bay Station in Anarctica (*Roscoe* et al., *1996*).

The system on Svalbard consists of a spectrometer, a Czerny-Turner type with a focal length of 275 mm, coupled to a Schmidt-Cassegrain telescope with a primary mirror diameter of 356 mm (Celestron C14) by an optical fiber bundle. The single fibers have a diameter of 200 μm and they are arranged with distinct distances from each other. The star is focussed on the central fiber. Thus, a two dimensional CCD-detector array allows the detection of the spectrum of the star itselv and the surrounding sky-background separately. This background could interfere with the spectrum of the star in case of Aurora. The wavelength range at which the spectrometer was operated this winter lies between 340 nm and 490 nm, allowing the detection of ozone, NO_2 and OClO.
The star choosen for this purpose has to be a hot star with sufficient intensity in the blue and near ultraviolett spectral region. This is providet by Vega, the brightest star in the northpolar sky. Spectra have been taken during several nights in February 1997, while Vega could be observed throughout almost its whole declination range from the lowest elevation angel of 27° in the evening and its highest elevation of 50.6° in the morning, when weather conditions allowed.

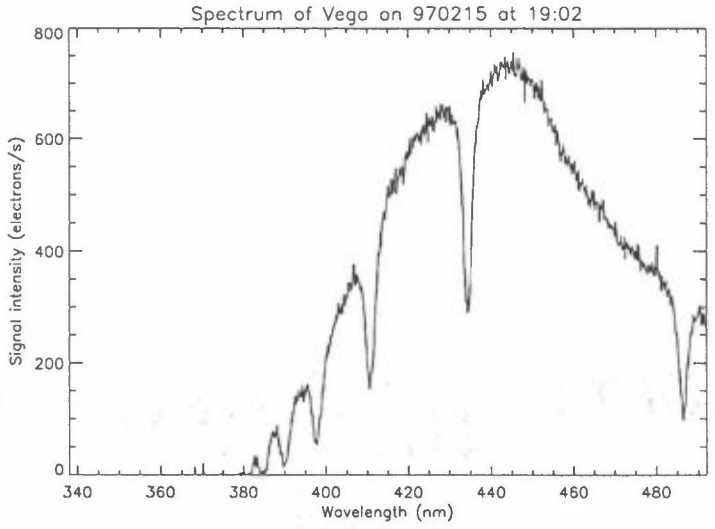

Figure 1: A spectrum of Vega integrated over 10 min taken on February, 15, 1997 at an elevation angle of 27. 2°.

Figure 1 shows a typical spectrum of Vega taken on February, 15, 1997. The Balmer lines in the spectrum of the star, origin from its atmosphere, are clearly visible and allow an independent wavelength calibration for each spectrum. Thus, the instrument is less sensitive to temperatures changes of its surroundings.

All spectra measured with a CCD sensor will be affected by the different sensitivities of the CCD-pixels. To measure this interpixel variabilty, the smooth spectrum of a tungsten lamp has been measured. The spectrum in Figure 1 has not been corrected for interpixel variability.
The spectra are intendet to be analysed by DOAS algorithm. Briefly, the ratio of two spectra of the same star at different elevation angles leads to a differential spectrum, containing the absorption features due to the constituents in the Earth atmosphere. This spectrum will be fittet to differential laboratory spectra giving the difference in the amounts of the trace gases between the two slant pathes of both measurements. The vertical amount of the trace gases is deduced from the angles at the different measurements.

In winter 1997/98 the instrument is planned to be placed on top of the Plateau-Mountain near the Longyearbyen airport in 500 m altitude. This location is shieldet against light from the town of Longyearbyen and strong winds and haze, which occur often in the valleys, can be avoidet. Additionally a better horizon is achieved which allows the use of stars with low elevations close to the horizon to observe a larger air mass than by using Vega.

Investigations of the polar middle atmosphere by miniturized rocket payloads

In the middle atmosphere above about 40 km one can only obtain in situ observations by the use of rockets. Recent observations of strange phenomena near the mesopause has increased the interest for both remote and in situ observations. These strange phenomena include the noctilucent clouds (NLC) and recently observed large quantities of subvisual dust, abnormally strong radar echoes (PMSE) from the NLC regions, layering of increased abundance of several elements such as Na (Sudden Sodium layers) and metals (sporadic

E-layers), and large "bite outs" and "bulges" of decreased and increased electron and ion densities (*Thomas, 1991*). It also appears that the strength and occurance rate of NLC has increased by a factor of about 10 since they were first observed in 1883. This, together with a decrease of the average temperature near the mesopause of about 0.5 K per year during at least the last 30 years (*Golitsyn* et al., *1996*) make it relevant to poise the question if we in the middle atmosphere see clear indications of climatic changes. We have developed a miniturized payload for a standard passive single stage high G (150 G) rocket. The payload contains four scientific probes, full housekeeping and telemetry. The rocket and payload (MINIDUSTY) has a total weight of only 47 kg as compared to the usual large instrumented rockets with a total weight from 1100 kg and upwards. The instrumentation of the present MINIDUSTY is one ion and one electron probe on booms and a dust probe which measures direct impacts of dust and possible secondary plasma production during impacts. It will be used to study plasma and dust conditions in the mesosphere simultaneously with the EISCAT radar. Simultaneous measurements with other groud-based instrumentation such as Lidars and optical cameras and photometers are also of interest. The EISCAT radar samples a limited number of parameters over long times and large volumes, with a height resolution of about 100 m. MINIDUSTY is able to examine the small scale structures and processes down to 0.5 m and less but only for the duration of the flight. We have an ongoing program for reducing the size of electronics and probes and for building other types of instruments for the small payload both to increase the number of simultaneous scientific measurements and also to have a set of probes which can be changed according to needs. We are considering photometers, impact counters, temperature measurements and trace gas detectors. Due to the drastically reduced price and weight of the new rocket system many new possibilities opens up for pioneer investigations of the polar middle atmospheres. Our first aim is to launch from the high polar latitude of Ny-Ålesund since these typical polar phenomena has not been studied north of 70° latitude yet.

References

Golitsyn, G.S., A.I. Semenov, N.N. Shefov, I.M. Fishkova, E.V. Lysenko, S.P. Perov, Long-term tremperature trends on the upper atmosphere, *Geophys. Res. Lett.*, **23**, 1741, 1996.

Oikarinen, L., H. Saari, K. Rainio, J. Graeffe, and H. Astola, Star-pointing spectrometer for measurements of atmospheric ozone, *Proc. SPIE*, Denver, 1996.

Roscoe, H.K., R.A. Freshwater, R. Wolfenden, R.L. Jones, D.J. Fish, J.E. Harries, A.M. South, and D.J. Oldham, Using stars for remote sensing of the Earth's stratosphere, *Appl. optics*, **33**, 7126, 1994.

Roscoe, H.K., W.H. Taylor, J.D. Evans, A.M. Tait, R.A. Freshwater,D.J. Fish, E.K. Strong, and R.L. Jones, An automated ground-based star-pointing UV-Visible spectrometer for stratospheric measurements, *Appl. optics*, 1996.

Thomas, G.R., Mesospheric clouds and the physics of the mesopause region, *Rev. Geophysics*, **29**, 553, 1991.

UV and Ozone Measurements with Multi Channel Filter Instrument at Ny-Ålesund

Arne Dahlback, NILU

The national UV monitoring network in Norway was established in 1995. The network consist of 8 multi channel filter instruments from Southern Norway (58N) to Ny-Ålesund (79N). The instruments (GUV-511) measure irradiances in five UV channels with centre wavelengths at 305 nm, 313 nm, 320 nm, 340 nm and 380 nm all with bandwidths around 10 nm. The instruments are temperature stabilised at 40C and the time resolution is 1 minute. The data are transferred to a central data base daily via internet. One of these instruments is carefully maintained and frequently calibrated. Once a year this reference instrument is sent around to all sites and possible instrumental drift may be determined.

The most important factors controlling the variability of solar UV-B-radiation at the surface are solar elevation, clouds, total ozone abundance and surface albedo. Thus, the variability in UV dose rate at noon measured with a GUV instrument at Ny-Ålesund in 1996 shown in Figure 1 are a result of variability of all these factors. To detect trends in solar UV-B radiation that are due to trends in total ozone, an UV monitoring network should measure UV radiation, total ozone, cloud- and albedo effects.

It has been shown (1) that by using radiative transfer calculations combined with measured irradiances from the instruments biologically weighted UV dose rates, cloud effects and total ozone abundance can be accurately derived. By using the derived cloud effect and the total ozone abundance as input to a multiple scattering radiative transfer model (2,3) a complete spectrum from 290 nm to 400 nm with 1 nm resolution can be reconstructed. These spectra can be applied to a variety of action spectra to predict any biological effect.

Figure 2 shows total ozone derived from the GUV instruments at Ny-Ålesund compared with AD direct sun measurements from Dobson instrument #8 in 1996. A similar comparison for a two year period in Oslo showed a average difference in derived ozone between GUV and Dobson < 1% with standard deviation 1.9%.

References

1 Dahlback, A. (1996), Measurements of biologically effective UV doses, total ozone abundances and cloud effects with multi-channel moderate bandwidth filter instruments. Appl. Opt. 35, 6514-6521.

2. Stamnes, K., Tsay S.-C., Wiscombe, W. and Jayaweera, K. (1988) Numerically stable algorithm for discrete-ordinate-method radiative transfer in multiple scattering and emitting layered media, Appl. Opt. 27, 2502-2509.

3. Dahlback, A., and Stamnes, K. (1991). A new spherical model for computing the radiation field available for photolysis and heating at twilight, Planet. Space Sci, 39, 671-683.

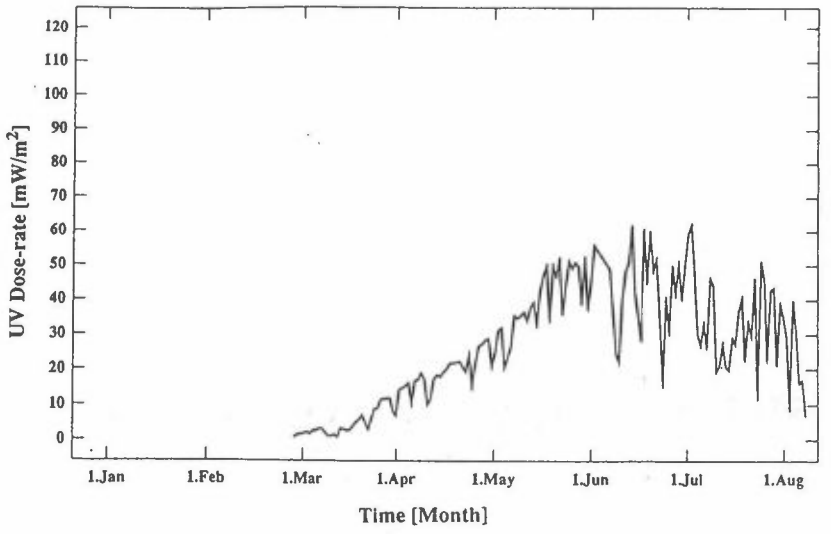

Figure 1: CIE weighted UV dose rates at solar noon measured with a GUV instruments at Ny-Ålesund in 1996.

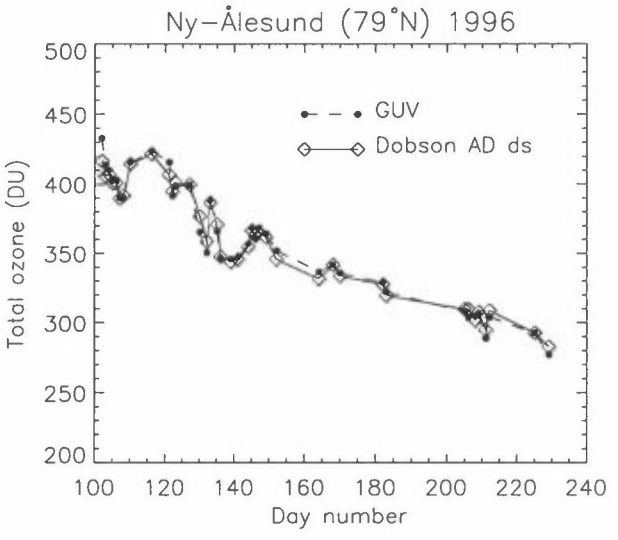

Figure 2: Total ozone abundance can be accurately derived from UV irradiance measurements with a GUV-instruments. Total ozone derived from GUV are compared with ozone derived from Dobson AD direct sun measurements at Ny-Ålesund in 1996.

Bipolar Intercomparison of Surface Radiation Fluxes

Gert König-Langlo, Andreas Herber

AWI

Measurements

Since 1992 the Alfred-Wegener-Institute has made radiation measurements in the Antarctic (Neumayer, $70^0$39'S, $8^0$15'W) and together with the NORSK POLARINSTITUTT in the Arctic (Koldewey, Ny Ålesund, $78^0$56'N, $11^0$56'E).

The radiation measurements are taken along with co-located surface and upper-air meteorological observations in the framework of the international "Baseline Surface Radiation Network" (BSRN). The uniform and consistent measurements thoughout the network are centrally archived in the World Radiation Monitoring Centre and used:

1. to monitor the background short-wave and long-wave radiative components and their changes with the best methods currently available,
2. to provide data for the calibration of satellite-based estimates of the surface radiative fluxes, and
3. to produce high-quality observational data to be used for validating the theoretical computation of radiative fluxes by models

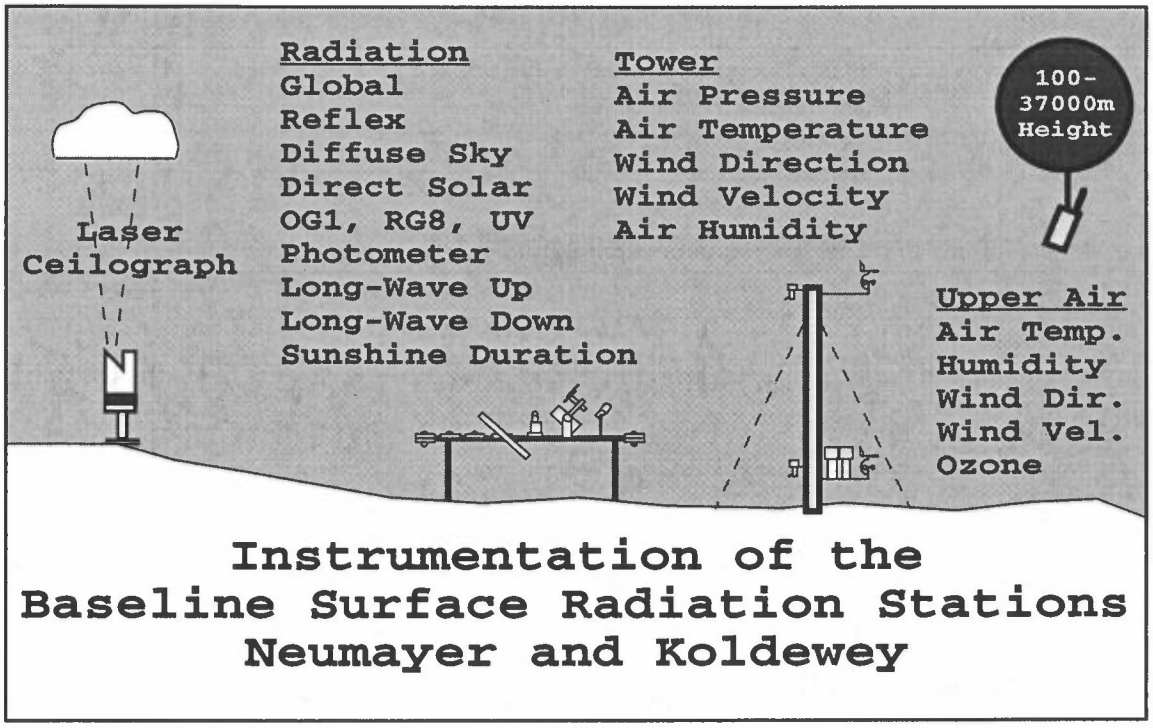

Annual Variation of the Surface Radiation Balance

Whilst at Neumayer the surface is covered by snow continuously, Koldewey is snow-free from about midsummer to early winter.While the Earth's surface is covered by snow, the downward and upward radiation fluxes compensate each other to a remarkable extent, which results in rather small net surface radiation balances in the Arctic and Antarctic. During snow free periods at Koldewey, all balance components increase drastically.

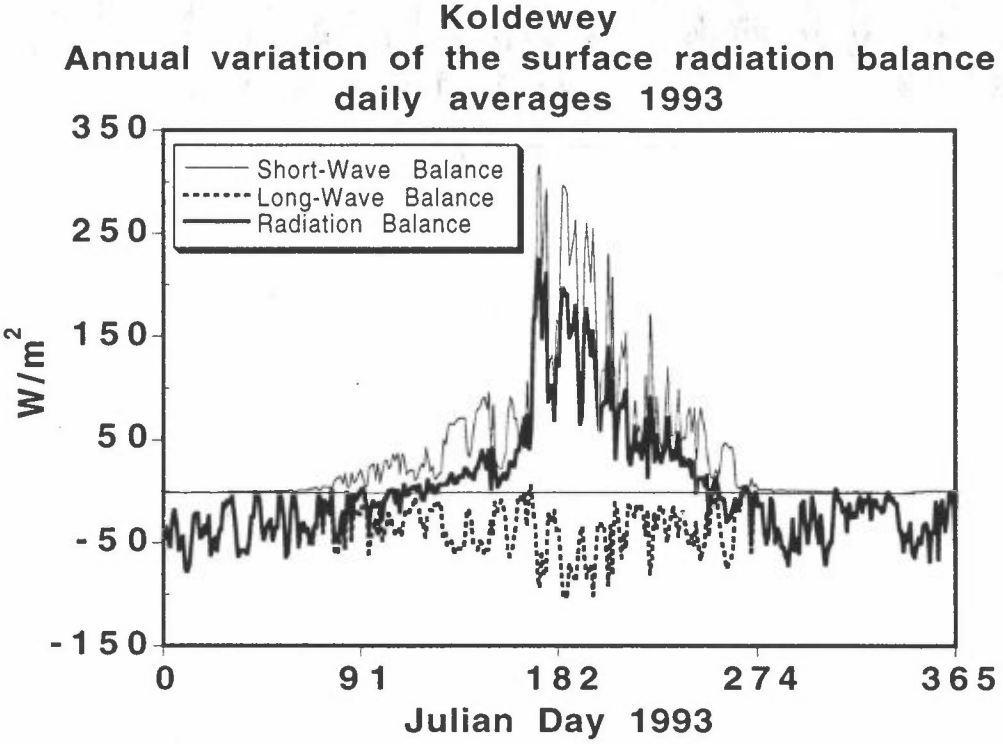

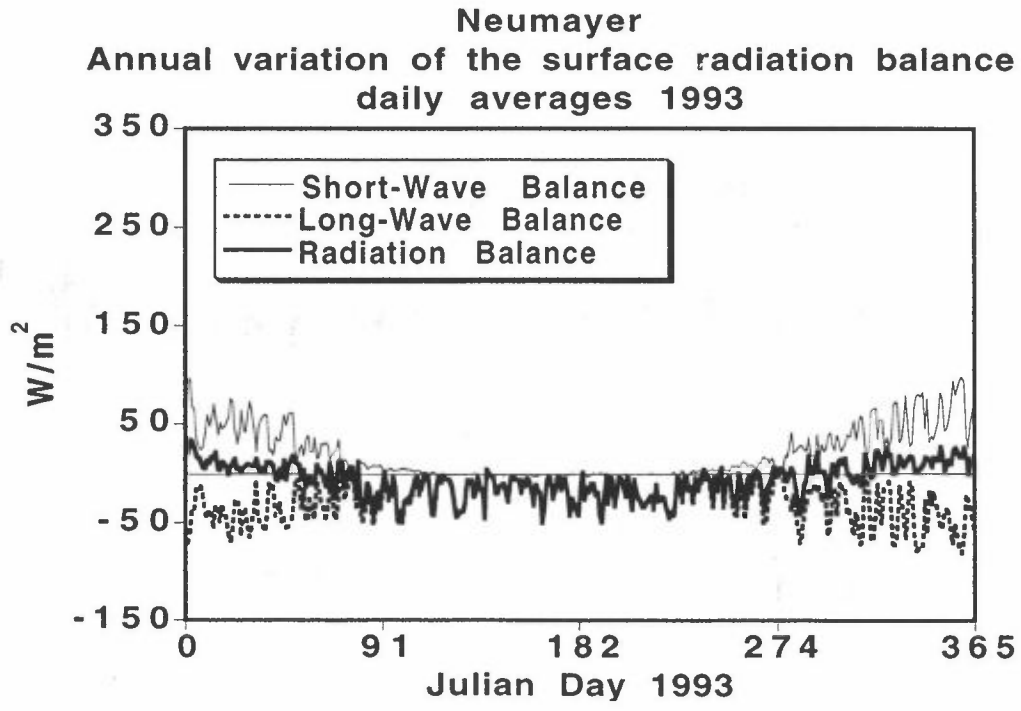

Cloud Coverages and Sunshine Duration

The relative sunshine duration (ratio between measured and astronomically-possible, daily sunshine duration) provides a reasonable measure of daylight cloud coverages.

At Neumayer, the relative sunshine duration is rather constant throughout the year. The relative global radiation can be described reasonably as a linear function of the relative sunshine duration. At Koldewey, the relative sunshine duration reaches maxima values during spring. Significant less clear sky cases exist during summer and autumn. The increasing amount of opaque clouds at Koldewey during summer and autumn and the decreasing albedo are responsible for the decreasing relative global radiation in the second half of the year.

Global Radiation

Due to multireflection between the Earth's surface and the cloud base, the surface albedo controls the impact of clouds on the global radiation. At Neumayer, where the daily averaged albedo is constantly very high (80-85%), about 45-85% of the extraterrestrial insolation reaches the ground as daily averaged global radiation. The corresponding numbers of the so-called relative global radiation for Koldewey are significantly lower (10-75%).
The main reason for the observed differences in the relative global radiation is the comparable low albedo at Koldewey. The differences in the cloud-free cases (85% at Neumayer, 75% at Koldewey)are also due to the different albedo values, and additionally due to the different sun elevations and only to a minor extent due to differences in the atmospheric turbidities.

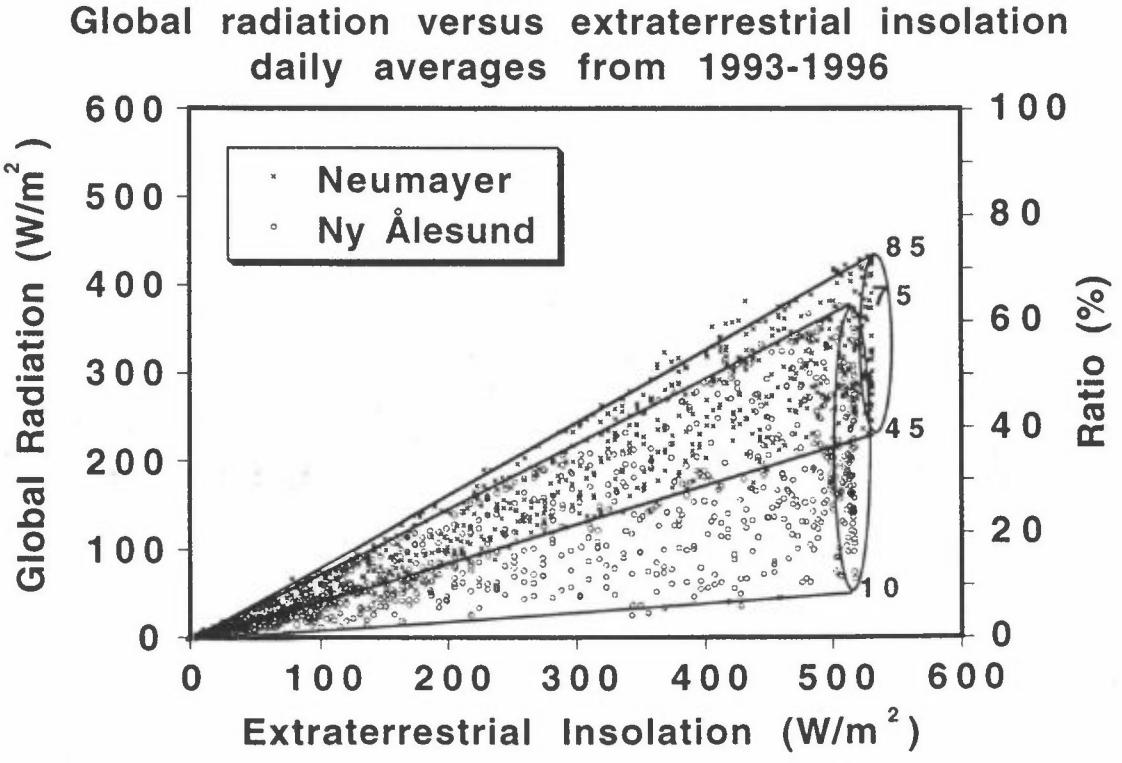

Downward Long-Wave Radiation

Various parameterization schemes for the downward long-wave radiation at the Earth's surface have been tested with the aid of the measurements taken at Koldewey and Neumayer. All of these concepts are based on the Stefan-Boltsmann radiation law. They use the measured surface air temperature at 2 m height and an empirically derived effective emissivity which typically depends on the the total cloud amount, cloud types, low level atmospheric water pressure, temperature, etc.

The downward long-wave radiation from Koldewey and Neumayer can be described by using the same parameterization scheme which takes the effective atmospheric emissivity proportional to the third power of the observed total cloud coverages. But no other influences e.g. due to falling ice crystals (diamont dust) could be detected as significant. And the low level atmospheric water pressure needs not to be considered explicitly in the formulae.

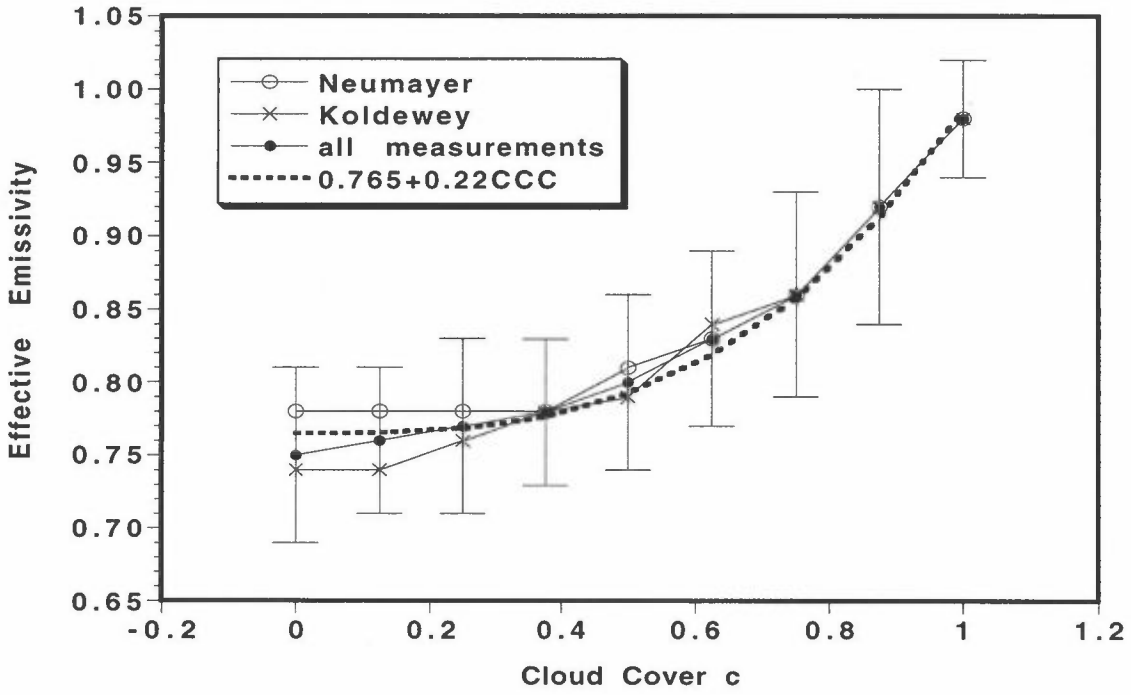

Broadband UV Radiation (290 - 380nm)

The broadband UV rate of the global radiation depends on clouds, sun elevation, surface albedo, and to a minor extend on the total ozone. The cloud dependence is less prononced if the relative broadband UV radiation (broadband UV radiation versus extraterrestrial insolation) is considered.

The relative broadband UV radiation taken at Neumayer exceedes the values from Koldewey. The highest relative broadband UV radiation was measured at Neumayer during austral spring, when the total ozone drops below 200 dobson. The lowest relative broadband UV radiation values have been observed at Koldewey during autumn, when the albedo is low and opaque clouds are predominant.

Abstract to the Scientific Seminar "Atmospheric Research in Ny-Ålesund" at NILU, Norway, April 9-11, 1997

Measurements of the Surface Radiation Budget in Ny-Ålesund

by
Jon Børre Ørbæk
Norwegian Polar Institute, P.Box 5072 Majorstua, 0301 Oslo

Introduction

Surface radiation budget (SRB) measurements have been performed by NP on a permanent basis in Ny-Ålesund during the past 20 years since 1974. The main objective of the activity is the continuation of a long term environmental monitoring program for the investigation of the long and short term variations in the Arctic radiation climate as related to different atmospherical, glaciological and oceanographical factors. The activity is a basis for multidisciplinary programs studying the interaction between the changing environmental conditions and Arctic ecosystems, as well as giving the possibility to detect global change signals as early as possible, for the purpose of giving the environmental management high quality scientific information as basis for their decisions. GCM-models show that the Arctic is very sensitive to climate perturbations, and that radiation processes and feedback mechanisms are very important for the Arctic climate and energy balance. The radiation and energy budget parameters may therefore be used as diagnostics for possible climate warming in the Arctic.

Since 1994 the surface radiation budget measurements are performed within the framework of the BSRN-network (Baseline Surface Radiation Network) in co-operation with AWI. The main objective of this activity is to evaluate high quality and high time resolution surface radiation budget data, in order to provide data for the calibration of satellite-based estimates of the surface radiative fluxes, as well as to provide data for validation of the model computation of radiative fluxes.

Surface Radiation Budget Measurements

Measurements:

The SRB station by the Norwegian Polar Institute monitors the following radiation components (the table list the number of instruments running in parallel at the station):

Radiation Component	Type of Instrument	Nb. of Instr. Measuring
Global shortwave irrad.	Eppley PSP and K&Z CM11	1 Eppley + 2 K&Z
Diffuse shortwave irrad.	K&Z CM11	2 (1 shaded ring + 1 track-ball)
Direct shortwave irrad.	Eppley NIP + AHF	1 NIP + 1 AHF (Cavity)
Reflected shortwave irrad.	Eppley PSP	2 (1 with shading ring)
UV-irradiance	Eppley TUVR	1
Longwave Downw. irrad.	Eppley PIR	3
Longwave Upward irrad.	Eppley PIR	1
UVB erythemal doses	Solar Light Comp. SL501	1
Spectral UV 200 - 600 nm	Bentham DM150	1 (Single monochrom.)
Solar Tracker	Scitec 2AP	1 (with tracking shading balls)
	Eppley SMT3	1

The diffuse irradiance is measured in 2 different ways: One with shading ring and the other with a tracking ball on the solar tracker. The shading ring method need a correction algoritm to account for the part of sky that is shaded apart for the sun. One of the instruments measuring the reflected irradiance is protected from direct sunlight on the dome with a shading horizontal ring, in order to prevent direct sunlight on the inverted dome during low solar elevation conditions. The direct solar radiation measured by the NIP are corrected by the cavity radiometer (AHF) at times of stable solar radiation conditions. One of the longwave instruments are placed on the solar tracker with a trackball shading the dome, in order to prevent possible heating of the dome. All instruments are ventilated to prevent dew-formation and snow, etc. on the domes. The datalogging system is based on a datalogger from Fluke instruments with subsequent dedicated computer-based data-acquisition, storing and presentation of data. The system is connected to the station network for transfer data of data to an Internet connected server once a day.

Calibration:

The shortwave global and direct sun radiation instruments are calibrated on site with the sun as a source by the automatic self calibrating cavity radiometer type AHF (Hickey Frieden traceable to WRR) at the platform of the radiation observatory during April/May every year by means of the standard irradiation/shade method. April/May is selected because the clear weather conditions are favourable at that time. The instruments are also extensive inter-compared with parallel running instruments at all times as well as side by side during spring time with primary instruments stored at the station. The normal incidence pyrheliometer (NIP) is automatically inter-compared with the AHF.

Instrument inter-comparison is used also for the Longwave instruments (Eppley PIR) and the TUVR (UV-radiation). However, these instruments are also calibrated by the factory at regular intervals. The UV-Biometer has been calibrated and characterised in Nordic and WMO inter-comparison campaigns (Leszczynski et al., 1997).

The high number of calibration and inter-comparison lines ensure high quality data and traceability to WRR.

Quality check:

The instruments and measurements are monitored by the station engineers every day. Plots and validation statistics are produced daily and checked. Each radiation parameter is measured by at least 2 instruments, which gives the possibility for early warning of possible faulty instruments, as well as the possibility to correct and replace bad data. The domes are checked daily for possible snow, dew or dust, the silica gel is replaced at regular intervals at least once each month, and the shading-rings etc. are also adjusted when needed.
The computer clocks are adjusted at regular intervals by automatic routines as well as manually daily by the station engineers to the station standard clock, which again is corrected through the Omega system.

Validation:

The validation process use the following data:

- Daily plots of all channels with duplicate measurements of the different parameter,
- Daily tables of measurement/quality statistics based on defined quality rules,
- Daily tables of the difference in % between the different duplicate instruments, the interrelation between Global, Diffuse and Direct radiation, as well as processed quantities like albedo, etc. ,

- Daily measurements logs.

These data-sources give a high probability to detect bad data as well as any sensitivity changes of the instruments during the whole year. Bad data on the main instruments may also be replaced by the secondary instruments measuring side by side. If so, this action is documented through a validation/correction log.

Radiation Database

A surface radiation budget database for Ny-Ålesund is now established at the Norwegian Polar Institute, containing data from 1974 - 1996. The database includes minute-samples, hourly sums, daily sums and monthly sums of the following parameters: Global, Diffuse, Direct, Reflected, UV, UVB, Longwave Downward and Longwave Upward Radiation, as well as Shortwave Net, Longwave Net and Net Radiation, and Albedo.

The database is currently used as basis for investigation of the Arctic radiation climatology and for statistical analysis of the surface radiation budget related to other parameters such as seasonal snow cover, atmospheric variability and meteorological conditions. Figure 2 shows an example of the radiation budget with plots of the shorwave and longwave net radiation form 1995. The plot illustrates the permanent negative longwave radiation balance as well as the polar night and polar day conditions with a net positive radiation balance only about 3 months from end of May to the end of August.

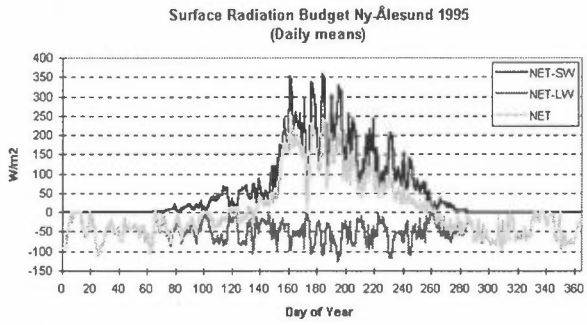

Fig. 1: Plot of the shortwave net, longwave net and net radiation from Ny-Ålesund, 1995.

References

Vinje, T., 1974-79: "Radiation Conditions in Spitsbergen in 1974-79", in
Norwegian Polar Institute Yearbook 1974-79

Hisdal, V., 1987: "Spectral distribution of global and diffuse solar radiation in Ny-Ålesund, Spitsbergen",
Polar Research 5, 1-27, 1987

Hisdal, V., Finnekåsa, Ø. and Vinje, T., 1992: "Radiation measurements in Ny-Ålesund, Spitsbergen 1981-87",
NP-Meddelelser Nr. 118, Norwegian Polar Institute, 1992

Hisdal, V. and Finnekåsa, Ø., 1996: "Radiation measurements in Ny-Ålesund, Spitsbergen, 1988-92",
Meddelelser Nr. 142, Norwegian Polar Institute, 1996

Yamanouchi, T. and Ørbæk, J.B., 1995: "Comparative study of the surface radiation budget at Ny-Ålesund, Svalbard and Syowa station, Antarctica, 1987",
Proc. of the NIPR Symp. on Polar Meteorol. and Glaciol., No.9, 1995

Leszczynski, K., Jokela, K., Ylianttila, L., Visuri, R. and Blumthaler, M., 1997: "Report of the WMO/STUK intercomparison of erythemally weighted solar UV-radiometers",
WMO-GAW Report No.112, WMO-TD No. 781

Monitoring of UV-B Radiation at Koldewey Station

H. Tüg, AWI; T. Hanken, isiTec

Introduction

Although stratospheric ozone depletion causes an increase of solar UV, ozone measurements gives only poor information about the radiation to which the biosphere actually is exposed. Main reasons for this are cloud cover and solar zenith angle which both vary widely depending on day time, season and geographic location. Continuous recording of highly resolved spectra in the cut-off range between 280 and 320 nm (UVB) will be necessary to derive dose weighted irradiances, which is the convolution of measured spectral irradiance with a spectral weighting function determined to express the potential of UV irradiance for causing damage.

Instrumentation

Field spectroradiomters for continuous recording of solar UVB irradiance are commercially not available. Funded by the German science foundation BMBF a system was developed at the AWI which originally was used to detect UVB in the water column (project: UV damage of phytoplankton), but which turned out to be also applicable for atmospheric field measurements. It consists of a double monochromator with extended centre slit using a microchannel plate for single photon detection in 32 parallel channels (optical resolution 1.35 nm, sensitivity $<10^{-8}$ W/m2 nm at S/N 1 and a dark current of less than 0.2 counts per sec and channel). The loss of stray light suppression due to the enlarged centre slit is compensated by a special filter to reduce the light level above 310 nm. Fig. 1 shows a diagram of detector and electronic unit. The instrument has no moveable optical components and seems to have a very stable sensitivity over long observing periods. It will be part of an arctic network and is proposed to participate in the NDSC network after upgrading to the UVA to meet the NDSC specifications.

Observations

In September 1995 a prototype was installed on top of the NDSC building in Ny-Ålesund, Svalbard. After successful tests it was sent back to Bremerhaven in February 96 for inspection and recalibration. In March 96 it was installed again at the same place and kept in operation continuously until October 96.
A complete UVB spectrum is measured each second but only mean values over 5 minutes were stored in this long-term monitoring program. While the instrument keeps in full operation permanently data recording runs automatically only at a signal level above 1 count per second and channel. Service normally can be reduced to regular inspection (and cleaning) of the spherical quartz dome. The collected data are sent periodically to Bremerhaven.

Data Applications

High time resolution, continuous data recording from sunrise to sunset, and the parallel measuring mode together with photon statistics offer a wide field of applications, for example:

- Evaluation of radiation transfer models at fast varying cloud conditions and large solar zenith angles (high scattering)
- Integration over daily, monthly or annual irradiance values for trend measurements
- Computation of the spectral dose for the investigation of biological damaging effects
- Correlation of UVB radiation with meteorological parameters and trace gases like ozone or radicals.
- Calculation of irradiance ratios (indices) using selected channels (e.g. at 300 and 320 nm). These ratios are almost unaffected by clouds or albedo and useful for the comparison of measurements at different locations using the same airmass or for correlations with total column ozone

Unfortunately the various types of instruments which are in use for UVB monitoring programs (like narrow or wide bandpass filter radiometers, scanning double-monochromators or instruments with array detectors) make it difficult to compare the data sets. Due to the sharp cut-off in the solar UVB a slight difference of optical resolution, wavelength and sensitivity lead to significant deviations.

Results

Some preliminary results of our UVB monitoring during the observing period March to October 1996 are given in Fig. 2 to 4.
Fig. 2 shows the daily integral of the spectral irradiance at 307 nm, which was chosen because of its adopted maximum damaging effect to human skin (erythem function). While the shape of the function indicates the seasonable solar zenith distance the daily fluctuations are mainly due to weather conditions like cloud cover or precipitation overlayed by variations of stratospheric ozone, trace gases, aerosols and albedo.
Daily integrals of the solar irradiance covering the spectral range 290 to 320 nm are shown in Fig. 3 together with the minimum airmass at noon for the location of Ny-Ålesund. The daily dose around midsummer (minimum airmass 1.8) is 5 to 10 times higher than in spring during expected stratospheric ozone depletion (minimum airmass around 5).
The influence of ozone to solar UVB radiation is not obvious from Fig. 2 or 3 because of the many overlapping effects but becomes more evident if the ratio of selected channels are used. In Fig. 4 channel numbers 15 and 30 corresponding to the wavelengths 300 and 320 respectively. were taken to correlate daily integrals with total ozone values available from radio soundings at Ny-Ålesund. The comparison shows the expected increase of UVB with decreasing ozone and reverse. Only those days were selected from the UVB data set on which soundings could be achieved.

Acknowledgement

The development of the UVB spectroradiometer was funded by the BMBF under reference number 03PL000A. Six identical instruments are available now and partly in operation for ground-based operation (Neumayer Station in Antarctica, Ny-Ålesund, research vessel Polarstern). Technical support and service during 1996 was due to Hauke Schütt (AWI). The ozone data for comparison purposes were provided by Thomas Seiler.

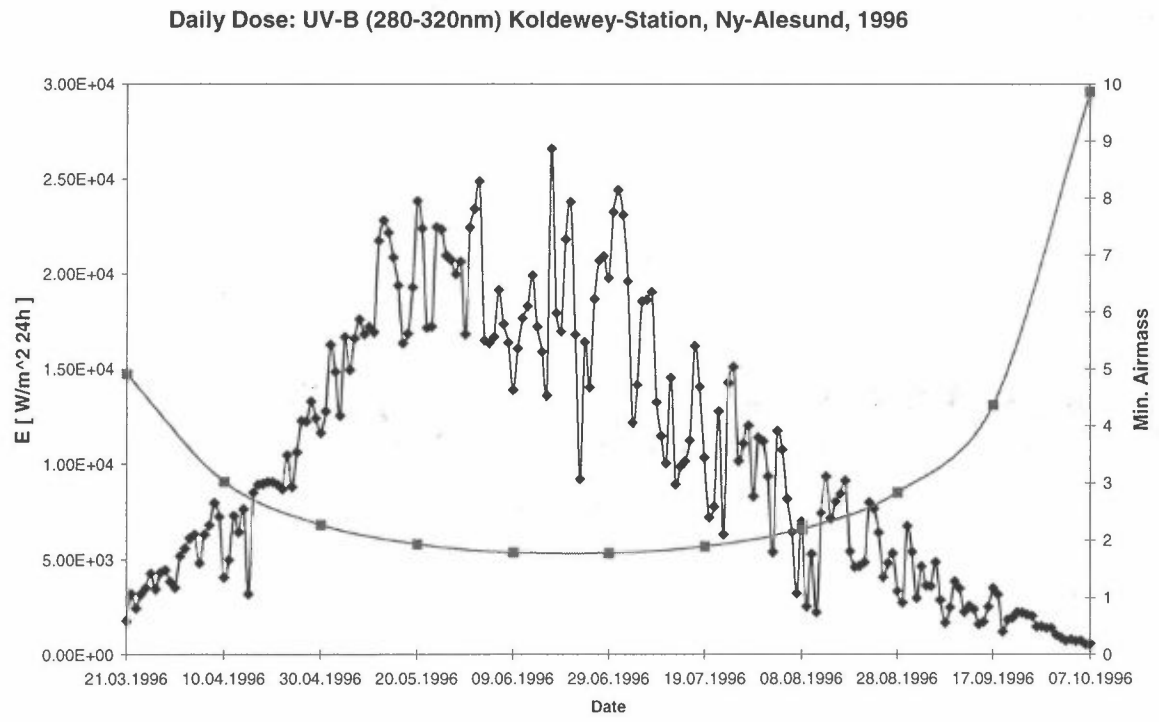

Fig. 3: Daily spectral irradiance integrated over whole UV-B range still influenced by the same parameters as in Fig. 2

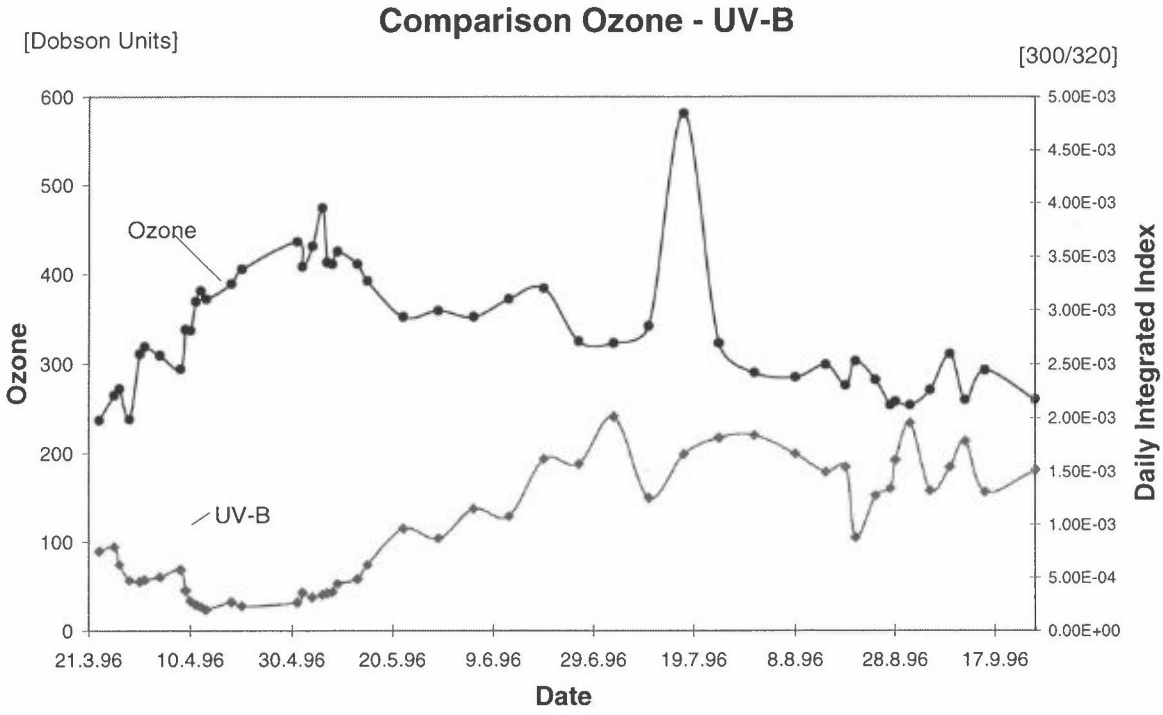

Fig. 4: Daily integrated index derived from spectral irradiances at 300 and 320 nm for suppression of cloud and albedo effects compared with total ozone column

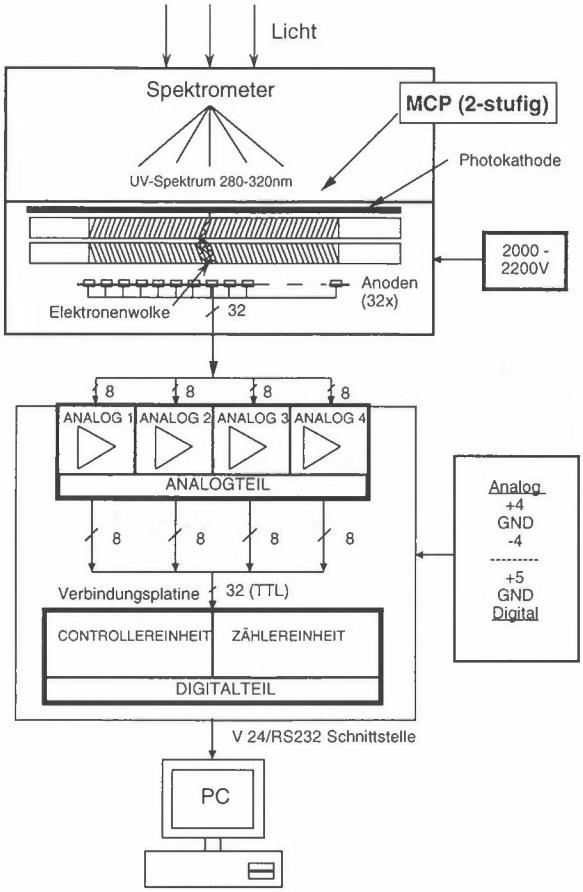

Fig.1: Detector and electronic unit of the AWI-spectroradiometer

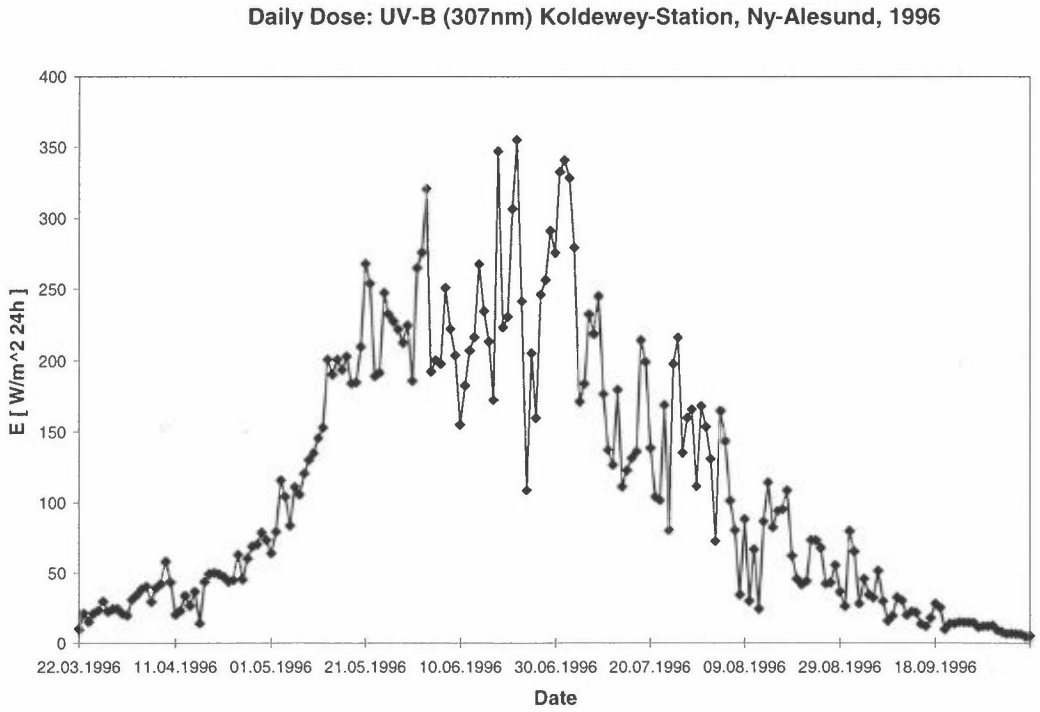

Fig. 2: Daily spectral irradiance at 307 nm (erythem maximum) mainly influenced by cloud cover, solar angle, albedo and total column ozone

Arctic Stratospheric Ozone Depletion Rates Measured with the Match Technique During Four Winters

P. von der Gathen, M. Rex, J. Steger, G.O. Braathen,N.R. P. Harris, E. Reimer, A. Beck, R. Alfier, R. Krüger-Carstensen, B.M. Knudsen, M. Chipperfield, D. Lucic, M. Allaart, H. De Backer, D. Balis, H. Claude, H. Dier, V. Dorokhov, H. Fast, A. Gamma, M. Gil, S. Godin, M. Guirlet, B. Kois, E. Kyrö, Z. Litynska, I.S. Mikkelsen, G. Murphy, F.M. O'Connor, F. Ravegnani, S.J. Reid, M. Rummukainen, C. Varotsos, J. Wenger, V. Yushkov, C. Zerefos, I. Ziomas

A Lagrangian approach has been developed to use ozone sondes for in-situ observation of chemically induced ozone loss in the Arctic lower stratosphere. The technique is based on the statistical analysis of a large number of so called 'matches'. A match is defined as a pair of ozone sonde measurements where sondes are launched from different stations (with Ny-Ålesund as a key station) and at different times but probe the same air parcel as it passes by. To identify the matches, isentropic air parcel trajectories (which are corrected by modelled diabatic cooling rates) are used to track the motion of the air parcel between the measurements. We report on the results of the winters 91/92, 94/95 and 95/96 were the technique has been successfully used to assess the winter/spring Arctic ozone loss as well as on the preliminary results of the winter 96/97. Chemical ozone destruction rates were achieved in temporal and vertical resolution.

In each of the covered winters chemically induced ozone loss was found inside the polar vortex. The measured ozone loss rates reached values of 1.5 to 2 % per day during short periods. Maximal losses in some layers accumulated to about 60% during the winter 94/95 and 95/96. During the 91/92 and 94/95 winters the ozone loss periods coincided and slightly lagged periods with temperatures cold enough to form PSCs in the respective height level. Results from the 95/96 winter show an unusual long persistence of substantial ozone loss rates after temperatures have risen above the PSC threshold. This indicates that the vortex was considerably denitrified during this extremely cold winter.

Chemically induced ozone loss was found also outside the polar vortex in mid-latitudes. Fast loss rates seem to coincide with strong disturbances of the Arctic polar vortex.

A detailed statistical data analysis reveals that ozone loss occurs exclusively during sunlit periods along the trajectories. This and the observed temperature dependence of the loss rate confirm our current understanding of catalytical ozone destruction by chlorine radicals, released from man-made chlorofluorocarbons.

The Evolution of Polar Stratospheric Clouds above Ny-Ålesund

O. Schrems[1], K. Stebel[1], R. Neuber[2]
Alfred Wegener Institute for Polar and Marine Research
[1]D-27515 Bremerhaven, Germany
[2]D-14473 Potsdam, Germany

INTRODUCTION

The crucial role of polar stratospheric clouds (PSCs) in polar ozone depletion is well recognized. Two major types of PSCs have been originally distinguished by lidar measurements[1]. While type II is identified with water ice, the composition and phase of type I PSCs are still under discussion. Type Ia PSCs are described as large aspherical Nitric Acid Trihydrate (NAT) particles, while type Ib are probably small spherical particles composed of a ternary liquid solution of sulfuric and nitric acid [2,3,4]. Small nonspherical particles (type Ic, probably metastable solid phase HNO_3, H_2O) have recently been suggested [5].

Spitsbergen is a very good location for PSC observations in the Arctic since the polar vortex and the region with the lowest stratospheric tempertures are regularly displaced from the North Pole to the European sector of the Arctic. However, temperatures are not cold enough in every winter to allow the formation of PSCs.

PSCs are continuously monitored by AWI's groundbased lidar at the primary Arctic NDSC station in Ny-Ålesund since 1989 (NDSC = *Network for Detection of Stratospheric Change*). In winter 1995/96 type I PSCs could be observed above Spitsbergen over a period of 11 weeks. This was the longest 'PSC season' observed so far in the Arctic.

INSTRUMENTATION

Measurements of PSC's at the primary NDSC station Ny-Ålesund (79°N, 12°E) are performed with AWI's Aerosol & Ozone LIDAR. This LIDAR system consists of the following: A frequency doubled Nd:YAG laser (532 nm, 190 mJ/pulse at 30 Hz, linear polarized) an Excimer laser (308 nm, 200 mJ/pulse at 100 Hz; laser pulses at 353 nm are generated by stimulated H_2-Raman scattering), a 0.6 m diameter modified Cassegrainian telescope (field of view α = 0.8 mrad) and a multiwavelength detector for 7 simultaneous channels. Lidar returns are recorded by a photon counting system. A mechanical chopper prevents saturation of the photodetectors by signals from low altitudes.

RESULTS

The high variability of the minimum temperatures in the Arctic is reflected in the observation frequencies of PSCs above Spitsbergen [6,7] The frequency of lidar measurements and PSC occurence during the last eight winters (1988/89 - 1995/96) is displayed in figure 1. The plot shows a quite stable frequency of lidar observations with 40 - 60 days per winter, mainly between November and March. PSC appearance varies strongly from year to year. There were no PSC detections during winter 1990/91, a weak signal on December 6, 1991 and a single late PSC event on February 28 and March 1, 1994. During the other five years a good set of data of PSC obsevations could be collected. Each winter, 6 - 28 days show PSC signatures. The 'PSC season' usually lasts from December to February, with the highest probabiltity for PSC appearance in January. 31 % of all lidar measurements during the first five weeks of the year show PSC signatures.

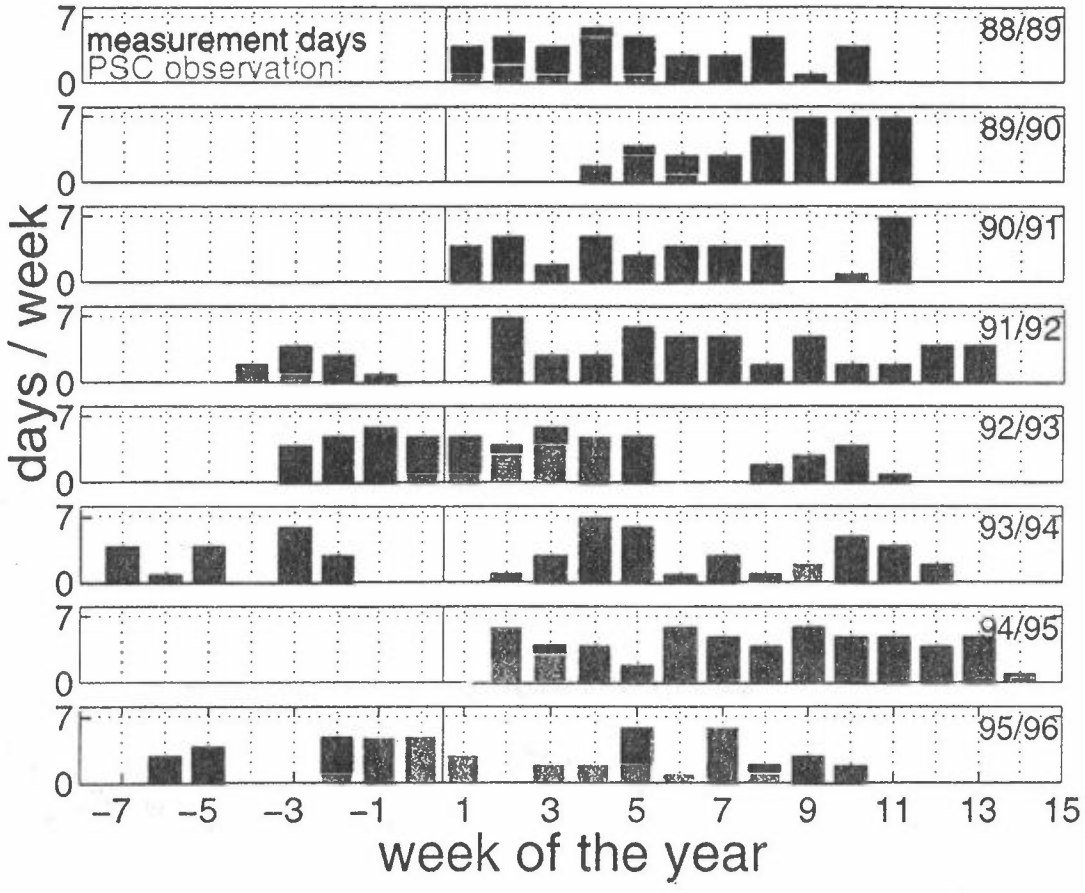

Figure 1: Lidar observations at the NDSC station Ny-Ålesund and PSC statistic for a period of eight winters

The lidar data of winter 1992/93 clearly show that the volume densities of PSC type Ib and Pinatubo aerosols have the same temperature dependence. The separation of both types of aerosols is possible because the volcanic aerosol layer is located below 425 K, in the lower part

of the main PSC layer (400-500 K). There is only a small altitude range where interaction is possible. Data from winter 1995/96 show typical PSC development during a cold winter with normal background aerosol content. Since Spitsbergen is an island without high mountain ranges, we can exclude effects of orographically induced waves. Thus our data should be representative for the normal devlopment of PSCs in the Arctic.

Lidar measurements with high resolution (1 min., 15 m) can detect the high spatial and temporal varibaility of PSCs. Figure 2 shows, as an example, the rapid development of PSC layers observed on February 13, 1996. At that time Ny-Alesund was inside the polar vortex and situated in the centre of the area of cold stratospheric air. Local temperatures were below the existence temperature of NAT (T_{NAT}) between 15-23 km, but well above the frost point of ice (T_{ICE}). This high variablitiy indicates two inhomogeneous 'patchy' PSC layers, moving across the field of view of the lidar.

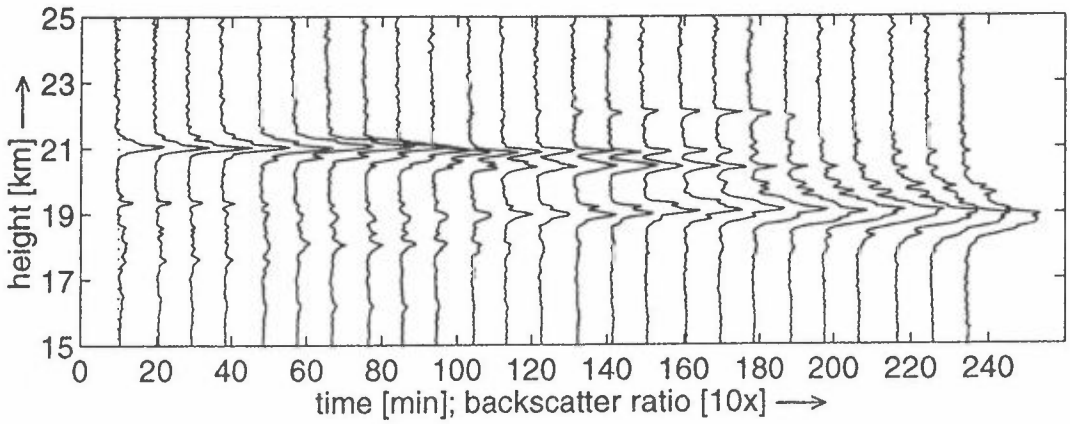

Figure 2: Profiles of means (10 min) of backscatter ratios at 532 nm measured at Ny-Ålesund on February 13, 1996

SUMMARY

Polar stratospheric clouds have been monitored at Ny-Ålesund by ground-based Lidar measurements since 1989. The high variability of the minimum temperatures in the Arctic is reflected in the observation frequencies of PSCs above Spitsbergen. PSCs have been found to be mainly of type I, as temperatures rarely reach the water frost point. Lidar depolarization measurements in combination with back trajectory analyses of airmass thermal history of PSCs are used to distinguish destinct classes of type I PSCs.

While during winter 1991/92 no PSCs could be detected, in the other winters PSC occurence was most likely in January. In the winters 1994/95 and 1995/96 the 'PSC season' was much longer than in previous years. Minimum temperatures have decreased and the altitude range of temperatures below T_{NAT} has increased, thereby enhancing the probability of PSC occurence.

ACKNOWLEDGEMENTS

Financial support of this research by the Bundesministerium für Bildung, Wissenschaft, Forschung und Technologie Bonn (Project: 01 LO 9407/5) and the Commission of the European Community, Brussels, DG XII (Project: ESMOS/Arctic) is greatly acknowledged.

REFERENCES

1. Browell, E. V., Butler, C. F., Ismail, S., Robinette, P.A., Carter, A. F., Higdon, N.S., Toon, O.B., Schoeberl, M.R., Tuck, A. F.: Airborne lidar observations in the wintertime Arctic stratosphere: Polar stratospheric clouds. Geophys. Res. Lett. **19** (1990), 385-388

2. Toon, O.B., Browelle, E.V., Kinne, S., Jordan, J.: An analysis of lidar observations of polar stratospheric clouds. Geophys. Res. Lett. **17** (1990) 393-396

3. Drdla, K., Tabazadeh, A., Turco, R. P., Jacobson, M.Z., Dye, J.E., Twohy, C., Baumgardner, D.: Analysis of the physical state of one arctic polar stratospheric cloud based on observations. Geophys. Res. Lett. **21** (1994) 2475-2478

4. Beyerle, G., Luo, B. P., Neuber, R., Peter, T., McDermid, I.S.: Temperature dependence of ternary solution particle voulumes as observed by lidar in the Arctic stratosphere during winter 1992/93. submitted to J. Geophys. Res. (1996).

5. Tabazadeh, A., Toon, O.B., Hamill, P.: Freezing behavior of stratospheric sulfate aerosols inferred from trajectory studies. Geophys. Res. Lett. **22** (1995) 1725-1728

6. Stebel, K., Neuber, R., Beyerle, G., Biele, J., Scheuch, P., Schütt, H., von der Gathen, P., Schrems, O.: Lidar Observations of Polar Stratospheric Clouds above Spitsbergen, in: Advances in Atmospheric Remote Sensing with Lidar, Ansmann, A. Neuber, R., Rairoux, P., Wandinger, U. (Eds.), Springer-Verlag, New York (1996), p. 509-512

7. Stebel, K., Schrems, O., Neuber, R., Beyerle, G., Biele, J., Beninga, I., Scheuch, P., Schütt, H., von der Gathen, P.: Polar Stratospheric Clouds above Spitsbergen, submitted to Proceedings of the 1996 Quadrennial Ozone Symposium

Analysis of SAOZ UV/Vis Measurements from 1991 to 1996

Britt Ann Kåstad Høiskar and Geir O. Braathen
Norwegian Institute for Air Research

Introduction

NILU has operated a UV-Visible spectrometer of the SAOZ type (SAOZ = System for Analysis of Observations and Zenith) since the autumn of 1990. With this instrument one can measure total columns of ozone and NO_2. NILU has participated in several EU projects with data from this instrument. The first EU project (STEP-13) lasted from 1990 to 1992. In addition to carrying out measurements NILU studied the effects of Pinatubo aerosols on SAOZ, Brewer and TOMS measurements (Dahlback et al., 1994). The second EU project was SCUVS (Stratospheric Climatology by UV-Vis Spectroscopy) that lasted from 1992 through 1993. In this project NILU started the development of a technique whereby total ozone is deduced from the ultraviolet part of the spectrum. Other contributions to this project included calculation of airmass factors with NILU's radiative transfer model, comparison of Dobson, Brewer and UV-Visible instruments, and dynamical modelling of the northern stratosphere. The third EU project was SCUVS-2 that lasted from 1994 through 1995. Here NILU contributed with further development of the UV analysis and with calculation of the seasonal dependence of the airmass factors for ozone. Currently NILU participates in SCUVS-3 that lasts from 1996 through 1997. Some examples of NILU's work are described in more detail in the following sections. Figure 1 shows the instrument deployed in Ny-Ålesund.

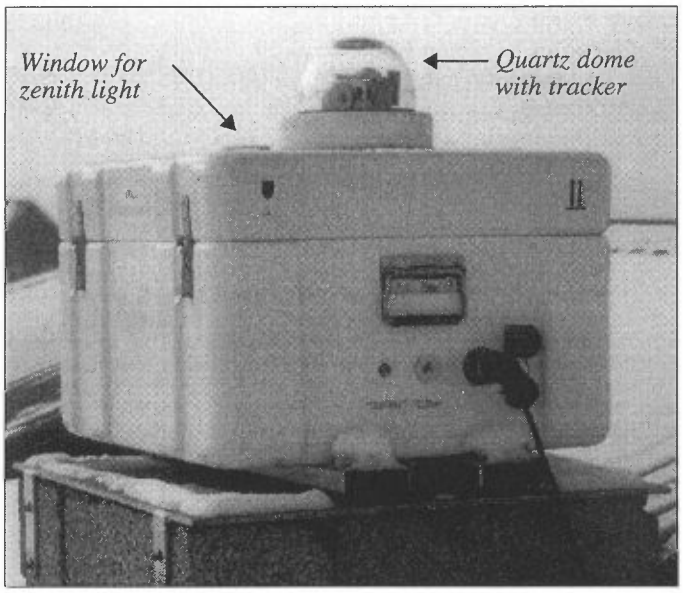

Figure 1: *Photograph showing the SAOZ instrument deployed in Ny-Ålesund on the observation platform of the Research Station of the Norwegian Polar Research Institute. The quartz dome contains a pointing device that enables the instrument to measure direct radiation from the sun or the moon. The light scattered from zenith enters the spectrometer through a window to the left of the quartz dome.*

The SAOZ instrument in Ny-Ålesund is part of a large international network of such instruments with stations in the Arctic, at northern middle latitudes, the tropics and Antarctica. Figure 2 shows the Northern Hemispheric part of this network.

Instrument description

In its original configuration, the SAOZ spectrometer consists of a holographic concave grating and a 512 elements diode array. The spectral range is 290-590nm and the spectral resolution is approx. 1nm. Figure 3 shows the various components of the instrument. In January 1996 the spectrometer was upgraded with a 1024 elements diode array. A new grating was also installed in order to disperse the same spectral range onto the new detector, which is twice as long as the original one. The main advantage of this upgrade lies in the oversampling, which is now doubled. In late 1996 the old HP computer was replaced

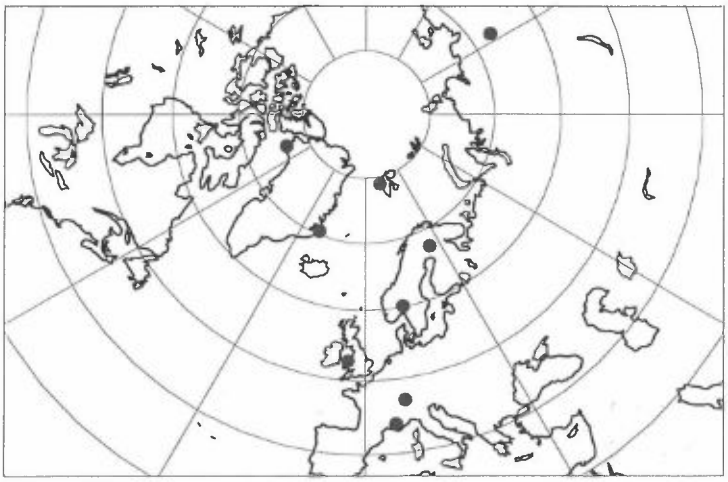

Figure 2: The Northern Hemispheric part of the SAOZ network consisting of stations in Ny-Ålesund, Thule, Scoresbysund, Sodankylä, Zhigansk, Aberystwyth, Jungfraujoch and the Observatoire de Haute Provence. The site in Southern Norway is equipped with another type of UV-Vis instrument.

with a PC based acquisition system. This makes the subsequent reanalysis of the data much quicker.

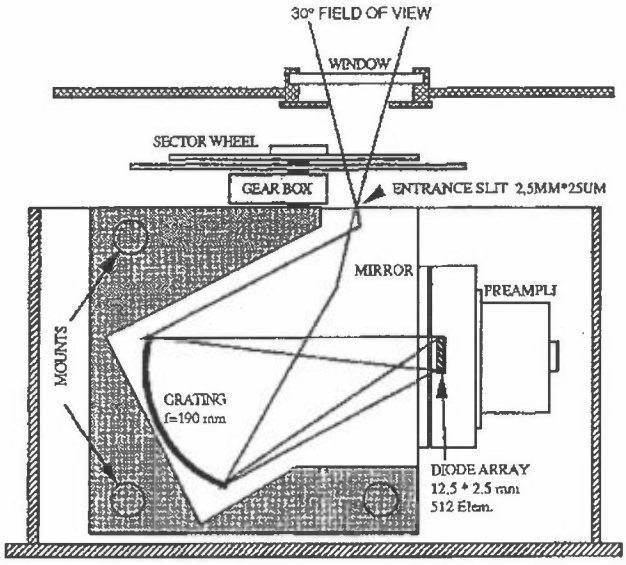

Figure 3: Schematic description of the configuration of the SAOZ instrument.

The SAOZ instrument observes sunlight scattered from zenith. The spectral range used by the standard SAOZ retrieval software to calculate the ozone column is the 450 - 580nm region, the so-called Chappuis band. The absorption by ozone in this region is quite weak, so the best measurements are obtained when the sun is close to the horizon and the light path through the ozone layer is long. This makes the SAOZ instrument ideal for measurements at sites where the sun is too low in the sky for Dobson or Brewer measurements. Since the instrument measures the light scattered from zenith one obtains in the first instance a so-called slant column, i.e. a column along the path followed by the light. When the sun is close to the horizon this path is typically 15-20 times larger than the vertical path. The ratio between the slant column and the vertical column is the co-called air mass factor (AMF). The AMF can be calculated with radiative transfer models. The vertical column is hence obtained by dividing the measured slant column with the AMF. However, the exact determination of the AMF is not without problems, as described below.

Analysis of the UV part of the spectrum 3

As mentioned above, the SAOZ instrument is ideal for location where the sun is low on the sky. The solar zenith angle (SZA) range that gives the best signal to noise ratio is 86 -91°. If the SZA is larger than 91° the calculated AMFs are uncertain. If the SZA is less than 86° the distance travelled by the light through the ozone layer is too short to give sufficient absorption in the Chappuis band. In Ny-Ålesund the useful measurement season is from mid February to the end of April and from mid August to late October. During the winter the sun is too low in the sky to give a sufficient signal and in the summer the sun is too high in the sky for the Chappuis band to give sufficient absorption. In order to increase the duration of the measurement season NILU has developed a technique whereby the ultraviolet part of the

spectrum is used. The absorption by ozone in this region (300 - 310nm) is much stronger than in the Chappuis band. The technique used is quite similar to the technique used to derive total ozone from Dobson measurements. The details of this method is described by Høiskar et al. (1996).

Seasonal variation of air mass factors

Intercomparison between SAOZ measurements and Dobson/Brewer measurements has revealed an annual cycle in the relative difference between the two data sets. The amplitude of this seasonal variation increases with increasing latitude. A technique for quantifying the seasonal variation of the AMF has been developed at NILU and described by Høiskar et al. (1997a). Figure 4 shows the relative deviation of the AMF in Ny-Ålesund as a function of time through the year. The relative error introduced by using a constant AMF throughout the year can be seen directly from the figure. It can be seen that a significant error is introduced by using a time invariant AMF.

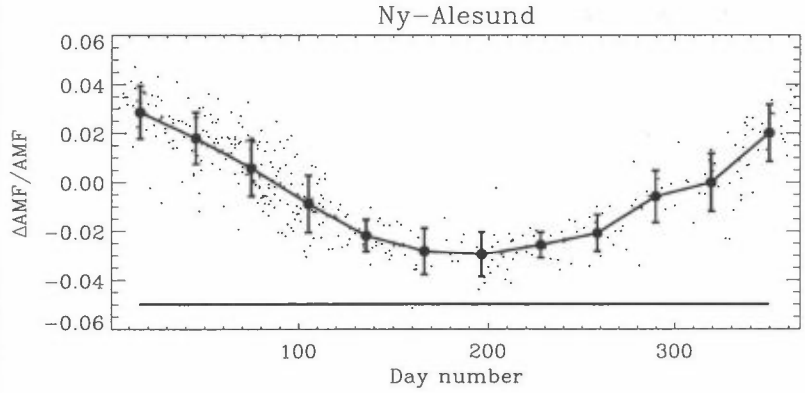

Figure 4: *The relative deviation of air mass factors (AMF) from the annual average AMF based on ozonesonde data from Ny-Ålesund. The small dots represent AMFs for individual launches and the large dots represent monthly averages with 1 σ error bars. The long horizontal bar at the bottom represents the standard AMFs used by the SAOZ algorithm.*

Comparison of SAOZ with other data

Total ozone from the SAOZ instrument has been compared to total ozone from the Dobson spectrophotometer operated by the Physics Department of the University of Oslo and with total ozone from ozonesondes launched by the Alfred Wegener Institute. Figure 5 shows the comparison between total ozone as obtained with the SAOZ and total ozone as measured by other techniques for the 1995 and 1996 spring periods. The comparison between total ozone from SAOZ and from ozone sondes shows a fairly good agreement in 1995, although the sondes show somewhat less ozone in the early winter and somewhat more ozone in the late spring. In 1996, however, total ozone from the sondes is systematically lower than from the SAOZ. The reasons for these discrepancies is still a matter of investigations. The middle panels show the potential vorticity (PV). It can be seen from the figure that ozone and PV are quite well anti-correlated. This can be taken as a sign of chemical ozone depletion. A detailed analysis of SAOZ data including comparison with meteorological data and model results is under way (Høiskar et al., 1997b).

References

Dahlback, A. B. Stein, M. Del Guasta, L. Stefanutti, E. Kyrö, N. Larsen and G.O. Braathen, 1994: Effects of Stratospheric Aerosols from the Mt. Pinatubo Eruption on Ozone Measurements at Sodankylä, Finland in 1991/92. *Geophys. Res. Lett.*, **21**, 1399-1402.

Høiskar, B.A. Kåstad, A. Dahlback, C.W. Tellefsen and G.O. Braathen, 1996: Retrieval of total ozone abundances from the UV region of spectra recorded with a UV-Visible spectrometer. *Appl. Optics*. Submitted.

Høiskar, B.A. Kåstad, A. Dahlback, G. Vaughan, G.O. Braathen, F. Goutail, J.-P. Pommereau and R. Kivi, 1997a: Interpretation of ozone measurements by ground-based visible spectroscopy - a study of the seasonal dependence of airmass factors for ozone based on climatology data. *J. Quant. Spectrosc. Radiat. Transfer*, **57**, 569-579.

Høiskar, B.A. Kåstad, G.O. Braathen, M. Chipperfield, 1997b: Analysis of total ozone data as observed with a UV-Vis spectrometer in Ny-Ålesund, Spitsbergen for the winters 1991 through 1996. In preparation.

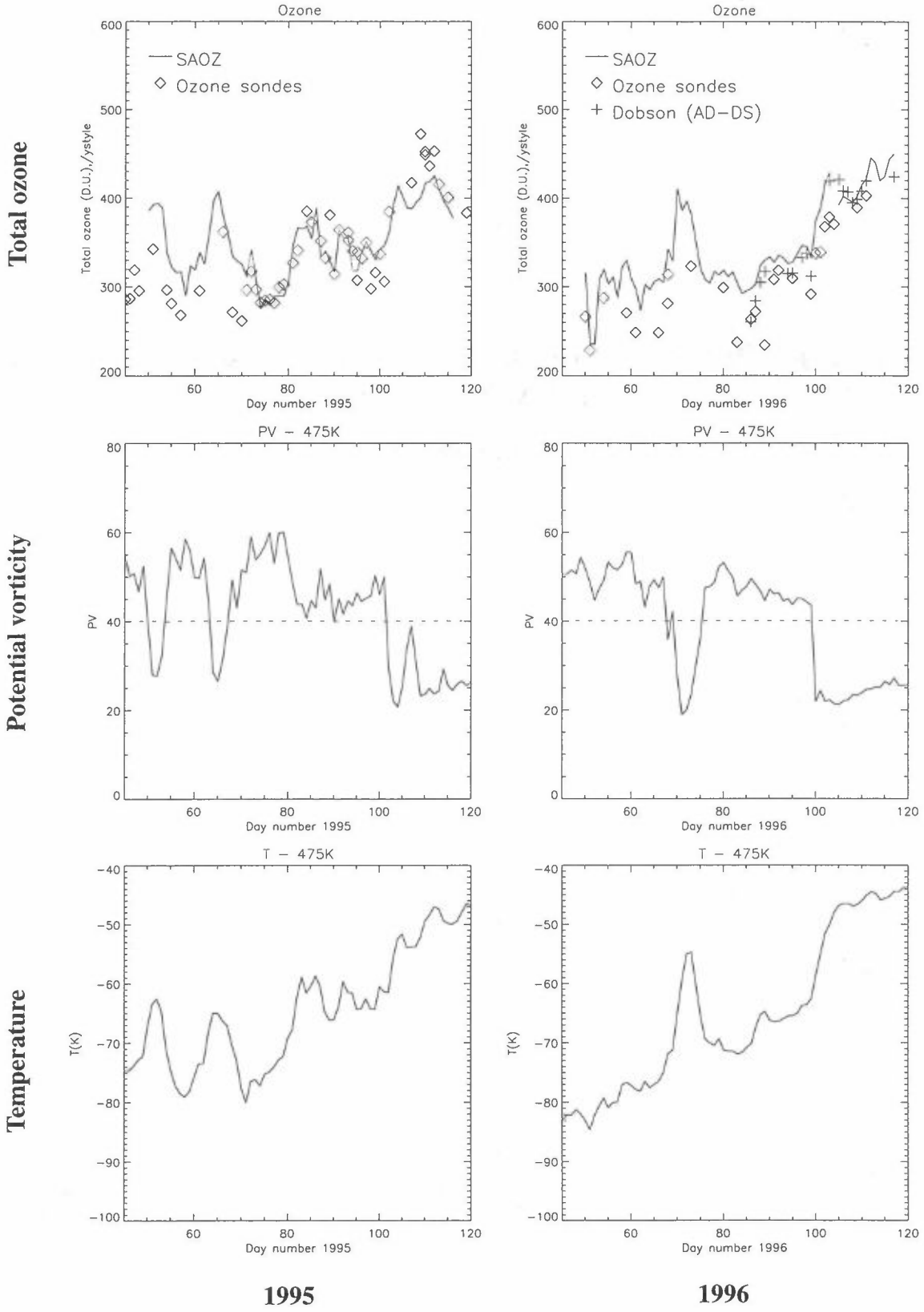

Figure 5: *The two upper panels show total ozone measured in Ny-Ålesund. The left panel shows data for 1995 (days 50 to 120) and the right panel for 1996. The solid line represents SAOZ measurements, the crosses (+) Dobson measurements and the diamonds (◊) total ozone from ozonesondes. Dobson data for 1995 are not available. The two middle panels show the temporal development of potential vorticity at 475 K for the two winters and the two lower panels show the temperature for the two winters also at the 475 K level. The dashed line at 40 PV units represents a fairly conservative limit for being outside/inside the polar vortex.*

Seasonal variations of atmospheric trace gases in the high Arctic at 79°N

J. Notholt*, G. Toon**, F. Stordal***, S. Solberg***, N. Schmidbauer***,
E. Becker*, A. Meier*, and B. Sen**

*Alfred Wegener Institute for Polar and Marine Research,
P.O.Box 600149, 14401 Potsdam, Germany

**Jet Propulsion Laboratory, California Institute of Technology,
4800 Oak Grove Drive, Pasadena CA 91109, USA

***Norwegian Institute for Air Research,
P.O.Box 100, 2007 Kjeller, Norway

Introduction

The high latitude regions have the largest atmospheric seasonal variations of anywhere on earth. Observations made throughout the year, from continuous sunlight to continuous darkness, therefore provide a unique test of our capability to correctly model the photochemical, heterogeneous, and dynamical processes which control the distribution of atmospheric trace gases.

Here we present 4 years of observations of the complete seasonal cycles of the column abundances of several tarce gases. The column data have been combined with in-situ observations for three compounds, to infer additional information about the variation of the VMR profiles with altitude and season.

Experimental and data analysis

Spectra were recorded with the BRUKER IFS 120M FTIR spectrometer (see Notholt, 1994). While the solar absorption spectra (March to September) were recorded typically at a resolution of 0.011 or 0.004 cm^{-1} (resolution=1/retardation). The analysis of the FTIR spectra was performed using the GGG software of the JPL MkIV Interferometer task, a further development of the ATMOS Data Analysis software (Norton and Rinsland, 1991).

Since 1989, in-situ measurements have been performed from Zeppelin Mountain, located about 1 km away from the FTIR spectrometer. Samples were collected manually into stainless steel bottles every second day. The subsequent analysis was performed at NILU using a gas chromatograph equipped with a flame ionization detector (see Schmidbauer and Ohme, 1986).

1. Trace gases

During winter and beginning of spring Ny-Ålesund is most of the time well inside the polar vortex. Mixing of midlatitude air into the Arctic occurs mainly during the middle/end of March after the final warming (Schoeberl et al., 1992). The total, columns of HCl are given in Figure 1a. Figure 1b gives the sum of $HCl+ClONO_2$ divided by HF, to account for the subsidence. Due to the large uncertainty in the lunar HF data, the winter ratio shows big error bars.

Chemical repartitioning of HCl into $ClONO_2$ starts in November, immediately after the onset of the polar night before the widespread production of PSC's. Already small regions with PSCs can behave like flow reactors, leading to a substantial conversion of HCl to $ClONO_2$. At the beginning of the polar night the circulating airparcels still sometimes see sunlight at lower latitudes. This maintains sufficient NO_2, from photolysis of N_2O_5 and HNO_3, so that any heterogeneoulsy formed chlorine is immediately converted to $ClONO_2$. However, by December, the complete darkness together with increasing concentrations of active chlorine, lead to a major loss of NO_2 in the lower stratosphere, preventing the formation of $ClONO_2$ and leading to a decrease of the sum of HCl and $ClONO_2$.

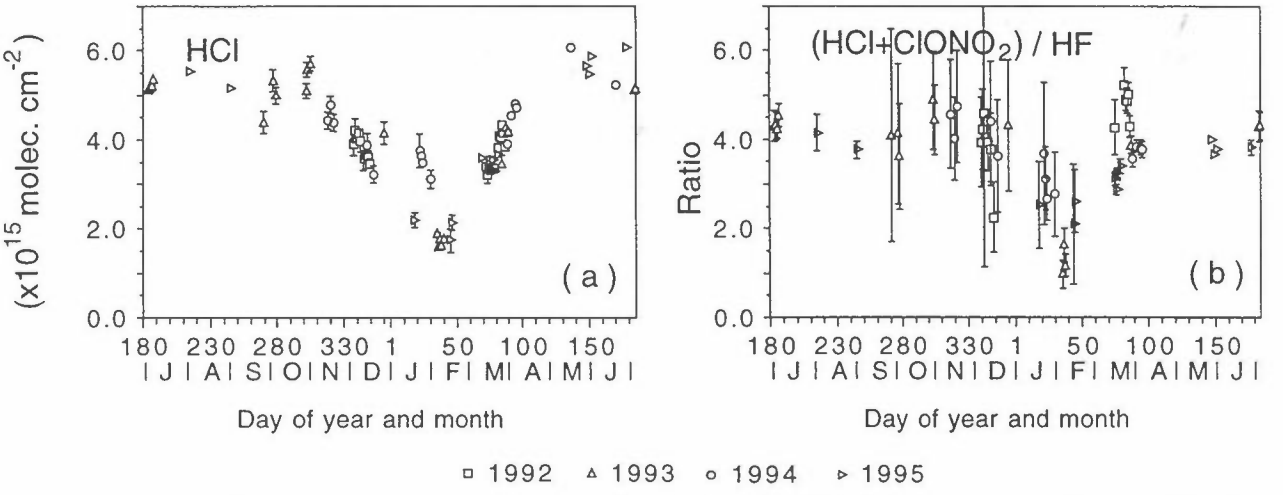

Figure 1: Seasonal variations of HCl and (HCl+$ClONO_2$)/HF.

C_2H_6 (Figure 2a), C_2H_2 and CO all show strong seasonal cycles with a maximum during the winter. These compounds are produced mainly at midlatitudes. Since their main removal pathway is the reaction with OH, which disappears in the dark, these gases accumulate during the winter. A model analysis has been performed by Isaksen et al. (1985), revealing the strong seasonal cycles for these compounds in reasonable agreement with in-situ measurements.

In contrast to C_2H_6, C_2H_2 and CO, the seasonal cycle of CH_2O (Figure 2b) shows two maxima, one during the summer and a second during the winter. The maximum during the summer can be assigned to its formation by methane oxidation. The maximum during the winter is possibly caused by the direct transport from the continents during the polar night.

The similarity of total column measured in Europe (Moscow and Switzerland) with the Ny-Ålesund winter values for C_2H_6, C_2H_2 and CO and the second maximum of CH_2O during the winter confirm the strong transport of midlatitude air into the Arctic during the winter and indicate, that during this time span no significant removal by OH occurred during the transport to the Arctic.

2. Effective layer thickness

In order to learn more about the vertical distributions of C_2H_6, C_2H_2 and CFC-12 (CCl_2F_2) we have studied the ratio of the total columns to the in-situ vmrs. The ratio has been expressed as an effective layer thickness H_x, which is defined as the altitude to which the compound would be mixed under the assumption of a constant mixing ratio.

The effective layer thickness of C_2H_6 (Figure 3a) is seen to be higher than that of C_2H_2 (Figure 3b) and shows much less variations. This is consistent with the fact that C_2H_6 has a

longer chemical lifetime of the two, and is therefore allowed to be transported to somewhat higher levels. Furthermore, the effective layer thickness of C_2H_6 shows a clear seasonal cycle,

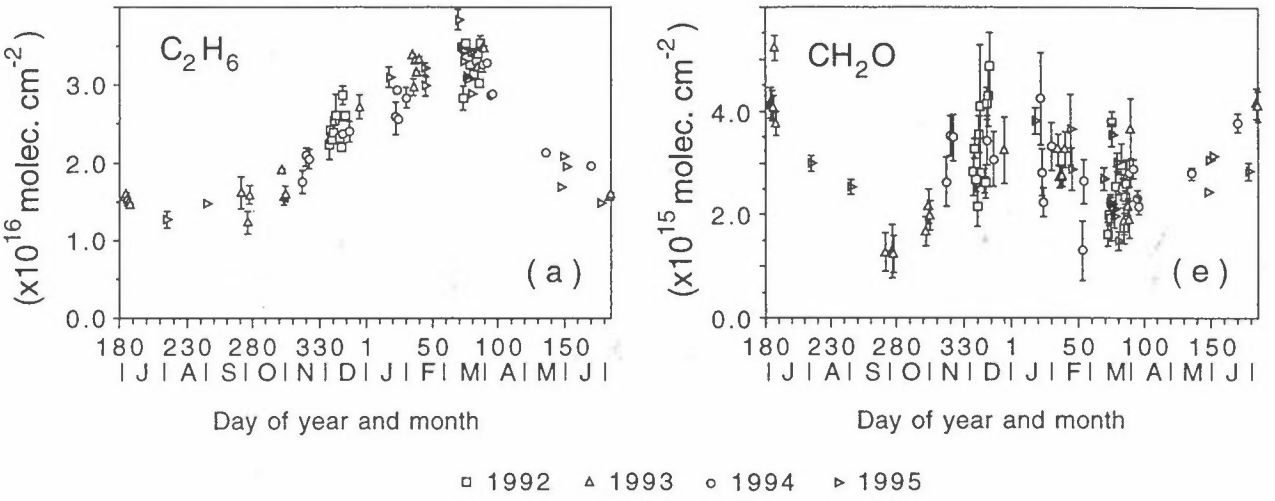

Figure 2: Seasonal variations of the total columns of C_2H_6 and CH_2O.

which is similar to that of the tropopause height, with a minimum during the winter. Parts of the seasonal cycle in the effective thickness of C_2H_6 is therefore believed to be due to the cycle of the tropopause altitude. This is reasonable for a compound that fills most of the troposphere, as the troposphere is relatively well mixed. The seasonal variations in the layer thickness can also be due to variations in the surface concentration that do not have a counterpart in the free troposphere, as the surface mixing ratio is used as a scaling factor in the definition of the thickness. For CFC-12 a nearly constant scale height of 12 km results, as expected for this trace gas which is uniformly mixed in the troposphere and the lower part of the stratosphere.

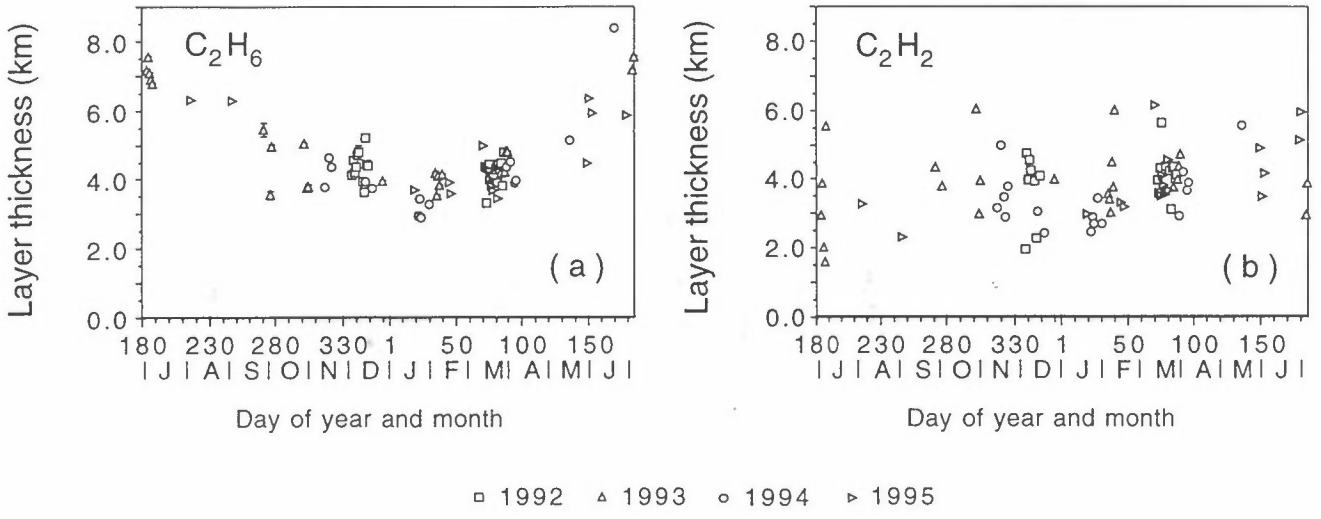

Figure 3: Seasonal variations of the effective layer thickness of C_2H_6 and C_2H_2.

References

Isaksen, I. S. A., O. Hov, S. A. Penkett, and A. Semb, Model analysis of the measured concentration of organic gases in the Norwegian Arctic, J. Atm. Chem., 3, 3-27, 1985.

Norton, R.H., and C.P.Rinsland, ATMOS Data Processing and Science Analysis Methods, Appl. Optics, 30, 389-400, 1991.

Notholt, J., The moon as light source for FTIR measurements of stratospheric trace gases during the polar night: Application for HNO_3 in the Arctic, J. Geophys. Res., 99, 3607-3614, 1994.

Schmidbauer, N. and M. Ohme, Improvement of a cryogenic preconcentration unit for C2-C5 hydrocarbons in ambient air at ppt levels, J. High Res. Chromatogr. & Chromatrogr. Commun., 9, 502-505, 1986.

Schoeberl, M. R., L. R. Lait, P. A. Newman, and J. E. Rosenfield, The Structure of the Polar Vortex, J. Geophys. Res., 97, 7859-7882, 1992.

Microwave Measurements of Stratospheric Ozone, Chlorine Monoxide and Tropospheric Water Vapor at Ny-Ålesund, Spitsbergen, 1994-1996 *

U. Raffalski, U. Klein, J. Langer, B. M. Sinnhuber and K. F. Künzi

Institute of Environmental Physics, University of Bremen, PO Box 33 04 40, D-28334 Bremen, Germany
e-mail: uwe@schalk.physik.uni-bremen.de

Abstract. With the Radiometer for Atmospheric Measurements (RAM) we have obtained a set of microwave emission measurements from which arctic stratospheric ozone, chlorine monoxide (ClO) and tropospheric water vapor content was derived. Measurements were performed during winter 1994 and continuously since November 1994. Ozone and ClO VMR profiles cover the altitude range of 15-55 km with a vertical resolution of 10 km and a high temporal resolution of less than one hour for ozone. The error of the ozone profiles due to uncertanties of the measurements is estimated to be less than 5% or ±0.1 ppmv, whichever is larger. The very high temporal resolution of our ozone measurements enables us to detect shortterm variabilities. These profiles have been used to evaluate the calculations from a 3D chemical transport model (SLIMCAT). In general the two data sets compare quite well, but deviations of ~20% near 20 km altitude were found. ClO profiles from RAM measurements agree very well with profiles from the Airborne Submm-wave Radiometer, ASUR, and both are quite well reproduced by SLIMCAT calculations. The threshold for successful ClO measurements is determined by the tropospheric water vapor content. It was found that our ClO measurements are only feasible for less than 1 mm of precipitable water vapor, corresponding to an opacity of 0.15 Neper. Values of tropospheric water vapor content derived from the microwave measurements show good agreement with those calculated from the relative humidity data of radiosonde in-situ measurements.

Introduction

Since 1988, the Arctic station Ny-Ålesund/Spitsbergen at 78.9N/11.9E evolved into an important site for the international Network for the Detection of Stratospheric Changes (NDSC). Ny-Ålesund is now part of the Arctic primary site of the NDSC and contributes to national (e.g. German ozone research program OFP) and european programs. The station is jointly operated by the Alfred-Wegener-Institute for Polar and Marine Research, AWI, the Institute of Environmental Physics of the University of Bremen, IUP, (both Germany) and the Norwegian Institute for Air Research, NILU.

Among other instruments a microwave radiometer is installed to provide stratospheric ozone and chlorine monoxide profiles. This "Radiometer for Atmospheric Measurements" (RAM) was built by the IUP. Until 1994 mm-wave measurements by the RAM were mainly done on a campaign basis. Since November 1994 the RAM is part of the permanent installation at this NDSC site and year-round measurements are now performed from the newly built NDSC-station.

The RAM was developed for continuous ground-based millimeter-wave observations of trace gases in the stratosphere and the lower mesosphere. It can operate in the frequency range from 100-300 GHz. In its most recent configuration it consists of a 142 GHz and a 204 GHz receiver for the observation of O_3 and ClO, respectively For a detailed instrumental description see *Langer et al.* [1996].

* *Printed in Proceedings of the Quadr. Ozone Symp, L'Aquila, Italy, 1996*

The Basics of mm-Wave Radiometry

At microwave frequencies the width of a thermal emission line from a molecular transition is proportional to pressure. Since the atmospheric pressure increases with decreasing altitude, the pressure broadening of the line leads to a characteristical line shape, depending on the vertical distribution of the observed species. Emission from high altitudes contributes to the line center whereas the outer line wings are dominated by the low altitude contribution. Mathematically this process can be described by the radiative transfer equation (RTE). By inverting the RTE the vertical distribution of the molecule under investigation can be estimated from the shape of the spectrum (*Janssen, 1993*).

Measurement Requirements

The altitude range covered by the RAM is approximately 15-55 km given by the total bandwidth (950 MHz) of the acousto-optical spectrometer (AOS) and its resolution of 1.3 MHz. The vertical resolution of the profile is roughly 10 km. The detection limit of the RAM is about 20 mK mainly due to tropospheric instabilities producing varying baseline effects. The integration time depends on the signal to noise ratio needed in order to perform a successful retrieval. Since line amplitudes of 15 K are expected for ozone and only 50 mK for chlorine monoxide, integration times of several seconds for ozone and several hours for ClO are neccessary.

The ClO spectral emission line near 204 GHz originates from rotational transitions and is composed of several hyperfine components due to chlorine nuclear-spin transitions. The line cluster appears as one single line in the spectrum with a brightness temperature of 50-200 mK. In order to retrieve the ClO profile, we have to subtract nighttime from daytime spectra making use of the fact, that ClO in the lower stratosphere nearly completely disappears at night. The ClO spectra need to be integrated over approximately 20 hours (including the nighttime measurements) requiring a stable troposphere for the entire period. Because tropospheric conditions - of main concern is the total amount of water vapor - tends to vary very rapidly above Ny-Ålesund, this poses a severe limitation to our ClO measurements. Furthermore instrumental effects (baseline) are very critical for detecting weak lines like ClO. In order to minimize nonlinearities and instabilities in the back-end the reference beam method (described by *Parrish et al., 1988*) is used for the ClO measurements.

The ozone emission line is quite strong. Therefore the influence of tropospheric water vapor is not as important as for ClO measurements. This leads to a very short integration time of <10 min to achieve an ozone spectrum of good quality. From each 10 min sample an ozone profile can be retrieved. Thus, the AOS can be operated in a time sharing mode. Measurements are performed 24 hours a day, alternating between 15 min of ozone and 50 min of ClO measurements.

Tropospheric Water Vapor

The continuum emission of tropospheric water vapor is included in an emission spectrum measured at ground level. This signal depends on the meteorological conditions and changes occur within a few minutes. Fig. 1 shows variations of atmospheric opacity due to tropospheric water vapor as calculated from the microwave measurements during March 1995. These data were compared with calculated opacities from radiosonde water vapor data. The systematical deviation between the two data sets is still under investigation, but we assume a major cause for the difference are the different air masses measured by the sonde and the radiometer.

For stable meteorological situations with very low water vapor content, such as found for March, 3 and 4 (days 63 and 64), the agreement is much better. However, the large water vapor variability over the winter period detected by the mm-wave radiometer is remarkable.

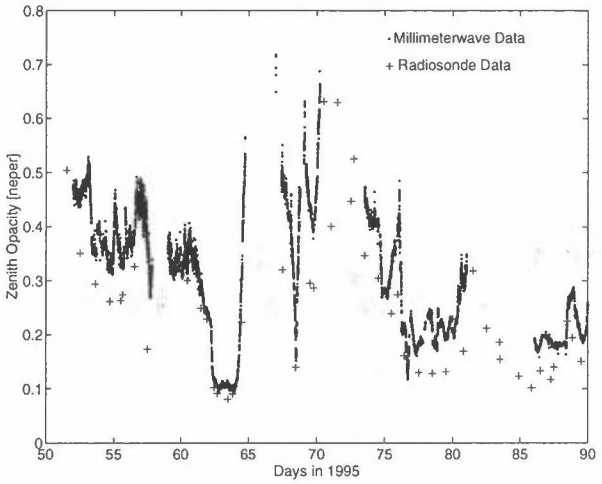

***Figure 1**: Zenith opacity at Ny-Ålesund at 204 GHz in 1995 as calculated from ClO measurements and radio sonde data.*

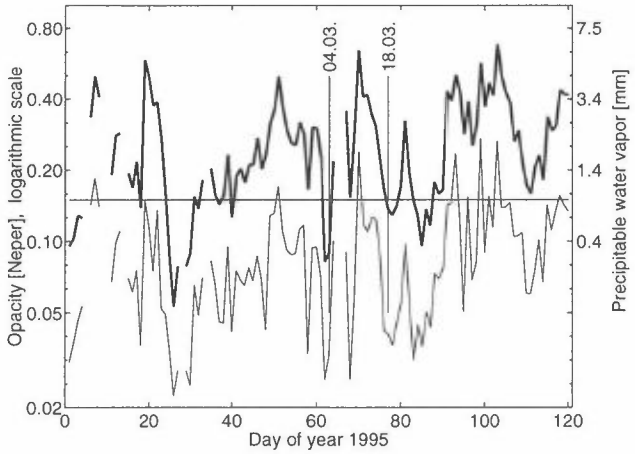

***Figure 2**: Atmospheric opacities due to tropospheric water vapor at 204 GHz as calculated from radio sondes launched at Ny-Ålesund in winter 1995. The dashed line represents the calculated opacities for an observation level of 2000 m. The precipitible water vapor content given at the right side is only an estimate, but it is roughly linear with the opacities (Janssen et al.).*

For our measurements we found, that we can only retrieve ClO profiles for meteorological conditions with tropospheric opacities lower than 0.15 Neper over the entire integration period. This corresponds to a transmissivity of ≥0.54. An analysis of the meteorological sonde data for the winter periods (January throughout March) for the years 1993-1996 at Ny-Ålesund shows, that favorable conditions to measure stratospheric ClO are quite limited. In Fig. 2 we present the zenith opacities for two different observer altitudes. The difference between a site at sea level and at 2000 m, which is nearly the highest point at Spitsbergen, is evident. In Table 1 the percentage of favorable observing time with opacities lower than 0.15 Neper is shown for the 1993-1996 winters. The three presented altitudes are the NDSC building (0 m), the Zeppelin Mountain close the NDSC building (500 m) and 2000 m. This very clearly shows the advantage of a high altitude site, however at present no such site is easily accessible in the Arctic.

Table 1: *Percentage of time in winter periods (Jan-April) with opacities lower than 0.15 Neper as calculated from sonde data for different altitudes.*

z \ year	1993	1994	1995	1996
0 m	17 %	11 %	15 %	8 %
500 m	38 %	22 %	35 %	21 %
2000 m	80 %	77 %	82 %	61 %

ClO Measurements

As explained earlier only very few good observing periods were available over the past three years. An example of a ClO profile for March 4, 1995 is shown in Fig. 3. The RAM profile (solid line) shows two peaks. The lower maximum near 20 km indicates slightly disturbed chemistry. Satellite measurements from the same period do not show significantly enhanced ClO (*Manney et al.*, 1996). The RAM data were also compared to profiles from SLIMCAT (the 3D chemical transport model from the university of Cambridge) and the ASUR instrument, an airborne submm-wave radiometer (see *Urban et al., 1996*), that was flown towards Spitsbergen on March 4, reaching 75.9N/17.7E.

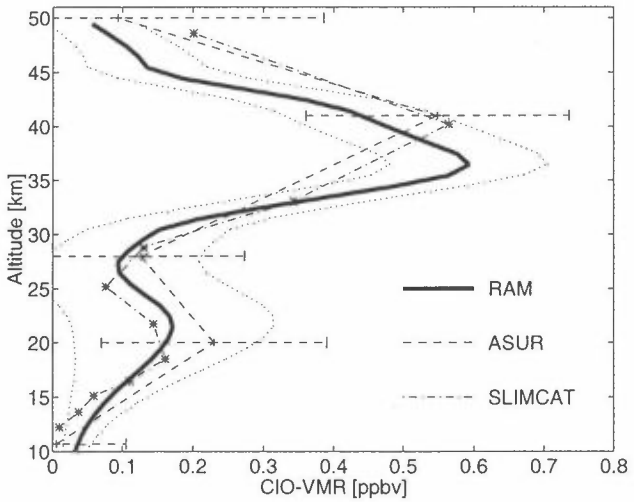

Figure 3*:ClO-profile (solid line) with corresponding uncertainty (dotted lines) from March 3-4, 1995, compared with data from SLIMCAT-model and ASUR.*

Although the ASUR measurements have been performed ~5° south from Ny-Ålesund the good aggreement between RAM and ASUR data is evident. The SLIMCAT model excellently reproduces the measurements.

Ozone Measurements

Ozone measurements are almost unaffected by meteorological conditions. Since the RAM has been installed permanently in the NDSC building in November 1994 continuous measurements provide data throughout the year. Vertical profiles are retrieved by using the Optimal Estimation Method. The error of the profiles is less than 5% or ±0.1 ppmv, whatever is larger. A comparison with sonde data shows very good agreement.

Fig. 4 shows RAM measurements and SLIMCAT calculations for February and March 1995. Especially at higher altitudes the model reproduces the mm-wave measurements extremly well. In the layer near 20 km differences start to increase on day 70, with the model overestimating the ozone. This is most likely due to an underestimation of the chemical ozone

depletion by the model. This ozone depletion has been confirmed by other investigators (*Rex*, personal communication).

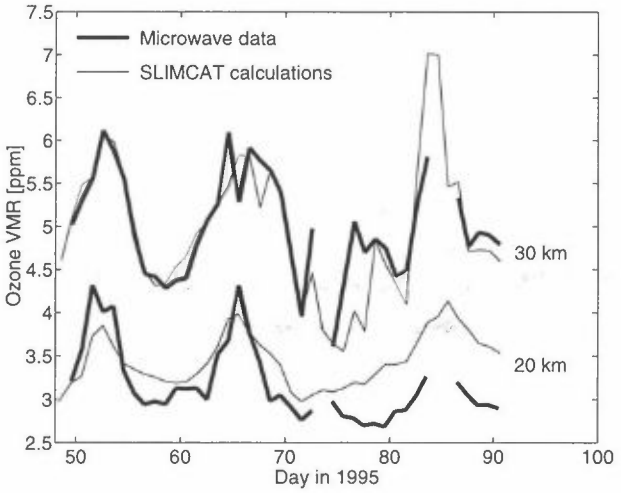

Figure 4: *RAM data and SLIMCAT calculations for February and March 1995 for two different altitudes.*

Since the RAM data have been time averaged to match the time resolution of SLIMCAT (one day), the rapid variations of stratospheric ozone can not be seen to their full extent.An analysis of our data clearly shows rapid ozone variations such as 1 ppmv in the layer at 20 km within a few hours. Most likely this is due to dynamical effects like filaments intruding into the vortex passing Ny-Ålesund. (*Sinnhuber et al., 1996*).

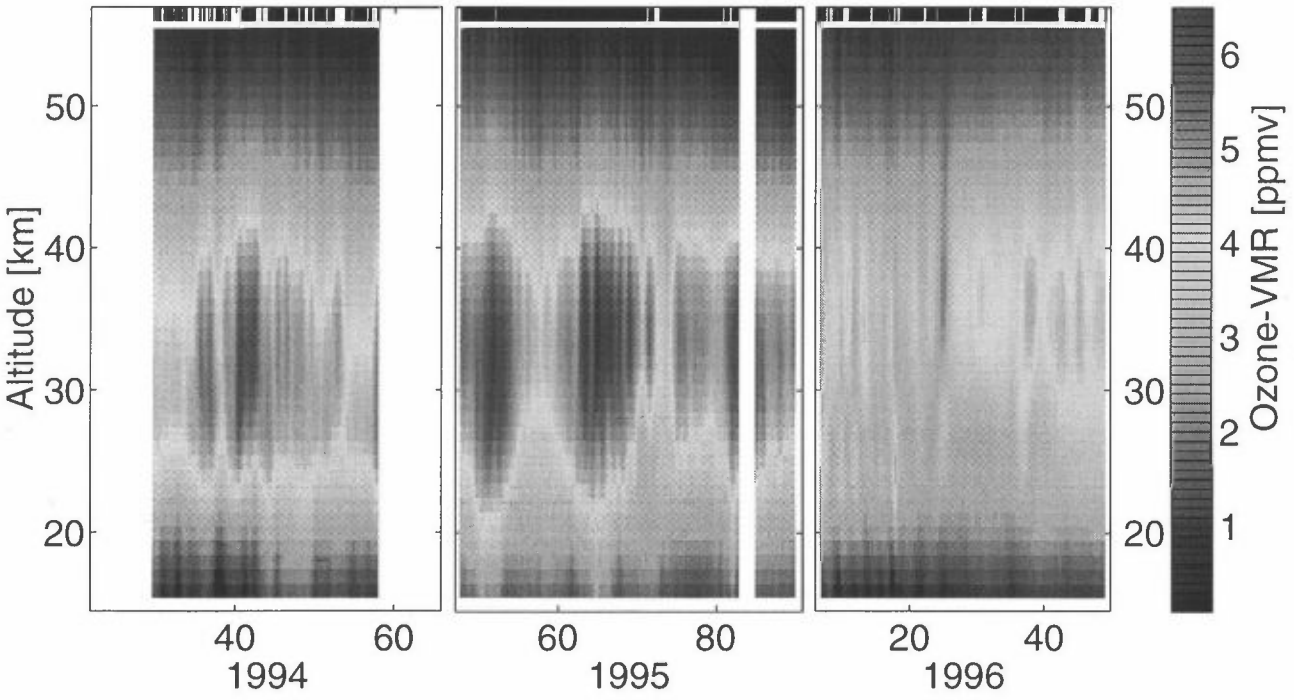

Figure 5*: Wintertime ozone volume mixing ratio above Ny-Ålesund versus Julian day number and altitude for 1994-96. In all three years strong variations of ozone could be observed. Black marks at the top of the graphs indicate single measurements.*

The contour plot presented in Fig. 5 shows the ozone for the winters of 1994-1996. Low ozone is associated with a polar vortex position over Ny-Ålesund and vice versa. The most

prominent feature is seen around day 75 in 1995 with an exceptionally low ozone VMR near 30 km.

The 1996 winter period from January to the end of February in Fig. 5 shows data of reduced quality until day 36 (February 5). This is due to an instrumental misalignment together with very unfavorable weather conditions. Starting with day 37 the RAM configuration was improved significantly. A better suppression of baseline effects (*Langer et al., 1996*) was achieved. This led to a higher quality of the retrievals.

Conclusion

We have obtained profiles of stratospheric ozone and ClO retrieved from measurements with the microwave radiometer RAM at the Arctic NDSC station Ny-Ålesund/Spitsbergen. The instrument enables us to conduct continuous measurements covering an altitude range of 15-55 km with a vertical resolution of 10 km.

The ozone measurements with a temporal resolution of one hour show shortterm ozone variations over a wide range. These data have been used to validate the SLIMCAT model showing good agreement in general. An underestimation of the ozone depletion was found in the layer near 20 km. The total error of the ozone profile is < 5% or ±0.1 ppmv, whatever is larger. The RAM has proven to be a powerful instrument for monitoring ozone nearly unaffected by meteorological conditions with very high temporal resolution.

We have calculated the attenuation due to tropospheric water vapor for a four years period (1993-1996) showing that unfavorable weather conditions - especially the high variability - severly impair microwave measurements of ClO at 204 GHz. The threshold for successful ClO retrievals was found to be 0.15 Neper corresponding to a transmissivity of ≥0.54 for the present configuration of the radiometer.

Two ClO profiles could yet be retrieved for the winter 1995. Both profiles show only slightly disturbed chemistry at altitudes near 20 km at the time of observation. The profile from March 4 was confirmed by the airborne submillimetre ASUR measurements and well reproduced by SLIMCAT calculations. Presently the RAM instrument is the only permanently available ClO sensor in the Arctic.

Acknowledgments. We thank the staff from the Koldewey-Station at Ny-Ålesund for their hospitality and their support during our various campaigns. We also thank H. Gernandt from the Alfred-Wegener-Institute, Potsdam, for providing us with sonde data. This work was funded by the German Ministry for Education and Research (BMBF), the Alfred-Wegener-Institute and the European Community.

References

Janssen, M. A., Atmospheric Remote Sensing by Microwave Radiometry, Wiley, New York, 1993.

Langer, J., U. Klein, K. F. Künzi, U. Raffalski, G. W. Schwaab, B.-M. Sinnhuber, A versatile millimeter-wave radiometer for spectroscopic measurements of atmospheric trace gases, *Proceed. of the Quadr. Ozone Symp, L'Aquuila, Italy, 1996.*

Parrish, A., R. L. de Zafra, P. M. Solomon, and J. W. Barrett, A ground-based technique for millimeter wave spectroscopic observations of stratospheric trace constituents, *Radio Sc.*, 23, 106-118, 1988.

Sinnhuber, B.-M., J. Langer, U. Raffalski, K. F. Künzi, On short- and longterm variability of arctic stratospheric ozone, *Proceed. of the Quadr. Ozone Symp, L'Aquuila, Italy, 1996.*

Urban, J., V. Eyring, H. Küllmann, K. F. Künzi, G. Mellmann, J. Wohlgemuth, Observations of stratospheric ClO, HCl, O3, N2O and HO2 at high latitudes during winter 1995 and 1996 with the Airborne-Submillimeter-SIS-Radiometer, *Proceed. of the Quadr. Ozone Symp, L'Aquuila, Italy, 1996.*

Manney, G. L. et al., Arctic Ozone Depletion Observed by UARS MLS during the 1994-1995 Winter, *Geophys. Res. Lett.*, 17, 85-88, 1996

Modelling Arctic Stratospheric Ozone

Ivar S.A. Isaksen and Bjørg Rognerud
Institutt for Geofysikk, University of Oslo

1. The ozone depletion problem

The ozone depletion issue has been on the scientific agenda almost continuously since Paul Crutzen and Harold Johnston in 1971 pointed out that a projected fleet of supersonic aircraft could harm the protecting ozone shield around the Earth. It is well known that ozone is generated in the stratosphere through the photodissociation of molecular oxygen by short-wave solar radiation. This production occurs in the middle stratosphere at low latitudes where the solar short-wave radiation is strongest. The ozone is redistributed by transport processes taking place in the lower stratosphere (heights between approximately 15 and 30 km). The transport is particularly important for the ozone levels at high latitudes where ozone column densities (vertically integrated amount of ozone from the surface to the outer part of the atmosphere) are largest. There are large variations in the ozone distribution and in the column amount of ozone; with latitude and longitude, and with season. This was well known before the ozone depletion issue was raised.

A key point in connection with the ozone issue is how the chemical loss process controls the overall ozone distribution in the stratosphere through different catalytic chemical reactions. Our present state of knowledge of the ozone depletion problem is a result of a large and concentrated research effort over the last 25 years. The focus has been on understanding man's impact on stratospheric ozone through the emission of certain chemical compounds (e.g. nitrogen, chlorine and bromine containing compounds). This research consists of laboratory studies, atmospheric measurements and model simulations of atmospheric processes. All together, the studies have advanced our understanding of atmospheric processes in general, and of the impact of man's activities in particular over the last two to three decades.

Studies have shown that the impact on ozone from enhanced levels of ODS (ozone depleting substances) is most pronounced at high latitudes. This is due to two conditions: a) High latitude ozone is far away from the source region making loss during transport more efficient, b) loss through heterogeneous processes are more efficient at high latitudes where the loss process is enhanced by the presence of heterogeneous processes on PSCs (Polar Stratospheric Clouds). The PSCs occur during late winter leading to impact on the ozone which can be detected during late winter and early spring when the effect of perturbed composition has been observed.

The main consequence of ozone layer depletion is: Reduction in stratospheric ozone will lead to a reduction in the total ozone column, thereby allowing more harmful ultraviolet (UV-B) solar radiation to penetrate to the Earth's surface.

Solar flux observations over the Antarctica show that the intensity of the short-wave solar radiation are more enhanced during the period of the "ozone hole" in the spring months (October) than at mid-summer (end of December) when the ozone distribution is back to normal for that time of the year. These particular observations are a clear result of the observed behaviour of the ozone layer.

The relation between ozone depletion and enhanced UV-B radiation has not been as clearly demonstrated at northern latitudes as we have seen in the Southern Hemisphere, although there are evidences of ozone depletion at Northern polar latitudes. However, it has been shown that the significant ozone reductions which has been observed over Europe during the last 5 years has led to enhanced UV-B fluxes. This is for instance very clearly shown in solar flux observations over Thessaloniki in Greece after 1991.

The current situation with ozone-climate interactions suggest that there are available data which link the observed ozone decreases during the last years to enhanced harmful solar radiation. Changes in the height profile of ozone, particularly in the lower stratosphere and in the upper troposphere are of relevance for the Earth's climate. Observations have shown reduced temperatures in the lower stratosphere over the last couple of decades which are likely to be connected to reduced ozone levels.

The result of the observed ozone decreases is, according to model studies, that there will be a cooling effect, particularly at high latitudes in the two hemispheres where the largest ozone reductions are observed. As it now has been clearly demonstrated that the ozone loss to a large extent is a result of enhanced CFC levels, the secondary effect of ozone cooling should be taken into account when the radiative heating from the very potent climate gases CFCs are considered. The result of this is that the CFCs are becoming less important climate gases, than previously assumed when chemical effect on gases like ozone was not considered.

2. Current status of stratospheric ozone loss in polar regions

The most recent analysis of the decrease in total ozone column densities, based on satellite observations, show a global average decrease of 4 to 6 % over the last two decades. However, what is important is that the significant winter/spring-time decreases in the two polar regions are positively identified to be a result of human activities. It is well established that there is a significant springtime (October) decrease of ozone of 50 % or more ("ozone hole") in the total ozone column over the Antarctic continent . The last few years the decrease has been as large as ever (covers an area of approximately 20 million km^2).

Observations performed by European scientists in the Northern polar region during the last 3 - 4 winter seasons show a significant ozone loss in the lower stratosphere (at heights around 20 km.) that can be traced back to enhanced chlorine levels. The ozone loss has been particularly large during the 1995 and 1996 winter seasons. In some cases chemical induced local ozone losses over 30 % have been observed.

The man induced ozone losses at Northern latitudes are of particular interest since these losses occur close to or in some cases over populated areas.

3. Model studies of ozone loss at high Northern latitudes

Global 2-D and 3-D CTMs (Chemical Tracer Models) have been used to study ozone distribution and changes due to man made emissions of CFCs and bromine compounds. The studies include both long term studies (years to decades) and studies during seasons when the ozone loss is efficient (e.g. late winter spring). The focus of the studies has been on Northern middle to high latitudes (Zerefos et al., 1997; Rummukainen, 1996). 2-D model studies of the

total ozone reduction during 1996 compared to the distribution in 1990 at Northern latitudes is given in Figure 1. The calculated reductions are largest at high latitudes with ozone reductions exceeding 7 % between 1990 and 1996 during the spring months.

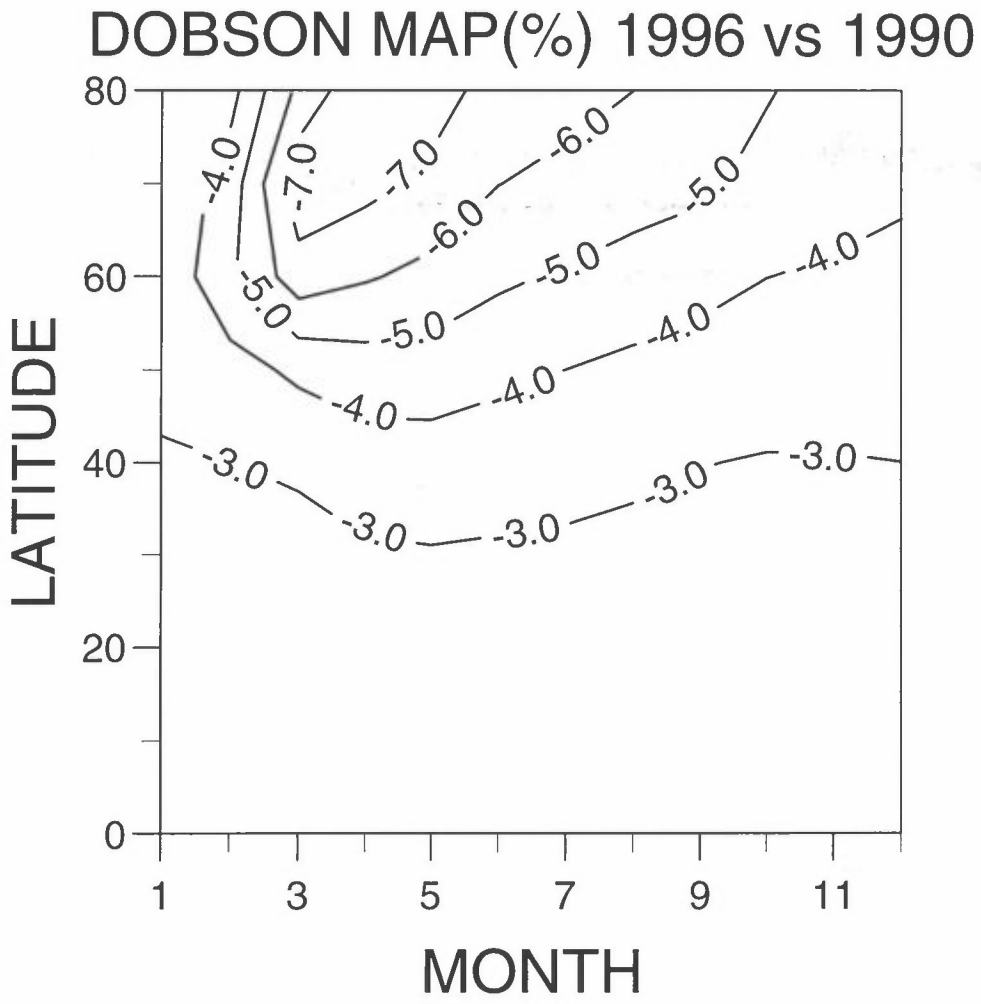

Figure 1. Monthly reductions in total ozone at northern latitudes between 1990 and 1996.

Figure 2 shows how the ozone loss has increased at different height over the time period 1990 to 1996 during the month of March when the impact from particles are most efficient. Increased ozone loss of 10 % at high northern latitudes around 20 km is a result of the presence of PSCs which during that particular year were particularly efficient in perturbing the ozone loss chemistry. There is also significant loss of ozone in the upper stratosphere in the polar regions where particles are not present. Comparisons with observations indicate that the calculated loss in this height region is somewhat overestimated. This overestimation is also found in other model studies. Observations of the ozone loss in the lower stratosphere are ambiguous. Satellite observations give larger ozone losses, while analysis of sonde observations are more in line with the calculated ozone loss in the lower stratosphere.

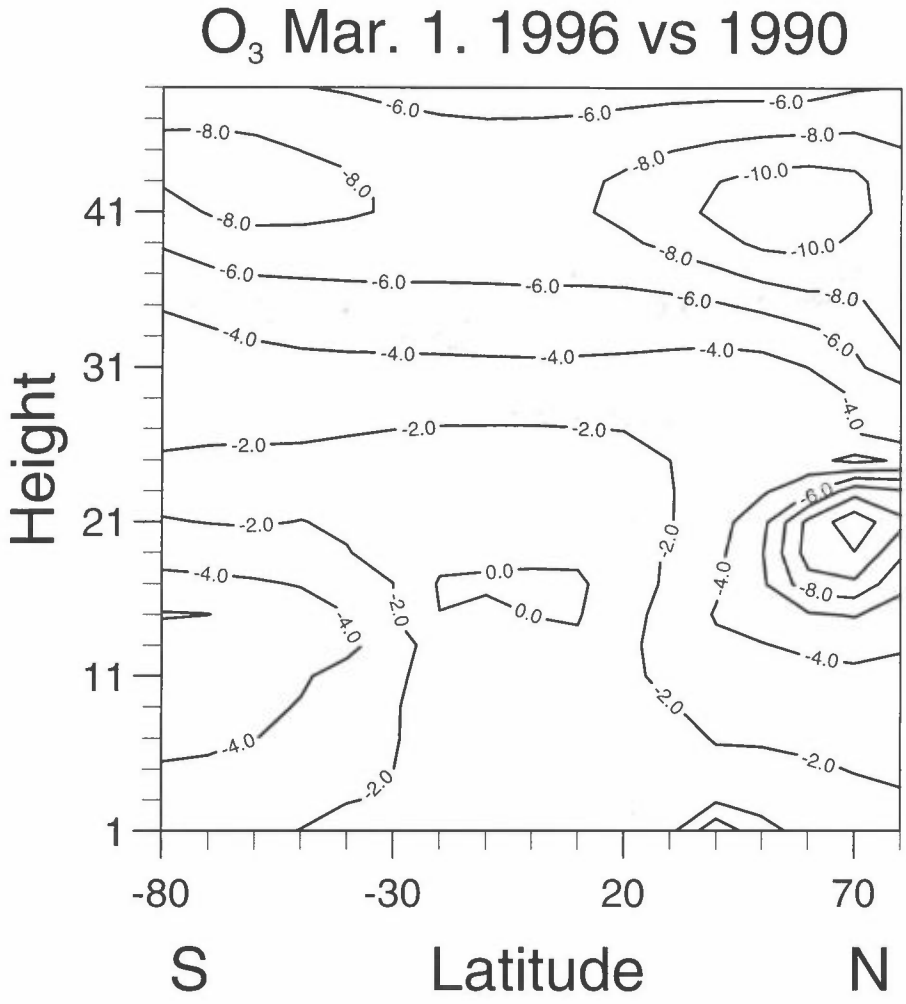

Figure 2. Calculated ozone reduction between 1990 and 1996 for the month of March as a function of latitude and season (in %).

Observations of the atmospheric concentrations of the major man emitted chlorine compounds have shown reduced growth rate during the last few years, undoubtedly a result of reduced emissions of the major CFCs. It will therefore be important to follow closely the development in the ozone layer and in the chemical composition of ozone depleting gases over the next decades. 2-D model studies of the ozone change over the next decades show that there will be a gradual increase in ozone column densities after the turn of the century if reductions in emissions continue as planned.

4. References

Zerefos, C., Tourpali, K., Bojkov, B., Balis, D.S., Rognerud,B., Isaksen, I:S:A:, Solar activity relationships. Observations and mode studies with heterogeneous chemistry. J. Geophys. Res., 102, 1561-1569, 1997.

Rummukainen, M., I.S.A., F. Stordal. Global 3-D model calculations of ozone during a northern hemispheric Winter. To appear in proceedings from The XIII Quadrennial Ozone Symposium, L´Aquila, Italy, 12-21, 1997.

MODEL SIMULATIONS OF TROPOSPHERIC LONG-RANGE TRANSPORT TO THE ARCTIC.

Trond Iversen
Department. of Geophysics
University of Oslo
P.O.Box 1022, Blindern
N-0313 Oslo, Norway

EXTENDED ABSTRACT

of invited paper to be presented at the Scientific Seminar: "Atmospheric Research in Ny-Ålesund", The Norwegian Institute for Air Research, P.O.Box 100, N-2007 Kjeller, Norway, April, 9. - 11. 1997.

Background

The Arctic troposphere was long considered to be a region little influenced by anthropogenic pollution. The main anthropogenic origin of Arctic haze was not convincingly advocated to be probable before the beginning of the 1980s (e.g. Rahn and McCaffrey, 1980; Barrie et al., 1981; Ottar, 1981). Full three-dimensional model-calculation of the main mass-component of the arctic aerosol, particulate sulphate, was first reported after the mid-eighties (Iversen, 1987 and 1989; Barrie et al., 1989). Later on a few more models have been developed and applied for the specific aim of understanding Arctic air-quality, and the set of contaminants have been extended. In parallel, global models have been developed and used for investigating the global distributions and budgets of several contaminants with anthropogenic as well as natural origins. These models also include the Arctic as a sub-domain, but often they are used with a wider scope than the Arctic which frequently is only briefly mentioned in publications describing the model-results. An increasing amount of measurement data from Arctic areas documents, however, that understanding Arctic air quality is important to understand prcesses related to atmospheric chemistry, physics and even to climatic change. The present paper will address model-results for Arctic air quality which hopefully will illustrate some of these points. Some results are published, but considerable parts will treat unpublished results. The honour and responsibility for these results reside with the authors who very kindly have trusted me with the dearest of their scientific property: their latest modelresults. These are Dr. Jesper Christensen, Dr. Janusz Pudykiewicz, Dr. Leonor Tarrason, Mr. Øyvind Seland, and Dr. Terje Berntsen.

Modes of modelling

Transport of contaminants to the Arctic can take transport routes through several geophysical compartments; the atmosphere, the oceans and the freshwater flows in rivers and soils. The atmosphere provides the fastest transport route for most contaminants. Atmospheric transport modelling therefore also is modelling of the major transport pathway in most cases. From an atmospheric point of view it is natural to separate between two basically different types of contaminants. **One-hop compounds** are released into the atmosphere once, transported a distance away from its source determined by the atmospheric residence time, and finally deposited as dry deposition or through precipitation scavenging. **Multi-hop compounds** have the possibility to be recycled to the atmosphere after its deposition, and their environmental residence time determines their potential transport distance and not only their atmospheric residence time. Examples of one-hop compounds are those constituing Arctic haze (sulphate, soot, trace metals except mercury); examples of multi-hop compunds are several persistent organic pollutants (POP), mercury and carbon dioxide. Models aiming at one-hop compounds are often adequately studied by a pure atmospheric model with hemispheric-scale coverage; whilst multi-hop compounds in general require global coverage and ways to treat inter-compartment fluxes. In some applications recycling can be disregarded by prescribing concentrations in soils and waters, and run a pure atmospheric model over short time-spans (e.g. a year) to obtain temporal and detailed air-concentrations. Complete multi-hop cycle-modelling involves soil models and transport in oceans, including the oceanic deep waters. The latter requires transport simulation over decades and longer, and the degree of spatial and temporal detail in the results has to be limitted.

Transport modelling in the atmosphere, as well as in the oceans, requires knowledge of three-dimensional flow-velocities and their variation in time. Furthermore, parts of the transport can only be described quantitatively as diffusion, and atmospheric chemistry and deposition processes depend on several physical variables in the atmosphere. The information about wind, turbulent diffusion and other meteorological variables are generally provided by models for the atmospheric dynamics. These meteorological models are regularly run in a mode which include assimilation of metorological observations. Wind-vectors and diffusion coefficients taken from such models as input to contaminant dispersion models are necessary in order to be able to compare the results with measurements taken at specific places and times. The transport modelling is then considered to be **time-specific and time-resolved**. In this case interpolations of the meteorological fields are needed, and the transport is said to be estimated by **off-line modelling**. If the calculation of contaminant transport is an integral part of the model for the dynamics, we are doing **on-line modelling**. The latter is the more consistent procedure, but so far little success has been obtained by on-line modelling which is time-specific. This is due to the so-called spin-up problems. When meteorological observations are introduced intermittently during the integration of the meteorological model, noise is created and fields of relative humidity does not match the vertical motions

immediately after the data assimilation step. In extratropical regions it normally takes 6 to 12 hours of simulated integration before a new balance is achieved. As a consequence, on-line models are not time-specific and have to be validated by comparing model climatology with observed climatology. This basically requires much longer simulation periods than time-specific modelling. Another type of model-calculation which is nither time-spcific nor time-resolved is the use of climatologically averaged meteorological data. Such models can estimate climatological concentration and deposition levels without having to simulate over a very long period. In this case it is important that the climatological transport fields are representative for mass-transport. This is not a trivial problem, so it is questionable to what extent dispersion modelling based on climatological input is cost-efficient.

Models for one-hop compounds

Sulphur dioxide and particulate sulphate have been the subject for the bulk parts of model-studies with focus on Arctic air-quality. These aim at explaining Arctic haze which is observed regularly each late winter/early spring in the Arctic. Iversen (1989) developed and applied a hemispheric scale model with simplified chemistry by a prescribed oxidation rate for sulphur dioxide to sulphate. Based on emission data from Semb (1985) and meteorological data from US NMC, the model was run for March and June-July 1983. Seasonal contrasts as well episodic behaviour were reasonably well reproduced. Later the model was in addition run for October 1982 and January 1983, and with a more comprehensive validation (Tarrason and Iversen, 1982). More recently the model has been run for a full year (1988), with meteorological data from ECMWF and with updated emission data from GEIA (Tarrason, 1995). The model has been further developed into a more comprehensive aerosol model with several particle classes for sulphate depending on the oxidation pathway, and with black carbon included. The oxidation is now calculated based on oxidant-levels provided by a global photo-oxidant model (Berntsen, 1994), and on model-estimated cloudiness. BC-emissions have been obtained by Cooke and Wilson (1996) (Seland and Iversen, 1997). Furthermore, it has been redesigned by Tarrason (1997) to simulate transport of lead to the Arctic based on emission numbers from Pacyna et al. (1995) (GEIA).

Christensen (1995) developed a model for oxides of sulphur with almost hemispheric coverage also using ECMWF meteorological data. The model has later been applied for five consequtive years (1990-1994), with considerable success (Christensen, 1997). This model uses a similar oxidation rate as Tarrason and Iversen (1992), and is probably so far the best documantation of Arctic-wide haze with its typical seasonal cycle. The main contribution (50-75%) to Arctic haze is estimated to originate in Russia, whilst the major part of the remaining (20-35%) is coming from European areas outside of Russia. This source-allocation is similar to that made by Tarrason (1995), Iversen (1989) and Barrie et al. (1989).

Dastoor and Pudykiewicz (1996) simulated Arctic sulphur transport on-line in the Canadian global spectral model. A quite detailed oxidation scheme similar to that of Berge (1993) was used, coupled to the model's predicted cloud fields. The fields of in-cloud oxidating agents were not fully three-dimensional and seasonally varying. So far the model does not include feedbacks to the meteorological fields, but the results were promising.

Berntsen (1994) constructed a three-dimensional off-line global model for tropospheric oxidants, with meteorological data from the GISS climate model. The horizontal resolution is quite poor, but the model-results are convincing for many components. In the Arctic winter PAN is accumulating together with volatile hydrocarbons which constitute a potent mixture for photchemical activity when the sun rises above the Arctic horizon in spring. There is no chemistry in the model which enable the so-called ground-level ozone-hole regularly observed during polar sunrise, however.

Models for multi-hop compounds

To this author's knowledge there are no modelling results so far available for mercury which cover the Arctic areas. And he also only knows about modelling of one type of POP, namely the alpha and gamma isomers of Hexachloro-Cyklo-Hexane (HCH), of which the gamma-isomer (Lindane) is the more toxic component. HCH is amongst the volatile POPs, and thus is associated with particulate matter to a less extent than many other POPs. Strand and Hov (1996) disregarded the particulate phase completely in their HCH-model. This model is a multicompartment, two-dimensional model with height and latitude as independant variables (model for zonal averages). The atmosphere is separated into 4 layers up to 33 km with an increasing layer thickness with height: the atmospheric boundary layer (ABL), the lower free troposphere, the upper troposphere and lower stratosphere, and the main stratosphere. The ocean is separated into a upper mixed ocean layer (MOL) of 75 m and a 3750 m thick deep water layer. The soil compartment is modelled as one soil layer, separating between cultivated an un-cultivated land. Each compartment is separated into 30 degree latitude bands. Meteorological data are taken from Plumb and Mahlman (1987), and emission data for the two isomers are taken from Ottar and Semb (1989) and Semb and Pacyna (1989). Data on soil quality is taken from Jury et al. (1983) and oceanic transport data are from Siegenthaler and Joos (1992). The destruction and sedimentation of HCH is prescribed by compartment-specific time-constants. In the atmosphere no chemical turnover is assumed since the timescale of transformation from the gamma- to the alpha-isomer is believed to be much slower than the atmospheric loss-rate by deposition. The Henry's law coefficient for equilibrium between water and airborne HCH is taken from Kucklick et al. (1991). The model results for the ABL and MOL compares reasonably well with measurements. In the box representing the Arctic underestimations seem to be larger than at other latitudes. Model estimates of parameter-sensitivity indicate that the Henry-law

coefficient is the most decisive parameter for the atmospheric content of HCH.

Pudykiewicz (1997) is in progress with a three-dimensional atmospheric GCM with HCH included. This model is not multi-compartment, and thus is used on a shorter time frame (a year) to better estimate the distribution of HCH in the atmosphere. Considerable amounts are modelles at high latitudes in the Northen Hemisphere, but no model validation is so far available.

REFERENCES

Barrie, L.A., R.M. Hoff and S.M. Daggupaty, 1981, The influence of midlatitudinal pollution sources on haze in the Canadian Arctic. *Atmos. Environ.*, **15**, 1407-1419.

Barrie, L.A., M.P. Olson and K.K. Oikawa, 1989, The flux of anthropogenic sulphur into the Arctic from mid-latitudes in 1979/80. *Atmosph. Environ.*, **23**, 2505-2512.

Berntsen, T.K., 1994, Two- and three-dimensional model calculations of the photochemistry of the troposphere. PhD.-Thesis, University of Oslo, Norway.

Christensen, J.H., 1995, Transport of air pollution in the tropoosphere to the Arctic. PhD.-thesis, National Environmental Institute, Roskilde, Denmark.

Christensen, J.H., 1997, *Personal communication.*

Cooke, W.F. and J.J.N. Wilson, 1996, A global clack carbon aerosol model. *J. Geoph. Res.*, in press.

Dastoor, A.P. and J. Pudykiewicz, 1996, A numerical global meteorological sulfur transport model and its application to Arctic air pollution. *Atmos. Environ.*, **30**, 1501-1522.

Iversen, T., 1987, Simulation of the atmospheric transport of sulphur dioxide and particulate sulphate to the Arctic. NILU OR 83/86. The Norwegian Institute for Air Reserarch, Kjeller, Norway.

Iversen, T., 1989, Numerical modelling of long range atmospheric transport of sulphur dioxide and particulate sulphate to the Arctic. *Atmos. Environ.*, **23**, 2571-2595.

Jury, W.A., W.F. Spencer and W.J. Farmer, 1983, Behavior assessment model for trace organics in soil: model description. *J. Environ. Qual.*, **12**, 558-564.

Kucklick, J.R., D.A. Hinckley and T.F. Bidleman, 1991, Determination of Henry's law coefficients for Hexachlorocyclohexanes in distilled water and artificial seawater as a function of temperature. *Marine Chemistry*, **34**, 197-209.

Ottar, B., 1981, The transfer of airborne pollutants to the Arctic region. *Atmos. Environ.*, **15**, 1439-1445.

Ottar, B. and A. Semb, 1989, Emisions, atmospheric transport, deposition and mass flows of chlorinated hydrocarbons. *8th Int. Conf. of Comité Arctique International (CAI)*, Oslo, Norway. The Norwegian Institute for Air Research, Kjeller, Norway.

Pacyna, J.M., M.T. Scholtz and Y.-F. (Arthur) Li, 1995, Global budget of trace metal sources. *Environ. Rev.*, **3**, 145-159.

Plumb, R.A. and J.D. Mahlman, 1987, The zonally averaged transport chracteristics of the GFDL general circulation/transport model. *J. Atmos. Sci.*, **44**, 298-327.

Pudykiewicz, J., 1997, *Personal communication.*

Rahn, K.A. and R.J. McCaffrey, 1980, On the origin and transport of the winter Arctic aerosol. *Ann. New York Acad. Sci.*, **338**, 486-503.

Seland, Ø, and T. Iversen, 1997, Preliminary, unpublished results.

Semb, A., 1985, Circumpolar SO_2 emission survey. NILU OR 69/85, The Norwegian Institute for Air Research, Kjeller, Norway.

Semb, A. and J.M. Pacyna, 1988, Toxic trace elements and chlorinated hydrocarbons: sources, atmospheric transport and deposition. *Nordic Council of Ministers, Copenhagen, (NORD 1988:74).*

Siegenthaler, U. and F. Joos, 1992, Use of a simple model for studying oceanic tracer distribution and the global carbon cycle. *Tellus*, **44B**, 186-207.

Strand, A. and Ø. Hov, 1996, A model strategy for the simulation of chlorinated hydrocarbon distributions in the global environment. *Water, Air and Soil Poll.*, **86**, 283-316.

Tarrason, L., 1995, Dispersion of sulphur in the Northern Hemisphere. PhD.-thesis, University of Oslo, Norway.

Tarrason, L., 1997, *Personal Communication.*

Tarrason, L. and T. Iversen, 1992, The influence of north American anthropogenic sulphur emissions over western Europe. *Tellus*, **44B**, 114-132.

Flaring of Gas in Western Siberia, an Overlooked Source for CO_2 and Other Anthropogenic Species During Arctic Haze episodes ?

Magnuz Engardt and Kim Holmén
Department of Meteorology, Stockholm University
S-106 91 Stockholm, SWEDEN

Abstract. In order to test recent compilations of anthropogenic CO_2 emissions, we employ a limited-area transport model centered over the Arctic but including the majority of the industrialized regions in Siberia and Europe. The model is run for a winter period using anthropogenic CO_2 emissions only and the results are compared with CO_2 measurements taken at the Zeppelinfjellet monitoring station on Spitsbergen.

We find that the industry centers and the gas-fields in the lower-Ob region (60°-72° N, 65°-80° E) have a very large impact on the CO_2 measurements at Spitsbergen during the studied period. We suggest that flaring of gas may be a significant but overlooked CO_2 source in the former Soviet Union. We also briefly discuss transport patterns into and out of the Arctic and conclude that the polar region is efficiently ventilated in winter; the e-folding time of the Arctic troposphere is of the order of 10 days in our study.

Transport model description

MATCH (Meso-scale Atmospheric Transport and CHemistry modelling system), is a flexible, "off-line", transport model developed at the Swedish Meteorological and Hydrological Institute (SMHI). It is, in the present study, driven by the initialized analysis of the European Centre for Medium Range Weather Forecast. The horizontal resolution is 110 km × 110 km, and the time-step 5 minutes. The model atmosphere is divided into 31 unequally spaced layers; the lowest 1 km is comprised of ~5 layers. Vertical winds are calculated in MATCH after an adjustment of the horizontal wind (see Heimann and Keeling, 1989). The model use an advection scheme similar to Bott (1989a,b) with only little numerical diffusion.

Diurnal and spatial variations in the turbulent transport are parameterized as a function of a vertical exchange coefficient K_Z, and from the local vertical gradient of CO_2 mixing ratio. The current version of the MATCH model has no sub-grid vertical diffusion outside the planetary boundary layer, nor an inclusion of parameterized convective transport in clouds. Studies with passive tracers (Robertson et al., 1996) have nevertheless shown realistic simulations of Radon-222 in the lower troposphere.

To investigate the significance of the initial conditions in this study, we performed a number of tests were we initialized the model with completely different boundary and initial conditions but retained an identical CO_2 source at the surface. Although the initial conditions and boundary values varied considerably, the resulting time-series at Zeppelinfjellet appeared mainly as parallel shifted. This implies that the background mixing ratio is determined by the amount of CO_2 on the model-boundaries, while the synoptic variability are generated by the sources within the model domain.

To calculate the ventilation of the domain, we initialized the whole model with a constant mixing ratio. The tagged air was allowed to flow out of the domain; incoming air was free of tracer. The e-folding time of the air in layer 1-20 of the domain (i.e. up to ~10 km) was 11 days for the period January 10 through February 28, 1993. The efficient ventilation of the Arctic is not compatible with some previous studies (e.g. Shaw and Khalil, 1989) which describe a distinct air mass which tend to be locked away from the circulation at the mid-latitudes in winter. Based on these results, we conclude that there is no stagnant Arctic air-mass where anthropogenic pollutants are gradually accumulating

throughout the winter. Rather, there seem to be a vigorous transport of air across the polar regions, carrying polluted air into and out of the Arctic. Tongues of Arctic haze are swept into the region from the mid-latitudes by migrating cyclones on the Arctic-front. The age of the pollution in these tongues is, at least at Spitsbergen, typically no more than a week.

Results

In the following simulations we neglect any sinks for atmospheric CO_2 that may occur in the domain during the studied period. We also neglect all sources for CO_2 except the anthropogenic emissions. Figure 1 illustrate the two different estimates of fossil fuel CO_2 emissions used in this study. Figure 1a shows the Andres et al. (1996) (A96) inventory mapped to the MATCH domain. A96 spread CO_2 emissions *within each country* based on population densities. Figure 1b shows an alternative emission estimate which is derived from the SO_X-emissions by Benkovitz et al. (1996) but scaled such that the total CO_2 emissions are the same as A96 in the MATCH domain, namely 1.9 Pg C year^{-1}.

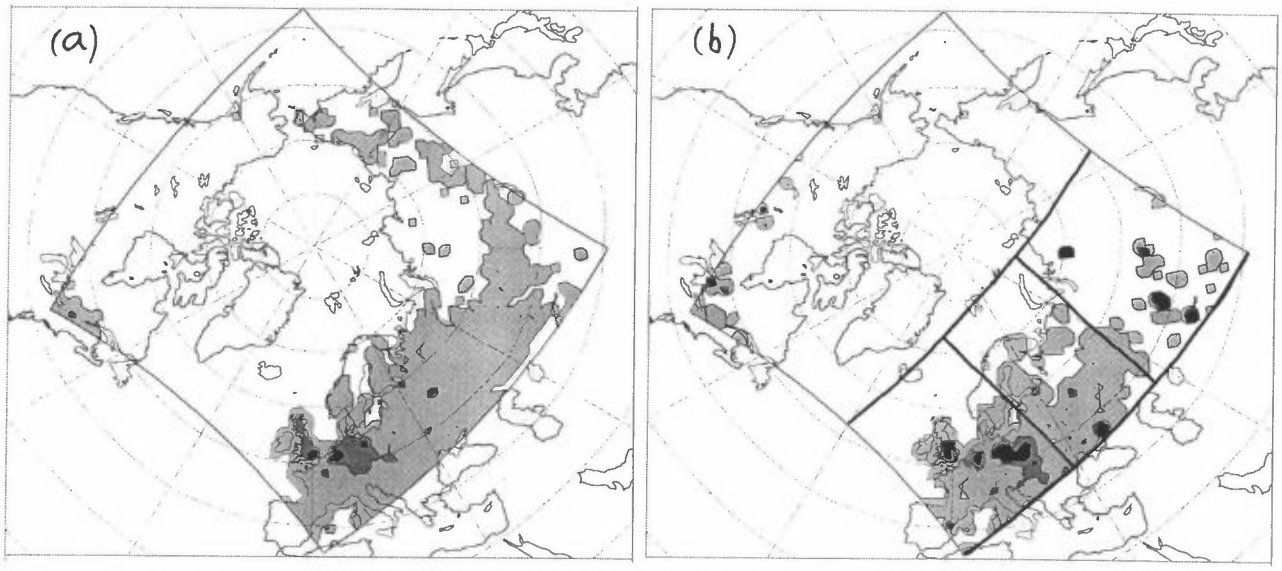

Figure 1. Anthropogenic CO_2 emissions (in g C m^{-2} day^{-1}). (a) from Andres et al. (1996), (b) Constructed from SO_X-data from Benkovitz et al. (1996). Light grey is 0.001-1; dark grey is 1.0-2.0; black denotes emissions greater than 2.0 g C m^{-2} day^{-1}. In (b) the three regions "*W. Europe*", "*E. Europe*", and "*Siberia*" are indicated.

In Fig. 2 we compare the model results at Zeppelinfjellet when using the A96 inventory and the alternative, SO_X-derived source function. In these, and the following simulations, the CO_2 mixing ratios in the domain are set to zero at the beginning of the integrations and the lateral boundaries are treated such that the incoming air is always be free of CO_2. The data is plotted after 3 weeks of spin-up. We note that the SO_X-derived emission field corresponds much better with the measurements than the "state-of-the-art" A96 data. The correspondence with the measured data is, in fact, surprisingly good. Several of the hot spots for SO_X emissions in Siberia emanates from metallurgic activates which should not be accompanied with high CO_2 emissions (but they may affect σ_{sp}, which is mostly determined by anthropogenic sulphate-particles). We therefore suspect that the correlation between CO_2 and SO_X emissions in Siberia is partly coincidental; there are often other, potentially important, but ignored, activities going on in the same regions. We suggest that flaring of gas may be a significant but overlooked CO_2 source in the former Soviet Union (FSU). This hypothesis is also supported by the high correlation between combustion products such as CO_2 and aerosol-particles with CH_4 (Conway and Steele, 1989; Trivett et al., 1989) which may have a large non-combustion source from leakage in connection to natural gas exploitation and transportation (Müller, 1992).

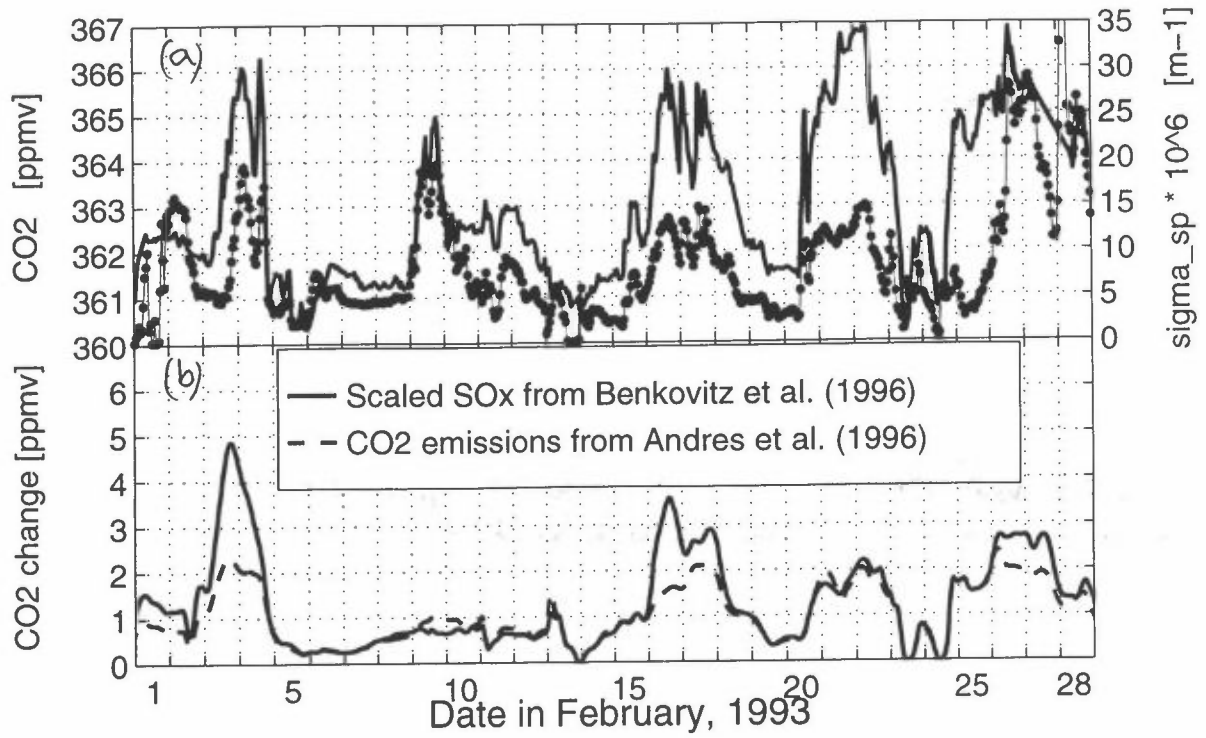

Figure 2. Measured and modelled time-series of CO_2 at Zeppelinfjellet in February 1993. (a) Solid line is hourly median CO_2 from a continuously operating NDIR analyzer, dotted line is half-hour median scattering coefficient of aerosol particles, σ_{sp}, measured by an integrating nephelometer. (b) Instantaneous CO_2 mixing ratio, in the lowest model-layer, plotted every 1 hour. Dashed line is the resulting time-series when the original CO_2 emission inventory from A96 was used, solid line is when the emission were taken from the scaled SO_X-emissions.

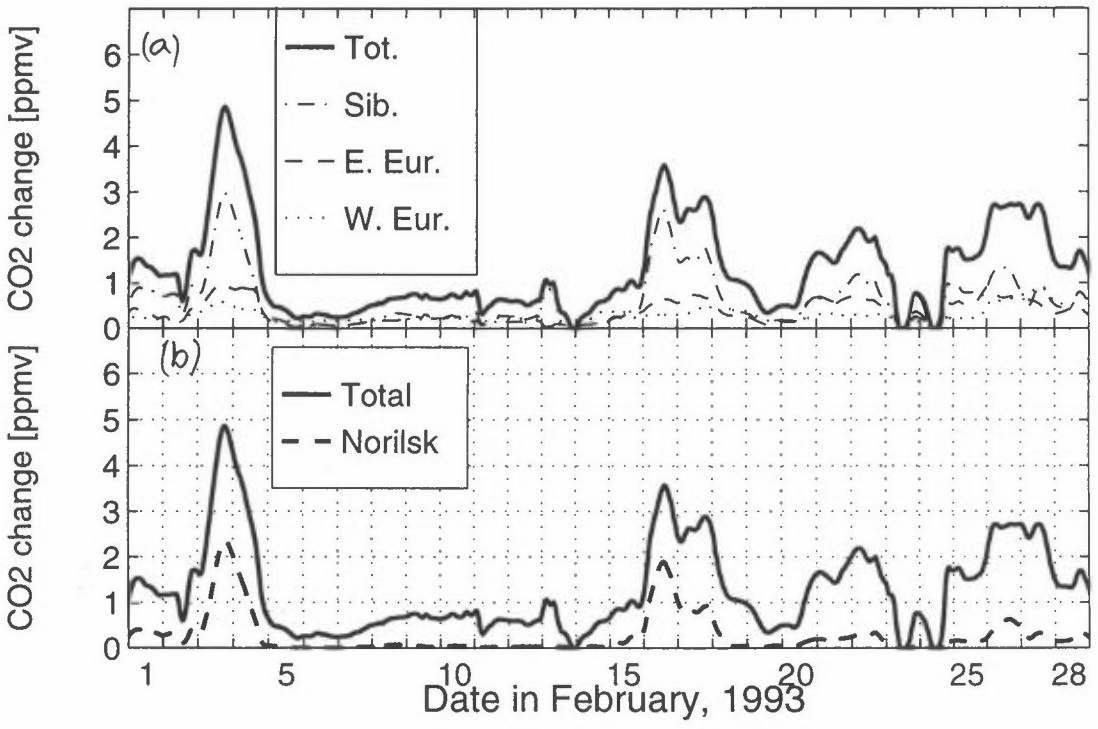

Figure 3. Modelled time-series of CO_2 at Zeppelinfjellet in February 1993. (a) Instantaneous CO_2 mixing ratio, in the lowest model-layer, when only a fraction of the SO_X-derived CO_2 emissions field was used, see Fig. 1b. Dotted line is when only western European emissions are used (1.0 Pg C year^{-1}). Dashed line is when the eastern European emissions are used (0.44 Pg C year^{-1}); Dash-dotted line corresponds to Siberian emissions only (0.36 Pg C year^{-1}). Solid line is the full emission scenario (1.9 Pg C year^{-1}) (i.e. solid line in Fig. 2b). (b) As in a, but dashed line corresponds to emissions from Norilsk only (0.08 Pg C year^{-1}), solid line is the full emission scenario (same as in Fig. 3a).

In order to further investigate which geographical regions that have the greatest impact on the CO_2 measurements at Zeppelinfjellet in winter we divided the SO_X-derived Eurasian emissions into three sub-regions (cf. Fig. 1b), and performed experiments were we retained only the emissions in each one of these regions, see Fig. 3a. As can be seen, the sources in Siberia have a very large impact on the measurements at Zeppelinfjellet, despite the fact that they only comprise ~15% of the amount of CO_2 emitted in the MATCH domain.

The Siberian emissions may be even further split up to illustrate the importance of a small distinct region. Figure 3b displays the result of a simulation where all sources but Norilsk (69°N, 88°E) were masked away. As can be seen, the emissions from Norilsk often make up half, or more, of the signal during the pollution events at Zeppelinfjellet. The ultra-high SO_X emissions from Norilsk mostly emanates from the roasting of copper and nickel ores and is not accomplished by high CO_2 emissions. However, in the adjacent lower-Ob region (60°-72° N, 65°-80° E) there are huge gas-fields and we suggest that this specific area is actually one of the main sources for the haze layers measured throughout the Arctic in winter.

Acknowledgements. J. Langner, C. Persson, and L. Robertson at the SMHI are acknowledged for providing access to the MATCH model. The European Commission (through the support of ESCOBA) and the Nordic Council of Ministers are acknowledged for financial support. The CO_2 monitoring at Zeppelinfjellet is financed by the Swedish Environmental Protection Agency.

References

Andres, R.J., Marland, G., Fung, I. and Matthews. E. 1996. A 1° × 1° distribution of carbon dioxide emissions from fossil fuel consumption and cement manufacture, 1950-1990. *Global Biogeochem. Cycles* **10,** 419-429.

Benkovitz, C.M., Scholtz, M.T., Pacyna, J., Tarrasón, L., Dignon, J., Voldner, E.C., Spiro, P.A., Logan, J.A., and Graedel, T.E. 1996. Global gridded inventories of anthropogenic emissions of sulfur and nitrogen. *J. Geophys. Res.* In press.

Bott, A. 1989a. A positive definite advection scheme obtained by nonlinear renormalization of the advective fluxes. *Mon. Wea. Rev.,* **117,** 1006-1015.

Bott, A. 1989b. Reply. *Mon. Wea. Rev.,* **117,** 2633-2636.

Conway, T.J. and Steele, L.P. 1989. Carbon dioxide and methane in the Arctic atmosphere. *J. Atmos. Chem.,* **9,** 81-99.

Heimann, M. and Keeling, C.D. 1989. *A three-dimensional model of atmospheric CO_2 transport based on observed winds: 2. Model description and simulated tracer experiments.* In: Aspects of Climate Variability in the Pacific and the Western Americas (ed. D.H. Peterson). American Geophysical Union, Washington, DC, pp 237-275.

Müller, J.-F. 1992. Geographical distribution and seasonal variation of surface emissions and deposition velocities of atmospheric trace gases. *J. Geophys. Res.* **97D,** 3787-3804.

Robertson, L., Langner, J., and Engardt, M. 1996. *MATCH - Meso-scale atmospheric transport and chemistry modelling system. Basic transport model description and control experiments with ^{222}Rn.* Swedish Meteorological and Hydrological Institute, **Report RMK-70**, 37 pp.

Shaw, G.E. and Khalil, M.A.K. 1989. *Arctic haze.* In: The Handbook of Environmental Chemistry, Vol 4B, (ed. O. Hutzinger). Springer-Verlag, Berlin Heidelberg, pp 69-111.

Trivett, N.B.A., Worthy, D.E.J., and Brice, K.A. 1989. Surface measurements of carbon dioxide and methane at Alert during an Arctic haze event in April, 1986. *J. Atmos. Chem.,* **9,** 383-397.

Atmospheric Transport of Mercury to Ny-Ålesund. Comparison of Model Results with Measurements.

Jerzy Bartnicki[1], Torunn Berg[2], John Munthe(3), Andrzej Mazur[4], Jaroslaw Hrehoruk[4]
[1]Norwegian Meteorological Institute (DNMI), Oslo, Norway
[2]Norwegian Institute for Air Research (NILU), Kjeller, Norway
[3]Swedish Environmental Research Institute (IVL), Goteborg, Sweden
[4]Institute for Meteorology and Water Management (IMGW), Warsaw, Poland

Introduction

A large part of pollution deposited in the Arctic environment comes from the distant anthropogenic sources in Europe, America and Asia. Natural sources can also significantly contribute to measured concentrations and deposition of some pollutants. One example of such pollutants are heavy metals and especially mercury. Concentrations of different species of mercury have been measured at Ny-Ålesund in 1995 and also during three-weekly campaigns in 1996. To estimate the role of long-range transport of mercury to the Arctic from European sources, a modified version of the Heavy Metals Eulerian Transport (HMET) model has been used in the present study.

Measurements of mercury at Ny-Ålesund

Gaseous mercury, particulate mercury in air, methylmercury and total mercury in precipitation have been measured by NILU and IVL. Typical concentrations for gaseous mercury measured at Ny-Ålesund were in the range of 1-2 ng m^3. Particulate mercury was below 5 pg m^{-3} and total mercury in precipitation was in the range 3-30 ng l^{-1}. Measured daily values of gaseous mercury are shown in Figure 1 for 1995 and in Figure 2 for 1996.

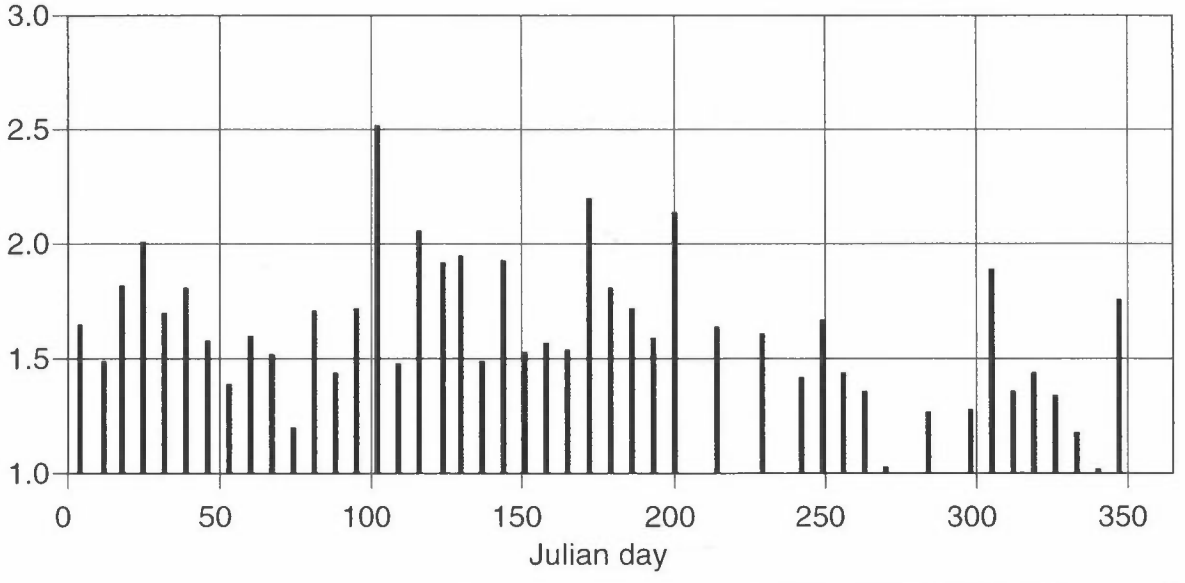

Figure 1. Measured concentrations of gaseous mercury in air in 1995 (SFT 663/96). Units: ng m^{-3}.

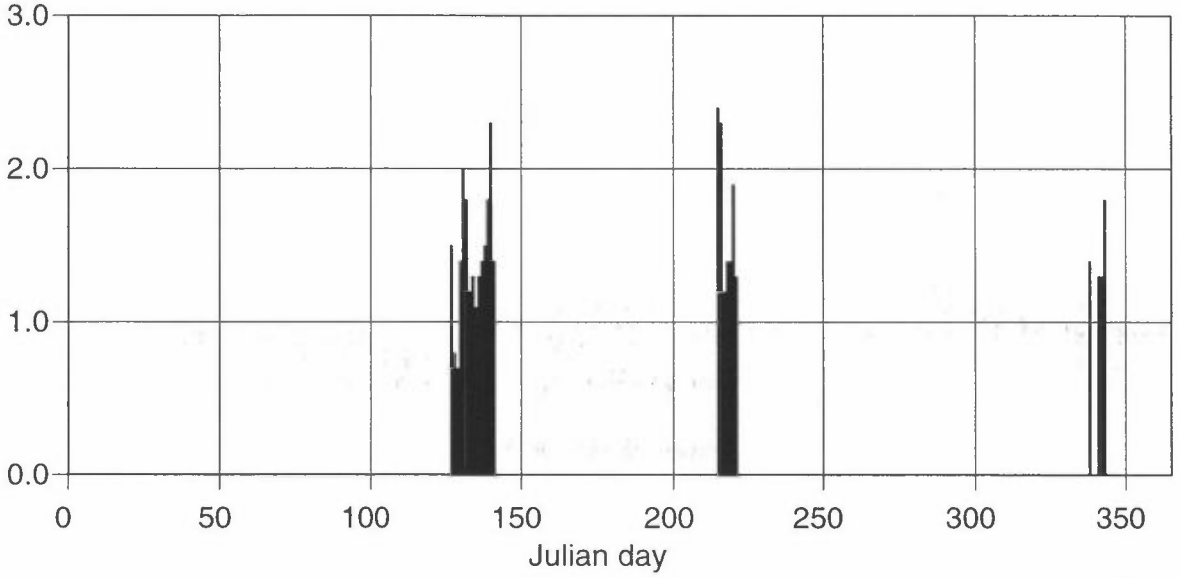

Figure 2. Measured daily concentrations of gaseous mercury in air in 1996. Units: ng m^{-3}.

Measured values of particulate mercury in air in 1996 in Ny-Ålesund are given in Table 1 and the values of total mercury in precipitation are presented in Table 2.

Table 1: Concentrations of particulate mercury measured at Ny-Ålesund in 1996.

Period			Concentration
From		To	ng m^{-3}
2 September	-	3 September	0.0020
3 September	-	4 September	0.0021
6 September	-	7 September	0.0003
7 September	-	8 September	0.0008
8 September	-	9 September	0.0006
2 December	-	3 December	0.0003
3 December	-	4 December	0.0004
4 December	-	5 December	0.0008
6 December	-	7 December	0.0001
7 December	-	8 December	0.0002
8 December	-	9 December	0.0005

The HMET model

The mercury version of the HMET model has been previously validated, in a preliminary way, by comparing its results for 1987 with available observations in Scandinavia. Approximately "factor of two" agreement between measured and computed mercury concentrations was reached in the comparison, but in the future more measurement data are necessary for a better validation of the HMET model. The model is of the Eulerian type and has two dynamic layers,

Table 2: Total mercury in precipitation measured at Ny-Ålesund in 1996.

Period			Concentration
From		To	ng l^{-3}
1 July	-	5 August	31
5 August	-	2 September	3.8
2 September	-	9 September	10
9 September	-	1 October	17

in vertical, so mercury transported above the mixing height is also taken into account. As meteorological input: wind, precipitation, mixing height, surface pressure, temperature at 2 m, turbulent stress and vertical velocity for 1995 were used in the simulations. Simulations for 1996 will also be performed within the project framework, as soon as meteorological data for 1996 are available. In the model computations, we have used 1987 annual emission inventories for three components: elemental mercury (Hg^0), divalent inorganic mercury (Hg(II)(g)) and particulate mercury Hg(part.). Total European emission of mercury in 1987 was 726 tonnes. Emission inventories in the model grid system were kindly provided by Prof. Petersen and Dr. Krüger from GKSS. Since, the latest emission inventories for mercury are available for 1987 (and the same for 1988), we have used these emission inventories to simulate transport from Europe to the Arctic in 1995. Annual average concentration maps of gaseous and particulate mercury are presented in Figures 3 and 4 as examples of the model results for 1995.

Comparison of model results and measurements

Computed model concentrations of mercury were compared with observations at Ny-Ålesund. In case of gaseous mercury, minimum, average and maximum measured values in 1995 were 1.02 ng m^{-3}, 1.66 ng $m^{-3}$and 2.52 ng m^{-3}, respectively. Computed from the HMET model, minimum, average and maximum air concentrations are 1.81 ng m^{-3}, 1.85 ng m^{-3} and 1.92 ng m^{-3}. Agreement between average measured and computed concentration is good but mainly because of the background value, 1.8 ng m^{-3} applied in the model computations. Without a background value, model underestimates measured concentrations of gaseous mercury by almost two orders of magnitude. Also computed air concentration of particulate mercury in air in 1995 - 0.00002 ng m^{-3}, is one order of magnitude lower than measured in 1996 - 0.0007 ng m^{-3}.

Preliminary conclusions

Since the project has not been finished yet, the results presented here should be considered as preliminary. They indicate, that on annual average basis, transport of mercury to Ny-Ålesund can not satisfactory explain the concentrations measured there. Therefore, for the future studies, it will be important to take global anthropogenic sources as well as natural sources into account. A large difference between measured and computed concentrations of mercury can be also partly caused by re-emission processes. In this context, parameterization of the exchange processes between sea and air is an important issue for the future investigations.

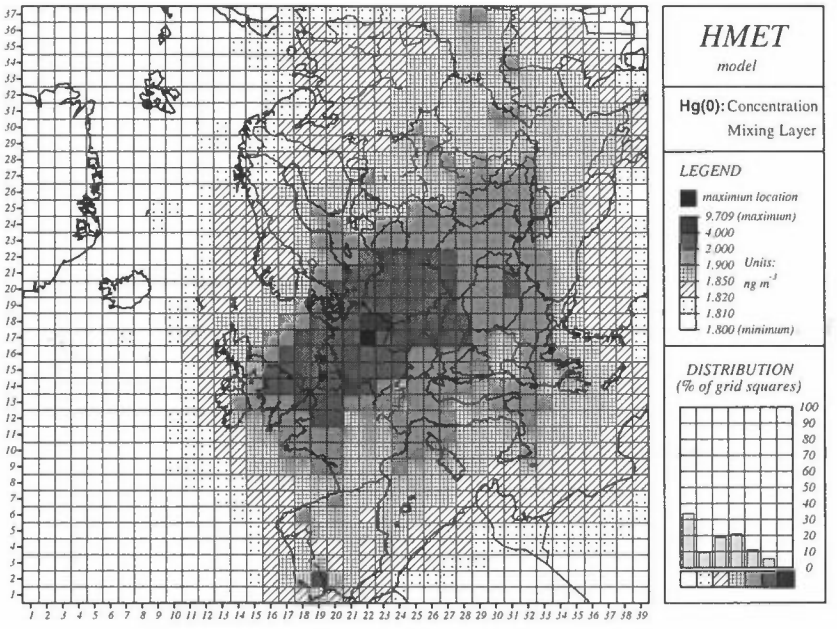

Figure 3. Annual average concentration of gaseous mercury in 1995 computed by the HMET model.

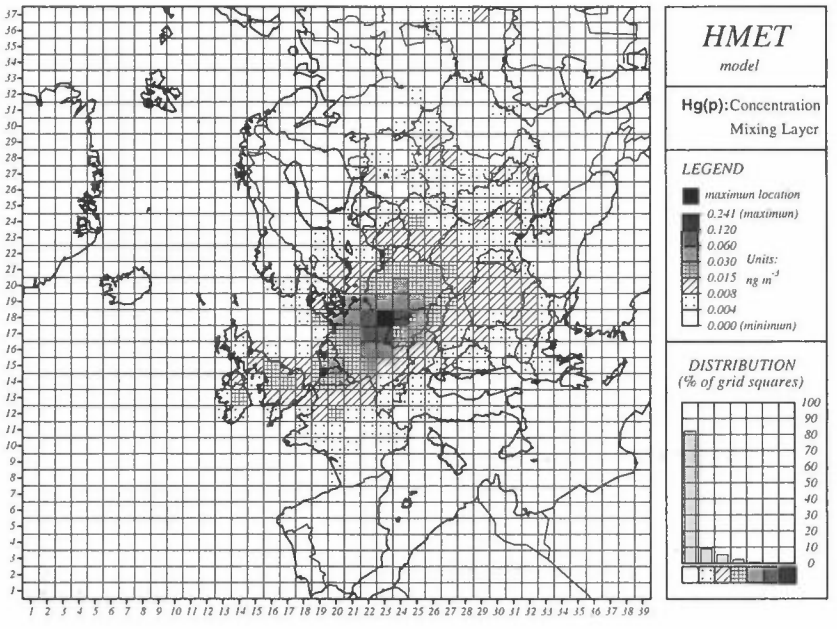

Figure 4. Annual average concentration of particulate mercury in 1995 computed by the HMET model.

Long-term measurements of volatile organic compounds at Ny-Ålesund

Sverre Solberg, Norbert Schmidbauer and Christian Dye
Norwegian Institute for Air Research
P.O. Box 100
N-2007 Kjeller
Norway

Non-methane hydrocarbons have been measured occasionaly at Spitsbergen since the early 1980'ies and regularly on the Zeppelin Mountain near Ny-Ålesund since September 1989 (Hov et al., 1984; Hov et al., 1989; Solberg et al., 1996). Grab samples have been collected in pressurized steel canisters twice a week for some of the time, although there are periods of missing data, as well as periods with sampling each day. The filling of the canisters takes about 10-20 min. The subsequent laboratory anlysis is done by gas chromatography with flame ionisation detection by an automated Chrompack VOC-AIR instrument (Schmidbauer and Oehme, 1986; EMEP/CCC, 1995). The samples were analysed for C2-C5 hydrocarbons in 1989-1991 and extended to include C6-C7 components, as well as aromatics from 1992.

Carbonyl compounds were measured on the Zeppelin Mountain during campaign periods in 1994-1996 (Solberg et al., 1996). The carbonyls were sampled by drawing air through a cartridge which contains silica coated with 2,4-dinitrophenylhydrazine (2,4-DNPH) packed in a polyethylene tube. The sampling time is about 8 hours and the total air sample volume is 750 litres. In the laboratory the cartridges are eluated with acetonitrile, and the sample extract is analysed by reversd phase high-performance liquid chromatography by UV detection, using a Hewlett Packard 1050 modular system equipped with a diode array detector (Slemr, 1991; EMEP/CCC, 1995).

The concentration of the VOCs in the air are determined by emissions (mainly anthropogenic), atmospheric transport processes and chemical reactions. Comparison with measurements in Central- and Northern-Europe indicates that the alkanes become well mixed from Europe into the Arctic during winter. This is explained by the reduced oxidation due to the low concentration of OH radicals. The correlations between individual hydrocarbons at Spitsbergen during winter is very high, also indicating efficient mixing and ineffective chemistry. For acetylene and the alkenes the European concentrations are significantly higher than measured at Spitsbergen even in winter. This could be explained by a combination of alkene + ozone reactions, which is effective also without solar radiation, and the proximity to traffic emission sources (for acetylene).

The average winter concentrations of ethane and propane were higher at Spitsbergen than at Birkenes in southern Norway. The number of data is, however, too few to draw firm conclusions. Sector analysis based on trajectories indicate that elevated concentrations of ethane and propane were associated with transport from across the Arctic basin or from southeast.

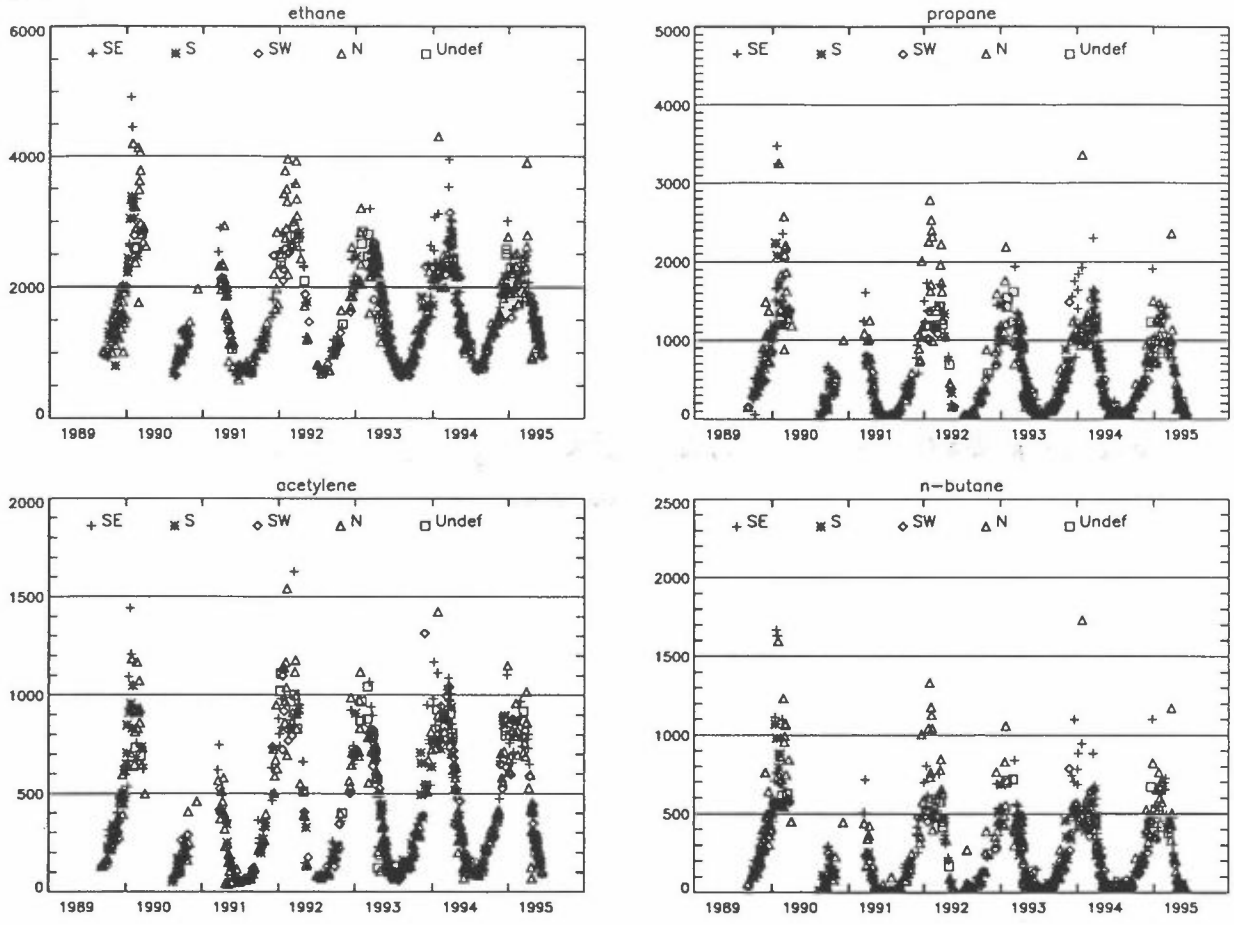

Figure 1. *Measured concentrations of four hydrocarbons at Spitsbergen 1989-1995. The symbols mark different transport sectors.*

References

EMEP/CCC, 1995: Manual for sampling and chemical analysis. Kjeller, Norwegian Institute for Air Research (EMEP/CCC-Report 1/95).

Hov, Ø., Penkett, S. A., Isaksen, I. S. A., and Semb, A., 1984: Organic gases in the Norwegian Arctic, *Geophys. Res. Letters*, **11**, 425-428.

Hov, Ø., Schmidbauer, N., and Oehme, M., 1989: Light hydrocarbons in the Norwegian Arctic. *Atmos. Environ.* **23**, 2471-2482.

Schmidbauer, N. and Oehme, M. 1986: Improvement of a cryogenic preconcentration unit for C2-C5 hydrocarbons in ambient air at ppt levels, *J. High Res. Chromatogr. & Chromatogr. Comm.* **9**, 502-505.

Slemr, J., 1991: Determination of volatile organic compounds in clean air, *Fresenius J. Anal. Chem.*, **340**, 672-677.

Solberg, S., Dye, C., Schmidbauer, N., Herzog, A., and Gehrig, R., 1996: Carbonyls and nonmethane hydrocarbons at rural European sites from the Mediterranean to the Arctic, *J. Atmos., Chem.*, **25**, 33-66.

Seasonal variation and origin of the atmospheric aerosol over Spitsbergen related to the Arctic Sulfur Cycle.

Caroline Leck
Department of Meteorology, S-106 91 Stockholm University, Sweden

Tropospheric chemistry and related measurements

Data collected at the air chemistry station on Zeppelinfjellet (79°N; 12°E, 474 m asl) at Ny-Ålesund, Spitsbergen provides a long-term record of many parameters relevant to cycling of sulfur and climate.

We shall discuss the results from 6 years of submicrometer aerosol measurements. Long-term and seasonal variation of aerosol composition, including soot (EC), biogenic and anthropogenic sulfate (SO_4^{2-}) and methane sulfonate (MSA) will be viewed with an emphasis on segregating the influence on marine biological and anthropogenic sources. These trends will also be related to changes in the general weather circulation of the Arctic region.

For interpretation of the aerosol chemistry samples, results from two particle counters and an integrating nephelometer were available. The history of the air masses sampled was derived from 5-day receptor originated 3D-trajectories.

While non-sea-salt-SO_4^{2-} and EC data showed the typical Arctic Haze seasonality, based on strong inputs of polluted air during November to April, the summer peak in MSA and the second maxima in nss- SO_4^{2-} were related to marine biogenic regional Arctic or high latitude Atlantic or Pacific sources. MSA concentrations fell to winter levels in October.

To provide further characterization of the Arctic natural aerosol and its precursor gas dimethyl sulfide (DMS), attention is also given to the results from two extensive ice breaker expeditions between latitude 75°-90°N in the summers of 1991 and 1996.

Persistent organic pollutants in air measured at the Zeppelin mountain

Martin Schlabach
Norwegian Institute for Air Research (NILU), Kjeller, Norway

Introduction

The Arctic Monitoring and Assessment Programme (AMAP) was established in 1991. The following countries participate in this programme: Canada, Denmark, Finland, Iceland, Norway, Russia, Sweden and USA. The goal of the programme is to investigate the level and trend of antropogenous pollutants in all parts of the Arctic, and its consequences for Arctic ecosystem, including human populations. The monitoring of persistent organic pollutants, heavy metals and radioactivity are issues of major concern. As part of AMAP, NILU started weekly measurements of persistent organic pollutants and hevy metals in April 1993.

The following organic contaminants are included into the measurement programme: hexachlorocyclohexanes (HCH, 2 compounds), hexachlorobenzene (HCB), chlordanes (4 compounds), DDT (6 compounds), polychlorinated biphenyls (PCB, 10 compounds), and polycyclic aromatic hydrocarbons (PAH, 33 compounds).

Sampling

The sampling station is located at Zeppelin mountain (78°55' N, 11°53' E, 474 m above sea level) about 2 km south of Ny-Ålesund, Spitsbergen (figure 1). Today the small settlement Ny-Ålesund hosts different research activities and some touristical activities during the spring and summer months. The former coal mine is closed after a large explosion in 1962.

A sample of approximately 1000 m^3 of air was collected over a period of 48 h once every week. A high-volume sampler was employed using a flow of approximately 20 m^3/h. Particles were collected on glass fiber filters (cut off >99% for 0.2 μm), which had been pretreated at 450 °C for 8 h. Compounds in vapor phase were adsorbed on two sequential polyurethane foam (PUF) plugs.

Sample Extraction and Clean-up

Prior to sample extraction, internal standards were added to the first PUF plug. The glass fiber filter and the PUF plugs were Soxhlet extracted separately for 8 h with 150 and 300 mL of n-hexane/diethyl ether (9:1). The extracts were combined since earlier studies had shown that at the temperatures prevalent at Arctic stations, only a very minor fraction of HCHs (< 3 %) is present in the particle phase. This is reflected in very low concentration levels in the filter extract, which in most cases were close to detection limits and blank values.

Quantification by Gass Chromatography-Mass Spectrometry

All compounds were quantified using high-resolution gas chromatography combined with low or high resolution mass spectrometry.

Quality Control

A rigorous quality control scheme for determination of organic compounds in air, based on the requirements in the European quality norm EN 45001, was carried out. Blank and control samples were run through the complete clean-up procedure frequently and parallel with the air samples. The filter and PUF plug I and II from selected air samples were analysed separately. The particle bound fraction of HCHs consituted less than 1 % of the total amount of HCHs.

Results

The average air concentration of hexachlorocyclohexanes (sum of α- and γ-HCH) was about 76 pg/m^3 in 1995 with variation from 38 to 115 pg/m^3. There was no pronounced seasonal variation. Compared to the results of NILU's measurements from 1981 and 1984, the concentration of α-HCH had decreased. The average reduction of α-HCH through the last three years was about 6-8 pg/m^3 each year. This reduction corresponds to the replacement of technical HCH with γ-HCH (lindane). For γ-HCH no similar reduction was detected during the last ten years.

The concentration of chlordanes (sum of *trans*- and *cis*-chlordane and *trans*- and *cis*-nonachlor) varied between 1 and 5 pg/m^3 . There was no pronounced seasonal variation. The average air concentration of the sum of chlordanes was 2,64 pg/m^3 (1993), 2,96 pg/m^3 (1994), and 2,20 pg/m^3 (1995).

In 1995 the average air concentration of sum DDT (6 compounds) was about 2,0 pg/m^3. The concentration ranged from 0,33 to 6,14 pg/m^3. There was a pronounced saisonal variation with a winter maximum due to meteorological situatuations which allow long range transport from lower latitudes. This is different from the situation at mid and low latitudes with the highest DDT levels occuring during the summer.

During 1995 the air concentration of HCB was about 100 pg/m^3 (41 - 211 pg/m^3).

The yearly average air concentration of sum PCB (10 compounds) was 13,1 pg/m^3 in 1993. In the beginning of 1994 there was a dramatic increase of the three most volatile PCB congeners (28, 31, and 52) which resulted in a higher average for 1994: 112,2 pg/m^3 and 1995: 68,2 pg/m^3. A contamination from local PCB-sources in Ny-Ålesund cannot be excluded.

Polycyclic aromatic hydrocarbons show the same saisonal variation as the DDTs with a winter maximum caused by long range transport from the south. The same trend was observed in the Canadian Arctic. The most volatile compound (PAH) represents about 70 - 90 % of the sum of PAH. The yearly averaged PAH-concentration was 7,2 pg/m^3 (1994) and 5,12 pg/m^3 (1995).

During two special measurement campaigns in the spring and summer 1995, the sampling time was extended to five days. The extracts from four samples were combined and analysed for either toxaphene or polychlorinated dibenzo-p-dioxins and furans (PCDD/PCDF). It was possible to detect both toxaphene and PCDD/PCDF with air concentration of between 0,7 and 1,4 pg/m^3 (sum of tox-26, 50 and 62) and between 1 and 2 fg TE/m^3 (PCDD/PCDF).

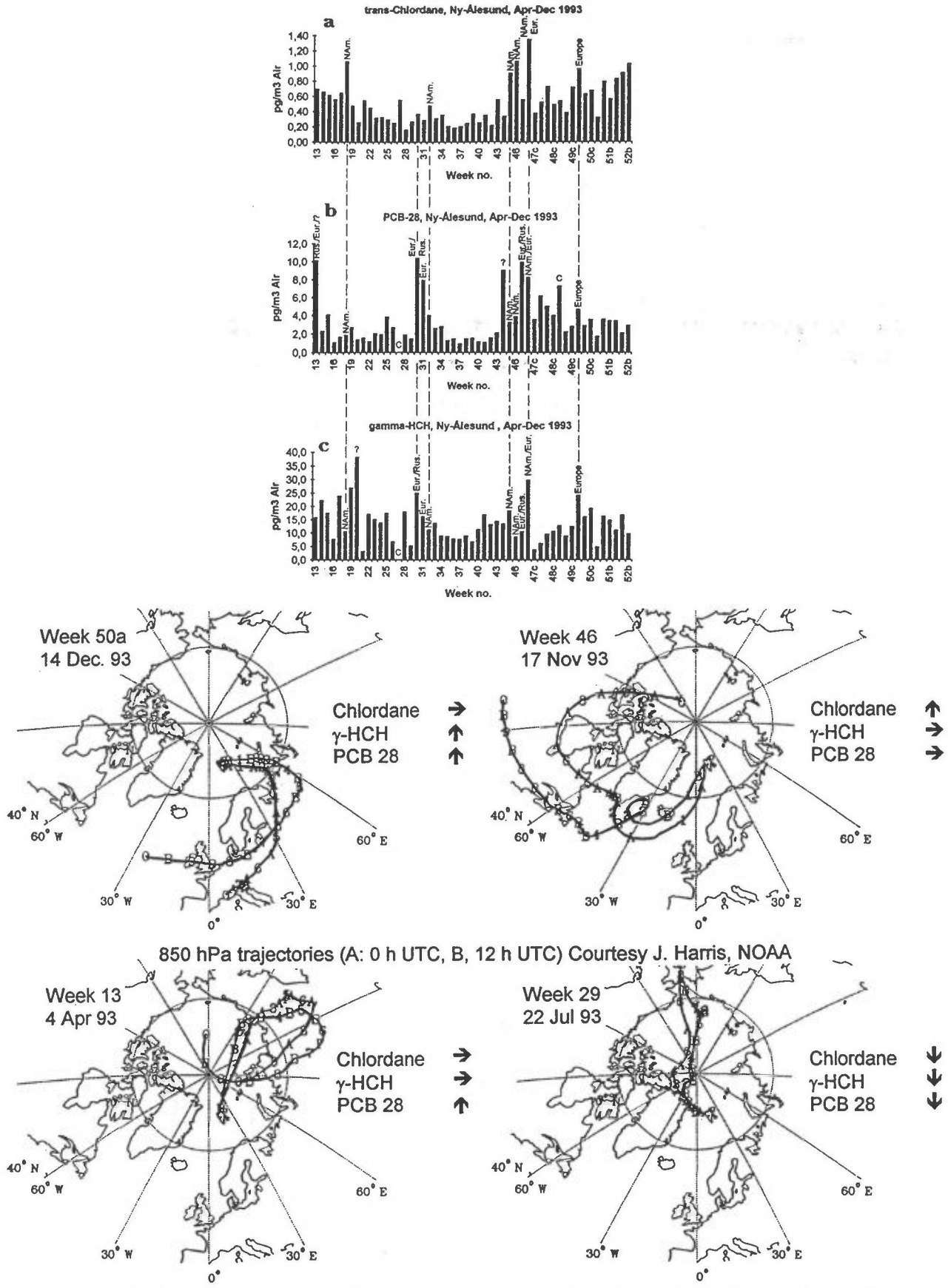

Figure 1a: Weekly concentration profiles of trans-chlordane, PCB-28, and γ-HCH. Long range transport episodes are marked with the origin of the air masses.
Figur 1b: Selected situations of long range air transport to Ny-Ålesund.

Long range transport episodes

Long range transport episodes with long stability can have considerable influence on the air concentration of persistent organic compounds. For some compounds it was possible to demonstrate that short term concentration changes are influenced by the origin of air masses. During long range transport mainly from Europe, levels of both γ-HCH and PCB-28 increased, while *trans*-chlordane remained unchanged. The opposite was the case for transport from North America. Air masses from Siberia showed an increase of PCB-28, but not of the two other compounds. Finally, when clean air was transported via the North Pole, the lowest concentrations during this campaign were observed.

Conclusions

With the described method and a rigorous quality control programme it is possible to sample and analyse the most abundant persistent organic pollutants in Arctic air. During two campaigns in 1995 with extended sampling time (up to four weeks!) it was even possible to determine toxaphene and PCDD/PCDF. Furthermore, significant long range transport episodes could be observed for many pollutants. The input of persistent organic pollutants is dominated by long range transport from sources outside the Arctic.

Star Photometer Measurements During Polar Night

Andreas Herber[1], Siegrid Debatin[1], Hartwig Gernandt[1], Michail Lamakin[2], German Sakunov[2], Axel Naebert[3] and Karl-Heinz Schulz[3]

1 Alfred Wegener Institute Potsdam, Germany
2 Arctic and Antarctic Research Institute St. Petersburg, Russia
3 Dr. Schulz & Partner GmbH Buckow, Germany

Since March 1991 the Alfred Wegener Institute runs integral aerosol measurements in the Arctic (Ny-Ålesund, 78°56'N, 11°56'E) which different types of Sun photometers, additional Moon measurements were performed during the polar night since January 1995. Significant features of aerosol variations could be detect in the Arctic atmosphere, like stratospheric aerosol loading by volcanic aerosol or Arctic Haze.

Measurements during the polar night were carried out with a high sensitive Star photometer since January 1996, which is developed in framework of a research project between AWI Potsdam and Dr. Schulz & Partner GmbH Buckow. This Star photometer is installed in order to perform spectral aerosol optical depth measurements during the whole polar night, whereby the light from different fix stars is used. A typical seasonal variation was observed with the highest values of the aerosol content in winter and spring. The presence of polluted aerosol and lower tropospheric ice-crystals affects this turbidity.

This new ground-based instrument STAR01 works in the same spectral range as the combined Sun- and Moon photometer (390 nm - 1050 nm). Presently we use two different detectors. The first detector is a photon counter on the semiconductor basis (SPCM 200-PQ from EG&G Canada) for the whole wavelength range, whereby the detector area is very small, only 50 mm^2. The second detector is a photomultiplier (R1878 from Hamamatsu, Japan) with a detector area from approximately 12 mm^2, but the spectral range is only from 390 nm to 850 nm. First results of these observations and the experiences with both detectors will be shown.

Rapid Surface Ozone Loss - The Role of Halogen Species

Ulrich Platt

Institut für Umweltphysik, Univ. Heidelberg, INF 366, D-69120 Heidelberg, Germany

Introduction

About a decade ago the phenomenon of complete boundary layer ozone depletion was first noticed by Bottenheim et al. [1986]. Since then sudden, episodic loss of O_3 has been observed at several arctic sites (Fig. 1) including Alert, Canada [Barrie et al. 1988, 1994, Bottenheim et al. 1990, Mickle et al. 1989]; Barrows, Alaska [Sturges et al. 1993], Ny-Ålesund, Spitsbergen [Solberg et al. 1994], Thule [Rasmussen et al. (1996)], and Söndre-Strømfjord [Rasmussen et al. (1996)].

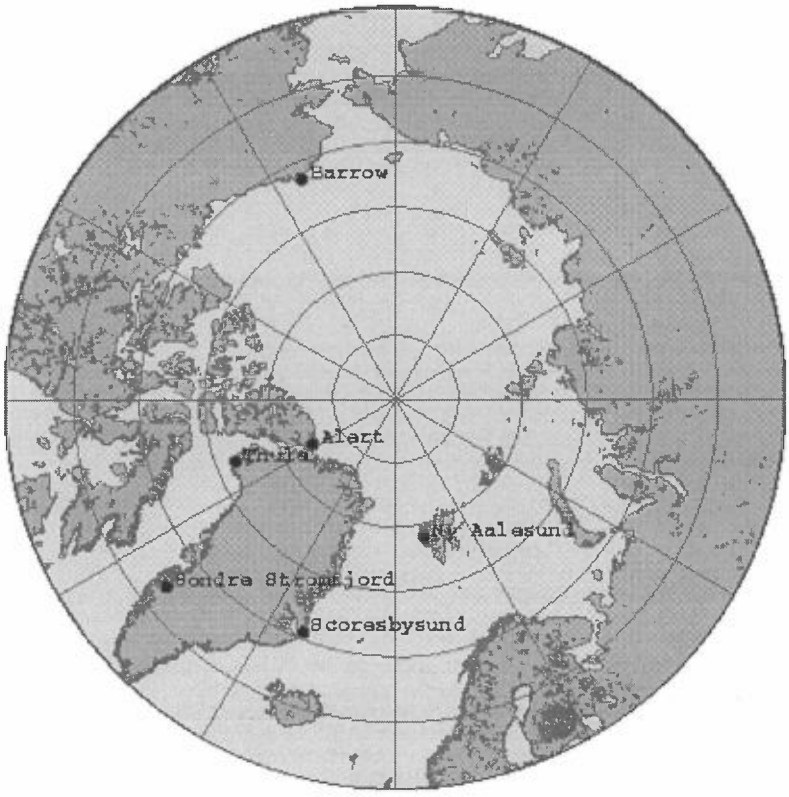

Fig. 1: Episodic destruction of surface ozone has been observed at several arctic sites: Alert, Canada Ny-Ålesund, Spitsbergen, Scoresbysund, Greenland, Söndre Strømfjord, Greenland, Thule, Greenland (from: ARCTOC final report 1996).

A typical springtime Arctic ozone record, as observed during the ARCTOC campaigns at Ny-Ålesund, is presented in Fig. 2. Recently a very similar phenomenon was reported during Austral winter and spring (August, September and early October) from several Antarctic stations: Syowa [Murayama et al. 1992], Neumayer [Wessel 1996], and Arrival Heights [Kreher 1996]. Apparently ozone depletion episodes only occur after polar sunrise. In the Arctic they are most frequent during late April and begin of May. During these episodes O_3 levels drop from the normal 30 - 40 ppb to mixing ratios unmeasurable by standard equipment (< 2 ppb).

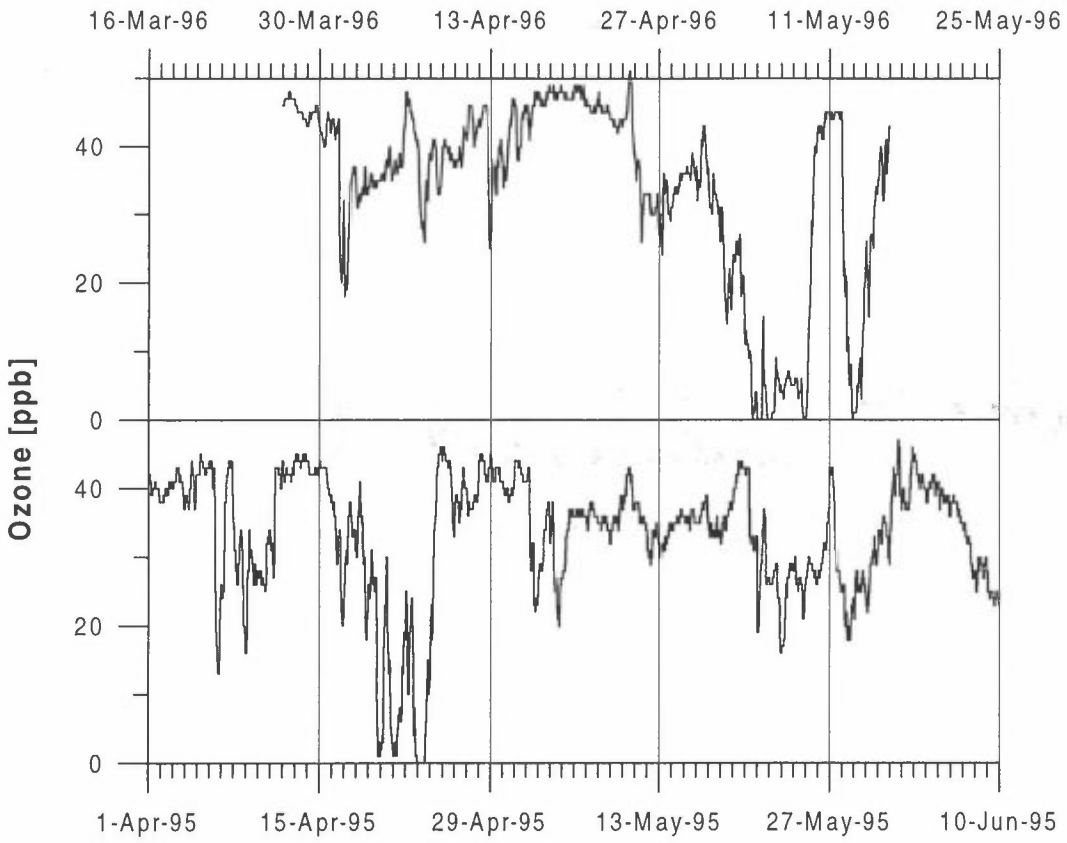

Fig. 2: Ozone variability during the ARCTOC campaigns 1995 and 1996 at Ny-Ålesund /Svalbard

Despite many attempts to explain the phenomenon, the reasons for this phenomenon are only partly understood today. Already early observations showed a striking anticorrelation between ozone and levels of filterable bromine (f-Br), i.e. bromine compounds that can be collected on cellulose aerosol filters [e.g. Barrie et al. 1988, Lehrer et al. 1996] leading to the hypothesis of BrO_x- [Barrie et al. 1988, Bottenheim et al. 1990, Finlayson-Pitts 1990], BrO_x + ClO_x- [LeBras and Platt 1995], or IO_x- [Solomon et al. 1994] catalysed reaction cycles being responsible for the observed ozone destruction. All theories have in common that they assume ozone destruction by the reaction sequence:

$$X + O_3 \rightarrow XO + O_2 \quad \text{(R1)}$$

$$Y + O_3 \rightarrow YO + O_2 \quad \text{(R2)}$$

$$XO + YO \rightarrow X + Y + O_2 \quad \text{(R3)}$$

with the net result:

$$2\,O_3 \rightarrow 3\,O_2 \quad \text{(R4)}$$

In fact recent expeditions unequivocally verified the presence of BrO [Hausmann and Platt 1994] and ClO [Unold et al. 1997, Tuckermann et al. 1997] in the arctic boundary layer. Efficient destruction mechanisms would involve X = Y = Br or X = Br, Y = Cl and possibly X = Br, Y=I (see Table 1). The combination X = Br, Y = Cl or I would be considerably more effective compared to the BrO + BrO reaction. The effect of the IO + IO reaction on ozone is still unclear, but it appears that it is only partly active (depending on the relative importance of the various product channels) with respect to the ozone budget.

Table 1: *Halogen oxide self- and cross reactions and their potential for tropospheric ozone destruction, data from Atkinson et al. [1992], if not otherwise noted.*

No.	Reaction XO + YO	Absolute k_{xy} 10^{-12} cm^3s^{-1} (at 263K)	Relative $k_{xy}/k_{BrO+BrO}$	Remark
1	ClO + ClO	(0.9) 0.01		unstable dimer formed, probably no effect on tropospheric O_3 other products
2	ClO + BrO	8.4[a]	2.6	most likely cause for arctic boundary layer O_3 depletion
3	ClO + IO	6.1[d]	1.9	probably negligible
4	BrO + BrO	3.2[b]	1.0	most likely cause for arctic boundary layer O_3 depletion
5	BrO + IO	69±27[c]	22	potentially very important
6	IO + IO	108[e]	34	effect on trop. O_3 unknown

An additional ozone destruction cycle involves the reaction of HO_2 with halogen oxides:

$$XO + HO_2 \rightarrow HOX + O_2 \qquad (R5)$$

where k_5 (in units of 10^{-11} cm^3s^{-1}) is 0.7, 4.5, and 8.4 for X = Cl, Br, I, respectively. Followed by:

$$HOX + h\nu \rightarrow X + OH \qquad (R6)$$

$$OH + CO \text{ (or VOC)} \rightarrow HO_2 + CO_2 \text{ (or other products)} \qquad (R7)$$

Together with R1/R2 the net effect of the cycle R5 to R7 is also equivalent to R4, while R5 usually will be the rate-determining step. In addition the reaction sequence R5 + R6 plays a similar role in the HO_x cycle as the reaction of NO with HO_2.

It is interesting to note that the halogen oxide self- and cross reaction mechanism (R3) as well as the HO_2 mechanism (R5 + R6) are of zero order in O_3 as long as the ozone concentration does not become too low. In other words the rate of ozone destruction does not dependent on the ozone concentration leading to a nearly linear decay of the ozone mixing ratio.

The total ozone loss rate-limited by the self- and cross reactions of halogen oxides (Table 1) is therefore given by:

$$-\frac{d}{dt}[O_3] = 2\cdot\sum_i ([XO]\cdot[YO])_i \cdot k_i + \sum_j [HO_2]\cdot[X_jO]\cdot k_{Hj} \qquad (\text{Eq. 1})$$

Where i denotes the XO-YO pairs as given in Table 1, while j refers to the different halogens (i.e. X_1 = Cl, X_2 = Br, X_3 = I). The following Table 2 summarises typical rates of ozone destruction expected from measured levels of halogen oxides [Hausmann and Platt 1994, Tuckermann et al. 1997, ARCTOC final report 1996]. Total rates of ozone destruction of the order of 1-2 ppb per hour can easily be reached. While these rates are comparable to observation it is likely that the rates of change in ozone are actually due to advection of airmasses with different ozone levels to the measurement site.

Table 2: Rates of ozone destruction (ppb/hour) by halogen oxide self- and cross reactions

ClO/ppt	BrO/ppt	IO/ppt	d/dt [O_3]
-	32	-	0.33
25	32	-	0.67
-	32	1	0.22

Tropospheric Sources of Reactive Halogen Species

The most important question concerning the ultimate cause of surface ozone loss is the source of reactive halogen species in the troposphere. Unlike the stratosphere, where the dominating source of reactive halogen species is photochemical degradation of fully halogenated compounds, in the troposphere reactive halogen species can only originate from less stable precursors. Many primary liberation processes are thought to yield species like X_2 or XNO_n [Behnke et al. 1993, Finlayson-Pitts et al. 1989], that are easily photolysed to release halogen atoms, which are subsequently converted to XO radicals (R1).

Liberation of from sea salt (aerosol or deposits). Sea salt contains (by weight) 55.7 % Cl, 0.19 % Br, and 0.00002 % I and thus could be a significant source of gaseous halogen species. The magnitude of this source has not been accurately established but there is substantial evidence for its existence. In particular reactions of the nitrogen oxides NO_2 or N_2O_5 with sea salt X^- (aerosol or deposits) can lead to the formation of gaseous XNO or XNO_2, (X = Br, Cl) respectively, which can easily photolyse. [Finlayson-Pitts et al. 1989, 1990; Behnke et al. 1993]. In addition reactions of autocatalytic nature can release RHS from sea salt even in an NO_x free environment [Mozurkewich 1995]. For instance heterogeneous reactions like

$$HOX + (X^-)_{aq} \rightarrow X_2 + (OH^-)_{aq} \qquad (R8)$$

will convert one gas-phase RHS molecule into two. In fact reaction cycles involving R8 can lead to a self-accelerating autocatalytic release of reactive halogen species from sea salt (deposited on ice or aerosol), the so called '**Bromine Explosion**' [Platt and Lehrer 1996].

Degradation of partially halogenated organic compounds, which are emitted by a variety of natural and man-made sources [Sturges et al. 1992]. The former include the oceans, which emit a wide variety of halocarbons such as the methyl halides - CH_3X. (estimated source strength (100-400)$\times 10^9$g CH_3Br/a, $\approx 4\times 10^9$g CH_3I/a [Schall and Heumann 1993]) as well as polyhalogenated species such as bromoform, $CHBr_3$ or CH_2Br_2. Some contribution is also expected from biomass burning (10-50$\times 10^9$g CH_3Br/a [Manö and Andreae, 1994]) and from industrial processes.

Conversion of hydrogen halides: There are substantial direct sources of HF and HCl, as well as of Cl_2 from industrial processes [e.g. Singh and Kasting, 1988]. Probably more important is production of HX by halogen-atom attack on saturated hydrocarbons (R9) or aldehydes. Also likely is liberation from sea salt aerosol by the action of strong acids, such as H_2SO_4 and HNO_3 originating from man made or natural sources [Behnke et al. 1993]. Heterogeneous reactions may convert HX to halogen atoms and thus recycle RHS, as - for instance - suggested by Fan and Jacob [1992], Mozurkewich [1995], Vogt et al. [1996] or Platt and Lehrer [1996]. Homogeneous reactions are less efficient in converting HX to X (see R10 below). In any case recycling of HX to the RHS reservoir is a most critical - yet not understood - process, given the short conversion time RHS $\rightarrow$ HX.

Chemical Cycles of Reactive Halogen Species

The following Fig. 3 illustrates the simplified reaction scheme of reactive halogen species in the troposphere [Platt and Janssen 1996].

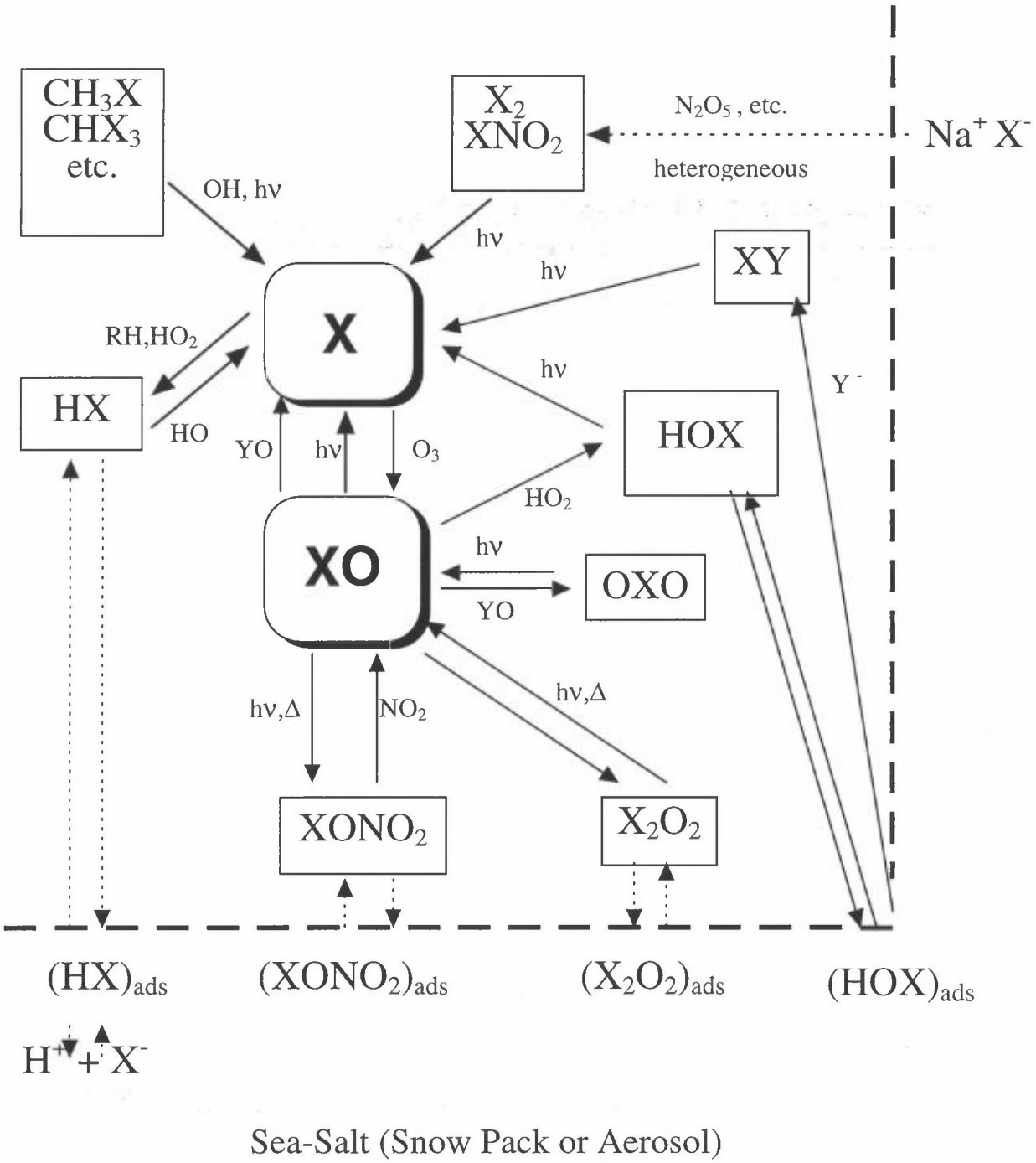

Fig. 3: Simplified scheme of the inorganic halogen reactions in the boundary layer (X = Cl, Br, I) after Wayne et al. [1995]. Sources are release from sea-salt (aerosol or deposits) or photochemical degradation of organohalogen species. Important questions concern the XO/X interconversion and recycling from hydrogen halides (HX). Fat lines: ozone destruction cycles.

Since most RHS - sources directly or indirectly produce halogen atoms the tropospheric fate of X atoms has to be analysed. In particular light X-atoms are highly reactive towards hydrocarbons, forming hydrogen halides through hydrogen abstraction (addition occurs in reactions with olefins),

$$X + RH \rightarrow HX + R \qquad (R9)$$

while Br-atoms can only abstract hydrogen atoms from HO_2 or aldehydes, I-atoms are even less reactive. The fate of the resulting HX is important when assessing stationary state RHS concentration. Since HX is highly water soluble it is likely to be irreversibly removed from the atmosphere by wet or dry deposition. The only other important gas phase removal mechanism of HX is reaction with OH,

$$HX + OH \rightarrow X + H_2O \qquad (R10)$$

which will return the halogen atom to the RHS reservoir. R10 is endothermic for X=F, also F $\rightarrow$ HF conversion is extremely rapid in the troposphere, so essentially any reactive F species will be quickly and irreversibly converted to HF. Other reactions of F-atoms are therefore not considered here. The alternative to R9 is oxidation of the halogen atom by O_3 (R1). Because of the decreasing reactivity of the heavier halogens towards H-containing compounds to form HX, the fraction of halogen atoms being converted to XO by reaction with atmospheric ozone (R1) is virtually zero for F, roughly 50% for Cl, ≈99% for Br, and essentially 100% for iodine. Therefore XO chemistry will be of great interest for X = Cl, Br, I. Halogen oxide radicals can undergo a number of reactions including oxidation of organic species (like DMS, see below), recombination with HO_2 (R5), or with another XO (R3). Kinetics and products of XO self reactions and XO-YO reactions have been investigated for a number of combinations as summarised in Table 2. Another important loss mechanism of halogen oxide radicals is reaction with NO (R11). In addition photolysis of XO can be of importance for X = I, Br, and to a minor extent Cl:

$$XO + h\nu \rightarrow X + O \qquad (J12)$$

Where $J_{12} \approx 3\times10^{-5}$ s^{-1}, 4×10^{-2} s^{-1}, 0.2 s^{-1} for X = Cl, Br, I, respectively. Ultimately the XO/X ratio is determined by reactions R1, XO+NO, XO+XO, and XO+YO reactions, and (during daytime) J12. Estimates of the stationary state [XO]/[X]-ratio are given in Table 3.

Table 3: Ratios of XO/X for various NO concentrations (and 40 ppb O_3)

Ratio	**Night (J_{12} = 0)**		**Day**	
	[NO] = 0	[NO] = 10 ppt	[NO] = 10 ppt	[NO] = 1 ppb
ClO/Cl	> 3600*	> 1600*	1000	30
BrO/Br	130*#	80*#	20	2
IO/I	?	≤ 190	≤ 5	1

* assuming 17 ppt BrO (5×10^8 molec. cm^{-3})

\# assuming 17 ppt ClO (5×10^8 molec. cm^{-3})

Tropospheric concentration of reactive halogen species

Overall there is not much information on the abundance of RHS in the troposphere. The available data come from (1) Indirect evidence for the presence of halogen atoms, mostly from observation of hydrocarbon ratios in airmasses of known chemical age, in marine and remote areas. While there is criticism of this method, the results nevertheless provide indications for the presence of other oxidants than OH in the troposphere. Also some indirect evidence for the presence of reactive Cl-species is due to observation of tropospheric HCl. (2) Direct observation of XO species in the troposphere.

*Table 4: Direct and indirect determinations of X-atom and XO conc. in molec./cm^3 (X=Cl, Br, I), quantities actually determined are shown in **boldface**, remaining data are calculated from assumed X/XO ratios (see Table 3)*

Author	Site	[Cl] 10^4	[ClO] 10^7	[Br] 10^7	[BrO] 10^7	[I] 10^7	[IO] 10^7
Finlayson-Pitts 1993[b]	Point Arena, CA, 39°N	**1.5**[a]	3[e]	-	-	-	-
Brauers et al. 1990	Brittany, France 53°N	-	-	-	-	< 0.2	< **1**[c]
Jobson et al. 1994	Alert and north >82°N	**1-8**[a]	2-16[e]	**1 - 6**[a]	100-600[e]	-	-
Solberg et al. 1994	Ny-Ålesund, Spitzbergen, 79°N	**3-6**[a]	6-12[e]	**3 - 10**[a]	300-1000[e]	-	-
Pszenny et al. 1993	Virginia Key, Florida, 26°N	1-10	2-20[e]	-	-	-	-
Wingenter et al. 1996	North Atlantic, 30°N - 41°N	**3.3**[a]	6.6[e]	-	-	-	-
Hausmann and Platt 1994	Alert, 82°N	-	-	≤ 0.5[e]	≤ **52**[c]	-	-
Unold et al. 1996	Ny-Ålesund 79°N	24[e]	**48**[c]	0.44[e] (≤ 0.9)	**44**[c] (≤ 90)	0.3[e]	1.5[d]

a Derived from relative rates of hydrocarbon decay
b Interpreting data from Parrish et al. [1992].
c Direct UV spectroscopic (DOAS) measurement
d From difference in DOAS data
e Values estimated from XO/X ratios

Table 4 summarises some estimates and measurements of XO and X-atom concentrations (assuming [XO]/[X] ratios typical for background conditions, see Table 3) based on those considerations. XO concentrations of up to several 10 ppt (X=Cl, Br) can be derived from the available indirect and direct data. Note that the BrO concentrations directly observed in the arctic (Alert, Ny-Ålesund) are up to two orders of magnitude higher than in the stratosphere

and thus constitute the highest levels of BrO found anywhere in the atmosphere. FO concentrations can be estimated to be <1 molec. cm^{-3}. It should be noted, however, that the observations presented in Table 4 are derived from observations in areas with presumably high levels of halogens, thus global average concentrations are likely to be much smaller. For instance an upper limit can be placed on the global average Cl concentration (and thus on the av. ClO levels) by assuming that in the global CH_4 budget an additional loss of ≤ 20% due to R9 could go unnoticed. This consideration yields $[Cl]_{glob.av.} \leq 8 \times 10^3$ molec. cm^{-3}, which is about one order of magnitude lower than most estimates in Table 4.

Conclusions

In summary, there is a growing body of evidence, that halogen species are present in the troposphere at concentration levels sufficient to influence chemical reaction cycles, in particular those related to its oxidation capacity. Although the available information on the tropospheric concentration of reactive halogen species pertain mostly to the boundary layer it should be kept in mind that the short lived trace species are degraded there. Summing the available information it becomes clear that the halogen oxide radicals can provide a considerable fraction of the oxidation capacity provided by the HO_x - system.
In addition it is now clear that the dramatic disturbances of the boundary layer O_3 reported from the polar regions are due to XO reactions and may occur in other regions as well. In any case the considerations presented here clearly show that more research is required and warranted to reduce the uncertainties in the budgets and concentration levels of those free radicals.

Literature

Barrie L.A., Bottenheim J.W., Schnell R.C., Crutzen P.J. and Rasmussen R.A. (1988), Ozone destruction and photochemical reactions at polar sunrise in the lower Arctic atmosphere, Nature 334, 138-141.

Behnke W., Scheer V. and Zetzsch C. (1993), Formation of $ClNO_2$ and HNO_3 in the presence of N_2O_5 and wet pure NaCl- and wet mixed $NaCl/Na_2SO_4$-aerosol, J. Aerosol Sci. 24, S115-S116.

Bottenheim J. W., Gallant A. C. and Brice K.A. (1986), Measurements of NOy species and O3 at 82° N latitude, Geophys. Res. Lett. 13, 113-116.

Bottenheim J.W., Barrie L. W., Atlas E., Heidt L. E., Niki H., Rasmussen R. A., and Shepson P.B. (1990), Depletion of lower tropospheric ozone during Arctic spring: The Polar Sunrise Experiment 1988, J. Geophys. Res. 95, 18555 - 18568.

Brauers T., Dorn H.-P. and Platt U. (1990) Spectroscopic measurements of NO2, O3, SO2, IO and NO3 in maritime air. In Physico-Chemical behaviour of Atmospheric pollutants, Proceeding of the 5. European Symp., Varese, Italia (edited by Restelli G. and Angeletti G.), pp. 237-242, Kluwer Academic, Doordrecht.

Fan S.-M. and Jacob D. J. (1992), Surface ozone depletion in the Arctic spring sustained by bromine reactions on aerosols, Nature 359, 522 - 524.

Finlayson-Pitts B. J., Ezell M. J. and Pitts J. N. (1989), Formation of chemically active chlorine compounds by reactions of atmospheric NaCl particles with gaseous N2O5 and ClONO2, Nature 337, 241-244.

Finlayson-Pitts B. J., Livingston F. E. and Berko H. N. (1990), Ozone destruction and bromine photo chemistry in the Arctic spring, Nature. 343, 622-625.

Finlayson-Pitts B. J. (1993), Indications of Photochemical Histories of Pacific Air Masses from Measurements of Atmospheric Trace Species at Point-Arena, California - Comment, J. Geophys. Res. 98, 14991-14993.

Hausmann M. and Platt U. (1994), Spectroscopic measurement of bromine oxide and ozone in the high Arctic during Polar Sunrise Experiment 1992, J. Geophys. Res. 99, 25,399-25,414.

Huie R.E., Laszlo B., Kurylo M.J., Buben S.N., Trofimova E.M., Spassky A.I., Miziolek A.W. (1995), The atmospheric chemistry of iodine monoxide, presented at the Halon Options Technical Working Conf., Albuquerque, NM, May 10, 1995.

Jobson B.T., Niki H., Yokouchi Y., Bottenheim J., Hopper F. Leaitch R. (1994) Measurements of C2-C6 hydrocarbons during Polar Sunrise Experiment 1992, J. Geophys. Res., 99, 25,355-25,368.

Le Bras G. and Platt U. (1995), A Possible mechanism for combined chlorine and bromine catalyzed destruction of tropospheric ozone in the Arctic, Geophys. Res. Lett., 22, 599-602.

Manö S. and Andreae M. O. (1994), Emission of methyl bromide from biomass burning, Science 263, 1255-1256.

Mozurkewich M. (1995), Mechanisms for the release of halogens from sea-salt particles by free radical reactions, J. Geophys. Res., 100, 14199-14207.

Parrish D. D., Hahn C. J., Williams E. J., Norton R. B., Fehsenfeld F. C., Singh H. B., Shetter J. D., Gandrud B. W. and Ridley B. A. (1992), Indications of Photochemical Histories of Pacific Air Masses from Measurements of Atmospheric Trace Species at Point Arena, California, J. Geophys. Res. 97, 15883-15901.

Platt., U. and Janssen C. (1996), Observation and role of the free radicals NO_3, ClO, BrO and IO in the Troposphere, Faraday Discuss 100, 175-198.

Platt., U. and Lehrer E., Eds. (1996), Arctic Tropospheric Halogen Chemistry (ARCTOC), final Report to EU.

Pszenny A.A.P., Keene W.C., Jacob D.J., Fan S., Maben J.R., Zetwo M.P., Springeryoung M. and Galloway J.N. (1993), Evidence of Inorganic Chlorine Gases other than Hydrogen Chloride in Marine Surface Air, Geophys. Res. Lett. 20, 699-702.

Schall C. and Heumann K.G. (1993), GC determination of volatile organoiodine and organobromine compounds in seawater and air samples, Fresenius J. Anal. Chem. 346, 717-722.

Solberg S., Schmidtbauer N., Semb A., Stordal F. (1996), Boundary-Layer Ozone Depletion as Seen in the Norwegian Arctic in Spring, J. Atmos. Chem., 23, 301-332.

Sturges W.T., Schnell R.C., Dutton G.S., Garcia S.R. and Lind J.A. (1993), Spring Measurements of Tropospheric Bromine at Barrow, Alaska, Geophys. Res. Lett. 20, 201-204.

Sturges W.T., Cota G.F. and Buckley P.T. (1992), Bromoform Emission from Arctic Ice Algae, Nature 358, 660-662.

Tuckermann M., Ackermann R., Gölz C., Lorenzen-Schmidt H., Senne T., Stutz J., Trost B., Unold W., and Platt U. (1997), DOAS-Observation of Halogen Radical-catalysed Arctic Boundary Layer Ozone Destruction During the ARCTOC-Campaigns 1995 and 1996 in Ny-Ålesund, Spitsbergen, Tellus, submitted.

Unold W., Lorenzen-Schmidt H., Lehrer E., Stutz J., Trost B. and Platt U. (1997), Arctic Boundary Layer Halogen Oxides during an Ozone Depletion Event in Ny Alesund, Spitsbergen (78°N), in prep.

Vogt R., Crutzen P.J., Sander R. (1996), A mechanism for halogen release from sea-salt aerosol in the remote marine boundary layer, Nature 383, 327-330.

Wingenter O.W., Kubo M.K., Blake N.J., Smith T.W., Blake D.R. and Rowland F.S. (1996), Hydrocarbon and halocarbon measurements as photochemical and dynamical indicators of atmospheric hydroxyl, atomic chlorine, and vertical mixing obtained during Lagrangian flights, J. Geophys. Res. 101, 4331-4340.

Wayne R.P., Poulet G., Biggs P., Burrows J.P., Cox R.A., Crutzen P.J., Haymann G.D., Jenkin M.E., Le Bras G., Moortgat G.K., Platt U. and Schindler R.N. (1995), Halogen oxides: radicals, sources and reservoirs in the laboratory and in the atmosphere, Atmosph. Environ., 29, 2675-2884.

Measurements of Halogen Compounds, O_3, NO_2 and SO_2 During the ARCTOC Campaigns in Spring 1995 and 1996

M. Martinez-Walter, T. Arnold and D. Perner
Max-Planck-Institut für Chemie, Joh. J. Becherweg 27, D-55128 Mainz

Abstract. Depletion of boundary layer ozone has been observed during the EC-sponsored Arctic Tropospheric Ozone Chemistry (ARCTOC) campaign in spring of 1995 and 1996. During intense depletion events at Ny-Ålesund the ozone dropped from about 40 ppb to very low values and only then up to 30 ppt bromine monoxide were observed by Differential Optical Absorption Spectroscopy. Total bromine collected from air and analysed by neutron activation was also enhanced during the strong ozone depletion, which apparently is caused by photochemical destruction involving bromine.

Introduction

Ozone, O_3, depletion events have been observed in the arctic lower troposphere during spring [Oltmans and Khomhyr, 1986]: in Alert, Canada [Bottenheim et al., 1986, 1990, Barrie et al., 1988, 1994, Mickle et al., 1989], in Barrows, Alaska [Sturges et al., 1993] and in Ny-Ålesund, Spitsbergen [Solberg et al., 1994]. Ozone decreases from normal levels to low and even unmeasurable levels within a few hours and increases again to normal values after a few days. In these air masses filterable bromine anticorrelated with ozone and recently also bromine monoxide, BrO, was observed [Hausmann and Platt, 1994].

Experimental

During spring 1995 and 1996 long path Differential Optical Absorption Spectrometry (DOAS) measurements were carried out in Ny-Ålesund at the west coast of Spitsbergen (78.9°N, 11.8°E). Light paths were set up between the North Polar Institute building (20 m a.s.l.) and Zeppelin mountain (474 m a.s.l., 2100 m distance). In 1996, retroreflectors were placed as well on Brøggerfjellet (410 m a.s.l., 5000 m distance). Therefore integrated values over these altitudes and distances were obtained. A Xe-arc lamp was used as light source. Measurements were performed in 1995 with a Czerny-Turner spectrograph (resolution 0.45 nm) and a photomultiplier detector and in 1996 with a holographic grating spectrograph (resolution 1 nm) and a photo diode array detector.

The trace gas concentrations along the light path were determined from least-squares fits of the reference spectra and a polynom [Stutz, 1995] to the air spectrum. Reference spectra were obtained by placing a quartz cell with the particular trace gas in the light path. The differential absorption cross sections were taken from literature spectra, which, in case of having a higher resolution, were degraded to the lower resolution of the experiment by folding with measured Hg-lines. Temperature dependencies of the spectra of O_3, BrO and SO_2 were taken into account.

The measured values show systematic errors caused by the instrument (which is the main limitation of the detection) and by the uncertainties of the absorption coefficients (3-10%). Statistical errors arise from photon statistics, detector noise and random residual structures of the instruments.

Species	wavelength of prominent band, nm	det. limit 1995	det. limit 1996	literature absorption coefficients
O_3	299	5 ppb	2 ppb	Bass et al. 1984
BrO	338	5 ppt	2 ppt	Wahner et al. 1988
ClO	295	50 ppt	25 ppt	Simon et al. 1990
IO	427	2 ppt	2 ppt	Laszlo et al. 1995
SO_2	300	150 ppt	50 ppt	McGee and Burris 1987
NO_2	349, 431	500 ppt, 280 ppt	250 ppt, 140 ppt	Schneider et al. 1987
HCHO	338	1.3 ppb	500 ppt	Moortgat et al. 1980

Additionally, in 1996 total bromine and total iodine were collected from air and analysed by neutron activation. Polyethene sampling tubes were packed with suitable active charcoal. The outside air streamed directly on the carbon at a flowrate of 0.7 m^3/h at maximum. The volume was measured by a dry gasmeter at the exit of the vacuum pump. During strong O_3 depletion events sampling times were reduced to 12 hrs from 24 hrs at normal O_3 levels.
Samples clogged by snow at the inlet showed no bromine but some iodine which was taken as background contamination of the active carbon and subtracted from all other samples. The sampling efficiency for all bromine compounds was taken as unity.
The Br^{80} and I^{128} sensitivities were calibrated by introducing solutions containing 1 µg Br^- and I^- to a fresh sample which then underwent the same neutron activation procedure.
The sensitivity of our measurements was 6 ng Br/sample (0.5 ppt in 6 m^3 air), 5 ng I/sample (0.3 ppt in 6 m^3 air), with a precision of about 10%.

Results

In 1995 already at the beginning of the campaign an ozone depletion event was encountered. The ozone was depleted to levels lower than 5 ppb. O_3 and BrO data for this event are shown in fig. 1. The O_3 mixing ratios measured with DOAS roughly agree with those measured by the ozone monitor at Zeppelin station, with deviations of up to 5 ppb, which could be explained by varying ozone mixing ratios with altitude. BrO was normally below the detection limit of 5 ppt, but during the event measurable levels up to 30 ppt were found. As would be expected, the bromine oxide mixing ratio is about zero when the ozone is very low, as bromine atoms must encounter ozone to form bromine oxide. The unperturbed air showed mixing ratios of about 40 ppb O_3.
The measurements for spring 1996 are shown in fig. 2. Two major ozone depletion events occurred, on May 4-9 and on May 12-14. The O_3 mixing ratio dropped below 5 ppb and BrO reached up to 20 ppt. Between May 6 and 8 O_3 showed levels of no more than 10 ppb and BrO was around 10 ppt, which may indicate vertical mixing with unperturbed air rich in ozone prior to its arrival at Ny-Ålesund. On several other occasions the ozone mixing ratio dropped by 10-20 ppb while BrO levels of 5 to 10 ppt were observed.
Total bromine ranged between 10 and 20 ppt during times of normal ozone levels which agrees with the anticipated content of CH_3Br and halons in the free northern troposphere. During ozone depletion events additional bromine typically three times the higher BrO levels detected spectroscopically was observed. This agrees with the expectation from the chemical manifold which contains mainly BrO or Br, HOBr, Br_2 and HBr. ClO and IO always remained

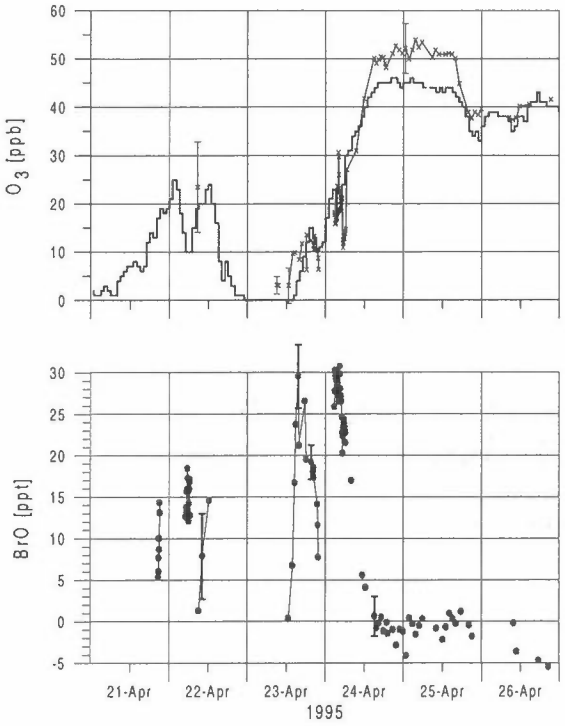

Figure 1. Ozone at Zeppelin Station (Monitor Lab), solid line, and by DOAS, crosses. BrO measured by DOAS in 1995.

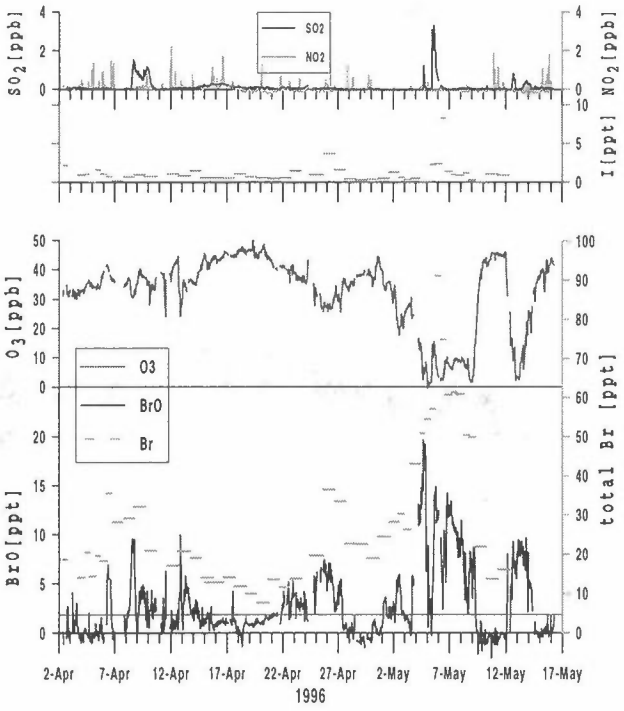

Figure 2. Ozone, BrO, total bromine, total iodine, NO_2 and SO_2 measured during the campaign in spring 1996.

below the detection limit even on May 6, 1996, when total iodine went up to 8 ppt from the normal level of 1-2 ppt.

The NO_2 mixing ratio stayed in general below the detection limit, except for several spikes due to local pollution. During ozone depletion events NO_2 spikes were less frequent because the ozone-driven conversion of NO from the pollution sources to NO_2 was less effective.

In 1995 the SO_2 mixing ratio only exceeded the detection limit on April 22, during the ozone depletion event, when almost 2 ppb were found. In 1996 SO_2 between 0.5 and 3 ppb was measured on five occasions again during ozone depletion events. These elevated SO_2 mixing ratios have not been accompanied by NO_2, as would be expected for local contamination, therefore the contamination source must be situated further away. During a period of calm weather between April 14 and 18 longer lasting SO_2 of about 300 ppt and frequent NO_2 spikes of up to 2 ppb appeared. The O_3 was not affected (fig. 2).

Discussion

Halogen atoms destroy ozone in a catalytic cycle:

$$\begin{aligned} Br + O_3 &\rightarrow BrO + O_2 \\ BrO + BrO &\rightarrow Br + Br + O_2 \qquad k = 1.9\times10^{-12} \\ &\rightarrow Br_2 + O_2 \qquad k = 5.7\times10^{-13} \end{aligned}$$

Similar reactions are possible for every combination of Cl, Br and I, but only bromine has been reliably detected during ozone depletion events. Because of the high amount of chlorine in sea-salt it should obviously be formed at first, but because of its fast reaction with methane to HCl it must be rapidly scavenged from the gas phase. Photochemistry of ozone leads to production of OH and HO_2, which react with Br and BrO to produce HBr and HOBr. While in the gas phase they are effective bromine sinks, HBr and HOBr can be recycled on the ice cap

by heterogeneous reaction as was first suggested by Fan and Jacob, 1990. Further, the same reaction can lead to autocatalytic release of sea-salt Br^- [Mozurkewich, 1995; Vogt et al., 1996; Tang and McConnell, 1996]. Therefore, bromine will be released to the gas phase as soon as photochemistry starts, under the assumption that there is enough sea-salt on the ice cap. During the ozone depletion event on May 4-9, 1996, the measured total bromine curve seems to peak at about 60 ppt, corresponding to 40-50 ppt inorganic bromine, except for two very high values of 91 and 75 ppt measured during the 24 hours following the highest SO_2 peak. Assuming this SO_2 peak was accompanied by NO_2 , possibly additional autocatalytic release by reaction of $BrNO_3$ with Br^- is responsible for these especially high total bromine levels.

A simple model can be used to understand the measured data. As long as an airmass moves over the ice cap, ozone destruction takes place. When it is transported to Ny-Ålesund, it passes over open sea, were heterogeneous reactions are of lesser importance. Bromine atoms and bromine oxide are then converted to HBr and HOBr. The BrO content of an airmass therefore depends on the mixing ratios of ozone and total bromine as well as on the time passed since the airmass left the ice cap.

Acknowledgements. The authors thank the CEC for financial support (CT93 0318). The neutron activation analysis by A. Trautmann and H. Zauner, Institut für Kernchemie, Gutenberg University, Mainz, is highly appreciated.

References

Barrie, L.A., J.W. Bottenheim, R.C. Schnell, P.J. Crutzen, R.A. Rasmussen, *Nature*, *334*, 138-141, 1988.

Barrie, L.A., S.M. Li, D.M. Toom, S. Landsberger, W. Sturges, *J. Geophys. Res.*, *99*, 25453-25468, 1994.

Bass, A.M., and R.J. Paur, *Proceedings of the Quadrennial Ozone Symposium, Greece* (ed. C. Zerefos and A. Ghazi), 606-617, 1984

Bottenheim, J.W., A.J. Gallant, K.A. Brice, *Geophys. Res. Lett.*, *13*, 113-116, 1986.

Bottenheim, J.W., L.W. Barrie, E.Atlas, L.E. Heidt, H. Niki, R.A. Rasmussen, P.B. Shepson, *J. Geophys. Res.*, *95*, 18555-18568, 1990.

Brauers, T., M. Hausmann, U. Brandenburger, H.-P. Dorn, *Applied Optics*, *34*, Nr. 21, 4472-4479, 1995.

DeMore, W.B., S.P. Sander, D.M. Golden, R.F. Hampson, M.J. Kurylo, C.J. Howard, A.R. Ravishankara, C.E. Kolb, M.J. Molina, *JPL Publication 94-26*, 1994.

Fan, S.-M., and D.J. Jacob, *Nature, 359*, 522-524, 1992.

Hausmann, M., and U. Platt, *J. Geophys. Res.*, *99*, 25399-25414, 1994.

McGee, T.J., and J. Burris, *J. Quant. Spectrosc. Radiat. Transfer*, *37*, No. 2, 165-182, 1987.

Mickle, R.E., J.W. Bottenheim, R.W. Leaitch, W. Evans, *Atmos. Environ.*, *23*, 2443-2449, 1989.

Oltmans, S.J., and W.D. Khomhyr, *J. Geophys. Res.*, *91*, 5229-5236, 1986.

Sander, R., and P.J. Crutzen, *J. Geophys. Res.*, *101*, 9121-9138, 1996.

Schneider, W., G.K. Moortgat, G.S. Tyndall, J.P. Burrows, *J. Photochem. Photobiol.*, *40*, 195-217, 1987.

Simon, F.G., W. Schneider, G.K. Moortgat, J.P. Burrows, *J. Photochem. Photobiol. A: Chem.*, *55*, 1-23, 1990.

Solberg, S., O. Hermansen, E. Joranger, N. Schmidtbauer, F. Stordal, O. Hov, *NILU Report OR 27/94*, ISBN 82-425-0575-6, 1994.

Sturges, W.T., R.C. Schnell, G.S. Dutton, S.R. Garcia, J.A. Lind, *Geophys. Res. Lett.*, *20*, 201-204, 1993.

Stutz, J., PhD thesis, University of Heidelberg, 1995.

Tang, T. and J.C. McConnell, *Geoph. Res. Letters, 23*, No. 19, 2633-2636, 1996.

Vogt, R., P.J. Crutzen, R. Sander, *Nature*, submitted, 1996.

Wahner, A., A.R. Ravishankara, S.P. Sander, R.R. Friedl, *Chem. Physics Letters*, *152*, No. 6, 507-512, 1988.

Tropospheric Ozone Depletion Related Air Mass Characteristics

Lehrer, E., Langendörfer, U., Wagenbach, D. and Platt, U.
Institut für Umweltphysik, University of Heidelberg, D-69120 Heidelberg, Germany

Introduction

During spring 1995 and 1996 intensive investigations in the phenomenon of tropospheric ozone depletion at Ny-Ålesund / Svalbard (79°N, 12°E) were performed within the framework of the EU project ARCTOC. As a result ARCTOC provides for the first time a springtime data set on tropospheric ozone depletion and related chemistry for the European sector of the Arctic comparable to former activities in the American Arctic (e.g. Polar Sunrise Experiment '88 and '92). Here we report on the results of continuos aerosol sampling and Radon measurements combined with trajectory calculations and meteorological observations.

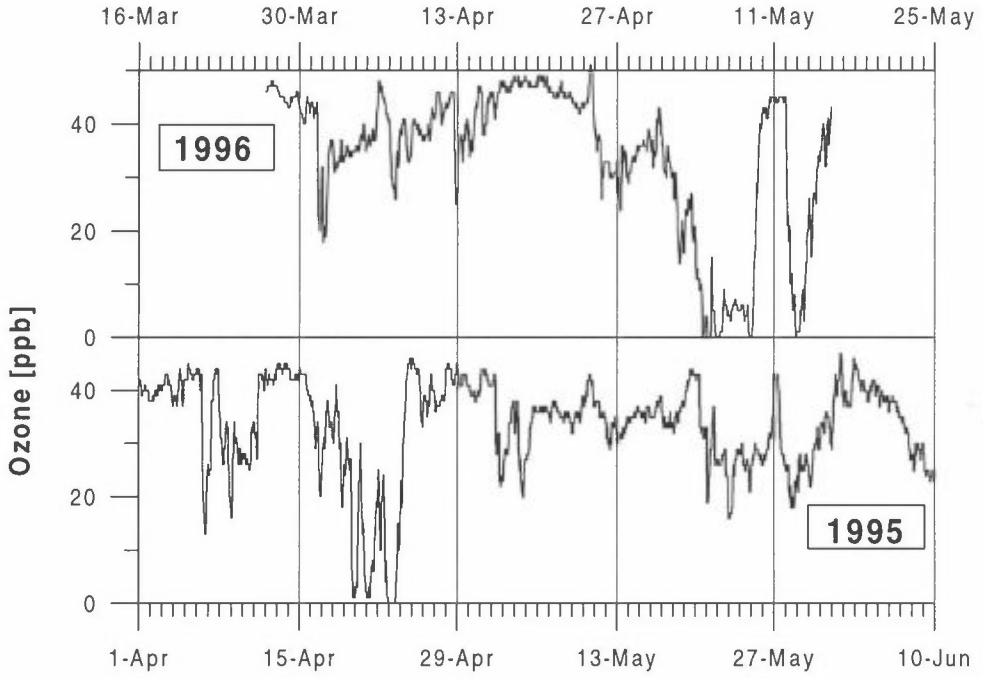

Figure 1: Ozone records during the ARCTOC campaigns 1995 and 1996 at Ny-Ålesund Svalbard. Ozone data measured by the Norwegian Institute for Air Research (NILU).

Experimental

Aerosol was sampled on a total of 121 cellulose filter pairs during the ARCTOC '95 campaign and on 421 pairs of cellulose filters in 1996, respectively. The filters were analysed by ion-chromatography at the Heidelberg Institut für Umweltphysik (IUP). For details about the experimental set-up and the analysis conditions see references [1] or [2]. In-situ Radon measurements were performed in a continuous α-counting device developed by the IUP [3].

Comparison of the ionic tracer concentration during ARCTOC '95 and '96

The ARCTOC measurements during 1995 and 1996 took place from 17.4. to 12.6. and 27.3. to 15.5., respectively and thus covered most of the spring season. The Arctic spring is characterised by a decreasing Arctic Haze influence and increasing biogenic activity. For the discussion of the 1995 and 1996 measurements it is helpful to separate the measuring campaign into two main periods. The herein defined late winter period lasted until begin of May 1995 followed by an early summer period. Both periods were characterised by significantly different aerosol compositions (compare [2]). In particular high sulphate concentrations up to several $\mu g/m^3$ could be found till the begin of May, whereas the early summer period was characterised by the onset of biogenic activity in the surrounding polar oceans (increase of the MSA concentration).

Ionic aerosol composition related to ozone depletion events

Ozone depletion events could be classified as total event in the case of almost total ozone loss and secondary ozone events, which are characterised by ozone depletions with $\Delta O_3 > 10$ ppb. During both ARCTOC campaigns an extended total ozone depletion event could be observed, which lasted in both cases for more than 48 hours. Secondary ozone events happened throughout both campaigns several times, but where not observed after May (see Fig 1 and [2]). Table 1 shows average concentrations of typical ionic species during total, secondary and no - ozone depletion periods.

Table 1: Typical ionic tracer concentrations in ng/m^3 during a) total ozone depletion, b) secondary ozone depletion and c) no depletion periods ('95 campaigns concentration before slash; '96 campaigns concentration after slash).

'95 / '96	a) Total ozone depletion	b) Secondary ozone depletion	c) No depletion period
Sea Salt	930 / 580	300 / 620	320 / 390
SO_4	1520 / 2030	530 / 1440	490 / 1200
NO_3	130 / 180	55 / 120	110 / 100
MSA	6 / 18	25 / 8	60 / 5

Origin of ozone depleted air masses

From the trajectory calculations by the Danish Meteorological Institute (DMI) and by the Atmospheric Environment Service (AES) / Canada some hints on the origin of the ozone depleted air masses could be found. During both campaigns total ozone depletion was only seen in air masses coming from the North over sea ice covered areas. Starting point of the 5 days back trajectories was in almost all cases the area north of either Greenland or Siberia (Figure 2). The source region determination for secondary ozone depletion events was not unequivocal, although a tendency for air masses to originate from the Arctic basin is seen, however.

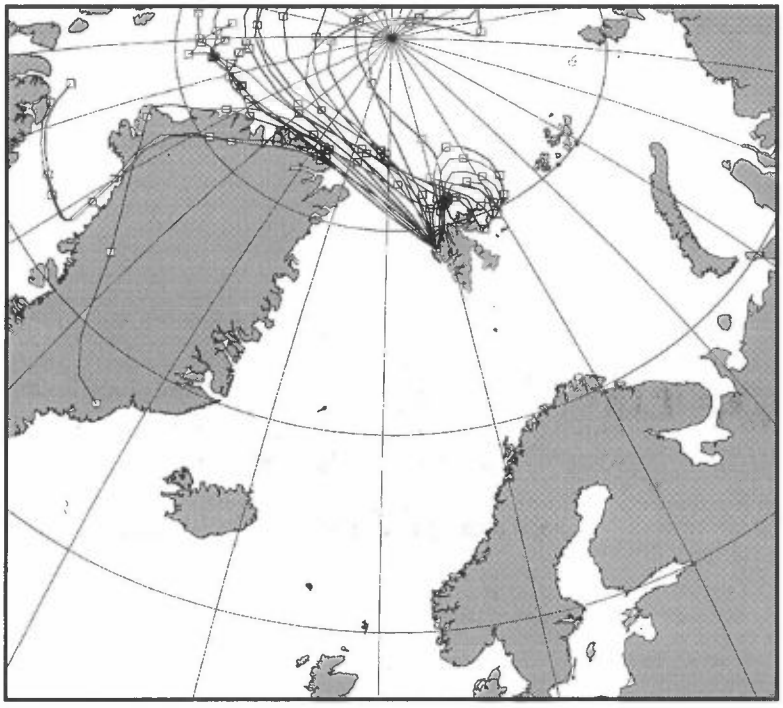

Figure 2: Origin of air masses in the case of total ozone depletion during the ARCTOC '96 campaign.

Radon measurements

We obtained two quasi-continuous ^{222}Rn records from the spring 1995 and 1996 campaigns, respectively. However, during the second year's campaign technical shortcomings led to gaps in the Radon data set.

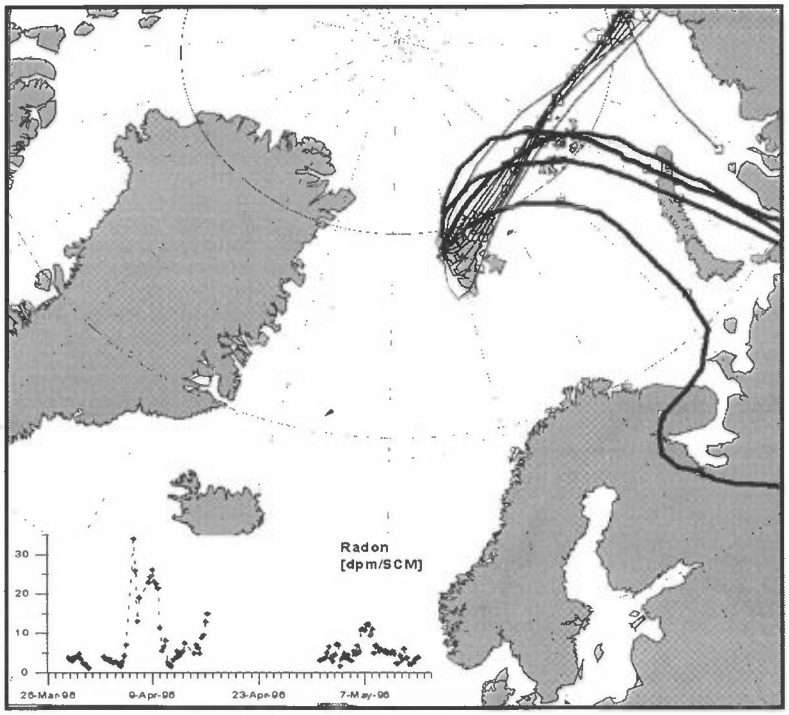

Figure 3: 5 days backward trajectories for the period between 6. April and 9. April 1996 for measured Radon concentrations > 10 dpm/SCM^{-1}. The thick lines mark the trajectories for 6. April 1996.

Radon concentrations at Svalbard were found to be 5 decays per minute and standard m^3 ($dpmSCM^{-1}$) on the average with background concentration of typically 3 $dpmSCM^{-1}$, but can also reach concentration of more than 30 $dpmSCM^{-1}$, when air masses are advected by fast transport from continental areas. Fig.3 shows 5 days backward calculated trajectories for the 1000 mbar pressure level from 6. April to 9. April 1996. During this period Radon concentrations of more than 10 $dpmSCM^{-1}$ could be observed. High Radon concentrations often coincide with high SO_4^{2-} levels. Low ^{222}Rn concentrations are generally associated with air mass subject to a relatively long residence time over ocean (or sea ice) areas.

Meteorological aspects of ozone depletion events

A positive correlation between temperature variability and the ozone concentration was found during both spring seasons. Ozone sonde measurements provided that ozone depleted air mass parcel could reach a vertical extension up to 2500 m and are topped by an inversion layer. The analyses of individual ozone depletion events show a faster rate of decrease than the subsequent increase rate (dO_3/dt) (see [4]).

References

[1] Lehrer E., Wagenbach D. and Platt U., Chemical Composition of the Aerosol during Tropospheric Ozone Depletions, Tellus submitted, 1996.

[2] Platt U. and Lehrer E., ARCTOC - Final Report to the European Union, 1997.

[3] Levin I. BOVOC final report to the European Union, 1995

[4] Tuckermann, M., Ackermann, R., Gölz, C., Lorenzen-Schmidt, H., Senne, T., Stutz, J., Trost, B., Unold, W., and Platt, U. (1996), DOAS-Observation of Halogen Radical-catalysed Arctic Boundary Layer Ozone Destruction During the ARCTOC-campaigns 1995 and 1996 in Ny-Ålesund, Spitsbergen, Tellus submitted, 1996.

DOAS-Measurements During the ARCTOC-Campaigns 1995 and 1996 in Ny-Ålesund, Spitzbergen

R. Ackermann, M.Tuckermann and U.Platt
Institut für Umweltphysik, Univ. Heidelberg, INF 366, D-69120 Heidelberg, Germany

1. Introduction

About a decade ago the phenomenon of complete boundary layer ozone depletion was discovered. Since then sudden, episodic loss of O_3 has been observed at several arctic sites after polar sunrise in spring. During the episodes ozone levels drop from the normal 30 - 40 ppb to mixing ratios unmeasurable by standard equipment (< 2 ppb). Despite many attempts to explain the phenomenon the reasons for this phenomenon are only partly understood today. Already early observations showed a striking anticorrelation between ozone and levels of filterable bromine (f-Br) [e.g. Barrie et al. 1988, Lehrer et al. 1996] leading to the hypothesis of BrO_x- [Barrie et al. 1988] BrO_x + ClO_x- [LeBras and Platt 1995], or IO_x- [Solomon et al. 1994] catalysed reaction cycles being responsible for the observed ozone destruction. Recently the presence of BrO has been unequivocally verified in the arctic boundary layer at Alert [Hausmann and Platt 1994]. Here we present a much more detailed data set of BrO and ClO observations at Ny-Ålesund during spring of '95 and '96 (ARCTOC campaigns)

2. Experimental

Measurements of the halogen oxide radicals were performed by Long Path Differential Optical Absorption Spectroscopy (LP-DOAS) observing the strongly structured absorption bands of ClO and BrO in the near UV and of IO in the blue spectral region.
The measurements were carried out in the Arctic at Ny-Ålesund, Svalbard (78.9°N, 11.8°E). To minimise contamination of the measurements by local air pollution, the experimental set up was installed in a laboratory located about 1.5 km to the west of Ny-Ålesund at an elevation of about 50 m a.s.l.. During the period described here from April 18 the sun was above the horizon all day.
A new design of a DOAS spectrometer [Stutz 1995, Unold 1995], based on the principle of Platt and Perner [1983], was used, it incorporates a unit of two coaxially arranged Newton type telescopes to send and receive the light beam. The light of a Xe-short-arc lamp was formed into a beam by the transmitting section of the telescope, reflected by a retroreflector array mounted in the field and recollected by the receiving section of the telescope. The spectrometer was coupled to the telescope by a quartz fiber, which also performed the task of a mode mixer as described by Stutz and Platt [1997]. Spectra in the UV and visible were recorded at a resolution of about 0.3 nm by a Czerny-Turner spectrograph with a focal length of 0.5 m (F=6.9, 1200 gr/mm grating, thermostated to +10±0.3°C) in combination with a photodiode array detector (RETICON RL 1024R, thermostated to -30±0.3°C). In 1996 the thermostating of the spectrograph and detector was changed to +15±0.3°C and -35±0.3°C, respectively.
The telescope combination could be pointed to either of three retroreflector arrays mounted at different sites in the field. Thus it was possible to use three light paths. The telescope/spectrometer unit was housed at slightly different locations in the two years. Resulting in the following full lengths of the folded light path in 1995 and 1996, respectively (the distance between telescope and array is half as long):

1. 3560 m / 3418 m in north-westerly direction, running over land in its full length.
2. 5672 m / 6226 m in westerly direction, running over land in its full length.
3. 11646 m / 11646 m in northerly direction, running across the Kongsfjord during most (ca. 10000 m) of its length to the Blomstrandhalvøya peninsula.

Spectra were taken in four wavelength ranges selected for optimum detection of ClO, BrO, NO_2, and IO, respectively. Bands of NO_2 and O_3 could be observed in several of the regions. In addition bands of HONO (1995 only), H_2O, SO_2, and oxygen dimers (O_4, 1995 only) were detectable (Table 1).

Table 1: Spectral intervals used for the DOAS measurements in Ny-Ålesund and list of species observed in the particular interval, absolute values of the differential cross sections were taken from the literature as indicated.

Spectral Interval [nm]	Species	Wavelength of prominent band [nm]	Differential Absorption Cross Section [10^{-20} cm^2/molec]	Mean detection limit	
				1995	1996
A: 275 - 305	ClO, O_3 SO_2	280 281.5 291	353[a] 10 68	19 ppt 1.2 ppb 0.04 ppb	8.5 ppt 0.8 ppb 0.03 ppb
B: 310 - 340	BrO O_3 CH_2O OClO NO_2	328 320 326 336 333	1040 0.6 6.2 980 7	1.7 ppt	3.1 ppt 690 ppt 1.3 ppt
C: 350 - 380 (1995 only)	BrO NO_2 HONO O_4	355 356 352	410 8.7 41	660 ppt	
D: 420 - 450	IO NO_2	427 430	1700 17	2.5 ppt 0.1 ppb	0.9 ppt 0.06 ppb

a Data were degraded to our resolution and used to scale relative laboratory spectra
Data corrected, U. Schurath private comm.
The DOAS measurements employed the Multi-Channel-Scanning Technique (MCST).

3. Results and Conclusions

Summarising the experimental results of the spring 1995 and spring 1996 campaigns the time series of ozone together with the halogen oxides BrO, ClO, IO, NO_2 and SO_2 are given in Fig. 1 and Fig.2 , respectively [c.f. Tuckermann et.al. 1997].
Up to 30 ppt of both, BrO and ClO were found to coincide with low ozone events (LOE). During periods of normal ozone average levels of BrO and ClO were closed to zero. Average ClO levels during LOE were considerably higher in 1995 (21 ppt) than in 1996 (3.3 ppt). IO

levels in individual measurements never exceeded 1-2 ppt. Average levels over LOE and periods of relatively stable ozone levels were below 0.2 ppt.

From the observed levels of halogen oxides rates of ozone destruction of the order of 1-2 ppb/hour can be concluded. Rate limiting steps in ozone destruction are the ClO + BrO reaction and the BrO self reaction, the IO + BrO reactions appears to be of minor importance (if it occurs at all). Even faster observed rates of ozone change (up to 7 ppb/hour [Tuckermann et al. 1997]) are due to advection of air masses to the measurement site.

In summary it can be said that halogen catalysed ozone destruction is the cause of the ozone depletion events in the arctic boundary layer. The remaining central question, of course, is what is the origin of these high levels of reactive halogen species?

References

Barrie L.A., Bottenheim J.W., Schnell R.C., Crutzen P.J. and Rasmussen R.A. (1988), Ozone destruction and photochemical reactions at polar sunrise in the lower Arctic atmosphere, Nature 334, 138-141.

Hausmann M. and Platt U. (1994), Spectroscopic measurement of bromine oxide and ozone in the high Arctic during Polar Sunrise Experiment 1992, J. Geophys. Res. 99, 25,399-25,414.

Le Bras G. and Platt U. (1995), A Possible mechanism for combined chlorine and bromine catalyzed destruction of tropospheric ozone in the Arctic, Geophys. Res. Lett., 22, 599-602.

Lehrer E., Wagenbach D., Platt U. (1997), Chemical aerosol composition during tropospheric ozone depletion at Ny-Ålesund / Svalbard, Tellus, this issue.

Platt U., and D. Perner (1983), Measurements of atmospheric trace gases by long path differential UV/visible absorption spectroscopy: Optical and Laser Remote Sensing, D.K. Killinger and A. Mooradian (Eds.) Springer Ser. Optical Sci., 39, 95-105.

Platt U. (1994), Differential optical absorption spectroscopy (DOAS), In: Air Monitoring by Spectroscopic Techniques, M.W. Sigrist, Ed., Chemical Analysis Series, Vol. 127, John Wiley & Sons, Inc.

Solomon S., Garcia R.R., Ravishankara A.R. (1994), On the role of iodine in ozone depletion, J. Geophys. Res. 99, 20491-20499.

Stutz J. (1996), Messung der Konzentration troposphärischer Spurenstoffe mittels Differentieller-Optischer Absorptionsspektroskopie: Eine neue Generation von Geräten und Algorithmen, Ph.D. Thesis, University of Heidelberg.

Stutz J. and Platt U. (1997), Improving long- path differential optical absorption spectroscopy (DOAS) with a quartz- fiber mode- mixer, Appl. Opt., 36, (6)1105 - 1115.

Tuckermann M., Ackermann R., Gölz C., Lorenzen-Schmidt H., Senne T., Stutz J., Trost B., Unold W., and Platt U., (1997), DOAS-Observation of Halogen Radical- catalysed Arctic Boundary Layer Ozone Destruction During the ARCTOC-campaigns 1995 and 1996 in Ny-Alesund, Spitsbergen, Tellus, submitted.

Unold W. (1995), Bodennahe Messungen von Halogenoxiden in der Arktis, Diploma Thesis, University of Heidelberg.

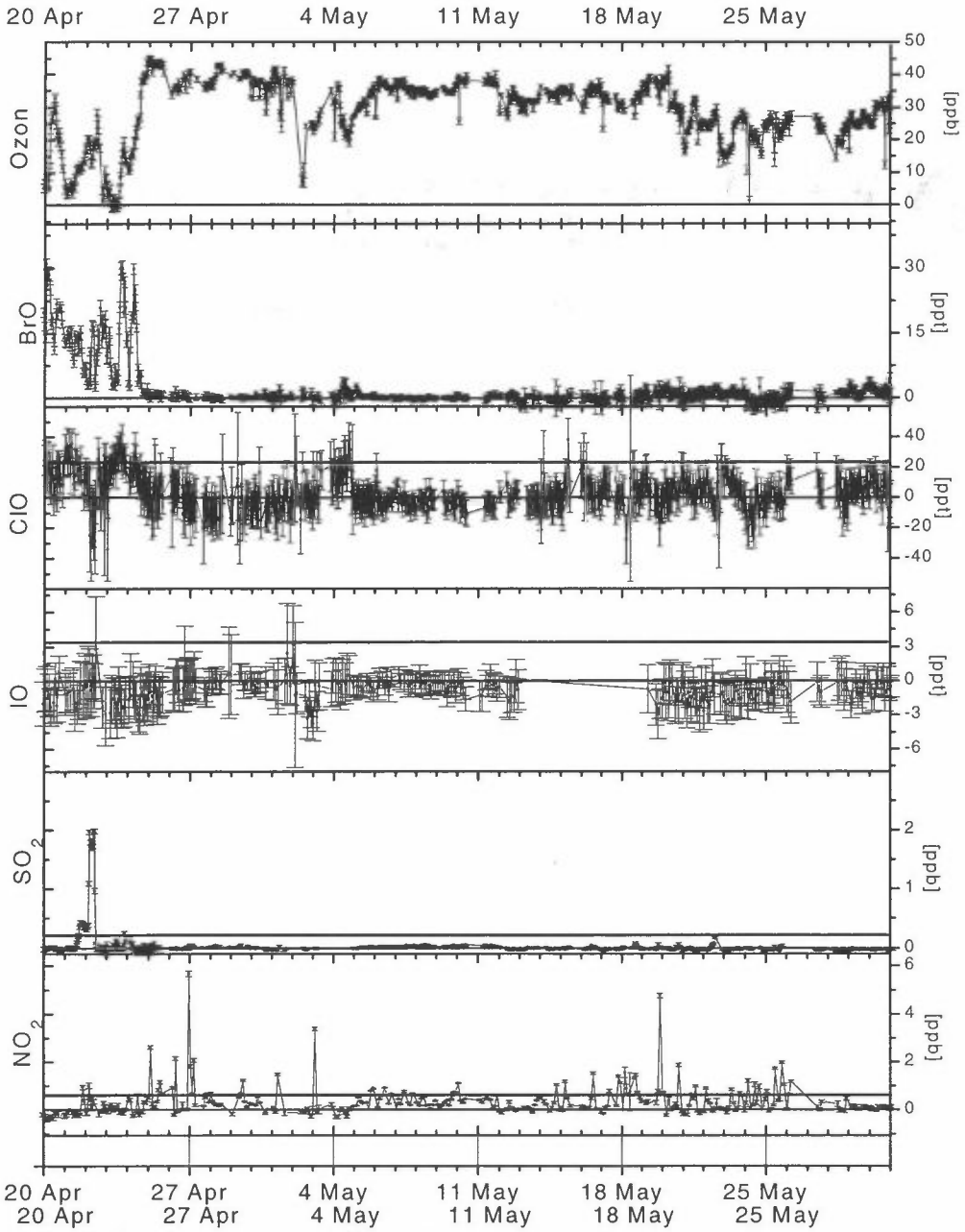

Figure 1: Time series of the halogen oxides ClO, BrO, IO, O_3, NO_2 and SO_2 during the entire period of the 1995 campaign.

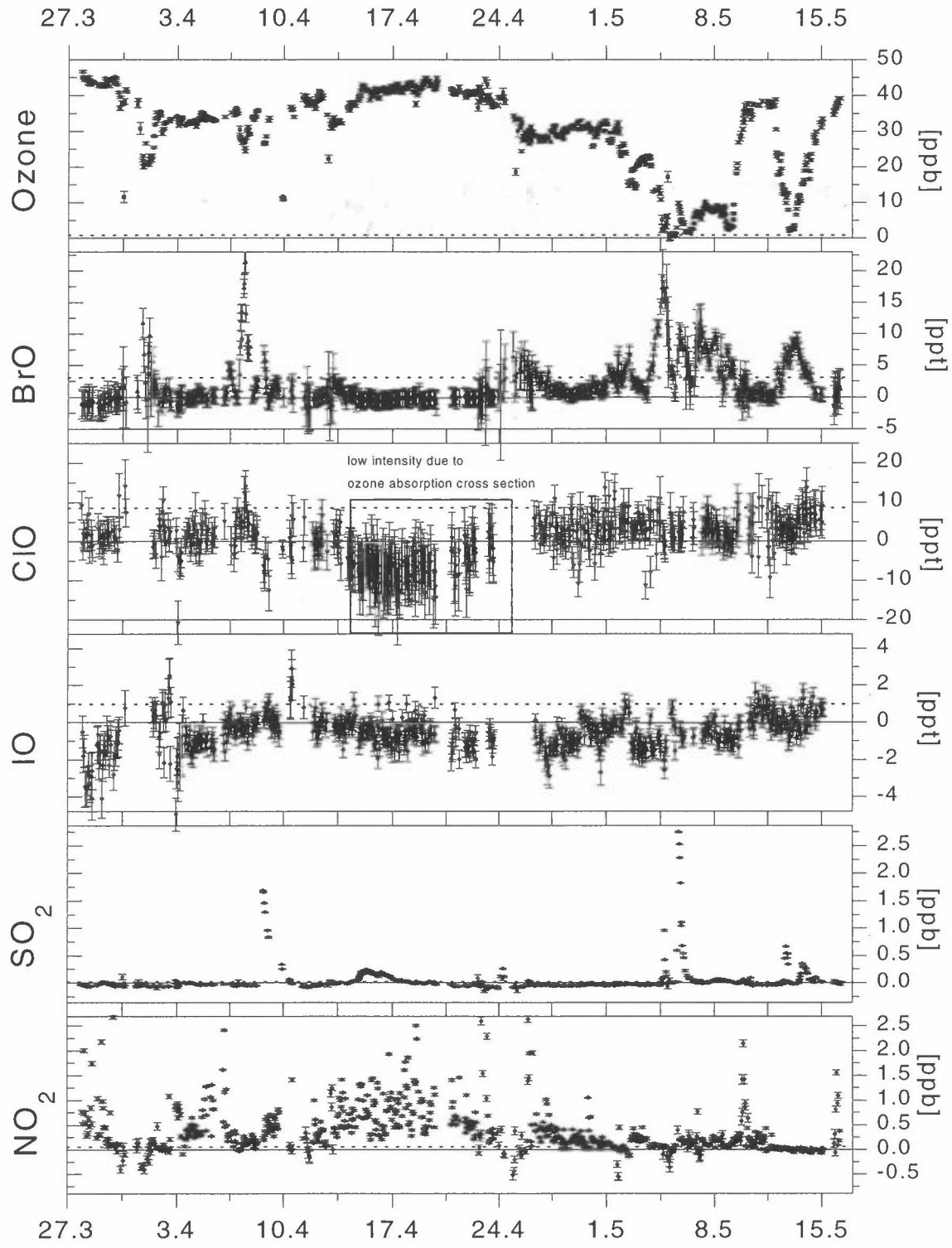

Figure 2: Time series (March 21 - May 18) of the halogen oxides ClO, BrO, IO, O_3, NO_2 and SO_2 during the entire period of the 1996 campaign.

Tropospheric Ozone Related Aerosol Chemistry Observed in High Time Resolution During ARCTOC '95 & '96 at Zeppelin Fjellet

Langendörfer, U., Lehrer, E., Wagenbach, D. and Platt, U.
Institut für Umweltphysik, University of Heidelberg, D-69120 Heidelberg, Germany

1. Introduction

Since the late eighties an anti-correlation between tropospheric ozone and so called filterable bromine (f-Br), bromine species that are sampled by cellulose filters, is observed at several Arctic sites, e.g. Barrow (Alaska) and Alert (Northern Canada). The phenomenon was not observed in the Eurasian Arctic sector yet. In the framework of the EU project ARCTOC (Arctic Tropospheric Ozone Chemistry) two field campaigns were performed in spring 1995 and 1996 at Ny-Ålesund / Svalbard. Here we report on the first Eurasian Arctic measurements which demonstrate the f-Br - ozone anti-correlation during ozone depletion events. The results will be discussed with a focus on the temporal changes of f-Br and its correlation to gaseous BrO in different ozone scenarios.

2. Experimental Procedures

Instrumental set-up

The aerosol sampling set-up during the campaigns in 1995 and 1996 was installed at the Norwegian Institute for Air Research (NILU) Air Monitoring Station on the top of Zeppelin Station. The station is located on a height of 474 m asl, 2 km south of the settlement Ny-Ålesund and air contamination on the station due to local emissions is believed do be negligible [Solberg et al., 1996].
The aerosol sampling routine was developed on the basis of the procedure we routinely apply at the German Antarctic overwintering station [Wagenbach, 1988]. A vertical inlet tube (∅ = 120 mm), continuously ventilated, was installed on the roof of the station. To reduce ice crystal sampling a protecting, downward-facing cylinder (∅ = 320 mm) was attached top of the inlet. Through a downward facing bow within the inlet tube the air was pumped through the filter. To get comparable results to those obtained by Barrie et al. [1988] and Berg et al. [1983] we used two cellulose filters in series as similar filter media. The usage of dual filters allowed the calculation of filter efficiency. The sampling parameters in 1995 and 1996 are given in Table 1.

Table 1.: Sampling parameters of the ARCTOC aerosol sampling in 1995 and 1996

	ARCTOC '96 27.03 - 15.05		**ARCTOC '95** 17.04 - 12.06
	High Volume	Low Volume	
time resolution	4 - 1 h	24 h	24 - 4 h
filter type	2 Whatman 541 Cellulose filter in series (A&B-filter), Ø 150 mm	combination of Cellulose filter (A-filter) and Nylon filter (B-filter) in series, Ø 47 mm	2 Whatman 541 Cellulose filter in series (A&B-filter), Ø 90 mm
number of filtersets	421	41	121
flow rate	54 m³/h (900 l/min)	2.5 - 5 m³/h	21 m³/h
pumping unit	DIGITEL DHA-80 (modified auto filter changing unit)	system '95	pump station, manual filter changing

Filter preparation and chemical analysis via Ion Chromatography (IC)

The filters were cleaned several times in ultra clean water (18 MΩ), underwent an ultrasonic bath treatment and were dried under clean air before being used for sampling. They were stored in pre-cleaned polyethylene bags until usage and cut immediately after sampling in pre-cleaned vials (Nalgene, 60 ml). Process blanks were taken to get information on total procedure contamination. For chemical analysis one half of the filter was extracted into 20 ml ultra clean water (18 MΩ) and underwent an ultrasonic bath treatment again. At the Heidelberg laboratory the filter extracts were analysed for major ions by ion chromatography [Minikin, 1994]. The anion analyses of MSA^-, Cl^-, Br^-, NO_3^- and $SO_4^=$ were performed on a DIONEX DX300 ion chromatograph (AS11 separating column, AG11 precolumn and a 200 µl sampling loop) applying a NaOH eluent gradient procedure. For the cation analysis (Na^+, NH_4^+, K^+, Mg^+ and Ca^+) the DIONEX DX4500i ion chromatograph with a DIONEX IonPac CG12A pre and separating column was used. These runs were performed isocratic with a 50 mM MSA eluent. The analytical IC detection limit for all presented ions was always below the process blank concentration and the overall detection limit was controlled by the 3 σ process blank variability. For a typical 100 m³ air sample the above defined overall detection limits correspond to atmospheric concentrations of 12, 7, 0.8, 0.12 and 3.6 ng/m³ for Cl^-, Na^+, $SO_4^=$, Br^- and NO_3^-, respectively.

3. Results and Discussion

Filterable Bromine

During the sampling periods in 1995 and 1996 a strong anti-correlation between f-Br and Ozone could be found (Fig.1). It was the first time, that this phenomenon was observed in the Eurasian Arctic. This clearly shows, that the sudden loss of tropospheric ozone and the

simultaneous enhancement of f-Br is not a local aspect. In 1995 there was an average f-Br concentration of 15 ng/m³ during the late winter period (till 2nd May) and of 2 ng/m³ during the early summer period. In 1996 the average concentration was 10.5 ng/m³ for the whole campaign. The ozone variability, here defined as the standard deviation of the hourly averaged ozone concentrations, in 1996 (33.7 ± 13.7 ppb) was higher than in 1995 (32.1 ± 10.5 ppb). Maximum f-Br concentrations which occurred during total ozone depletion events ($[O_3]$<2 ppb) were 121 ng/m³ in 1995 and 81 ng/m³ in 1996.

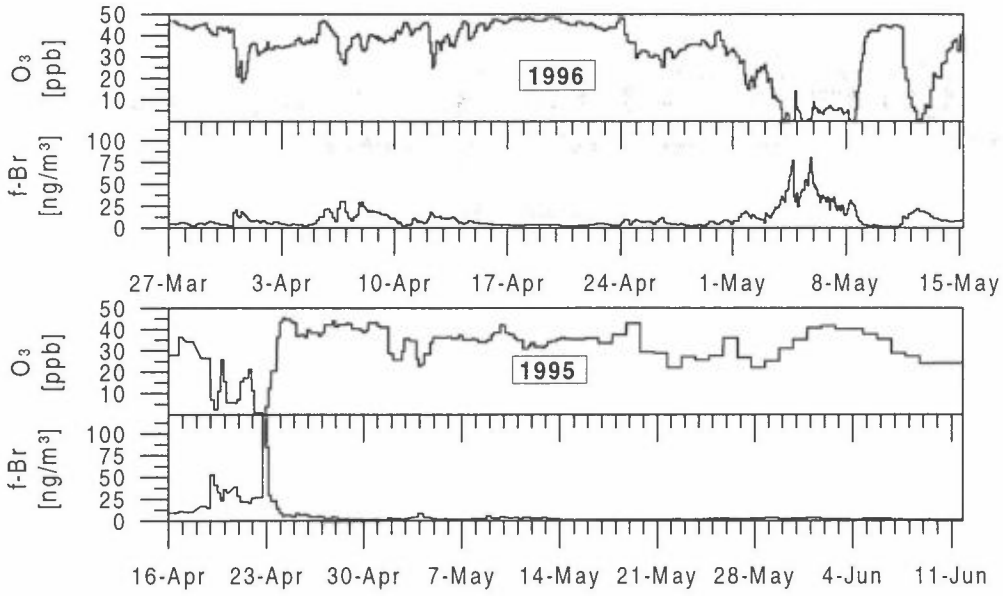

Figure 1: Ozone and f-Br concentrations during ARCTOC campaigns in spring 1995 & 1996

The results also show a significant enhancement of f-Br up to 30 ng/m³ during minor ozone depletion events (15 ppb < $[O_3]$ < 30 ppb). Even background ozone variabilities (35 ppb < $[O_3]$ < 50 ppb) seem to force f-Br behaviour to be strictly ozone anti-correlated in the range of 2-10 ng/m³. During total depletion events there is also a change in the rather linear anti-correlation between excess f-Br and ozone from an ozone threshold concentration of approximately 7 ppb (see Fig. 2).

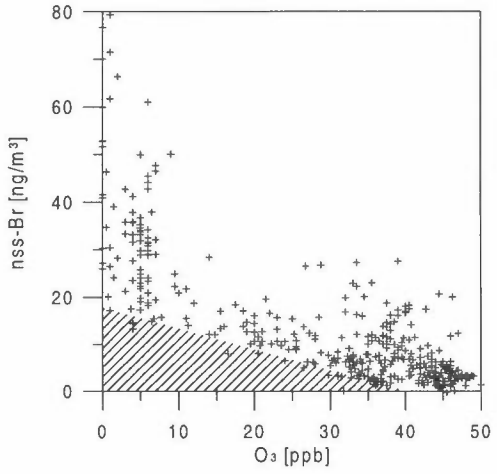

Figure 2: Non sea salt f-Br⁻ versus ozone in 1996

Due to a constant high time resolution in 1996 it was possible to observe that temporal changes in f-Br and ozone concentrations seem to be coincident for most of the observed variabilities. However the f-Br gradient in time tends to get positive after ozone got a negative gradient. Maximum f-Br values were only detected after ozone was below detection limit (<2 ppb). This 'maximum f-Br phase shift' is in the range of 6-12 hours. In 1996 a significant chloride excess up to 200 ng/m³ was observed during ozone depletion events.

Correlation to Bromine Oxide (BrO)

From differential optical absorption spectroscopy (DOAS) observations of BrO it became clear that the common anti-correlation between gaseous BrO and ozone changes to a correlation in the case of a total ozone loss, starting at an ozone concentration < 3 ppb [Tuckermann et al., 1996]. That behaviour suggests that BrO could not be formed anymore during such a period due to lack of ozone. Modelling simulations suggest that HBr is expected to be the Br species which may be formed with the greatest likelihood at extremely low ozone levels [Borken, 1996]. As plotted in Fig. 3 only during total depletion events f-Br exceeds the typical BrO/f-Br mole ratio of 2 by a factor up to 10.

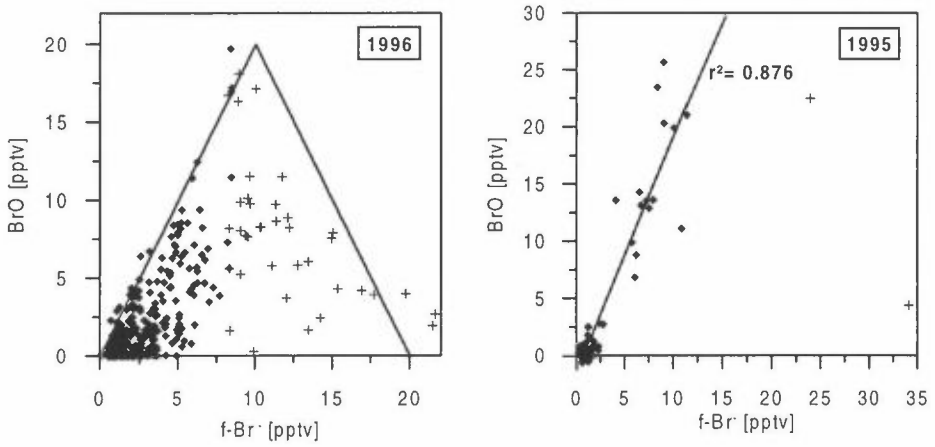

Figure 3: BrO - f-Br⁻ correlation in 1995 & 1996. The crosses mark ozone concentrations smaller than 7 ppb during total depletion events.

Consequently we expect the extremely high bromine concentrations found on the filters to be HBr. This interpretation is also supported by the results of the 1996 nylon filter samples. Nylon is expected to collect HBr with a very high efficiency [Barrie et al., 1989].

References

Barrie L.A., Bottenheim J.W., Schnell R.C., Crutzen P.J., Rasmussen R.A. (1988) Ozone destruction and photochemical reactions at polar sunrise in the lower Arctic atmosphere, In: Nature, Vol.334, pp. 138-141.

Barrie L.A., den Hartog G., Bottenheim J.W., Landsberger S. (1989) Anthropogenic Aerosols and gases in the lower troposphere at Alert Canada in April 1986, In: Journal of Atmospheric Chemistry, Vol.9, pp. 101-127.

Berg W.W., Speery P.D., Rahn K.A., Gladney E.S. (1983) Atmospheric Bromine in the Arctic, In: Journal of Geophysical Research, Vol. 88, No.C11, pp. 6719 - 6736.

Solberg S., Schmidbauer, N., Semb, A. and Stordal, F. (1996) Boundary-layer ozone depletion in the Norwegian Arctic in spring. Journal of Atmospheric Chemistry. 23, pp. 301-332.

Wagenbach D., Görlach U., Moser K., Münnich K.O. (1988) Coastal Antarctic aerosol: the seasonal pattern of its chemical composition and radionuclide content, In: Tellus, Vol. 40B, pp. 426 - 436

Minikin A. (1994) Spurenstoff-glaziologische Untersuchung von Eisbohrkernen des Filchner-Ronne-Schelfeises, Antarktis: Bestimmung der Tiefenverteilung und der Kontinentaleffekte ionischer Aerosolkomponenten. PhD Thesis, University of Heidelberg.

Tuckermann M., Ackermann R., Gölz C., Lorenzen-Schmidt H., Senne T., Stutz J., Trost B., Unold W. and Platt U. (1996) DOAS-observations of halogen radical-catalysed arctic boundary layer ozone destruction during ARCTOC-campaigns 1995 and 1996 in Ny-Ålesund, Spitsbergen. Tellus, submitted.

Borken J., (1996) Ozonabbau durch Halogene in der arktischen Grenzschicht: Reaktionskinetische Modellrechnungen zu einem Frühjahrsphänomen. Diploma Thesis, University of Heidelberg

Peroxy Radical Behaviour During ARCTOC Campaigns at Ny-Ålesund

T. Arnold, M. Martinez-Walter, D. Perner, and R. Seuwen
Max-Planck-Institut für Chemie, Joh. J. Becherweg 27, D-55128 Mainz

Abstract

In April 1995 and 1996 the EC-sponsored Arctic Tropospheric Ozone Chemistry (ARCTOC) investigations at Ny-Ålesund, Svalbard, consolidated the connection of bromine chemistry with the depletion of ozone in boundary air.
The in situ photochemistry was followed by the observation of peroxy radicals through a chemical amplification technique (ROx- Box). In sunny periods and under conditions undisturbed by bromine up to 8 ppt peroxy radicals were found around noon. The daily variation followed closely the photolysis rate of ozone decomposition into oxygen ^1D atoms, $J(O^1D)$. In the presence of BrO and low ozone the daily pattern changed. The mixing ratios of the radicals did not follow $J(O^1D)$ closely anymore. Elevated radical concentrations were observed also under reduced irradiation. The situation will be discussed with the help of a chemical box model.

Experimental

During spring 1995 and 1996 peroxy radical measurements by the chemical amplification technique [*Cantrell et al.*, 1984; *Hastie et al.*, 1991] were performed at Ny-Ålesund at the west coast of Spitsbergen ($78{,}9^0$ N, $11{,}8^0$ E). The instrument was set up at 'Gruvebadet' (ARCTOC 95) and 'Gruveverkstedet' (ARCTOC 96), both sites are situated 1,5 km south-west of Ny-Ålesund at an altitude of about 50 m a.s.l. and halfway between town and the base station of the cable car to the Zeppelin mountain.
The principle of the chemical amplification is the OH / HO_2 radical catalysed chain oxidation of CO to CO_2 and NO to NO_2. which is initiated by radicals (OH, HO_2, RO_2).

$$HO_2 + NO \rightarrow NO_2 + OH \qquad (1)$$
$$OH + CO \rightarrow CO_2 + H \qquad (2)$$
$$H + O_2 + M \rightarrow HO_2 + M \qquad (3)$$

The repetition of reactions (1-3) lead to the amplification of the peroxy radicals which are measured by the detection of the resulting NO_2 molecules. Organic peroxy radicals are converted to HO_2 by the reactions (4) and (5).

$$RO_2 + NO \rightarrow NO_2 + RO \qquad (4)$$
$$RO + O_2 \rightarrow R'CHO + HO_2 \qquad (5)$$

The chain is terminated by wall losses and by combination of the radicals. The efficiency of the chain reaction that means the number of molecules of NO_2 produced from one molecule HO_2 or RO_2 is called chain length (CL).

$$CL = \frac{[NO_2]_{on} - [NO_2]_{off}}{[HO_2]}$$

For the determination of the CL the photolysis of a mixture of water vapour with synthetic air at 185 nm was irridated with the 185 nm line from a mercury lamp [*Brune et al.*, 1995; *Schultz et al.*, 1995] and the O_3 formed was measured. The average CL value found in 1995 was 160 ± 15 (at 1σ) and in 1996 155 ± 10 (at 1σ).

The NO_2 detector a modified Scintrex LMA-3 was calibrated with mixtures of NO_2 permeation tubes in synthetic air. To reach a better NO_2 detector linearity, in 1996 a constant level of NO_2 was added at the air inlet [*Hastie et al.*, 1991].
For 10-minute-averages the detection limit of the peroxy radicals was 2 ppt in 1995 and 1 ppt in 1996. The estimated uncertainty (accuracy) of the measurements was ± 20 %, instrumental reproducibility (precision) based upon calibration was 6 %.
During the 1996 campaign $J(O^1D)$ was followed by two $J(O^1D)$ 2π-photoelectric filter radiometers (Meteorologie Consult) [*Junkermann et al.*, 1989; *Müller et al.*, 1995] one of them pointed upwards the other downwards. The uncertainty of these measurements is ± 30 % for solar zenith angles between 60^0 and 70^0 and ± 50 % for angles between 70^0 and 80^0 as stated by the company.

Results of the field measurements during low ozone events

1995: During 1995 periods of zero or almost zero ozone the peroxy radical mixing ratios were below the detection limit of the instrument (fig. 1).
In the beginning of the 1995 the measurements had just started when the major O_3 depletion event occurred and mixing ratios were low. At this time high wind speeds in combination with precipitation at low temperature were encountered.

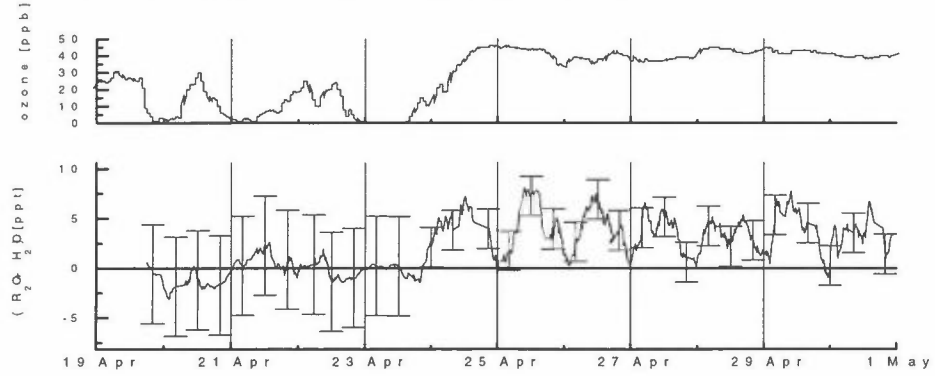

Figure 1: Mixing ratios of ozone at Zeppelin mountain (supplied by NILU) and of peroxy radicals during the low ozone period in 1995.

1996 : In 1996 the weather conditions during the ozone depletion event were different (fig.2).

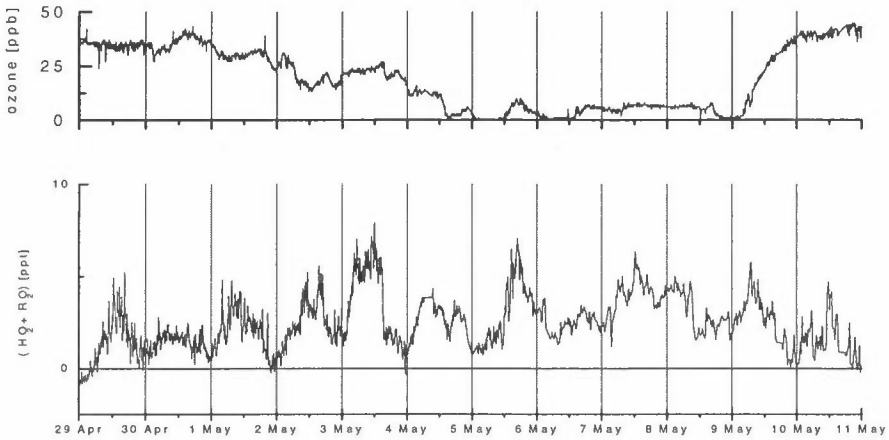

Figure 2: Mixing ratios of ozone as measured at Gruveverkstedet and of peroxy radicals around a ozone depletion event in 1996.

The sky was clear and cloudless.

Discussion : Before and after the depletion in both years the peroxy radical mixing ratios followed a diurnal cycle with maximum mixing ratios at local noon shown in Figures 3 and 4.

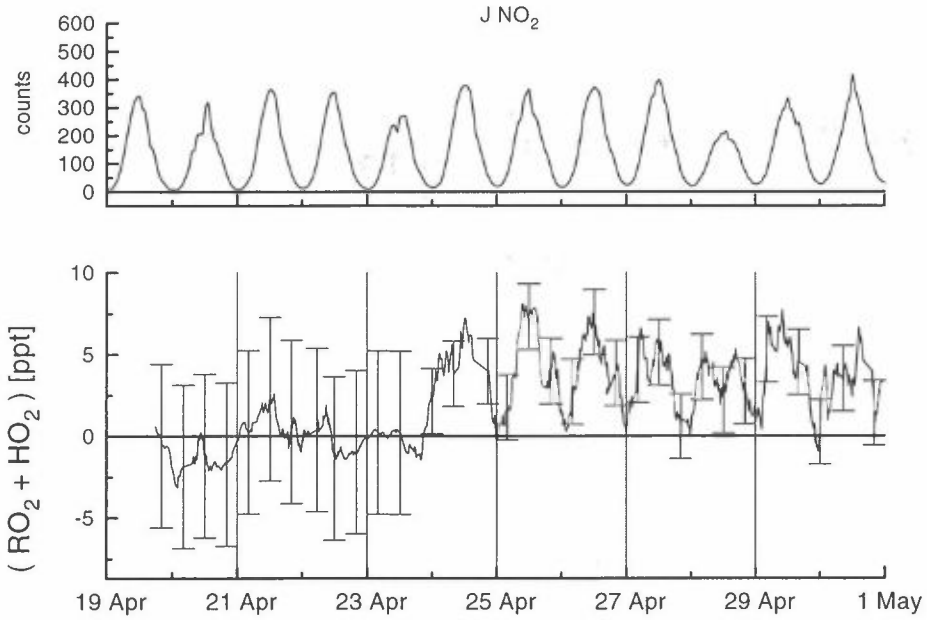

Figure 3: J(NO_2) photolysis data supplied by NILU and peroxy radical mixing ratios during the first 2 weeks of the campaign in 1995.

Under conditions of normal ozone the RO_2 mixing ratios reached up to 8 ppt and followed the radiative flux pretty well. In the presence of BrO and reduced ozone the RO_2 behaviour became somehow irregular. High mixing ratios at night were often followed by low values at noon(see for example 5 - 7 May).

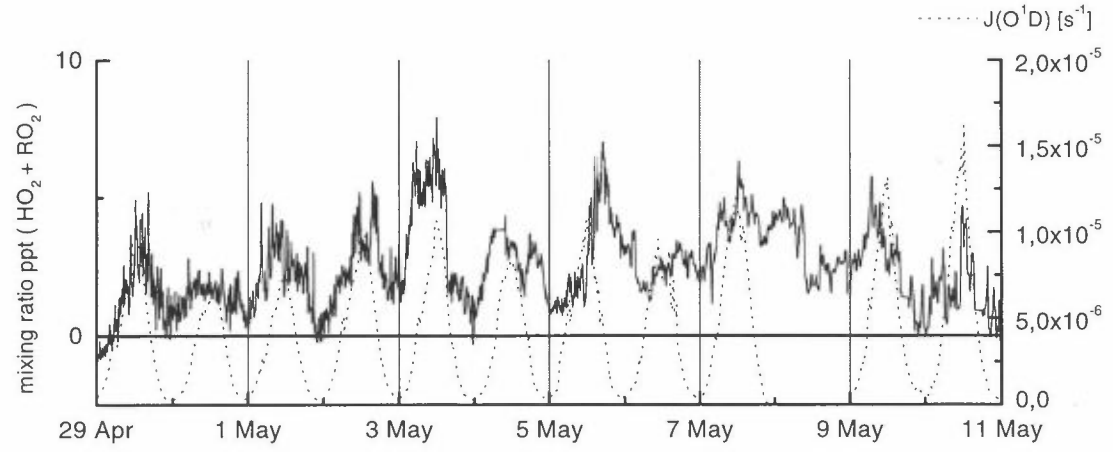

Figure 4 : J(O^1D) photolysis and peroxy radical mixing ratio during low ozone 1996.

Model calculations

In periods of 'undisturbed' ozone the data analysis by a chemical box model including only homogeneous gas phase chemistry and methane chemistry only showed good agreements of computed and measured peroxy radical mixing ratios.
When the model was initiated with 25 ppt of Br_2 and 10 ppb of O_3 the calculated levels of the peroxy radical mixing ratio dropped to 3 ppt at the noon but showed still the usual diurnal behaviour. After 12 hours the initial Br_2 was converted to HBr.
Including the chlorine chemistry (4 ppt Cl_2) and added hydrocarbons C_2H_6 (2 ppb), C_2H_4 (30 ppt) and H_2C_2 (350 ppt) did not change the peroxy radical behaviour. Already after 4 hours all chlorine was converted HCl.

Conclusions

The mixing ratio of the peroxy radicals was strongly dependent on the level of available ozone. If no ozone was present the peroxy radical levels were also close to or below the detection limit.
In the absence of BrO the peroxy radicals are produced by the photolysis of ozone. During the depletion event the peroxy radical chemistry became different probably due to the influence of inorganic halogen compounds, but the exact behaviour of the radicals could not be explained by the present gas-phase model.

Acknowledgements

The authors thank the CEC for financial support (CT93 0318)

References

Brune, W.H., P.S. Stevens, and J.H. Mather, Measuring OH and HO_2 in the troposphere by laser-induced fluorescence at low pressure, *Journal of the Atmospheric Sciences*, *52* (19), 3328-3336, 1995.

Cantrell, C.A., D.H. Stedman, and G.J. Wendel, Measurement of atmospheric peroxy radicals by chemical amplification, *Analytical Chemistry*, *56* (8), 1496-1502, 1984.

Hastie, D.R., M. Weissenmayer, J.P. Burrows, and H.G. W., Calibrated chemical amplifier for atmospheric RO_x measurements, *Analytical Chemistry*, *63*, 2048-2057, 1991.

Junkermann, W., U. Platt, and A. Volz-Thomas, A photoelectric detector for the measurement of photolysis frequencies of ozone and other atmospheric molecules, *Journal of Atmospheric Chemistry*, *8*, 203-227, 1989.

Müller, M., A. Kraus, and H. A., $O_3 \rightarrow O(^1D)$ photolysis frequencies determined from spectroradiometric measurements of solar actinic UV - radiation: Comparison with chemical actinometer measurements, *Geophysical Research Letters*, *22* (6), 679-682, 1995.

Schultz, M., M. Heitlinger, D. Mihelcic, and A. Volz-Thomas, Calibration source for peroxy radicals with built-in actinometry using H_2O and O_2 photolysis at 185 nm, *Journal of Geophysical Research*, *100* (D9), 18811-18816, 1995.

Hydrocarbon measurements in the Arctic troposphere: A probe for tropospheric ozone depletion

R. Koppmann, B. Ramacher and J. Rudolph
Institut für Atmosphärische Chemie
Forschungszentrum Jülich GmbH, 52425 Jülich, Germany

Abstract

Hydrocarbon measurements were carried out during the ARCTOC 95 and 96 field campaigns at Ny Ålesund, Svalbard (78°55'N, 11°56'E). In-situ measurements of C_2-C_8 hydrocarbons and C_1-C_2 halocarbons, canister sampling, and in-situ determination of carbon monoxide were done between April 16 and June 12, 1995 and March 29 and May 15, 1996. Tropospheric ozone depletions were observed in both years. In each case concurrent depletion of alkanes and ethyne, but no significant change in benzene, chloromethane, or CO mixing ratios were detected. For major ozone depletion periods time integrated chlorine and bromine atom concentrations were calculated from the depletion in ethane, propane, n-butane and ethyne. Time integrated Cl and Br radical concentrations are in the order of 10^{10} s/cm^3 and $5 \cdot 10^{12}$ s/cm^3, respectively. For strong ozone depletions the observed ozone losses can be explained quantitatively with these data. Our results show that free bromine atoms appear to be the major cause for ozone depletion.

Introduction

Since 1985 the phenomenon of tropospheric ozone depletion in the arctic during spring has been observed [1]. On time scales varying between hours and days the ozone mixing ratio drops rapidly from normal levels (30 - 40 ppb) to levels below the detection limit (1 ppb). Because of an anticorrelation of filterable bromine and ozone an ozone destruction mechanism via bromine atoms forming bromine oxide was suggested [2,3]. Later observations showed that some hydrocarbons are depleted in correlation with ozone, too [4-7]. This confirmed the idea of halogen atoms influencing the tropospheric chemistry during ozone depletion events. The purpose of this study was to improve the database of NMHC mixing ratios in order to provide more quantitative information for the suggested radical mechanism.

Methods

Two campaigns were conducted at Ny Ålesund, Svalbard (78°55'N, 11°56'E) in spring 1995 (April 16 - June 12) and spring 1996 (March 29 - May 15). A variety of organic trace gases were measured by several different methods. Nonmethane hydrocarbons (NMHC) as well as carbon monoxide (CO) were measured by in-situ gas chromatography at locations about 1.5 km away from the village of Ny Ålesund and about 50 m above sea-level ('Gruvebadet' in 1995; 'Gruvewerkstedet' in 1996). A road to Zeppelin Mountain is close to the locations but not used frequently (< 1 vehicle / h). Whole air samples were taken both at these locations and on Zeppelin Mountain (474 m a.s.l.) in evacuated 2 L stainless steel canisters. The measurement techniques have been described elsewhere [7]. For NMHC analyses detection limits range from 2 ppt to 60 ppt depending on the substance, the method, and the volume of preconcentrated air sample. Reproducibilities range from 2-38 % depending on the compound, but are better than 10% for most compounds. The CO detection limit is 2 ppb and the reproducibility is 1.2 %.

Results and Discussion

No significant deviations between the two in-situ methods and the canister sampling are found for most of the investigated substances [7]. For further interpretation the hydrocarbon data sets recorded with the different methods are combined.

The good comparability of the different NMHC measurement techniques emphasizes the quality of the data collected during the campaigns. Although most of the canister samples were collected on Zeppelin Mountain whereas in-situ measurements were carried out at sea level, there is no significant difference between the mixing ratios observed at the two sites. A comparison between samples from sea level and Zeppelin Mountain with overlapping sampling intervals shows that the variation is statistical within the error limits of the methods.

Figure 1 shows the time series of propane, benzene, and ozone for ARCTOC 96. In general, the correlation between NMHC and ozone is reasonable for light alkanes and ethyne for the major ozone depletion events. Weaker correlations are found for the pentanes. No positive correlation was found for benzene and methyl chloride. The correlation coefficients for the less intense ozone depletion periods are generally lower than those found for the strong depletion periods. For CO, benzene, and CH_3Cl the rates of reaction with Cl atoms is not significantly faster than for their reactions with OH-radicals. The reaction of alkanes or ethyne with Cl is a factor of 50 to 350 faster than with OH. The observation that benzene and CO show no change in their mixing ratios during the ozone depletion event supports the idea that changes in meteorology cannot explain the phenomenon. A chemical explanation based on halogen atoms seems much more likely and is able to account for the observed changes in NMHC pattern.

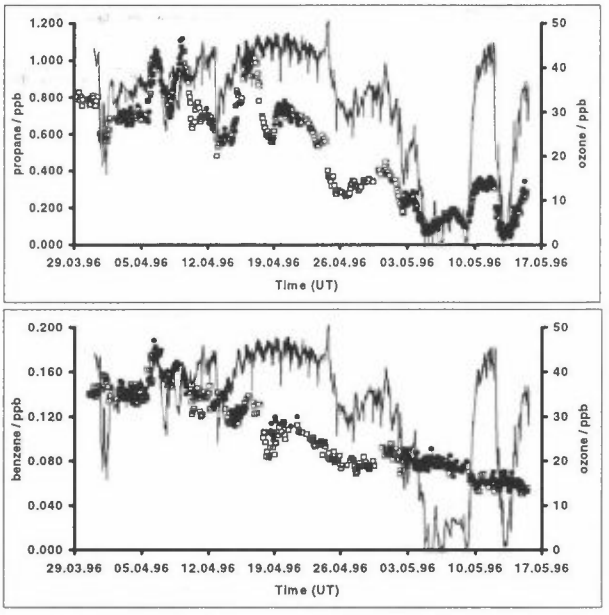

Figure 1: Plot of hydrocarbon time series. Open symbols: in-situ data GC 1, solid symbols: in-situ data GC 2, solid line: ozone (measured by T. Arnold, MPI Mainz)

From the change in hydrocarbon patterns during ozone depletion events, it is possible to calculate time-integrated halogen atom concentrations. The basic assumption is that the difference between 'normal' and 'depletion event' NMHC concentrations are caused by halogen atom reactions [5,6].

$$-\int [Cl]dt = \frac{1}{k_{HC,Cl}} \ln\left(\frac{[HC]_{depl.}}{[HC]_{initial}}\right) \qquad (1)$$

NMHC mixing ratios during ozone depletion ($[HC]_{depl.}$) were measured and the rate constants for the reaction with chlorine ($k_{HC,Cl}$) are known from literature. The unknown quantity in the equation is the initial NMHC mixing ratio ($[HC]_{initial}$) in an ozone depleted air mass before it was effected by chlorine radicals. The difficulty is that an ozone depletion event is always accompanied with a change in the air mass at the measuring site. However, since the arctic boundary layer seems to be quite well mixed, it can be assumed as a first approximation that an interpolation between the NMHC mixing ratios before and after the ozone depletion event is a measure for $[HC]_{initial}$. As mentioned before this assumption is supported by benzene,

carbon monoxide, methane, and PAN data, which do not show any significant changes during low ozone events.

The effect of Br-atoms can be derived from the depletion of ethyne. Ethyne is one of the few measured compounds which react fast enough with bromine atoms to see a significant effect on their mixing ratio. In order to obtain the time-integrated bromine atom concentration, the effect of the time integrated Cl concentration (calculated from the depletion of ethane and propane) was calculated. The corrected ethyne mixing ratio was then treated as $[C_2H_2]_{initial}$ and $\int[Br]dt$ was calculated from an equation equivalent to equation (1).

Table 1 shows the halogen atom concentrations calculated for the minor depletion episodes (May 2-5,1995; Apr. 1, 1996) and the three major depletions in April 95 and May 96, Table 2 gives the corresponding errors. The simple approach of calculating time integrated halogen atom concentrations from NMHC data is able to explain the major ozone depletion episodes quantitatively. From these data it is obvious that bromine is the main cause for ozone depletion (more than 95 %). However, this approach seems to fail in explaining minor depletion periods exactly.

Table 1: Time integrated halogen atom concentration during the ozone depletion periods estimated from changes in the mixing ratios of ethane, propane, ethyne and n-butane

	$\int[X\bullet]dt$ / $10^9 s \cdot cm^{-3}$				change of ozone mixing ratio / %			
Date	X = Cl (Ethane)	X = Cl (Propane)	X = Cl (n-Butane)	X = Br (Ethyne)	Cl induced	Br induced	Cl+Br	observed
April 21, 1995	9.8	8.4	8.1	9860	8.1	99.9	99.9	95.0
April 23, 1995	8.4	7.8	8.8	16000	7.7	100.0	100.0	99.0
May 3, 1995	2.7	2.8	3.3	955	2.8	47.6	49.1	23.5
May 4, 1995	4.8	3.9	2.4	1720	3.5	68.7	69.8	38.0
April 1, 1996	2.5	1.9	1.9	1340	2.0	59.6	60.4	48.4
May 4, 1996	13.7	13.5	10.9	6740	11.6	99.0	99.1	98.3
May 9, 1996	12.6	9.1	6.2	10000	8.6	100.0	100.0	97.7
May 12, 1996	14.7	10.4	9.2	8740	10.5	99.7	99.8	97.6

Table 2: Errors of the halogen atom concentrations and the change in ozone mixing ratios given in Table 1

	$\Delta\int[X\bullet]dt$ / $10^9 s \cdot cm^{-3}$		relative error of the calculated change of ozone mixing ratios / %
Date	X = Cl	X = Br	Cl+Br
April 21, 1995	0.9	3880	0.30
April 23, 1995	0.5	5090	0.01
May 3, 1995	0.4	1250	43.15
May 4, 1995	1.2	1240	25.31
April 1, 1996	0.3	1080	28.88
May 4, 1996	1.6	2070	1.29
May 9, 1996	3.2	2700	0.19
May 12, 1996	2.9	2930	0.48

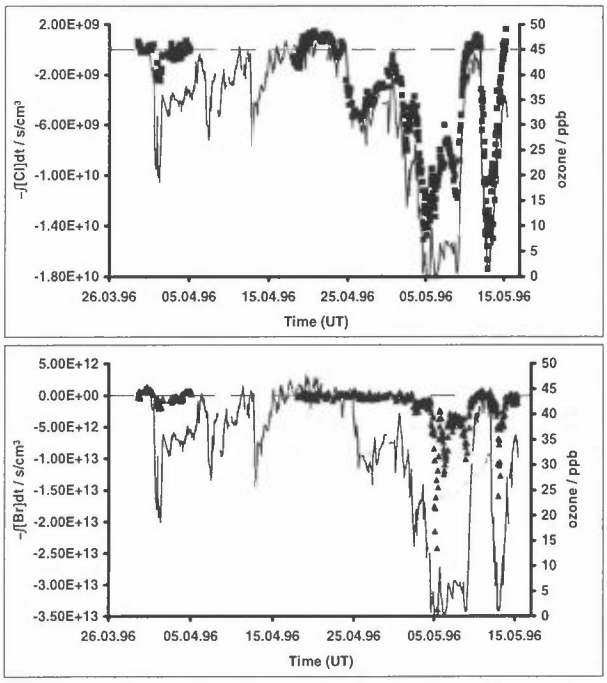

Fig. 2: Time series of the time integrated halogen atom concentrations. Symbols: halogen atom concentrations, solid line: ozone mixing ratio.

The good time resolution of the NMHC data allows the calculation of a time series of the time integrated halogen atom concentrations. NMHC data for 'normal ozone' are fitted by a trend curve and interpolated to the major ozone depletion period. Figure 2 shows the calculated integrated chlorine and bromine concentrations along with ozone data for the campaign in 1996 (the 1995 data give similar results). The correlation between the calculated radical concentrations and the ozone mixing ratio is obvious.

For normal ozone levels the mean values of $\int$[Br]dt and $\int$[Cl]dt were found to be $3 \cdot 10^{10}$ s·cm^{-3} (standard deviation of mean $84 \cdot 10^{10}$ s·cm^{-3}) and $-2 \cdot 10^{8}$ s·cm^{-3} (standard deviation of mean $8 \cdot 10^{8}$ s·cm^{-3}), respectively. These values are more than an order of magnitude lower than those derived for depletion episodes.

Achnowledgements

The assistance from Sverre Thom, Aanon Grimnes, Stig Osdal (Norsk Polarinstitutt) and especially Jan Wasseng (NILU) is gratefully acknowledged. This work was supported by EU Grant No. EV5V-CT93-0318.

References

[1] Bottenheim, J.W., Gallant, A.G., and Brice, K.A. (1986) Measurements of NO_y species at 82° N latitude. *Geophys. Res. Lett.*, **13**, 113-116.

[2] Barrie, L.A., Bottenheim, J.W., Schnell, R.C., Crutzen, P.J., and Rasmussen R.A. (1988) Ozone destruction and photochemical reactions at polar sunrise in the lower Arctic atmosphere. *Nature* **334**, No. 6178, 134-141.

[3] McConnell, J.C., Henderson, G.S., Barrie, L., Bottenheim, J., Niki, H., Langford, C.H., and Templeton, E.M.J. (1992) Photochemical bromine production implicated in Arctic boundary-layer ozone depletion. *Nature* **355**, 150-152.

[4] Bottenheim, J.W., Barrie, L.A., Atlas, E., Heidt, L.E., Niki, H., Rasmussen, R.A., and Shepson, P.B. (1990) Depletion of lower tropospheric ozone during Arctic spring: The Polar Sunrise Experiment 1988. *J. Geophys. Res.*, **95**, 18.555-18.568.

[5] Jobson, B.T., Niki, H., Yokouchi, Y., Bottenheim, J.W., Hopper, F., and Leaitch, R. (1994) Measurements of C2-C6 hydrocarbons during the Polar Sunrise 92 Experiment. *J. Geophys. Res.* **99**, 25355-25368.

[6] Solberg. S., Schmidbauer, N., Semb, A., and Hov, Ø (1996) Boundary-layer ozone depletion as seen in the Norwegian Arctic in spring. *J. Atmos. Chem.* **23**, 301-332.

[7] Ramacher, B., Rudolph, J., Koppmann, K. Hydrocarbon measurements in the spring arctic troposphere during the ARCTOC 95 campaign, submitted to *Tellus B* (Oct. 96).

[8] Lorenzen-Schmidt, H., Unold, W., Platt, U., Solberg, S., Stordal, F., Wessel, S., Gernandt, H. Ozone measurements in the European arctic during the Arctoc 1995 campaign, submitted to *Tellus B* (Oct. 96).

Tropospheric BrO and its Consequences for the Global Bromine Budget.

D. Perner, A. Grund, E. Hegels, T. Klüpfel and M. Martinez-Walter,
Max-Planck-Institut für Chemie, Saarstr. 23, D-55122 Mainz

Ib Mikkelsen
Danish Meteorological Institute, Lyngby Vej 100, DK-2100 Copenhagen

Abstract

Spring time low tropospheric ozone, O_3, in the arctic troposphere is associated with bromine monoxide, BrO, as was found in Alert (Hausmann and Platt, 1994) or in Spitsbergen by long path differential optical absorption spectroscopy, DOAS, in the boundary layer by using lamps. BrO appears to be independent of the organic bromide content and exceeds the latter often in concentration. Its most probable source is sea ice.

Recently tropospheric BrO has also been observed by groundbased zenith sky spectroscopy during tropospheric polar sunrise ozone depletion events in March in Greenland (Miller et al., 1996) as well as Svalbard (Wittrock et al., 1996). Here we report on the observation of episodes of large amounts of inorganic bromine compounds in tropospheric air later in the year namely in July/August 1995 from Söndre Strömfjord, Greenland and from the Jungfraujoch by using zenith scattered sunlight.

These experiments show the signature of tropospheric BrO at noon. The peculiar observations at both locations point to an unknown tropospheric reservoir of bromine. This inorganic bromine must be seen in addition to the organic bromine and may be transported into the stratosphere as well where it could explain the relatively large bromine content.

Observations

Day profiles of BrO slant columns of purely stratospheric BrO show a regular decrease from the morning until the highest sun elevation around noon. Then the columns increase again with increasing solar zenith angle. For about a week at Söndre Strömfjord in July/August 1995 peculiar day profiles indicated tropospheric BrO. Backtrajectories at that time point to the polar region as the source of those air masses.

The observations show a strong increase of BrO columns being about symmetric around noon under sunny conditions. The reversibility of this BrO absorption is readily explained by photolysis of a bromine reservoir at higher light fluxes and reformation with decreasing light intensities in the afternoon. The time regimes of both processes agree with photolysis of $BrONO_2$ and its reformation by the reaction of BrO with NO_2. Therefore $BrONO_2$ appears to be a tropospheric reservoir for bromine. Another possibility could be HOBr. Either compound seems to escape at least in part atmospheric washout processes and could be transported into the stratosphere.

Evidence already accumulated in the literature show the polar regions to be significant sources of atmospheric inorganic bromine during the sunlit period (Barrie et al., 1988; Vogt et al., 1996; Kreher et al., 1996). The bromine is ablated selectively from sea salt on the sea ice by an autocatalytic process. This cycle could be primarily initiated by photooxidation of probably gas phase hydrochloric acid. The strength of this source remains to be determined. Recent observations of BrO by the GOME instrument on the ESR2 satellite (Hegels et al., 1996) are very promising to solve this interesting question of BrO abundance and its global transport.

Acknowledgement:

This work has been supported in part by the CEC through grants EV5V CT93-0347, CT93-0318. The authors acknowledge the logistic support by the DMI meteorological office at Söndre Strömfjord.

Bibliography

Barrie, L.A., J.W. Bottenheim, R.C. Schnell, P.J. Crutzen and R.A. Rasmussen, Ozone destruction and photochemical reactions at polar sunrise in the lower Arctic atmosphere, Nature, 334, 138-141, 1988

Hausmann, M., and U. Platt, Spectroscopic measurement of bromine oxide and ozone in the high Arctic during polar sunrise experiment 1992, J. Geophys. Res., 99, 25399-25413, 1994

Hegels, E., P.J. Crutzen, T. Klüpfel, D. Perner, J.P. Burrows, A. Ladstätter-Weißenmayer, M. Eisinger, J. Callies, A. Hahne, K. Chance, U. Platt, W. Balzer, Satellite measurements of halogen oxides by the Global Ozone Monitoring Experiment, GOME, on ERS2: Distribution of BrO and comparison with groundbased observations, XVIII Quadrennial Ozone Symposium, Vol. Abstracts, p. 229, L'Aquila, Italy, 12-21 September, 1996

Kreher,K., P.V. Johnston, S.W. Wood, G.J. Keys, and U. Platt, Ground-based observations of OClO, BrO and NO2 during 1995 at Arrival Heights (77.8 S), Antarctica, XVIII Quadrennial Ozone Symposium, Vol. Abstracts, p. 302, L'Aquila, Italy, 12-21 September, 1996

Miller,H.L., Sanders, R.W., Solomon S. and A. Weaver, Potential processes involved in an arctic sunrise surface ozone disappearance event in Kangerlussuaq, Greenland, Europ. Geophys. Soc., XXI General Assembley, Vol. II of Abstracts C604, The Hague, The Netherlands, 6-10 May, 1996,

Vogt, R,. and P.J. Crutzen, Halogen chemistry in the marine boundary and their possible effect on ozone destruction, XVIII Quadrennial Ozone Symposium, Vol. Abstracts, p. 558, L'Aquila, Italy, 12-21 September, 1996b

Wittrock, F., M. Eisinger, A. Ladstätter-Weißenmayer, A. Richter, J.P. Burrows, Measurements of ozone, BrO, OClO, and IO in polar spring, Europ. Geophys. Soc., XXI General Assembley, Vol. II of Abstracts C607, The Hague, The Netherlands, 6-10 May, 1996

Abstracts from posters

Characterisation of Gas-Phase and Particulate Inorganic Components Collected at the Svalbard Islands

I. Allegrini, P. Masia, A. Ianniello
CNR-Istituto Inquinamento Atmosferico
Via Salaria Km. 29,300 - CP10, 00016 Monterotondo S. (Roma), Italy

Abstract

Sulphur and nitrogen containing compounds in gas phase and in particulate matter were measured at Ny-Ålesund, Svalbard Islands. These studies were carried out within the framework of a project specifically addressed to the understanding of the atmospheric chemical processes relevant to remote sites. Sampling has been performed on diffusion tubes (Denuders) designed for the efficient collection of several species in gas phase. Downstream the denuders, a cyclone and a filter pack were used for the collection of suspended particulate matter. After sampling, the ionic species were extracted with proper water solutions and analysed by mean of ion chromatography. Quality assurance on the sampling and analytical steps allowed a final accuracy better than 5% and minimum detectable amounts in the ppt range. In addition, particulate samples obtained with low pressure cascade impactor were collected and analysed. Data show that nitric acid can be detected at concentration levels down to a few ng/m^3 and that a significant fraction of fine particulate nitrate was evaporated but ammonium was not present.

Pollutant levels are usually very low (up to a few ng/m^3). However, when polluted air masses were sampled, adsorbed gaseous components on large and fine particles were detected. Experimental evidences show that nitrites could be present in particulate matter as the result of nitrous acid absorption. This finding is very important because the transport of particulate matter may be responsible for the transport of nitrous acid into relatively clean atmospheres. Such process may trigger the formation of OH radicals through the photodissociation of nitrous acid. Fine particulate nitrate and nitrite, although detected in the denuder line, were not found in the impactor stages. These is not surprising since losses of fine nitrates in impactors were also reported in other sites.

The sulphate size distribution obtained with cascade impactor shows a trimodal distribution. The accumulation mode, which was located always around 0.5 μm, takes into account for 85 to 99% of total sulphate mass. Most of the sulphate was obviously in the form of sulphuric acid from which gaseous species could be desorbed. Nitrates were found in the large size region, indicating a possible reaction between sea salt and gaseous nitrogen containing components such as nitrogen dioxide and nitric acid. Detailed results will be presented and compared with similar measurements carried out in Antarctica and in other European remote sites.

High resolution climate simulations over the Arctic with special emphasis on Spitsbergen

K. Dethloff 1), A. Rinke 1), I. Hebestadt 1),
J.H. Christensen 2), M. Botzet 3), B. Machenhauer 3)

1) Alfred-Wegener-Institute for Polar and Marine Research, D-14473Potsdam, Telegraphenberg A43, Germany
2) Danish Meteorological Institute, Copenhagen, Denmark
3) Max-Planck-Institute for Meteorology, Hamburg, Germany

Introduction

Data analyses and global circulation studies of the atmosphere indicate that the Arctic is a region of high climatic sensitivity. Climate simulations with global general circulation models are not very satisfactory over the Arctic. They produce significant biases in the simulated Arctic temperature and wind fields. The current deficiences of global climate models are related to the crudeness of model topography owing to the coarse horizontal resolution and the inadequate description and parameterization of typical Arctic processes. To evaluate the consequences of climate change, we need to develop climate models capable of simulating regional temperature and precipitation patterns with a high degree of fidelity in comparison of measurements. Therefore we apply a high resolution climate model on the whole Arctic north of 65 degree North.

Model description

The regional atmospheric climate model HIRHAM is based on the dynamical package of the High-Resolution Limited Area Model HIRLAM described in Christensen et al. (1996) and the physical parameterizations of the general circulation model ECHAM3/ECHAM4 described in Roeckner et al. (1992). It has been applied on the simulation of the Arctic climate of the troposphere and stratosphere up to 10 hPa at a 50 km horizontal resolution. The model has been forced at the lateral boundaries by ECMWF analyses and at the lower boundary by ECMWF analysed sea surface temperatures and sea ice fractions.

Results

Calculations for the winter and summer months of the year 1990 have been performed and described in Dethloff et al. (1996). The general spatial patterns of the meteorological variables mean sea level pressure, temperature, geopotential and humidity are in a good agreement with the ECMWF analyses.

Here we focus on a comparison of simulated and observed temperature and wind fields over Ny Alesund on Spitsbergen for January 1995 using the physical parameterizations of ECHAM4. Figure 1 shows the monthly averaged temperature profile for January 1995 from the model simulations and the observations indicating a good agreement. Largest deviations are visible in the planetary boundary layer below 900 hPa. The monthly averaged zonal and meridional wind components u and v from simulations and observations are also given and indicate deviations especially in the meridional wind component.
Figure 2 shows in the upper part the height-time section of the simulated temperature field over the whole January 1995 and in the lower part the corresponding observations. The agreement between simulations and observations in the temporal evolution of temperature is quite good. The largest deviations occur in the lower stratosphere above 25 km and in the planetary boundary layer below 2 km. The validation of the simulated temperature and wind components against station data over Spitsbergen indicates the necessity of further improvements in the physical parameterization packages. The use of the ECHAM4 physical parameterization leads to a reduction of the model bias compared against simulations with ECHAM3 physics as discussed in Rinke et al. (1997). The new radiation scheme and the planetary boundary layer parametrization in ECHAM4 improves the monthly mean model fields over the whole Arctic.

Literature

Christensen, J. H., O. B. Christensen, P. Lopez, E. van Meijgaard, M. Botzet, 1996, The HIRHAM4 regional atmospheric climate model, DMI Copenhagen, Scientific Report 96-4, 51 pp.

Dethloff, K., A. Rinke, R. Lehmann, J. H. Christensen, M. Botzet, B. Machenhauer, 1996, Regional climate model of the Arctic atmosphere, J. Geophys. Res., 101, 23401-23422.

Rinke, A., K. Dethloff, J. H. Christensen, M. Botzet, B. Machenhauer, Simulation and validation of Arctic radiation and clouds in a regional climate model, 1997, J. Geophys. Res., submitted.

Roeckner et al., 1992, Simulations of the present-day climate with the ECHAM model: impact of model physics and resolution, MPI Report No. 93, 171 pp.

Acknowledgment

The HIRLAM system was developed by the HIRLAM project group, a cooperative project of the national weather services in Denmark, Finland, Iceland, Ireland, the Netherlands, Norway and Sweden. We thank G. König-Langlo from AWI Bremerhaven for providing the observational data.

- **"Observation (rawinsonde data) vs Simulation (HIRHAM model)" for Ny Ålesund/Spitzbergen, January 1995**

Temperature [°C]

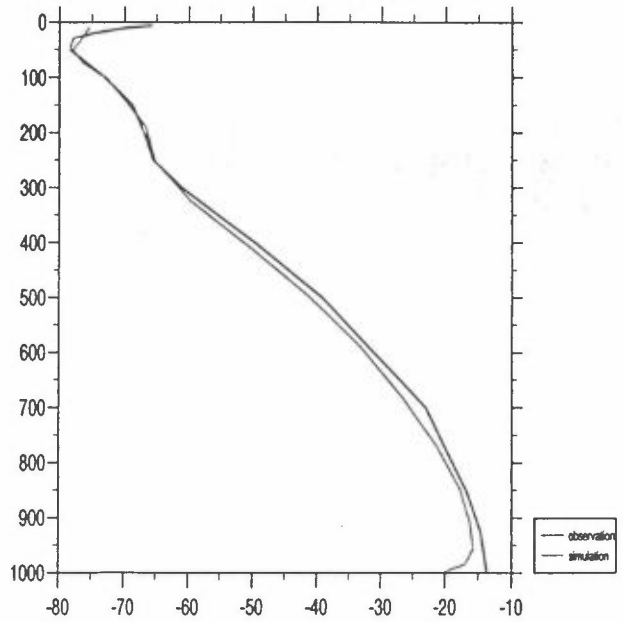

Wind [m/s]

u-wind

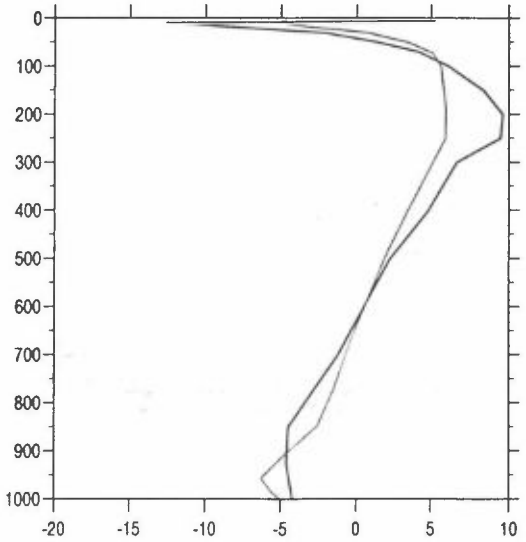

v-wind

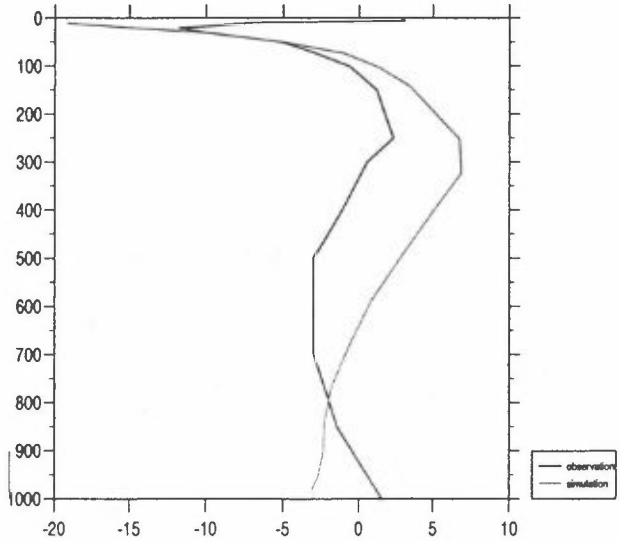

"Observation (rawinsonde data) vs Simulation (HIRHAM model)" for Ny Ålesund/Spitzbergen, January 1995

Height-Time-Section of Temperature

> Simulation

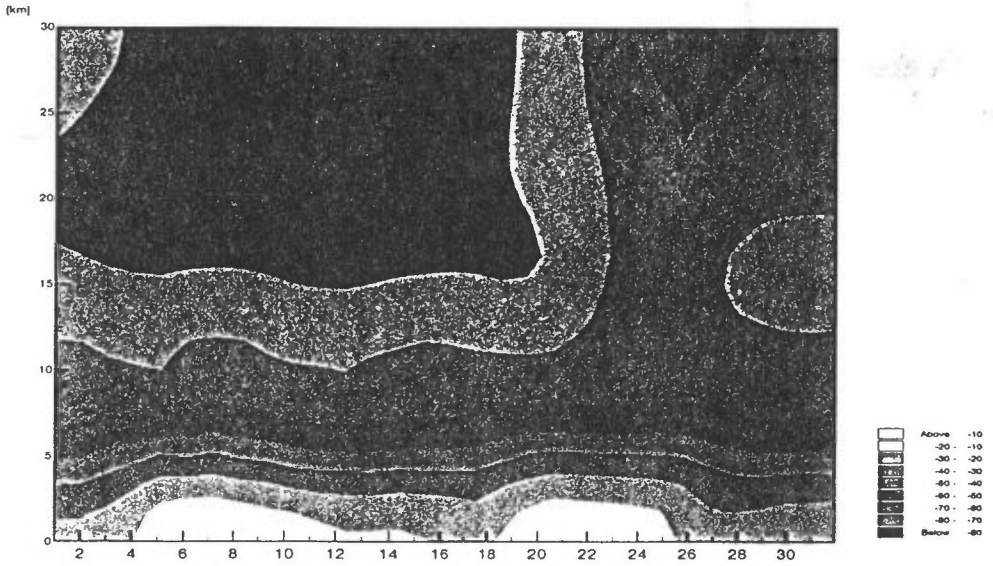

> Observation

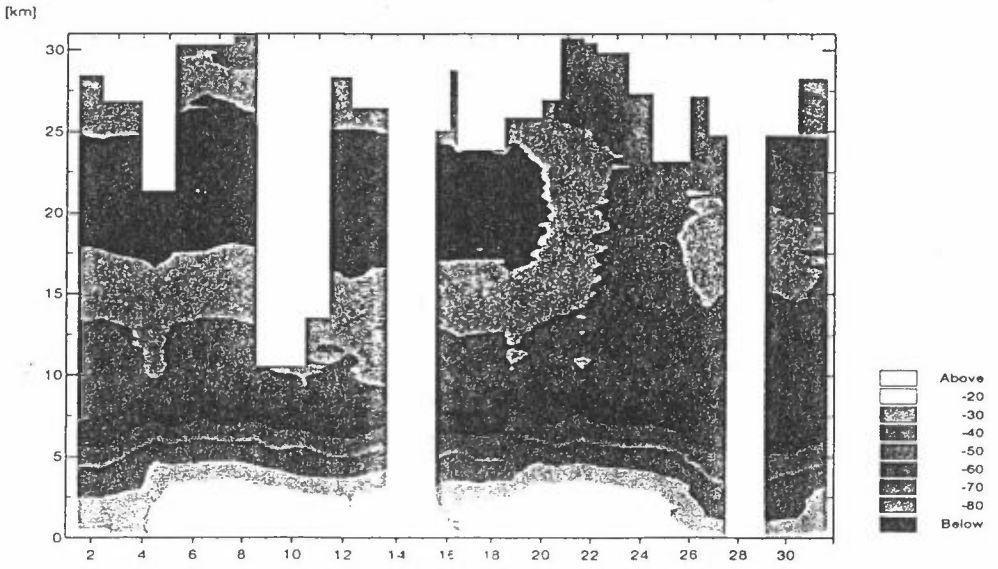

CFC trends at the Zeppelin mountain

Ove Hermansen, Norwegian Institute for Air Research

Background

NILU has been analysing halocarbons in air samples from Spitsbergen since 1990. The sampling and analysis of CFCs started as part of NILUs participation in the TOR project (Tropospheric Ozone Research) in the period 1990 to 1993. Samples were collected 3 times per week until May 1995 when regular sampling was ceased due to lack of funding. Samples are still collected for shorter periods once a year as part of measurement campaignes.

Sampling

Air samples are collected on stainless steel canisters. The canisters are electropolished inside to minimise adsorption problems. Cleaning is carried out by vacuumising (absolute pressure ~10^{-7} mbar). Air samples are filled into the empty canisters with a clean pump to 3 atm. pressure. All samples are sent to NILUs laboratories for analysis.

Analysis

Air samples are analysed by a gas chromatograph with an electron capture detector (GC/ECD). A specially designed injection unit with a cryo trap (figure 1) is used to introduce the sample into the gas chromatograph. The analysis method is used for the determination of five halocarbons, CFC-12 (CF_2Cl_2), CFC-11 ($CFCl_3$), CFC-113 ($C_2F_3Cl_3$), methyl chloroform (CH_3CCl_3) and carbontetrachlorid (CCl_4) as well as nitrous oxide (N_2O).

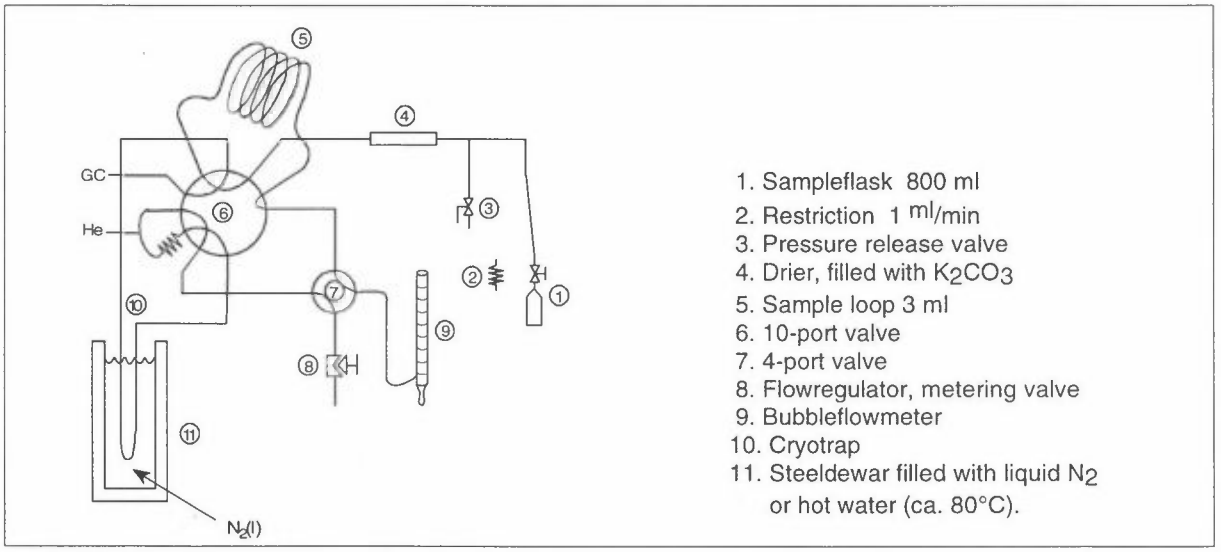

figure 1: Injection unit with cryotrap.

Trends

Former investigations has shown a steady growth in the amount of CFCs in the troposphere through the 1980s[1]. These investigations also indicated a decreasing growth in the beginning of the 1990s. Measurements from Mt. Zeppelin at Spitsbergen (figure 2) shows small changes in the levels of CFC-11, CFC-12 and CFC-113. The results indicates that CFC-11 might have

reached its maximum while CFC-12 and CFC-113 still might have a small increase (by mid 1995). Carbon tetrachlorid (CCl_4) shows a steady decrease through the period. The most rapid decrease is shown by metyl chloroform (CH_3CCl_3) which has the shortest atmospheric lifetime of these halocarbons.
The trends observed at Mt. Zeppelin are quite similar to trends observed elsewhere[2].

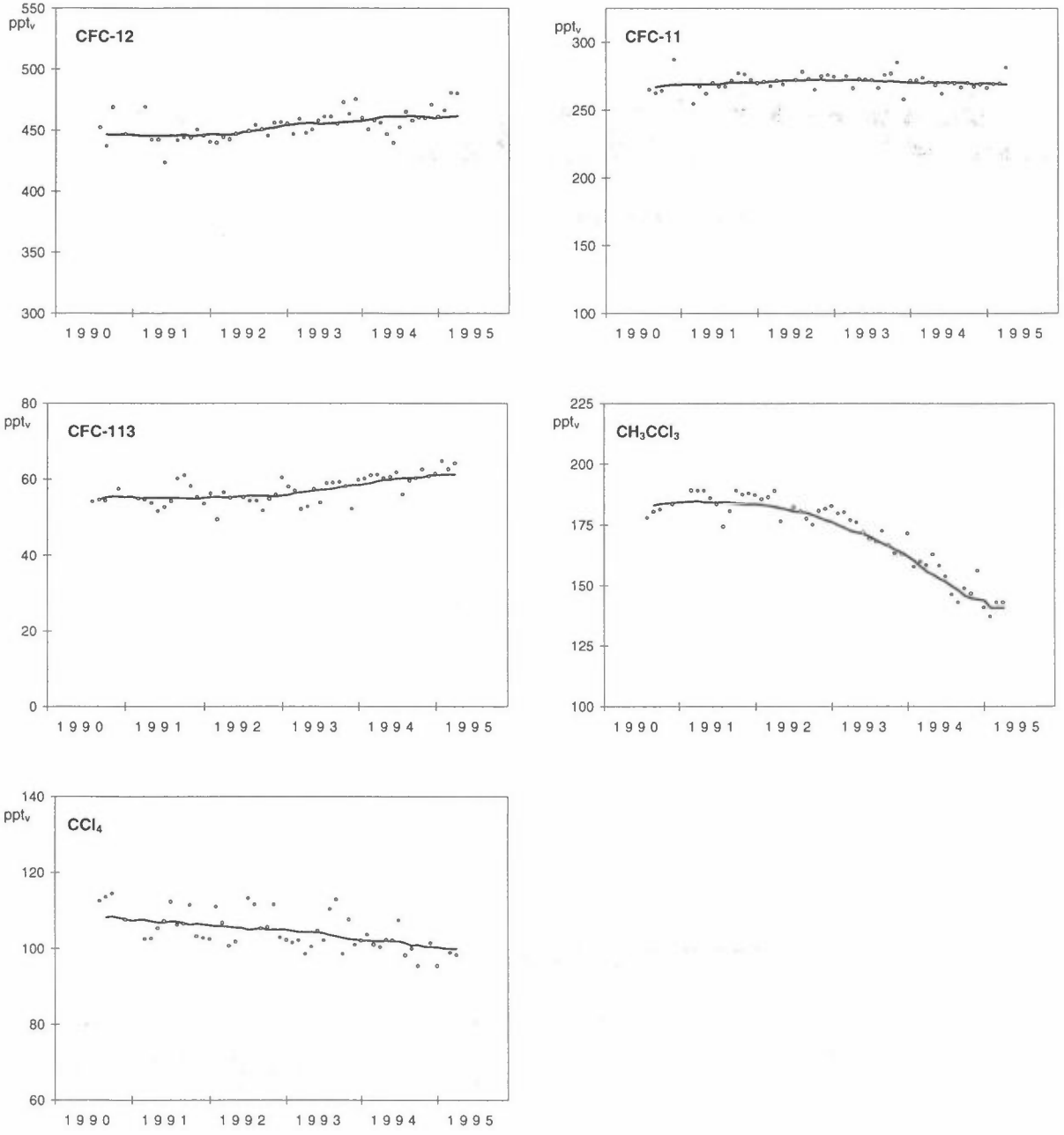

figure 2: Measurements of halocarbons at Mt. Zeppelin, Spitsbergen. Trend lines are shown as moving averages (± 12 months).

References

1. Elkins J. W.et. al., Nature vol 364, 26 August 1993, p. 780-783
2. Montzka S. A. et. al., Science vol. 272, 31 May 1996, p. 1318-1322

Atmospheric Research at Pallas in Finnish Lapland

Sirkka Juntto, Juha Hatakka and Yrjö Viisanen
Finnish Meteorological Institute, Sahaajankatu 20 E, FIN-00810 Helsinki
e-mail: Sirkka.Juntto@fmi.fi

GAW station Pallas-Sodankylä

In early 90's the Finnish Meteorological Institute established a monitoring station at Pallas-Ounastunturi National Park in western Lapland near the Swedish border (Fig. 1). In 1994, the station together with Sodankylä observatory were adopted as part of the Global Atmosphere Watch (GAW) network of the World Meteorological Organization (WMO). Radionuclides, ozone soundings, climatological and other meteorological measurements and upper-air soundings are carried out at the Sodankylä observatory, while tropospheric air composition and related boundary layer meteorological parameters are measured at Pallas.

Figure 1. Location of the atmospheric research station at Pallas.

Measuring sites

The main criteria for selecting the Pallas area as the site for tropospheric measurements were its remoteness, absence of local and regional pollution sources and the station maintenance. The main measuring site for GAW measurements is at the top of an arctic mountain (Sammaltunturi), at the height of 560 m a.s.l., over 300 m above the surrounding area. Another measuring site is situated inside a forest clearing on a hill (Matorova), at the height of 330 m a.s.l. The distance between the two measuring sites is 7 km.

At Pallas the height of the highest peaks are more than 500 m above the surrounding ground. This facilitates the measurement of temperature and wind profiles near the station to obtain information about the structure of the boundary layer in the area. The meteorological measurements are made using three automatic weather stations at different heights, and a present-weather sensor.

AMAP master station

In addition to being a GAW station, Pallas also serves as an AMAP master station. The aim of the Arctic Monitoring and Assessment Programme (AMAP) is to monitor the levels and assess the effects of anthropogenic pollutants in all compartments of the Arctic environment. The compartments are the atmosphere, the terrestrial environment, the freshwater environment, the marine environment and human health. During the first stage of its development, AMAP focuses on persistent organic pollutants (POPs), heavy metals, radioactivity and acidification.

The Finnish Meteorological Institute is responsible for the atmospheric part of the AMAP programme in Finland. Conventional air quality and deposition results from five stations in northern Finland are reported to the AMAP database. The measurements of POPs and mercury were started at the beginning of 1996 at Pallas/Matorova in cooperation with the Swedish Environmental Research Institute (IVL, Gothenburg), which is responsible for the analyses. The funding comes from the Swedish and Finnish environmental authorities. The ongoing GAW and AMAP measurements at Pallas and Sodankylä are presented in Table 1.

How clean is the air at Pallas?

The annual mean concentrations of the sulphur and nitrogen compounds collected daily in 1996 at Pallas/Matorova are in Table 2 compared with the annual means measured at Jergul and Zeppelin during 1991–1995, and at the Finnish EMEP station Oulanka (see Fig. 1) during 1991–1996. The mean concentrations of nitrogen compounds seem to be extremely low at Pallas. The concentration of sulphate at Pallas is about the same as at Jergul. The mean concentration of sulphur dioxide in 1995 measured by monitor at Pallas/Sammaltunturi was 0.45 $\mu g(S)/m^3$, which was somewhat lower than at Jergul, while in 1992–1994 the mean concentrations at the two stations where about the same.

The highest hourly sulphur dioxide concentration in 1991–1995 was 67 $\mu g(S)/m^3$, but on average the concentration is generally low; 90% of the hourly values are below 1.1 $\mu g(S)/m^3$ and 95% are below 2.3 $\mu g(S)/m^3$. The occasional brief episodes of high sulphur dioxide concentrations are mainly due to long-range transport from sources in the Kola Peninsula, 300 km north-east from Pallas. Most of the long-range transport episodes take place in winter and spring.

As an example of organic pollutants the monthly mean values of ethane, ethene, acetylene and n-butane at Pallas in 1994 are compared in Fig. 2 with those measured at Zeppelin and also at Birkenes in southern Norway. The concentrations at Pallas and Zeppelin were remarkably similar. At Birkenes the concentations of ethene, acetylene and n-butane were much higher, especially in wintertime. The results for the first year of measurements of air toxics will be presented at the AMAP symposium in Tromsø in June 1997.

International research

Air quality and meteorological research at Pallas will be developed on the basis of the permanent measurements. We already have some ongoing international projects concerning biogenic VOC emissions, as well as measurements and modelling of mercury.

Laurila, T. and Hakola, H., 1996. Seasonal cycle of C_2–C_5 hydrocarbons over the Baltic Sea and northern Finland. Atmospheric Environment 30, 1597–1607.

Lovén, L. and Salmela, S. (eds.), 1997. Pallas-symposium 1996. Finnish Forest Research Institute, Research papers 623, 1997.

Solberg, S., Dye, C. and Schmidbauer, N., 1996. VOC measurements 1994–1995. EMEP/CCC-Report 6/96, Norwegian Institute for Air Research, Kjeller.

Tørseth, K., 1996. Overvåking av langtransportert luft og nedbør. Atmosfærisk tilførsel, 1995. NILU OR 38/96, Norwegian Institute for Air Research, Kjeller.

Table 1. Ongoing GAW and AMAP measurements at Pallas and Sodankylä, April 1997.

Greenhouse gases	• flask sampling twice a week for CH_4 and N_2O • flask sampling once a week for CO_2 (with Atmospheric Environment Service, AES, Canada) • continuous CO_2 monitoring (with AES)
Ozone, total column and vertical distribution	• Sodankylä: O_3-soundings and total column O_3 measurements
Ozone, tropospheric	• O_3-monitor • Sodankylä: O_3-monitor
Other gases	• continuous SO_2, NO_x monitoring • SO_2, daily sampling, impregnated filter • flask sampling twice a week for volatile organic compounds (VOCs) • persistent organic pollutants (POPs), one week per month, polyurethane foam (with the Swedish Environmental Research Institute, IVL) • mercury, one day per week, goldtraps (with IVL) • Sodankylä: SO_2, two-week sampling, absorption solution
Atmospheric particles	• condensation nuclei and black carbon monitoring • daily filter sampling of sulphate, nitrate + nitric acid and ammonium + ammonia • heavy metals, weekly filter sampling • persistent organic pollutants (POPs), one week per month, filter (with IVL) • mercury, weekly filter sampling every other week (with IVL)
Precipitation chemistry	• bulk precipitation sampling on a daily basis: pH, conductivity, major ions • bulk precipitation sampling on a monthly basis: heavy metals, mercury (with IVL), POPs (only in summer, with the Finnish Environment Institute) • bulk sampling of POPs, one week per month (with IVL)
Radionuclides	• continuous ^{222}Rn monitoring • Sodankylä: daily ^{210}Pb, ^{7}Be, continuous ^{222}Rn monitoring
Solar radiation	• global solar radiation, $J(NO_2)$, $J(O1D)$ • Sodankylä: global, diffuse and reflected radiation, radiation balance, CIE-weighted UV-dose and spectral UV-B
Meteorological parameters	• three automatic weather stations at 300 m, 560 m and 790 m a.s.l., present-weather sensor, weather camera • Sodankylä: synoptic weather observations and upper-air soundings

Table 2. Annual mean concentrations of sulphur and nitrogen compounds from daily filter samples collected in 1996 at Pallas/Matorova, compared with the data of 1991-1995 from Jergul and Zeppelin and of 1991-1996 from the Finnish EMEP station of Oulanka (see Fig. 1).

Station	Year	SO_2 $\mu g(S)/m^3$	SO_4 $\mu g(S)/m^3$	NO_3+HNO_3 $\mu g(N)/m^3$	NH_4+NH_3 $\mu g(N)/m^3$
Zeppelin	1991	0.24	0.19	0.05	0.09
	1992	0.19	0.19	0.04	0.08
	1993	0.17	0.20	0.06	0.09
	1994	0.16	0.15	0.06	0.09
	1995	0.15	0.17	0.08	0.10
Jergul	1991	0.8	0.5	0.1	0.2
	1992	0.53	0.40	0.07	0.17
	1993	0.58	0.44	0.08	0.17
	1994	0.44	0.31	0.09	0.16
	1995	0.59	0.34	0.11	0.15
Pallas	**1996**	**0.32**	**0.34**	**0.05**	**0.07**
Oulanka	1991	0.93	0.68	0.08	0.25
	1992	0.70	0.57	0.08	0.19
	1993	0.70	0.58	0.08	0.17
	1994	0.50	0.44	0.07	0.12
	1995	0.55	0.44	0.07	0.13
	1996	0.60	0.48	0.07	0.16

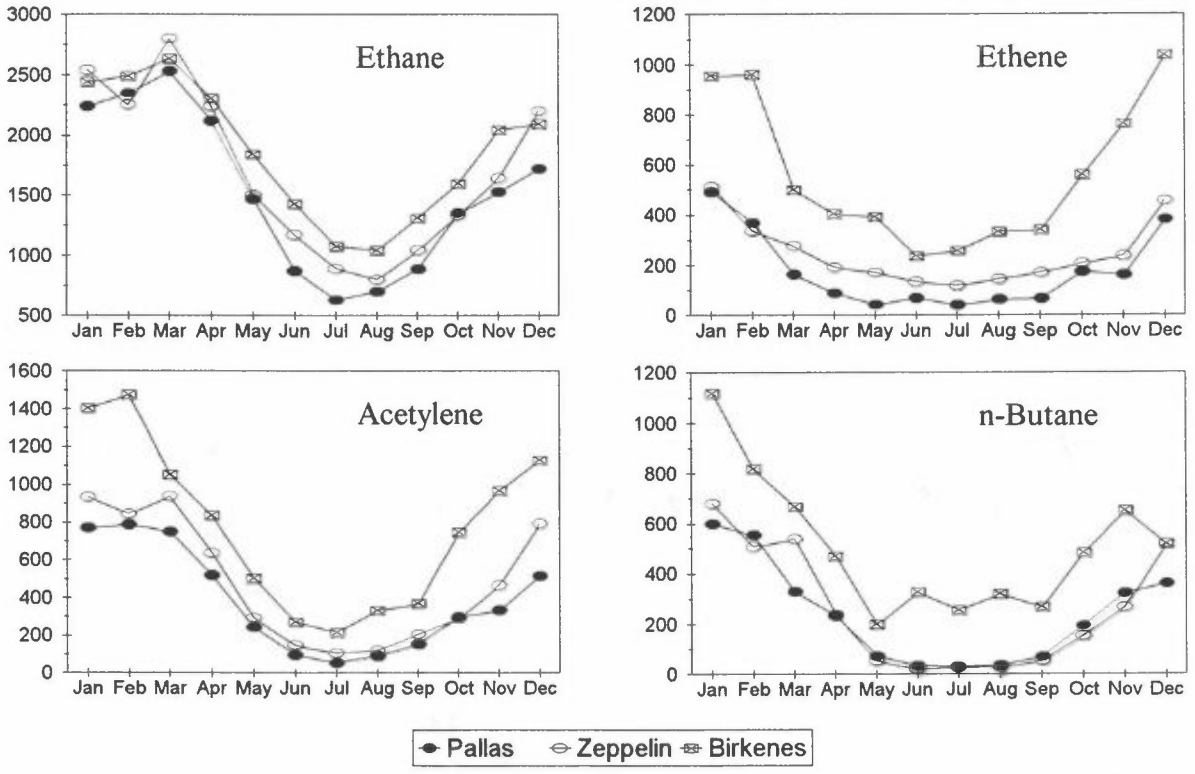

Figure 2. Monthly mean concentrations (pptv) of ethane, ethene, acetylene and n-butane measured in 1994 at Pallas, Zeppelin and Birkenes (see Fig. 1).

Ozone Mini Holes Above Svalbard Initiated by Energetic Solar Protons

E.A. Kasatkina, O.I. Shumilov
High-Latitude Geophysical Laboratory, St. Petersburg Filial of IZMIRAN,
P.O. Box 123, 184200 Apatity, Russia

O.M. Raspopov
St. Petersburg Filial of IZMIRAN, 191023 St. Petersburg, Russia

It is shown that high energy solar protons could produce so-called ozone "mini holes" (decrease of ozone total content up to 25%). Such a ozone "mini hole" was detected above Svalbard during solar proton events of Ground Level Event (GLE) type in May 1990.

The results of model calculations have shown that ordinary gas phase photochemistry can not explain the appearance of ozone total content depletion during GLE events. A possible trigger mechanism including ion-nucleation and heterogeneous chemistry is discussed. Lidar measurements at Kola peninsula and model calculations of aerosol concentration enhancement after another GLE event (16 February 1984) seem to support the trigger influence of solar protons on stratospheric aerosols and ozone layer.

Distribution of dimethylsulfide in the boundary layer at Spitzbergen

Ch. Kleefeld and O. Schrems
Alfred Wegener Institute for Polar and Marine Research
Am Handelshafen 12
D–27570 Bremerhaven, Germany

Introduction

The predominant gaseous biogenic compound of the global sulfur cycle is dimethylsulfide (DMS), emitted from the marine biosphere. Multi–step oxidation of DMS in the atmosphere leads to nss–sulfate and methanesulfonate (MSA) particles which are effective cloud condensation nuclei (CCN) and hence assumed to influence the cloud albedo.
About 80% of all contributions to the sulfur cycle in the northern hemisphere are attributed to anthropogenic emissions [1], masking the natural sulfur signal. This impact by human acivities is well seen in the Arctic region during spring and is associated with the Arctic haze phenomenon.

In this contribution we present results of two field campaigns performed at Ny–Ålesund. The DMS–measurements were conducted over a time period of two months in spring 1994 (Ark94) and in spring 1995 (Ark95).

Method

DMS was measured by gas chromatography (GC). It has been preconcentrated onto gold wool and subsequently analysed by GC with flame photometric detection (FPD). Calibration has been performed with certified permeation tubes.
Ambient air was enriched for 10 to 65 minutes at a flow rate of 2 l/min. Oxidizing compounds were removed from the air sample by scrubbing filters filled with cotton wadding. Two independent sampling channels were used in parallel for taking duplicate DMS samples.
The mean detection limit for atmospheric samples was estimated to be 0.5 pptv. The precision of the method was 12%.

During Ark94 duplicate DMS samples were collected three times a day and during Ark95 two times a day. Additionally, during the spring campaign 1995 DMS samples were taken two times a day at the air chemistry observatory on Zeppelinfjellet near Ny–Ålesund (Ark95/474m asl).

Results and discussion

The daily means of DMS mixing ratios observed during Ark94 and Ark95 are shown in Figure 1. The abscissa is divided in days of year (doy). The error bars denote the standard deviation of the mean values.

The DMS–time series indicate periods with low mean DMS mixing ratios of 0.8 pptv (Ark94 and Ark95) and with high mean DMS mixing ratios of 15.2 pptv (Ark94) resp. 33.1 pptv (Ark95).

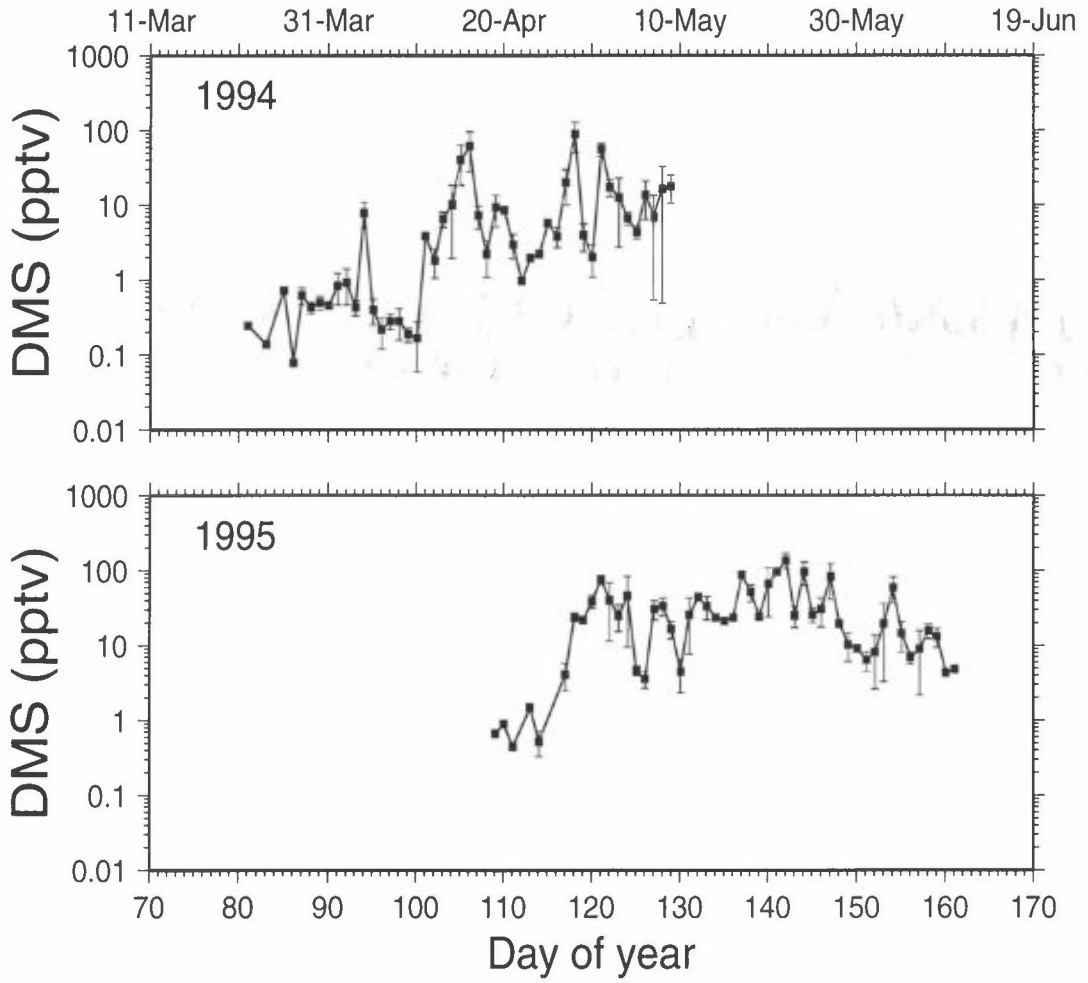

Figure 1: Time series of the DMS mixing ratios of Ark94 and Ark95.

The timing of the indicated periods and a statistical overview of the DMS concentrations is presented in Table 1.

The analysis of the air mass transport during the indicated DMS–periods is derived from 5–day backward trajectories on the basis of the 3dim. Global Model of the German Weather Service (DWD). Calculated trajectories for the surface level are grouped with respect to the different DMS–periods. Covariance ellipses around the mean locations at 5 days and 2.5 days before arrival of the trajectories define areas of the air mass origin. Figure 2 shows exemplarily the covariance ellipses calculated for the 1. period of Ark94. Additionally, the sea ice extend for the week before 03/28/94 is marked for the Svalbard area [2].

The covariance ellipses 5 days before arrival indicate a mean air mass advection from the sea ice covered Arctic Ocean and the Eurasian Continent. At 2.5 days before arrival air masses can origin from sea ice free areas of the Barents Sea and the ice edge zone. The same picture of air mass transport could be derived from the ellipses of the 2. period of Ark94 and the 2. period of Ark95. Since there is no change in air mass transport between the DMS–periods of Ark94 the elevated DMS level of the 2. period suggests the beginning activity of the biological DMS–

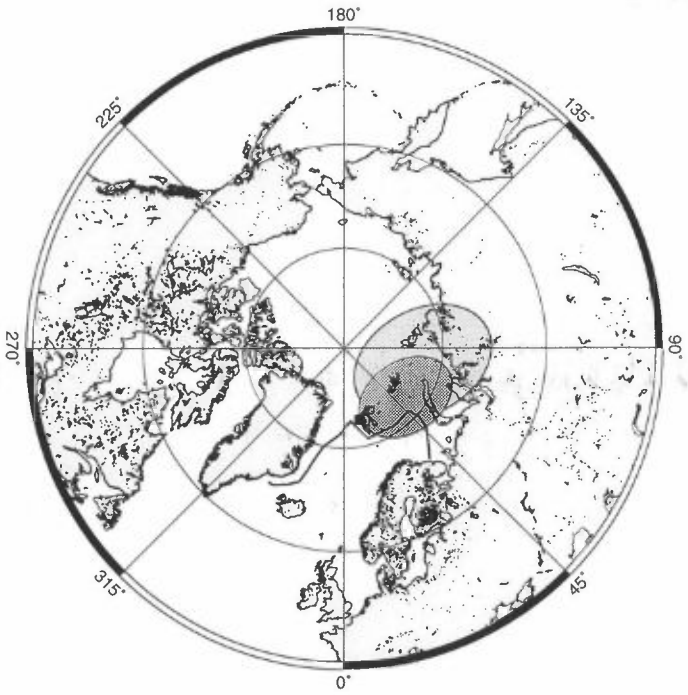

Figure 2: Covariance ellipses for the 1. period of Ark94 (03/22 until 04/10). The ellipses indicate mean air mass locations at 5 days (bright) and at 2.5 days (dark) before arrival. The sea ice extend is marked [2].

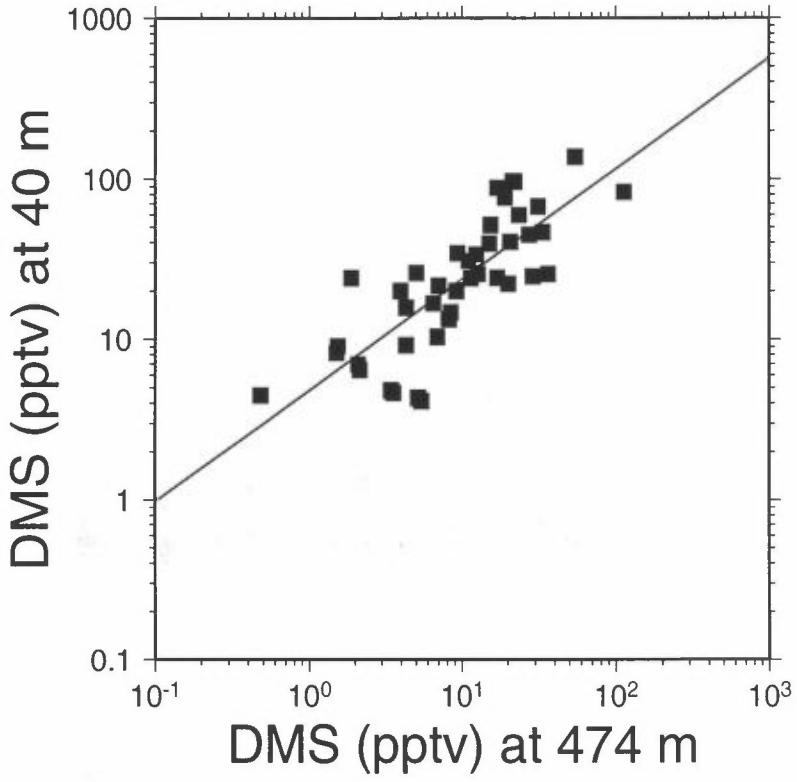

Figure 3: Correlation between daily means of DMS mixing ratios, measured in a height of 40m asl (Ark95) and 474m asl (Ark95/474m) (n=42, r^2=0.63).

Table 1: Statistical summary of the daily means of DMS mixing ratios (in pptv) during Ark94 and Ark95.

period	range	median	mean	1σ	n
Ark94					
03/22 – 04/10 (doy 81 – 100)	0.1 – 8.0	0.4	0.8	1.8	18
04/11 – 05/09 (doy 101 – 129)	1.0 – 89.6	7.0	15.2	20.6	29
Ark95					
04/19 – 04/26 (doy 109 – 116)	0.5 – 1.5	0.7	0.8	0.4	5
04/27 – 06/10 (doy 117 – 161)	3.6 – 138.9	24.3	33.1	30.1	45

source in mid–April. This result confirms investigations of MSA time series at Spitsbergen [3].

During the 1. DMS–period of Ark95 trajectories show an air mass advection from the probably DMS–source free Central Arctic Ocean. For this reason the onset of the activity of the DMS–source cannot be determined from the Ark95 DMS time series. The 1. period coincides with high BrO mixing ratios of about 15 pptv, measured during the ARCTOC 1995 campaign [4]. On the basis of the trajectory analysis the low mean DMS mixing ratios of 0.8 pptv are caused more likley by transport processes than by BrO–oxidation.

The DMS concentrations of Ark95/474m are lower by a factor of 2 than the DMS concentrations measured at sea level near Ny–Ålesund. The DMS mixing ratios of Ark95/474m and Ark95 show a striking good exponential correlation, which is presented in figure 3.

References

1 Berresheim, H., P.H. Wine and D.D.Davis, Sulfur in the atmosphere, in: Composition, chemistry and climate of the atmosphere, H.B.Singh (edt.), 251–307, Van Nostrand Reinhold Publishers, New York, 1995.

2 Sea ice charts of the Norwegian Meteorological Institute (DMNI), 1994.

3 Heintzenberg, J. and C. Leck, Tellus 46B: 52–67, 1994.

4 Platt, U., H. Lorenzen–Schmidt, W. Unold, E. Lehrer and M. v.König, Arctic Tropospheric Ozone Chemistry (ARCTOC), Environmental Research Programme, Progress Report No.2, 1996.

Measurements of heavy metals and ions in precipitation at Spitsbergen

M. Kriews, A. Ebbeler and O. Schrems
Alfred-Wegener-Institute for Polar- and Marine Research
D-27515 Bremerhaven, FRG

INTRODUCTION

Atmospheric transport from the highly industrialized areas at mid latitudes of the northern hemisphere is the main pathway of trace metals and ionic species to the arctic ecosystem. Removal processes of gaseous and particulate air pollutants from the atmosphere to snow-covered land or sea surfaces take place either by wet or dry deposition.

The highest concentrations of heavy metals in the arctic atmosphere have been observed in the winter/spring periods [1]. Through dry and wet deposition airborne pollutants reach the marine environment as well as the snow covered land areas. The scavenging of aerosol bound heavy metals by precipitation has been postulated as the most important process for cleansing the atmosphere. The aim of our investigations was to quantify the removal of trace metals and ionic species from the atmosphere by wet deposition via snow and rain as well as by dry deposition in the high Arctic (Ny-Ålesund, Spitsbergen 79°N, 10°E).

MATERIALS AND METHODS

Total deposition measurements are carried out at Ny-Ålesund since September 1993. A simple but very reliable total deposition sampler (TDS) is being used consisting of a well precleaned polyethylene funnel connected to an exchangeable bottle [3]. With this permanent open funnel wet and dry fall-out is collected. The total deposition samplers were placed at ground level at three different sampling sites in the vicinity of Ny-Ålesund. The annual distribution of wind directions shows that the winds mainly come from NW or SE [2].

In order to avoid contamination an extensive cleaning procedure of the sampling devices has to be carried out. All steps concerning the handling of material as well as the sample preparation have been performed under cleanroom conditions [3]. The preweighted sample bottles were stored after sample changing at -30°C, each packed in two polyethylene bags. The primary sample preparation steps were carried out in a laboratory at Ny-Ålesund under a clean bench (class 100). The precipitation height was estimated after melting by weighing the filled bottles. In samples with a water volume > 200 ml, the sample was subdivided into five portions. The minor portions were used for anion and nutrient analysis and measurements of pH-values as well as conductivity. The major subsample was used for filtration trough a 0.45 µm prewashed polycarbonate filter. This was necessary in order to get information about the dissolved and particulate element amount after the melting procedure.

For trace metal analyses the filtered and unfiltered samples were acidified immediately and stored in two polyethylene bags for transportation to the home laboratory, where further sample preparation steps [4] and element analyses were carried out by Graphite Furnace Atomic Absorption Spectroscopy (GF-AAS) for Al, As, Cd, Co, Cu, Cr, Fe, Mn, Ni, Pb and V. Flame Atomic Emission Spectrometry (F-AES) was applied for the determination of Na, Mg, K and Ca. Analyses of ionic species were carried by means of Ion chromatography for chloride, nitrate, sulphate, bromide and methanesulfonic acid (MSA) as well as for Na, K, Mg, Ca and ammonia.

RESULTS AND DISCUSSION

Results for the presumably anthropogenic elements Cd, Cr, Cu, Ni and Pb in deposition samples from a one year sampling period (February 1994 - March 1995) at Ny-Ålesund are shown. Supplementary results for Al as a tracer for earth crust weathering and for Na as a tracer for seaspray

are completing this data set. For the ionic species mentioned above data are partially available from February 1994 to November 1996. The median concentrations and deposition rates are shown in table 1. These are summarized data from snow, rain and mixed samples. The median was chosen, because the arithmetric means are susceptible for single extremly events, which can originate from contamination as well as from environmental conditions.

Table 1: Median element concentrations and deposition rates in total deposition samples from Ny-Ålesund

Earthcrust/Seas alt	Al	Fe	Ca	K	Na	Mg
(µg/kg)	196	140	456	186	1898	479
(µg/m²d)	67	40	142	76	687	189
Anthropogenic	Pb	Cd	Cu	Ni	Cr	Zn
(µg/kg)	0,89	0,033	0,58	0,57	0,72	22
(µg/m²d)	0,25	0,012	0,24	0,16	0,22	8,2
Anions	Nitrate	Ammonia	Sulphate	Chloride	MSA	Bromine
(µg/kg)	373	87	658	1281	12	28
(µg/m²d)	- -	- -	- -	- -	- -	- -

The strong variability of element concencentrations are exemplarily shown in figures 1 and 2 for the elements Al as a tracer for earthcrust weathering, Na and Cl as tracers for seaspray and the anthropogenic element Pb. It can be seen, that highest concentrations of all three categories are found in winter and spring. This is in good agreement with data from atmospheric aerosols [1]. In winter time element concentrations are about a factor of 10 higher than in the summer. However, the seasonal differences in trace metal concentrations are not obvious when deposition fluxes are considered. In summer and winter time we found comparable deposition fluxes due to the strong rain events during summer.

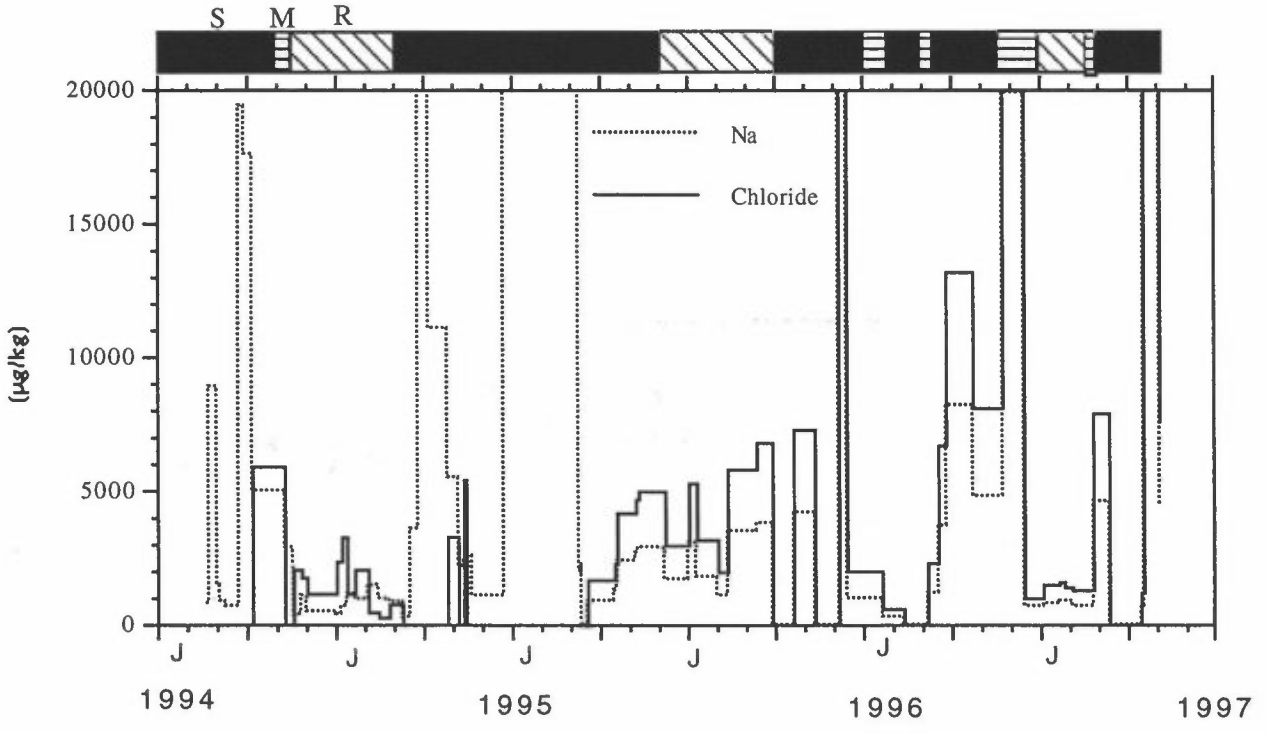

Figure 1: Na and Cl^- concentrations in total deposition samples from Ny-Ålesund (S=Snow, M=Mixed samples, R=Rain)

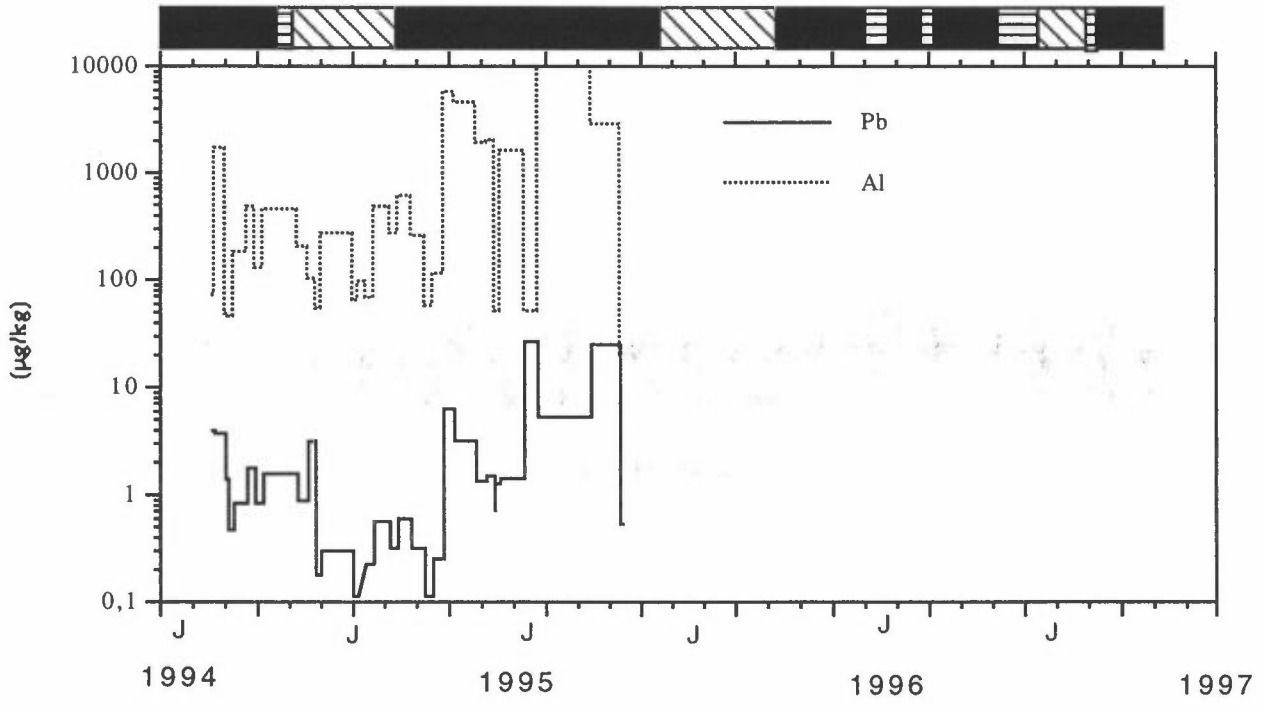

Figure 2: Al and Pb concentrations in total deposition samples from Ny-Ålesund

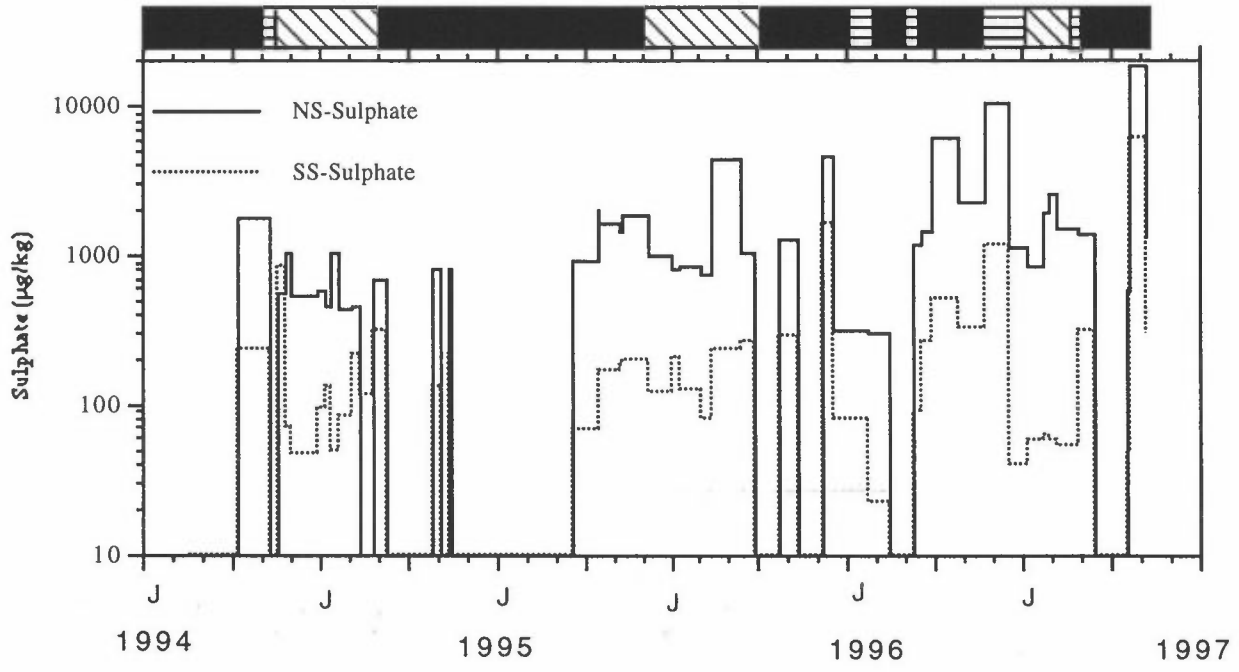

Figure 3: None seasalt-sulphate and seasalt-sulphate concentrations in total deposition samples

As an example for the variability of ionic species the time series for sulphate and MSA are shown in figures 3 and 4. Taking into account the sulphate/sodium ratio in seawater it is possible to distinguish between none seasalt-sulphate and seasalt-sulphate. The predominant sulphur species is none seasalt-sulphate which shows a 10-20 times higher concentration level than seasalt-sulphate.

The time series for another sulphur species which is from biogenic origin is shown in figure 4. Concentration maxima for methanesulfonic acid (MSA) could be found in summer time when the

Kongsfjord is free of ice and marine algaes are producing dimethyl sulfide (DMS). This gaseous species will be oxidised in the atmosphere to sulphate and MSA.

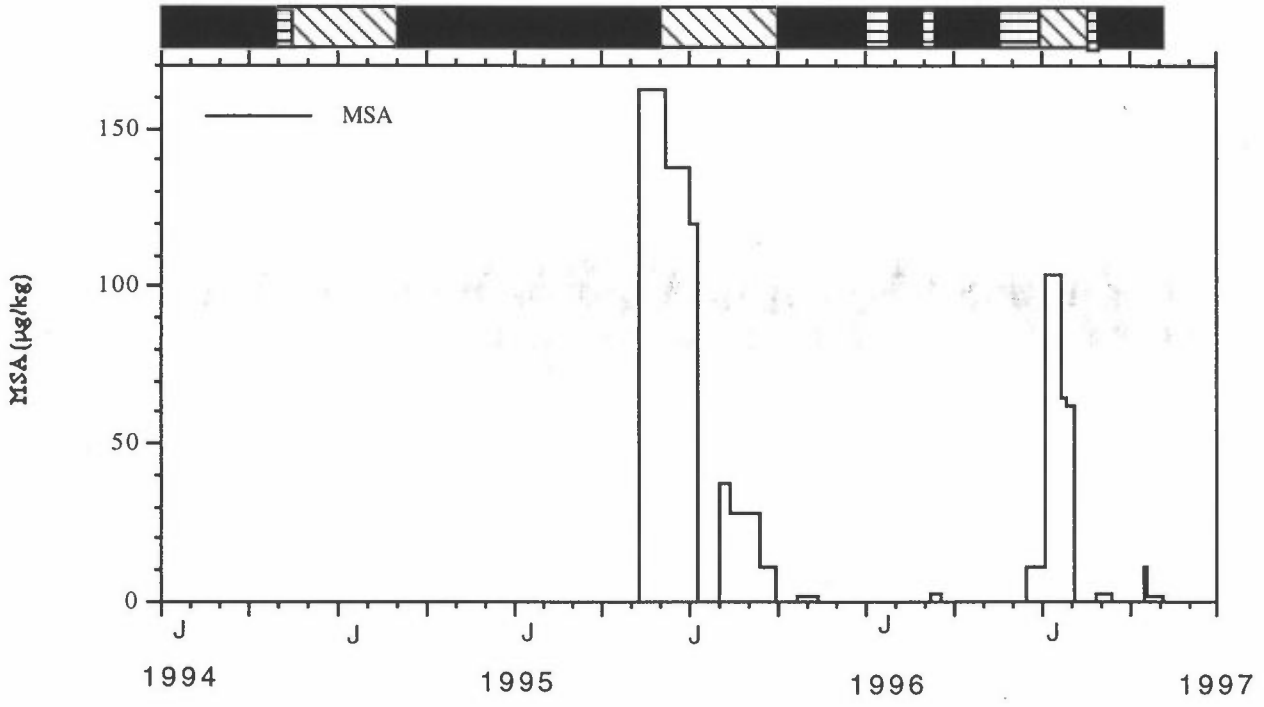

Figure 4: Methanesulfonic acid (MSA) concentrations in total deposition samples from Ny-Ålesund

CONCLUSIONS

The data obtained from our continuous wet and dry deposition measurements at Spitsbergen complement the sparse database for atmospheric trace metal fluxes to the Arctic basin. Element concentrations in the winter/spring period were found to be higher than in summer. However, the wet deposition fluxes in this period were similar due to the fact that there were strong rain events during summer. The winter appearance of anthropogenic pollutants is a well known phenomenon at sea level sites around the Arctic Ocean. In comparison to other areas of the northern hemisphere we observed relatively low deposition rates. A significant anthropogenic influence in this area from far away source regions is clearly documented. Further investigations to explain the strong seasonal change in trace metal concentrations are needed. Due to the fact that we found lower element concentrations during rain events in summer than during snow events in winter and spring, investigations of the wash-out efficiency of rain droplets and snow flakes in comparison to size separated aerosol samples should be included in future studies.

REFERENCES

[1] J.M. Pacyna and B. Ottar, *Atmos. Environ.* 19: 2109-2120 (1985)
[2] The climate of Spitsbergen, *DNMI rapport,* No. 39/90 (1990)
[3] M. Kriews, H. Giese and O. Schrems, *Colloquium Analytische Atomspektroskopie (CANAS`95)*, Welz B. (ed.) (1996)
[4] M. Kriews and O. Schrems, (1995): Pollution Analysis in the Arctic: Determination of Heavy Metals in Deposition Samples from Spitsbergen, in *Conference Proceedings HEAVY METALS IN THE ENVIRONMENT*, Vol.1, 371-374.

This is AWI publication No. 1233

PAN measurements at the Zeppelin Mountain 1994-1996

Terje Krognes, Harald J. Beine
Norwegian Institute for air research (NILU), Instituttveien 18, N-2007 Kjeller, Norway

Abstract

Measurements of peroxyacetyl nitrate (PAN) and ozone were made at the Zeppelin Mountain station near Ny-Ålesund, Svalbard during several years. PAN was measured with a custom built GC-ECD. Both PAN and ozone showed distinct annual cycles with maximum daily averaged mixing ratios of approximately 350 pptv and 36 ppbv, respectively, during spring. Mixing ratios of PAN and ozone were correlated. For each molecule of PAN, approximately 87 molecules of O_3 were present.

Introduction

PAN is a crucial component in the atmosphere. PAN is not emitted into the atmosphere, but rather produced from photochemical processes involving both NOx and VOC. PAN is thermally labile, but can be transported during winter into the Arctic, giving rise to a maximum during spring.

It was hypothesised [1,2] that the thermal break-up of PAN during spring can lead to *in-situ* ozone formation, and thus help explain the persistent ozone spring maximum that is observed at many northern hemispheric locations. This hypothesis has only recently been experimentally evaluated [3].

This work presents multiple yearly records of both PAN and ozone at Ny-Ålesund and explores their correlation to each other.

Measurements

PAN was measured with a custom built automated GC-ECD (NILU PANalyzer)[4]. Calibrations were carried out using a static dilution technique of a liquid PAN standard[6]. The PAN standards were transported to Ny-Ålesund packed in dry ice and stored in a freezer. The stability of PAN standards under such conditions has been demonstrated in an intercalibration project[5]. Preliminary data are presented with an estimated accuracy of 30%. Further evaluation of calibration results and outlier removal will be performed before final publication of the results.

Ozone was measured using a UV-absorption ozone analyser. We present here averaged daily values for the years 1991 - 1995 and 1994 - 1996 for ozone and PAN, respectively.

Results and discussion

The average mixing ratios and standard deviations for the two data sets have been summarised in table 1 below.

Table 1: Statistical overview of O_3 and PAN at the Zeppelin Mountain.

	O_3 [ppbv]	PAN [pptv]
Average	27.6	138.7
St. Dev.	2.9	61.6
Median	27.5	130

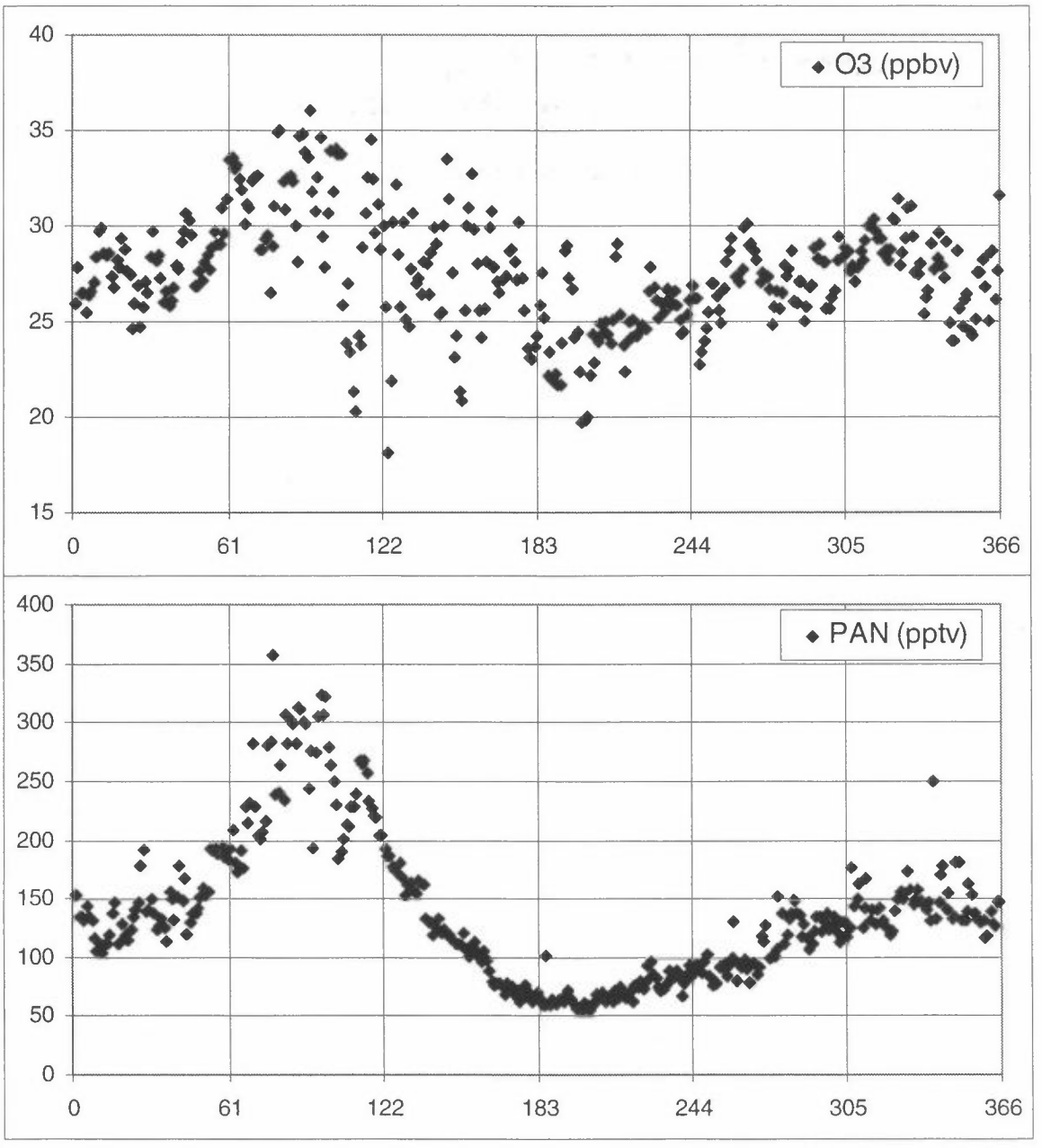

Figure 1. Mean annual cycles for ozone and PAN, plotted by the day of year (DOY). For each day of year, the measured mixing ratio from several years have been averaged.

Figure 1 above shows the mean annual cycles for both PAN and ozone. Both show maxima occurring during the spring, which agrees with measurements at other northern hemispheric locations[7,8,9,10]. The maxima occur in the period March to April.

The annual cycle of ozone shows the influence from boundary layer ozone depletion. On some occasions PAN mixing ratios are also reduced during these events. Ozone mixing ratios show a general tendency to episodic behaviour in the months March to July. PAN mixing ratios are more strongly episodic during a shorter period March to April.

Figure 2 shows that PAN and ozone are positively correlated.

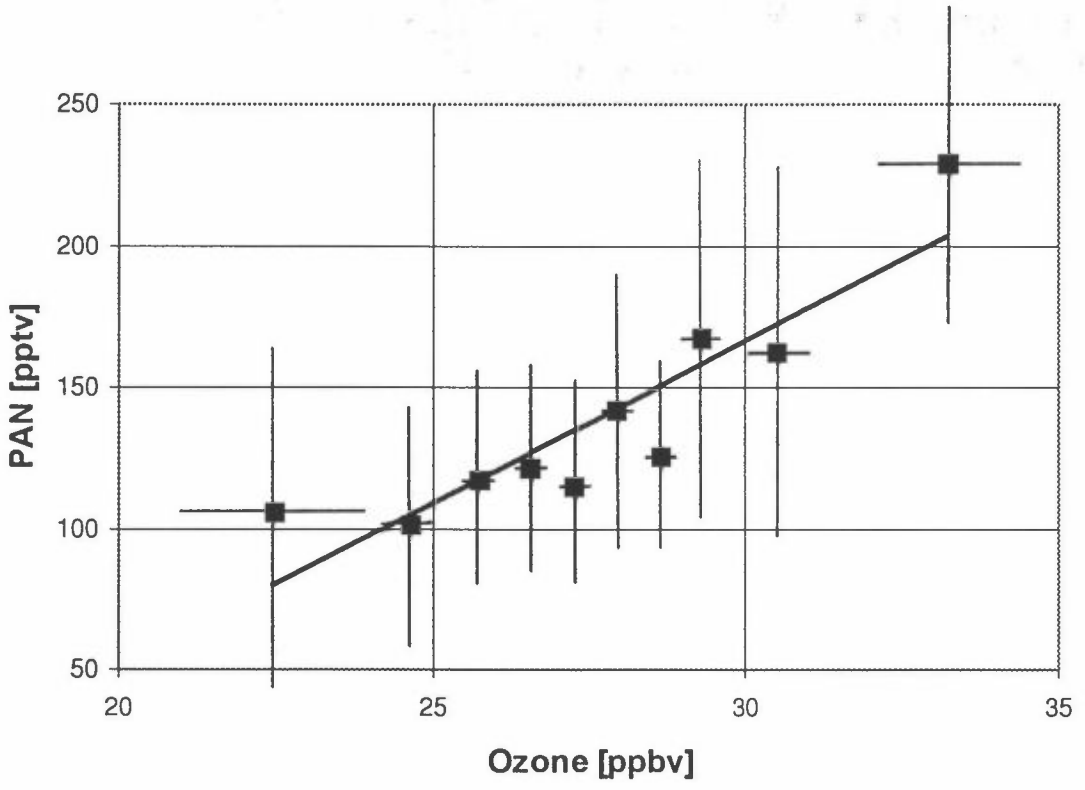

Figure *2. The corresponding ozone and PAN mixing ratios have been sorted by the ozone mixing ratio. Each marker represents the average PAN mixing ratio for a 10% fraction of the measured ozone data elements. The slope of the PAN mixing ratio is 11.46 pptv PAN pr ppbv ozone.*

Conclusions

- Multi-year records of PAN and ozone mixing ratios from the Zeppelin Mountain station at Ny-Ålesund are presented.
- The annual cycle of the PAN mixing ratios at the Zeppelin Mountain is consistent with other PAN data sets from the Arctic.
- The measured PAN mixing ratios are positively correlated to ozone mixing ratios.

References

1. Isaksen, I. S. A., et al., *J. Atmos. Chem.*, 3, 3-27, **1985**.
2. Penkett, S. A., Brice, K. A., *Nature*, 319, 655-657, **1986**.
3. Beine, H. J., et al., *J. Atmos. Chem.*, accepted for publication, **1997**.
4. Solberg, S. et al., *J. Atmos. Chem.*, accepted for publication, **1997**.
5. Krognes, T., et al., *Atmos. Environ.*, 30, 991-996, **1996**.
6. Nielsen, T., et al., *Atmos. Environ.*, 16, 2447-2450, **1982**.
7. Bottenheim, J. W. et al., *J. Atmos. Chem.*, 17, 15-27, **1993**.
8. Bottenheim, J. W. et al., *J. Geophys. Res.*, 99, 5333-5352, **1994**.
9. Muthuramu, K. et al., *J. Geophys. Res.*, 99, 25369-25378, **1994**.
10. Beine, H. J. et al., *J. Geophys. Res.*, 101, 12613-12619, **1996**.

Fresh Snow as Sampling Media for Reactive Halogen Species - Are f-Br Events Preserved in the Snow Pack ?

Lehrer, E., Langendörfer, U., and Wagenbach, D.
Institut für Umweltphysik, University of Heidelberg, D-69120 Heidelberg, Germany

The question if halogen activation leading to tropospheric ozone depletion is a natural or an anthropogenic phenomenon might be tackled (among others) by glacio-chemical ice core studies. In a pilot study fresh snow as well as several snow pits samples on a glacier site (Edithbreeen) about 15km Southeast of Ny Ålesund / Spitsbergen were sampled therefore during the ARCTOC campaign in spring 1996. All snow samples were analysed for bromide, major ions and MSA.
We will present here investigations on the scavenging conditions of fresh snow for halogens, in particular for non sea-salt bromine (nss-Br). Our results suggest that the f-Br signal is efficiently well preserved in snow and firn. Therefore Arctic spring Br (and consequently O_3 loss) events in the past (i.e. during the last decades or centuries) are expected to be recorded in ice cores from cold high Arctic glaciers. To extract the ice core information the search for a suitable drilling site, which fulfils a series of requirements: (low sea salt input, non tempered glacier, preferably at sea level, sufficiently low precipitation) as well as a sufficient detection limit of the instrumentation for Br is of major importance.

Long-term Measurements of the Atmospheric Aerosol Composition at Ny Ålesund, Spitsbergen

A contribution to subproject ASE

W. Maenhaut[1], K. Beyaert[1], G. Ducastel[1], V. Havránek[1], R. Salomonovic[1] and J.E. Hanssen[2]

[1]*Institute for Nuclear Sciences, Proeftuinstraat 86, B-9000 Gent, Belgium*
[2]*NILU, P.O. Box 100, N-2007 Kjeller, Norway*

Introduction

Since early 1991, size-fractionated aerosol samplings are performed on a continuous basis at the Zeppelin mountain station (78°54' N, 11°53' E, 474 m a.s.l.) in Ny Ålesund. The objectives are to investigate the temporal variability in the concentrations and size distributions of the various species and elements (both as a function of season and from year to year), to resolve the contributions from natural and anthropogenic origin for some important species (especially for fine non-sea-salt sulfate), to assess the sources, source processes and source regions of the species and elements, and to examine how the detailed elemental mass size distributions are modified during the long-range transport from the source regions or as a result of local meteorological processes. We previously reported on our results from the three summer seasons 1991 through 1993 [1]. Here, we present and briefly discuss some results from a period of almost five complete years (1991 through to September 1995) and from two different types of sampling devices.

Experimental

The collection devices used are (a) a modified Sierra-Andersen Hi-Vol cascade impactor, with one impaction stage and a back-up filter, providing two size fractions of > 2.5 μm and < 2.5 μm equivalent aerodynamic diameter (EAD) [2], and (b) a 1-L/min, Battelle-type PIXE Int. cascade impactor (PCI), with 7 impaction stages and a back-up filter [3]. Parallel samples are collected with the two devices according to a 2-2-3 day schedule. The back-up filters from the Hi-Vol sampler are analyzed for sulfate, methanesulfonate (MSA), nitrate, chloride, bromide and major cationic species by ion chromatography (IC) and for up to 42 elements by a combination of instrumental neutron activation analysis (INAA)

Presented at
EUROTRAC Symposium '96

and particle-induced X-ray emission (PIXE). The element list includes the sea-salt element Na, the halogens (Cl, Br, I), indicators for mineral dust (*e.g.* Al, Si, Ti) and tracer elements for a variety of anthropogenic activities (*e.g.* V, Zn, As, Se, Sb, Pb). The Hi-Vol impaction stages are only analyzed by IC, and only for the summer samples (June-July-August). Non-sea-salt (nss) sulfate and nss-Br in the Hi-Vol impaction stages and filter samples are obtained by correcting the sulfate and Br contents for the contribution from sea-salt, using Na as a sea-salt indicator and the sea water sulfate/Na and Br/Na ratios of Riley and Chester [4]. The PCI samples are analyzed by PIXE, and this yields raw mass size distributions (with mass per stage and per m^3) for the elements Na, Mg, Al, Si, S, Cl, K, Ca, Ti, Mn, Fe, Zn, Br and Pb.

Results and discussion

From a comparison of the data from the impaction surfaces with those from the back-up filters for the Hi-Vol sampler it appeared that (at least during summer) both sulfate and MSA are for 90 % or more associated with the fine (<2.5 μm EAD) particles. Furthermore, the fine sulfate was virtually all nss-sulfate. The means and associated standard deviations for MSA, nss-sulfate, and the MSA/nss-sulfate ratio (all for the < 2.5 μm EAD size fraction) for each of the 5 summers 1991 through 1995 and for all 5 summers combined are presented in Table 1.

Table 1. Means and associated standard deviations for MSA, nss-sulfate and the MSA/nss-sulfate ratio in the fine (<2.5 μm EAD) size fraction for the summer samples (MSA and nss-sulfate data are in ng/m^3)

Summer	MSA	nss-sulfate	MSA/nss-sulfate
1991	54 ± 41	250 ± 210	0.27 ± 0.20
1992	34 ± 31	240 ± 240	0.20 ± 0.14
1993	37 ± 66	470 ± 450	0.11 ± 0.11
1994	38 ± 43	144 ± 141	0.28 ± 0.16
1995	25 ± 22	220 ± 230	0.13 ± 0.08
5 summers	37 ± 44	260 ± 290	0.20 ± 0.16

Fig. 1 shows the atmospheric concentrations (in the < 2.5 μm size fraction) of As, nss-sulfate and MSA as a function of sampling date (Julian day) for the years 1991 through 1995. The anthropogenic element As exhibits a clear seasonal cycle, with about 50 times lower levels during summer than during winter/early spring. A similar seasonal cycle was observed for Sb. Occasionally, enhanced

levels of these pollutant elements are also seen during summer, particulary in 1993 (see *e.g.* days 190-200).

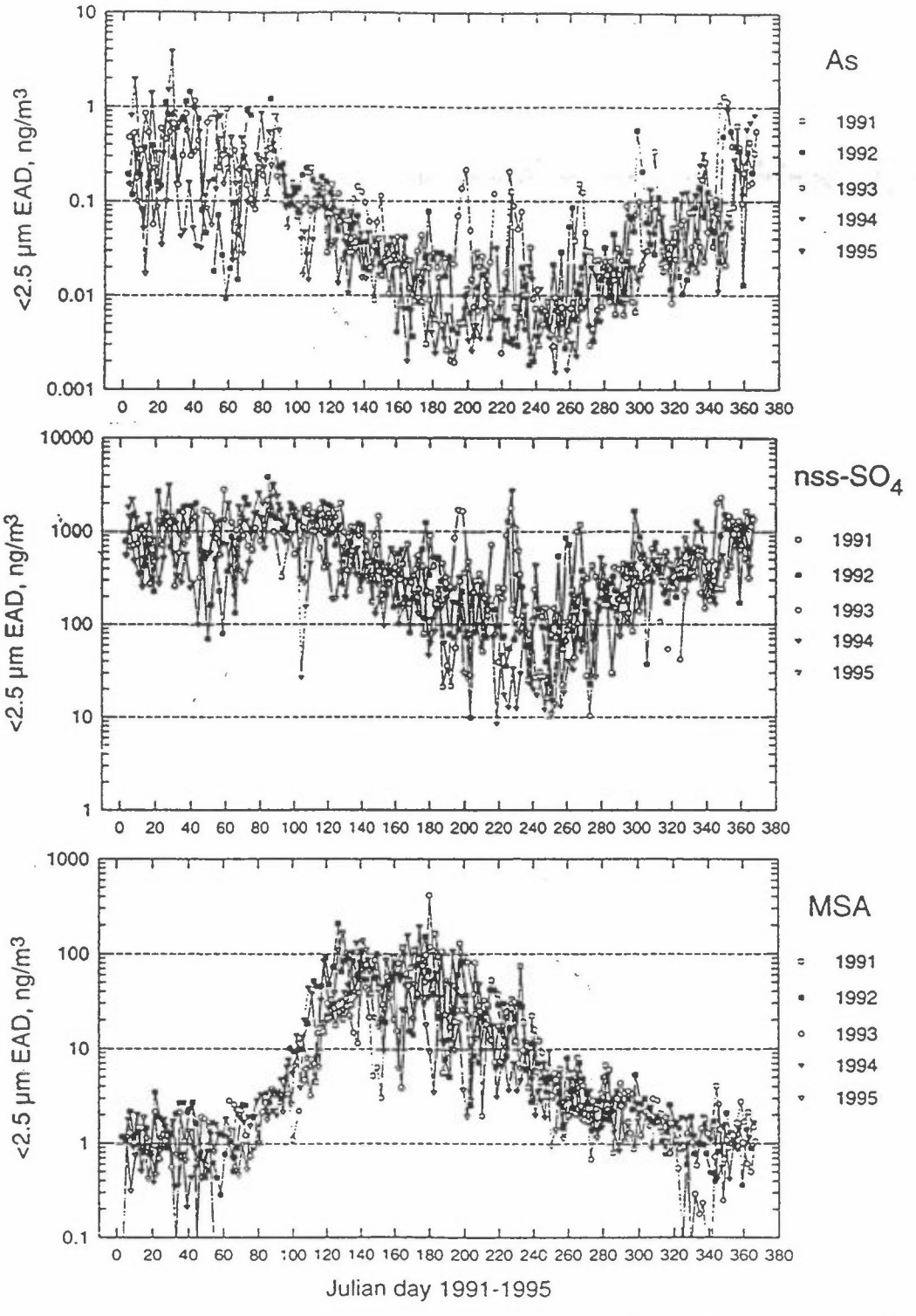

Fig. 1: Atmospheric concentrations (in the <2.5 µm size fraction) of As, nss-sulfate and MSA as a function of sampling date (Julian day) for the years 1991 through 1995.

Nss-sulfate is lower during summer than during the rest of the year, but the summer/winter difference remains limited to about a factor of 10, and is clearly smaller than for the anthropogenic metallic elements (As, Sb, etc.). There are occasionally episodes of high levels of nss-sulfate during summer, particulary in 1993, and they coincide with episodes of high levels for As. MSA, a gas-to-particle conversion product of dimethylsulfide (DMS) from marine phytoplankton, is very low during winter, increases steadily between day 100 and day 120 (~May 1), remains high during the entire summer, up to day 240 (~Sept. 1), but decreases with time after July 1. Both nss-sulfate and MSA exhibit significant variability during summer (June through August) and are sometimes well correlated with each other (particularly in 1991, 1992 and 1994). In these three summers, a higher mean MSA/nss-sulfate ratio was also found (see Table 1). Both observations clearly suggest that the contribution from marine biogenic origin was substantially larger during these three summers than during the summers of 1993 and 1995.

The raw mass size distribution data from the PCI samples were subjected to a data inversion, and lognormal curves were fitted to the inverted smooth size distributions [5]. For S, there was a tendency for the major (submicrometer) mode to have a lower diameter during summer than during the rest of the year. Summer/winter differences were also found in the size distributions of the mineral dust elements (*e.g.* Fe, Ca).

Acknowledgements

We are very grateful to J. Cafmeyer for technical assistance. This research was supported by the Belgian NFWO and IWONL and by the Impulse Programme "Global Change" and an EUROTRAC ASE grant from the Federal Office for Scientific, Cultural and Technical Affairs.

References

1. W. Maenhaut, G. Ducastel, K. Beyaert, J.E. Hanssen; in: P.M. Borrell, P. Borrell, T. Cvitas, W. Seiler (eds), *Proc. EUROTRAC Symp. '94*, SPB Academic Publishing bv, The Hague 1994, pp. 467-471.
2. W. Maenhaut, P. Cornille, J.M. Pacyna, V. Vitols; *Atmos. Environ.* **23** (1989) 2551-2569.
3. S. Bauman, P.D. Houmere, J.W. Nelson; *Nucl. Inst. Meth.* **181** (1981) 499-502.
4. J.P. Riley, R. Chester; *Introduction to Marine Chemistry*, Academic, New York (1971).
5. V. Havránek, W. Maenhaut, G. Ducastel, J.E. Hanssen; *Nucl. Inst. Meth.* **B109/110** (1996) 465-470.

Temporal Variability of the Aerosol and Atmospheric Optical Characteristics in the Russian Arctic

Vladimir F. Radionov
Arctic and Antarctic Research Institute, 38 Bering Str., 199397 St. Petersburg, Russia

A sharp increase in aerosol of anthropogenic origin in the atmosphere has been observed from the middle of this century. Observations show aerosol mass concentrations in industrial regions to be several times in excess of those measured in non-urbanised regions. Studies that were fairly active in the 1980s in the Arctic, have shown a high level of pollution of the Arctic atmosphere by aerosol of anthropogenic origin in the winter-spring period. It is mainly composed of the products of transformation of SO_2 with a large fraction of soot particles. During the cold period, the aerosol layers form what is called "arctic haze". Its occurrence is related to the increased meridional transfer in the winter months of polluted air masses from temperate latitudes. As to the observed high concentration of particles and their spreading over large areas, this is connected with the presence of inversions and a weaker mechanism of aerosol wash-out by precipitation in winter.

The life-time of aerosol particles in the troposphere does not exceed one month. Hence a considerable portion of aerosol particles has enough time to deposit on the surface of the Arctic Ocean and the marginal seas, polluting the snow cover, and accumulating in it during the polar night in greater quantities than in the atmosphere for each given moment in time. Actually, the entry of mixtures accumulating in the snow into the surface water as the snow intensively melts, may in principle, have a significant effect on the hydrochemical characteristics of the river and lake water and the upper freshened ocean.

The spatial distribution of mixtures at constant sources is governed by the meridional transfer pattern. At the system of macroprocesses that existed up to the early 1990s, mean meridional trajectories in the western sector of the Russian Arctic reached the Norwegian Sea, Spitsbergen and the Barents and Kara Seas. In the Pacific sector they reached the eastern East-Siberian Sea, the Chukchi Sea, the Beaufort Sea and the Canadian archipelago. Thus these regions of the Arctic corresponding to the tops of tropospheric ridges could most frequently be exposed to the influence of advection of anthropogenic mixtures. In other Arctic regions, one may expect the concentration of mixtures, formed at mixing air masses within the Arctic, to characterise their background level. Concentrations of mixtures in the atmospheric air, close to background ones, can be expected at the stations on the New-Siberian Islands, Severnaya Zemlya and in the sector 110°E to 160°E north of 80°N.

From the late 1970s, the observations of parameters directly or indirectly characterising the level of pollution of the surface air layer by aerosol particles were carried out at some points of the Russian Arctic. In particular, the size distribution function of aerosol particles in the surface air layer and the spectral aerosol optical depth of the atmosphere characterising total aerosol in the entire atmospheric column were determined. The observations were performed in different years in different Arctic regions: drifting station NP22 (72°-76°N, 135°W- 160°E), 1979; Severnaya Zemlya (79.5°N, 95.4°E), 1979, 1981- 1986, 1988; Vrangel Island (71.0°N, 178.5°W), April- June 1984, April- May 1985 and 1986; drifting station NP28 (82°N, 168°E), 1987; Dixon Island (73.5°N, 80.2°E), 1981, 1983- 1990; Kotelny Island (76.0°N, 137.9°E), 1985- 1989; expedition SEVER-44 (69°- 82°N, 60°- 118°E and 68°-76°N, 119°- 191°E), April- May 1992; expedition SEVER- 45 (72°- 82°N, 60°- 120°E), March-April 1993; Franz-Josef Land (81.0°N, 57.0°E), March- April 1994.

The measurements of the number of aerosol particles in the unit volume in the subsurface air layer at a height of 1.5-3 m were performed by means of a serial photoelectric counter A3-5. Before and after the expedition the instruments were calibrated by the plant manufacturer using the latexes of the prescribed size. The instrument measured total concentrations of particles N(d) with the effective sizes exceeding the prescribed size d. The size gradations were as follows: d=0.4; 0.5; 0.6; 0.7; 0.8; 0.9; 1;; 1.5; 2; 4; 7 and 10 μm.

For measuring the aerosol optical depth in the Arctic, three instruments were used. The first was a sun-photometer with a silicon photodetector and thirteen metal electric or dielectric light filters with the transmission maximums at about 350, 366, 405, 450, 501, 548, 680, 748, 800, 950, 1.010, 3.650 nm and the transmission band width within 8 to 30 nm. The second instrument, used at the arctic stations, was Yanishevsky thermoelectric actinometer M-3 with a set of five glass bandpass filters with their short-wave cut-offs at 0.38, 0.47, 0.53, 0.63 and 0.71 μm. The values calculated from such filter measurements of direct solar radiation are the aerosol optical depth at wavelength 0.5 μm, the Angstrom exponent and the Angstrom turbidity factor. Finally, the optical aerosol depths in January-February 1985 on Severnaya Zemlya were determined from measurements by a star-photometer, consisting of a telescope and a photometer for spectral regions of 0.3-0.8 and 0.5-1.0 μm.

The longest continuous measurement series of concentration of particles in the Arctic was obtained on the Severnaya Zemlya archipelago. Hence for characterising the features of variations of the aerosol component of the atmosphere within a year these data are the first to be analysed. Figure 1 presents mean concentrations of aerosol particles with a size of more than 0.4 m from April 1984 to October 1986 and their root- mean- square deviations.

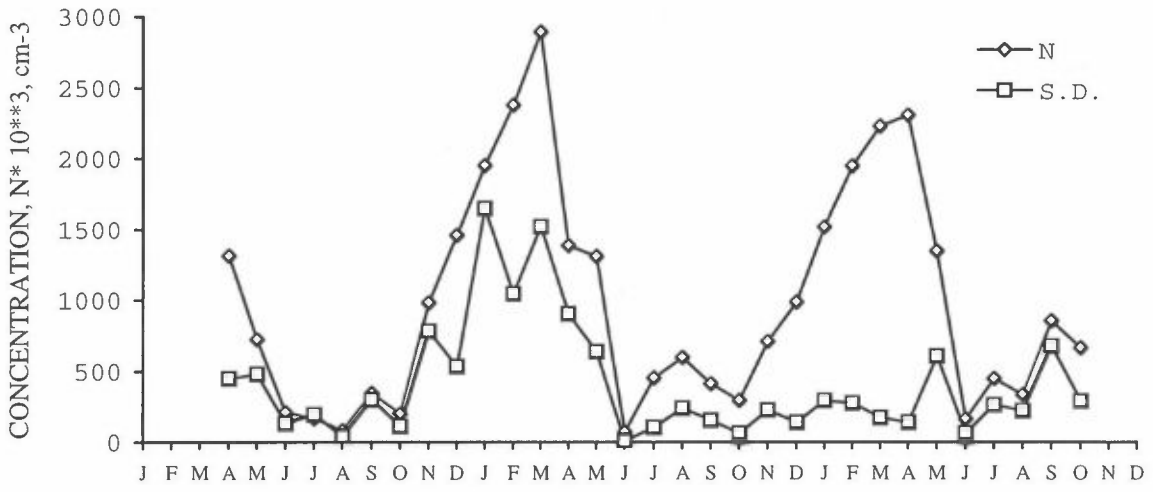

Figure 1. Mean monthly concentrations of aerosol and their standard deviations

The particles of precisely this size govern, on the one hand, the value of the aerosol extinction of solar radiation in the atmosphere and, on the other hand, make the main contribution to the mass concentration of aerosol substance in the air. The maximum concentration values in some series of measurements may 2-5 times exceed the presented mean values. Figure 1 demonstrates pronounced seasonal variations in the total concentration of particles with the maximum in February-March. The minimum concentrations were

observed from June to October. Similar pattern of aerosol concentration variations in the surface air layer within a year, was observed at all points of the Arctic where observations were performed in different years. This is the main feature of the aerosol component of the Arctic atmosphere. In all other regions of the globe the maximum of aerosol turbidity of the troposphere is recorded during the warmer period.

The majority of measurements of the aerosol size distribution function in the Arctic were performed by means of photoelectric counters allowing reconstruction of the particle size distribution function only for relatively large particles whose effective diameter exceeds 0.4 μm. Only twice, in May 1985 on Vrangel Island and in April 1994 on Tsigler Island and Franz-Josef Land, the measurements of aerosol characteristics covered the size range 0.005 to 10 μm.

On the whole, based on data of all measurements, in spite of the wide variability ranges of concentrations, the character of particle size distribution for a coarse fraction (a particle size of more than 0.4 μm) was preserved during a year and from year-to-year. The size spectrum of arctic aerosol is described in the first approximation by the Young's law $dN/d \log r \propto r^{-n}$. The index n at different points of the Arctic varied within 3 to 3.5. Only in May 1985 on Vrangel Island its mean value was n = 4. The aerosol size spectra measured during the cold and warm periods of the year also differ in that in the cold months the size range is wider. In summer, the particles with a size of more than 4 μm and in some cases of 1.5 and 2 μm were not, as a rule, recorded. From February to May the main contribution (60 to 80%) to the mass aerosol concentration was made by the particles with a size of more than 1 μm.

In the size range from 0.005 to 5 μm averaged from measurements on Franz-Josef Land and Vrangel Island, the modes (relative maximums) were observed within the volume spectra of aerosol particles localised near 0.02, 0.2 and 2 μm. On the whole, they are close to the modes observed in temperate latitudes. This fact is one of the indications of the common mechanisms of aerosol formation and evolution in these two regions in spite of significantly different conditions.

The levels of pollution in the surface atmospheric layer are closely connected with the character of temperature stratification in the lower troposphere. In particular, the concentration of aerosol particles near the surface was found to be related to the thickness of inversions, induced by radiation cooling of the subsurface air layer. The correlation coefficient of the values of aerosol particle concentration and surface inversion thickness (the thickness of the layer with a negative temperature gradient), r = 0.89.

Mean monthly values of aerosol optical depth at a wavelength of 500 nm are presented in Table 1. In spite of few data available (Table 1), they provide some understanding of the basic features of aerosol pollution in the Arctic. The stations in the Arctic Basin are characterised by the spring maximum of aerosol pollution of the atmosphere. It results from the accumulation of aerosol transported from the continent in the winter due to certain circulation processes. In a way, it is added to the arctic aerosol proper that is formed at low temperatures. Frequent inversions typical of the region also contribute to aerosol accumulation in the lower layers.

According to mean multi year data, the level of aerosol turbidity in spring is comparable to a similar level at the continental stations of Russia located beyond the influence of industrial zones.

By June, there is a fairly sharp decrease in aerosol pollution, the atmosphere is purified and the June to September period is characterised by a high transparency which especially increases by autumn.

Table 1. Mean monthly values of the aerosol optical depth at a wavelength 500 nm

Year/month	I - II	III	IV	V	VI	VII	VIII	IX
Vaida-Bay, Barents Sea								
1974, 84	-	-	-	-	-	0,17*	-	-
Severnaya Zemlya								
1981	-	-	0,17*	0,17*	0,18*	0,14*	0,09*	0,09*
1983	-	-	0,27*	0,22*	0,17*	0,13*	0,11*	0,08*
1984	-	-	0,18*	0,16*	-	-	-	-
1985	0,18**	0,18*	0,19*	0,14*	-	-	-	-
1986	-	-	-	0,12	0,08	0,06	0,05	0,06
1988	-	-	-	-	0,09	0,06	0,07	0,07
1989	-	0,22	0,18	0,18	-	-	-	-
mean	-	0,20	0,20	0,16	0,13	0,10	0,08	0,08
Dixon Island								
1981	-	-	0,23	0,20	0,23	0,11	0,08	-
1983	-	-	0,30	0,30	0,20	0,18	-	-
1984	-	0,22	0,24	0,24	0,12	0,10	-	-
1985	-	-	0,26	0,26	0,16	0,12	0,08	-
1986	-	0,15	0,24	0,24	0,28	0,19	-	-
1987	-	0,25	0,12	0,12	-	0,16	-	-
1988	-	-	0,18	0,18	0,07	0,08	0,10	-
1989	-	0,16	-	-	-	0,05	0,14	0,06
1991	-	0,13	0,11	0,11	0,03	0,06	0,08	0,06
mean	-	0,18	0,21	0,21	0,16	0,12	0,10	0,06
Vrangel Island								
1984	-	-	0,24	0,12	-	-	-	-
1987	-	-	-	-	0,10*	-	-	-
Kotelny Island								
1985	-	-	-	0,22	0,12	0,13	0,13	-
1986	-	-	0,20	0,21	0,15	0,10	0,11	-
1987	-	-	0,22	0,28	0,23	0,11	0,09	-
1988	-	0,20	0,27	0,12	0,07	0,05	0,05	-
1989	-	-	-	0,21	0,11	-	0,11	-
mean	-	-	0,23	0,21	0,14	0,10	0,10	-
NP- 22 drifting station								
1979, 12/5-3/7		-	-	-	0,04*	-	-	-

* sun- photometer measurements, ** star- photometer measurements, no asterisk - actinometer M-3 measurements

Surface Ozone Variations in Arctic in Summer 1995

O.I. Shumilov, E.A. Kasatkina
High-Latitude Geophysical Laboratory, St. Petersburg Filial of IZMIRAN,
P.O. Box 123, 184200 Apatity, Russia

O.M. Raspopov
St. Petersburg Filial of IZMIRAN, 191023 St. Petersburg, Russia

Surface ozone measurements were performed at Adventdalen Geophysical Station, Svalbard (78°N) in August 1995, with the help of Russian chemiluminescent ozone analyser AM-01. The mean surface ozone concentration is equal to 30 ppb and does not demonstrate diurnal course.

Several cases of rapid surface ozone depletion up to 80% with duration from ten minutes to some hours, and one intense enhancement of 120% value lasting about ten hours, were discovered. Nearly all variations can be interpreted as the influence of local topographically induced wind systems which brings high bromine concentrations from surface sea water to the observation point.

The surface ozone measurements were supported by ozone total content measurements with help of Russian M-124 filter ozonometer, and were compared with some meteorological and heliogeophysical parameters.

Human Health at Svalbard and Heliomagnetic Activity

O.I. Shumilov, E.A. Kasatkina
High-Latitude Geophysical Laboratory, St. Petersburg Filial of IZMIRAN,
P.O. Box 123, 184200 Apatity, Russia

O.M. Raspopov
St. Petersburg Filial of IZMIRAN, 191023 St. Petersburg, Russia

On the data of incident events and unexpected illnesses of Russian miners at Barentsburg (ϕ=74°), their possible connection to solar and magnetic activity (local magnetic activity and penetrating solar protons) was investigated. It was obtained that the extreme situation events (traumas, unexpected deaths, heart and nervous illnesses) correlated rather well with increase of solar and magnetic activity. During winter time not only enhanced level of activity, but also very low level of it, may influence on appearance of extreme situations. The infradian rhythms (with a period of about seven days) observed in variations of extreme situations level seem to be caused by heliogeophysical factors.
The results obtained may be used in forecast of extreme situation level increase during helio-geomagnetic disturbances far inside the geophysical polar cap.

Ozone Deficits in the Lower and Middle Stratosphere of the Arctic Polar Vortex

P. von der Gathen, H. Gernandt, R. Neuber, and M. Rex
Alfred Wegener Institute for Polar and Marine Research
P.O. Box 600149, D-14401 Potsdam, Germany

Since 1988 ozone and temperature profiles were measured above the NDSC station Ny-Ålesund/Spitsbergen by balloon borne sensors. As Ny-Ålesund is within the Arctic polar vortex most of the winter time it is a prime location for continuous and long term observations of characteristics of the Arctic stratospheric vortex.

In the winter months December to February we notice two different short-term trends of the ozone mixing ratios in the polar vortex. From 1990/91 on to 1995/96 mixing ratios decreased substantially in the middle stratosphere, e.g. by approx. 20 % at the 600 K potential temperature level and more than 25 % at 800 K. Such deficits are one order of magnitude larger than predicted by homogeneous chemically induced ozone destruction. We therefore assume a dynamical reason, i.e. the meridional transport of ozone in the middle and upper stratosphere is increasingly blocked year by year. First signs of these reductions can already be seen in the middle stratosphere when the vortex begins to form in August/September. As they propagate downwards by diabatic cooling these early mixing ratios in the middle stratosphere dominate the ozone column densities when they reach the altitude of the ozone concentration maximum in the late winter. In the recent winter 1996/97 the ozone amount increased slightly again.

We notice the second negative short-term trend in the lower stratosphere. One part is related to the dynamical effect as described above. We will outline that another part is consistent with our understanding of chemically induced ozone destruction with respect to heterogeneous chemistry on Polar Stratospheric Clouds (PSC). Ozone losses in the vortex are correlated to temperatures deep enough to form PSC as well as to the exposure to sun light. Ozone losses occurred already in the winter 1991/92 and even more in 1992/93. The winters 1994/95 and 1996/97 showed the largest ozone destruction in the Arctic polar vortex since we started recording ozone. Ozone had been depleted by 60 % at the maximum of the profile in the second half of March. With the exception of the winter 1993/94 chemically induced ozone losses increased from year to year since 1991/92 until 1995/96. We will report about the ozone layer of each winter including the recent winter 1996/97.

Measurements of Ozone, NO_2, BrO, OClO, and IO over Ny-Ålesund, Spitsbergen from 1995 to 1997

Folkard Wittrock, Marco Bruns, Silvia Dzienus, Michael Eisinger, Annette Ladstätter-Weißenmayer, Andreas Richter, and John P. Burrows
Institute of Environmental Physics, University of Bremen, Germany
E-mail: folkard@gome5.physik.uni-bremen.de

Abstract

Ground based observations of the light scattered from the zenith sky (ZS) made since 1995 at Ny-Ålesund were complemented by lunar occultation (LO) measurements in January and February 1997. This extends the retrieval of trace gas amounts from the period after the polar dawn into the polar night. The daily ZS measurements yield vertical columns of O_3 and NO_2 and slant column amounts of OClO, BrO and on a few occasions IO. Up to the present no evidence for significant absorption of OBrO has been found. The BrO differential slant columns (DSC) measured between 90° and 83° show large day to day and seasonal variability: the mean DSC being $1.7 \cdot 10^{14}$ molec/cm^2. OClO varies from 0.5 to $2.4 \cdot 10^{14}$ molec/cm^2 within the vortex; smaller amounts being observed occasionally outside of the vortex.
The lunar measurements provide independent measurements of O_3, NO_2 as well as NO_3 and OClO. The O_3 shows good agreement between ZS and LO. In contrast NO_2, which during daytime is strongly photolysed, has a significant diurnal variation.

Experimental Setup and Data Set

Zenith sky scattered sunlight is collected by a telescope and transmitted into two f/500-Czerny-Turner spectrographs (in 1997, in 1995-1996 only one) via a quartz-fibre bundle with scrambles the polarisation of the incoming light. For moonlight observations the same telescope is used in combination with a moontracker using a CCD camera to control the position of the moon.
A spectral range in the near UV/visible is simultaneous recorded with two Reticon diode arrays cooled to -35°C. Individual spectra were integrated for 300 s for ZS measurements and 100 s for LO measurements. The FWHM of the spectrograph in the range of 327- 492 nm is 0.64 nm for 1995/96 and 0.9 nm since February 1997. The second spectrograph has a FWHM of 0.8 nm in the visible range of 372- 700 nm. Both spectrographs are temperature stabilised to ±0.1K to minimise wavelength shift. Daily spectral and relative radiometric calibrations are performed using a HgCd lamp and a white lamp respectively.
For the zenith sky observation in the range 327- 492 nm the system functioned continuously since February 1995 except from short maintenance breaks and during the polar night. For moonlight spectroscopy the second spectrograph and the moontracker were brought into operation for January and February 1997. During the full moon phase observations were made with the lunar zenith angle (LZA) varying from 61° to 88°.

Data analysis

Slant columns of trace gases are derived by means of a Differential Optical Absorption Spectroscopy (DOAS) algorithm. This procedure uses a non-linear least squares fit in which the differential absorption cross-sections of all absorbers, an empirical „Ring" spectrum and a low order polynomial for the correction of Mie and Rayleigh scattering are fitted to the difference in optical depth between a twilight-spectrum and a reference-spectrum. Depending on the atmospheric trace gas of interest, a wavelength region exhibiting strong differential absorption features is selected for the fitting process. The „Ring" spectrum accounts for the filling in of Fraunhofer lines by Raman scattering in the zenith spectra.

Slant columns can be converted to vertical columns by division of air mass factors (AMF). These AMF express the enhancement in optical path through the atmosphere relative to the vertical optical path at every wavelength. In the case of zenith scattered light O_3 and NO_2 vertical columns were derived with AMF from radiative transfer calculations (GOMETRAN , *Rozanov 1996*). As a result of large diurnal variations in the amounts of species like OClO, BrO and IO the calculation of AMF is potentially error prone (*Fish, 1995*). Therefore only differential slant column densities (DSCDs) will be shown for the above-mentioned absorbers in this study. In contrast to straylight AMF the AMF for direct moon measurements can be calculated with high accuracy including spherical geometry and refraction from a knowledge of the viewing geometry.

For ozone and NO_2 the low temperature absorption cross-sections of *Dehn, 1995* were used after convolution to the instrument resolution. The relative absorption of IO was measured in the laboratory with a spectrometer identical to that of the field instrument (*Himmelmann, 1995*) and then scaled to the absolute values of *Stickel, 1988*. For BrO and OClO the data of *Wahner, 1988* and *Wahner, 1987* which have been shown to be similar to spectra taken in our laboratory were used; the O_4 data were taken from the measurements of *Greenblatt, 1990*. The Ring cross-section was determined with the crossed-polarise method described by *Solomon, 1987*.

Results and Discussion

Ozone and NO_2.

Vertical columns of O_3 and NO_2 are shown in figs 1 to 4. Both absorbers were retrieved in the visible using a fitting window of 435-481.5 nm except for the ozone measurement with moonlight spectra. In this case the 440-554 nm window is better suited. In addition the figures show the values of potential vorticity (PV) over Ny-Ålesund at 475 K-Level calculated by the European Centre for Medium Range Weather Forecasts. From fig 1 and 2 it is obvious, that high PV-values correlate with low amounts of O_3 and NO_2. On February 20 and February 21, 1996 values of ozone below 200 DU were observed. These low values are probably caused by dynamic effects resulting from an elevated tropopause. In both years the stratospheric NO_2 shows the expected behaviour, with extremely low column amounts ($< 1 \cdot 10^{15}$ molec/cm^2) occurring shortly after polar sunrise and increasing to $6 \cdot 10^{15}$ molec/cm^2 towards spring. The pm/am ratios of NO_2 are slightly larger outside the polar vortex than inside.

Figs 3 and 4 show the vertical columns of ozone and NO_2 in 1997. Both the direct moon and the scattered sunlight observations show good agreement with the ozone sondes in February and also in January. In NO_2 the LO values are larger than the ZS measurements and show an increase in February. Further analysis of this behaviour is under way.

Figure 1. Ozone vertical columns in 1995 and 1996

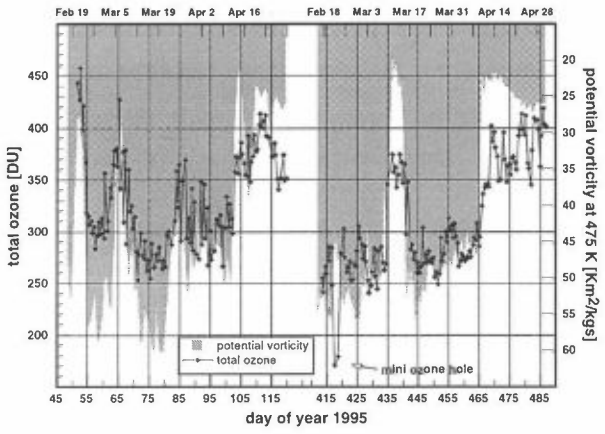

Figure 2. NO2 vertical columns in 1995 and 1996

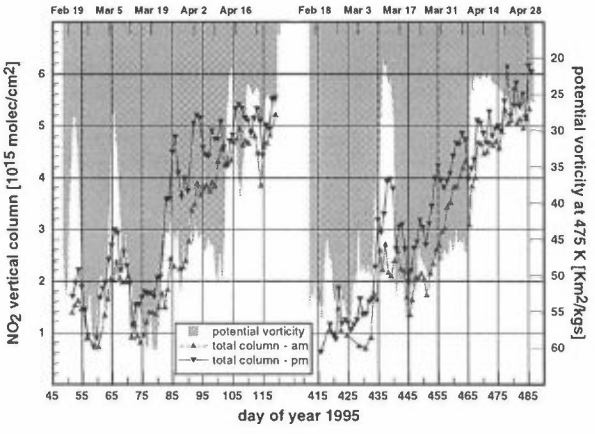

Figure 3. O_3 vertical columns in 1997

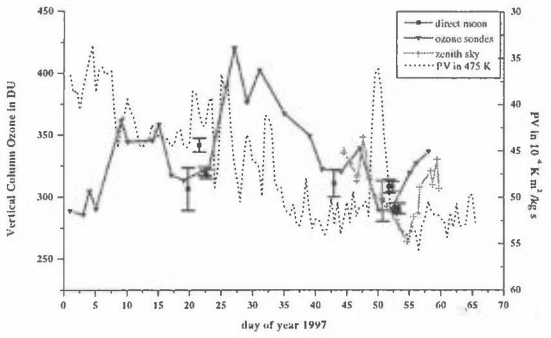

Figure 4. NO_2 vertical columns in 1997

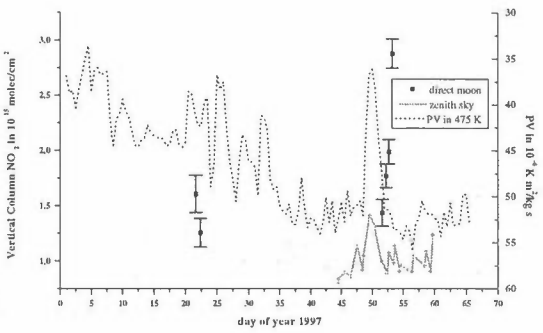

BrO and OClO.

The wavelength regions of 344.7-359 nm and 365-390 nm have been selected for the retrieval of BrO and OClO respectively. Differences in BrO slant columns between 90° and 83° SZA or higher are mostly in the range of $1.0 \cdot 10^{14}$ and $2.5 \cdot 10^{14}$ molec/cm^2 inside the polar vortex. Corresponding values of OClO are in the range of $0.5 \cdot 10^{14}$ and $1.5 \cdot 10^{14}$ molec/cm^2 with maxima higher than $2.0 \cdot 10^{14}$ molec/cm^2 in 1996.

In addition, OClO was occasionally found outside the vortex with amounts 40% lower than inside. Up to now it is not clear, whether the detected air parcels were exported from the vortex or originated outside the vortex.

Outside the vortex the differences in BrO slant columns are often negative. These results indicate large diurnal variation of BrO column with a maximum value around noon. Often the negative slant columns are accompanied by large variations in tropospheric ozone. These observations are best explained by elevated tropospheric BrO making a significant contribution to the total slant column. For this reason days with such behaviour are neglected in this report. A more detailed discussion of these events, when BrO was detected with negative slant columns, will be given in a forthcoming study.

In fig 5 the mean diurnal variation of the OClO respectively BrO DSCDs inside and outside the polar vortex are shown. Plotted are the DSCDs for solar zenith angles between 86° and 93° using a reference at 83° averaged for 1995 and 1996 data. Only values with a fitting error lower than 20% have been included.

Figure 5. Mean diurnal variation of OClO and BrO DSCDs

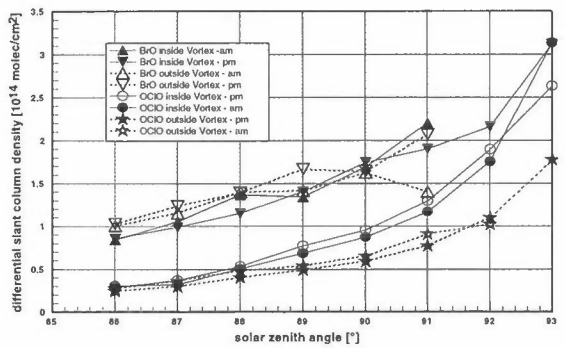

It is clear, that the mean DSCDs of OClO are symmetric around noon for SZAs lower than 92° for both inside and outside the vortex. The morning BrO DSCDs decrease for SZAs larger than 89° outside the vortex. This is in good agreement with model predictions published by *Fish, 1995* and is probably due to lower photolysis rates of $BrONO_2$/HOBr. Inside the vortex am and pm values of BrO DSCDs are nearly equal below 91° SZA within the error limits. Further the afternoon values extend to SZAs greater than 91°. This indicates a longer lifetime of BrO during the sunset. The BrO behaviour suggests, that BrCl/Br_2 rather than $BrONO_2$/HOBr is the main reservoir for bromine compounds inside the vortex.

IO.

For fitting IO, the spectral window 414-444 nm has been chosen in which IO exhibits three differential absorption peaks ((5,0),(4,0),(3,0)). In a few cases typically for a short time after polar sunrise it was possible to identify IO. The results have been checked for spectral interference with NO_2 and Ring, and up to now no indication for such interferences was found.

From 1995 to 1997 IO differential slant columns (92° to 83°SZA or higher) in the range of $0.3 \cdot 10^{14}$ and $0.7 \cdot 10^{14}$ molec/cm^2 were found inside the polar vortex.

Summary

O_3 and NO_2 values inside the vortex air are generally lower than those outside the vortex consistent with our current knowledge of vortex chemistry. The lowest values of O_3 observed on Feb 20, 1996 are better explained by a high tropopause than by a chemical destruction mechanism. Many periods in spring from 1995 to 1997 having vortex air with elevated OClO and possibly containing IO have been observed over Spitsbergen. Occasionally it was possible to identify OClO outside the vortex. The observed diurnal variations of BrO - neglecting days with negative values of DSCDs - are in good agreement with model predictions. The latter indicates the presence of tropospheric BrO, which is consistent with a bromine removal of tropospheric O_3.

Acknowledgements

Parts of this work have been funded by the University of Bremen, the DARA and the European Community via the SCUVS-II project (Contract No. EV5V-CT93-0334). We would like to thank the Alfred Wegener Institute for Polar and Marine Research, Research Unit Potsdam, in particular Dr. Roland Neuber, Dr. Hartwig Gernandt, Hauke Schütt, Rainer Lilischkis, Ingo Beninga, Thomas Seiler, Jens Warming and Silke Wessel for great assistance, without whom this work would not have been possible.

References

Chipperfield, M., et al, Comparison of SESAME data with a 3d chemical transport model, accepted by *J. of Atmospheric Chemistry*

Frank, H., and U. Platt, Advanced calculation procedures for the interpretation of skylight measurements, *First European Workshop, Schliersee 1990*, 1990

Greenblatt, G. D. et al., Absorption measurements of Oxygen between 330 and 1140 nm, *J. Geophys. Res.*, **D95**:18577-18582, 1990

Hausmann, M., and U. Platt, Spectroscopic measurement of bromine oxide and ozone in the high Arctic during Polar Sunrise Experiment 1992, *J. Geophys. Res.*, **D99**:25399-25413 1994

Himmelmann, S. et al, Time resolved absorption spectrum of iodine oxide by flash photolysis of a iodine ozone mixture, *Third European Workshop, Schliersee 1995*, 1995

Johnston, {unpublished results}

Richter, A. et al., Ground based uv/vis measurements of O3, NO2, BrO and OClO over Bremen (53° N), Quadrennial Ozone Symposium, *L'Aquila 1996*

Solomon, S. et al., On the role of iodine in ozone depletion, J. Geophys. Res., **D99**:20491-20499, 1994

Stickel, R. et al., Absorption cross sections and kinetic considerations of the IO radical as determined by flash photolysis/laser absorption spectroscopy, *J. Phys. Chem.*, **92**:1862-1864, 1988

Wahner, A. et al., Absorption cross sections for OClO as a function of temperature in the wavelength range 240-480 nm, *J. Phys. Chem.*, **91**:2734-2738, 1987

Wahner, A. et al., Absorption cross section of BrO between 312 and 385 nm at 298 K and 233 K, *Chem. Phys. Lett.*, **152**:507-512, 1988

Wittrock, F. et al., Ground based uv/vis measurements of O3, NO2, BrO and OClO over Ny-Ålesund (79° N, 12° E), Quadrennial Ozone Symposium, *L'Aquila 1996*

Poster to the Scientific Seminar "Atmospheric Research in Ny-Ålesund" at NILU, Norway, April 9-11, 1997

Presentation of the European Large Scale Facility in Ny-Ålesund

by
Jon Børre Ørbæk and Anne Kari Bjørge
Norwegian Polar Institute, P.Box 5072 Majorstua, 0301 Oslo

Under the Access to Large-Scale Facilities Activity of the Specific Programme for Research and Technological Development in the field of Training and Mobility of Researchers (TMR-Programme) of the European Community, access is provided for European researchers to the Large Scale Facility (LSF) entitled Ny-Ålesund International Arctic Environmental Research Station which is situated in Ny-Ålesund, Svalbard, Norway. The Norwegian Polar Institute is the co-ordinator of the Ny-Ålesund LSF, which is owned by the Norwegian Polar Institute (NP), the Alfred Wegener Institute for Polar and Marine Research (AWI), the Norwegian Mapping Authority (SK), and the Norwegian Institute for Air Research (NILU).

Interested scientists are invited to conduct environmental arctic research at the Ny-Ålesund LSF research installations and are encouraged to submit project proposals to the research facility specified below.

- Atmospheric Climate Research and Biological Research Facilities (NP)
- Atmospheric Air Research Facility (NP / NILU)
- Ozone/Stratospheric and Climate Research Facilities (AWI)
- Space Geodetic Research Facility (SK)

- Call for Proposals; Terms of Access and Funding, Eligibility Criteria
- General information about Ny-Ålesund

Interested Scientists should contact the Ny-Ålesund LSF and may submit project proposals to the facility at all times of the year. Next Call for proposals are scedules to 1 September 1997.

Program Manager:
Dr. Jon Børre Ørbæk
Norwegian Polar Institute
P.O.Box 5072 Majorstua, N-0301 Oslo - Norway
Telephone: +47 22 95 95 97 Telefax: +47 22 95 95 01
E-Mail: jonbo@npolar.no

Appendix A

Programme

Atmospheric Research in Ny-Ålesund

Scientific seminar 9–11 April 1997
Kjeller, Norway

Programme

Wednesday 9.4.1997

Opening

0900–1000	Registration, Coffee
1000–1025	Welcome
1025–1115	**Invited lecture**: Leonard A. Barrie, AES: "The Nature and History of Arctic Air Pollution"

Overview of research programs in Ny-Ålesund
Chair Pål Prestrud, NP

1115–1145	Frode Stordal, NILU: "NILUs Atmospheric Measurement Program in Ny-Ålesund"
1145–1215	Hartwig Gernandt, AWI: "The Koldewey-Station in Ny-Ålesund Contributions to Atmospheric Studies in the Arctic"
1215–1315	Lunch
1315–1345	Kim Holmén, MISU: "Climatically Active Species in Ny-Ålesund; a Synopsis of MISU Activities"
1345–1400	Makoto Wada, NIPR: "Overview of Observations of Clouds, Precipitation and Atmospheric Minor Constituents at the Japanese Ny-Ålesund Observatory"

1400–1415	Yasu-Nobu Iwasaka, Nagoya Univ. "Lidar and Balloon Measurements of Polar Stratospheric Aerosols at Ny-Ålesund"
1415–1445	Ivo Allegrini, CNR: "Italian Research in Tropospheric Chemistry at Ny-Ålesund"
1445–1515	Jon Børre Ørbæk, NP: "Overview of Research Activities Preformed by the Norwegian Polar Institute in Ny-Ålesund within Atmospheric Sciences"
1515–1545	Birgit Heese, UNIS: "Aurora, Ozone and Dust: Atmospheric research on Svalbard by UNIS"
1545–1600	Coffee

Solar radiation

Chair Kim Holmén, MISU

1600–1620	Arne Dahlback, NILU: "UV and Ozone Measurements with Multi Channel Filter Instruments at Ny-Ålesund"
1620–1640	Gert König-Langlo, AWI: "Bipolar Intercomparison of Surface Radiation Fluxes"
1640–1700	Jon Børre Ørbæk, NP: "Measurements of the Surface Radiation Budget in Ny-Ålesund"
1700–1720	Helmut Tüg, AWI: "Monitoring of UV-B Radiation at Koldewey Station
1720–1800	Oral poster presentations

Thursday 10.4.1997

Stratospheric physics and chemistry
Chair Hartwig Gernandt, AWI

0900–0920	Peter von der Gathen, AWI: "Arctic Stratospheric Ozone Depletion Rates Measured with the Match Technique During Four Winters"
0920–0940	Otto Schrems, AWI: "The Evolution of Polar Stratospheric Clouds above Ny-Ålesund"
0940–1000	Geir O. Braathen, NILU: "Analysis of SAOZ UV/Vis Measurements from 1991 to 1996"
1000–1020	Justus Notholt, AWI: "Seasonal Variations of Atmospheric Trace Gases in the High Arctic at 79°N"
1020–1110	Coffee, Poster session
1110–1130	Ulf Klein, Univ. Bremen: "Microwave Measurements of Stratospheric Ozone, Chlorine Monoxide and Tropospheric Water Vapour at Ny-Ålesund, 1994-1996"
1130–1230	**Invited lecture**: Ivar Isaksen, Univ. Oslo: "Modelling Arctic Stratospheric Ozone Loss"
1230–1330	Lunch
1330–1400	Poster session

Tropospheric physics and chemistry

Chair Makoto Wada, NIPR

1400–1500	**Invited lecture**: Trond Iversen, Univ. Oslo: "Model Simulations of Tropospheric Long-Range Transport to the Arctic"
1500–1520	Magnuz Engardt, MISU: "Flaring of Gas in Western Siberia, an Overlooked Source for CO_2 and other Anthropogenic Species During Arctic Haze Episodes?"
1520–1540	Jerzy Bartnicki, DNMI: "Atmospheric Transport of Mercury to Ny-Ålesund. Comparison of Model Results with Measurements"
1540-1610	Coffee
1610-1630	Sverre Solberg, NILU: "Long-Term Measurements of Volatile Organic Compounds at Ny-Ålesund"
1630-1650	Caroline Leck, MISU: "Seasonal Variation and Origin of the Atmospheric Aerosol over Spitsbergen Related to the Arctic Sulphur Cycle"
1650-1710	Martin Schlabach, NILU: "Persistent Organic Pollutants in Air Measured at the Zeppelin Mountain"
1710–1730	Andreas Herber, AWI: "Star Photometer Measurements During Polar Night"

Friday 11.4.1997

Low ozone events

Chair Len Barrie,

0900–1000	**Invited lecture**: Ulrich Platt, Univ. Heidelberg: "Rapid Surface Ozone Loss - The Role of Halogen Species"
1000-1020	Monika Martinez-Walter, MPI: "Measurements of Halogen Compounds, O_3, NO_2 and SO_2 During the ARCTOC Campaigns in Spring 1995 and 1996"
1020–1040	Eckard Lehrer, Univ. Heidelberg: "Tropospheric Ozone Depletion Related Air Mass Characteristics"
1040–1100	Ralf Ackermann, Univ. Heidelberg: "DOAS-Measurements During the ARCTOC-Campaigns 1995 and 1996 in Ny-Ålesund, Spitsbergen"
1100–1130	Coffee
1130–1150	Uwe Langendörfer, Univ. Heidelberg: "Tropospheric Ozone Related Aerosol Chemistry Observed in High Time Resolution During ARCTOC '95 & '96 at Zeppelin Fjellet"
1150–1210	Thomas Arnold, MPI: "Peroxy Radical Behaviour During the ARCTOC-Campaigns at Ny-Ålesund"
1210–1230	Ralf Koppman, FZJ: "Hydrocarbon Measurements in the Arctic Troposphere: A Probe for Tropospheric Ozone Depletion"
1230–1250	Dieter Perner, MPI: "Tropospheric BrO and its Consequences for the Global Bromine Budget"
1250-1400	Lunch

Appendix B

List of Participants

List of Participants

Ackermann, Ralf	University of Heidelberg Institute for Environmental Physics Im Neuenheimer Feld 366 D-69120 Heidelberg, Germany ac@uphys1.uphys.uni-heidelberg.de
Allegrini, Ivo	Istituto sull'Inquinamento Atmosferico Area della Ricerca di Roma Via Salaria Km 29.300 00016 Monterotondo Stazione, Roma, Italy allegrini@ntserver.iia.mlib.cnr.it
Arlander, Bill	Norwegian Institute for Air Research (NILU) P.O. Box 100 N-2007 Kjeller, Norway Bill.Arlander@nilu.no
Arnold, Thomas	Max-Planck-Institut für Chemie (MPI) P.O. Box 3060 D-55020 Mainz, Germany arnold@diane.mpch-mainz.mpg.de
Barrie, Leonard A.	Atmospheric Environment Service 4905 Dufferin Street, Downsview M3H 5T4 Ontario, Canada len.barrie@ec.gc.ca
Bartnicki, Jerzy	Norwegian Meteorological Institute (DNMI) P.O. Box 43 Blindern N-0313 Oslo, Norway jerzy.bartnicki@dnmi.no
Beine, Harry	Norwegian Institute for Air Research (NILU) P.O. Box 100 N-2007 Kjeller, Norway Harry.Beine@nilu.no
Bojkov, Bojan	Norwegian Institute for Air Research (NILU) P.O. Box 100 N-2007 Kjeller, Norway Bojan.Bojkov@nilu.no

Braathen, Geir O.	Norwegian Institute for Air Research (NILU) P.O. Box 100 N-2007 Kjeller, Norway Geir.Ole.Braathen@nilu.no
Bull, Ann Margit	Norwegian Pollution Control Authority (SFT) P.O. Box 8100 Dep. 0032 Oslo, Norway Ann.Margit.Bull@sftospost.md.dep.telemax.no
Dahlback, Arne	Norwegian Institute for Air Research (NILU) P.O. Box 100 N-2007 Kjeller, Norway Arne.Dahlback@nilu.no
Dzienus, Silvia	University of Bremen Institute of Environmental Physics, P.O. Box 330440 D-28334 Bremen, Germany sdz@gome5.physik.uni-bremen.de
Engardt, Magnuz	Stockholm University Department of Meteorology S-106 91 Stockholm, Sweden magnuz@misu.su.se
Flatøy, Frode	University of Bergen Geophysical Institute Allégaten 70 N-5007 Bergen, Norway frode@gfi.uib.no
Fløisand, Inga	Norwegian Institute for Air Research (NILU) P.O. Box 100 N-2007 Kjeller, Norway Inga.Floisand@nilu.no
Gernandt, Hartwig	Alfred-Wegener-Institute for Polar and Marine Research(AWI) Research Department Potsdam P.O. Box 60 01 49 D-14473 Potsdam, Germany gernandt@awi-potsdam.de

Hanssen, Jan Erik	Norwegian Institute for Air Research (NILU) P.O. Box 100 N-2007 Kjeller, Norway Jan.Erik.Hanssen@nilu.no
Heese, Birgit	University Courses on Svalbard (UNIS) PO Box 156/157 N-9170 Longyearbyen, Norway birgit@unis.no
Herber, Andreas	Alfred-Wegener-Institute for Polar and Marine Research (AWI) Research Department Potsdam P.O. Box 60 01 49 D-14473 Potsdam, Germany aherber@awi-potsdam.de
Hermansen, Ove	Norwegian Institute for Air Research (NILU) P.O. Box 100 N-2007 Kjeller, Norway Ove.Hermansen@nilu.no
Høiskar, Britt Ann Kåstad	Norwegian Institute for Air Research (NILU) P.O. Box 100 N-2007 Kjeller, Norway Britt.Ann.Kaastad.Hoiskar@nilu.no
Holmén, Kim	Stockholm University Department of Meteorology S-106 91 Stockholm, Sweden kim@misu.su.se
Ianniello, Antonietta	Istituto sull'Inquinamento Atmosferico Area della Ricerca di Roma Via Salaria Km 29.300 00016 Monterotondo Stazione, Roma, Italy baseartico@ntserver.iia.mlib.cnr.it
Isaksen, Ivar	University of Oslo Geophysical Institute P.O. Box 1022 N-0315 Oslo, Norway ivar.isaksen@geofysikk.uio.no

Iversen, Trond	University of Oslo Geophysical Institute P.O. Box 1022 N-0315 Oslo, Norway trond.iversen@geofysikk.uio.no
Iwasaka, Yasu-Nobu	Nagoya University Solar-Terrestrial Environmental Laboratory 3-13 Honohara, Toyokawa 442 AICHI, Japan
Johannessen, Tor	Norwegian Pollution Control Authority (SFT) P.O. Box 8100 Dep. 0032 Oslo, Norway Tor.Johannessen@sftospost.md.dep.telemax.no
Juntto, Sirkka	Finnish Meteorological Institute Air Quality Research Sahaajankatu 20 E FIN-00810 Helsinki, Finland sirkka.juntto@fmi.fi
Karlsen, Kjersti	Norwegian Institute for Air Research (NILU) P.O. Box 100 N-2007 Kjeller, Norway Kjersti.Karlsen@nilu.no
Kasatkina, Elena A.	High Latitude Geophysical Laboratory St. Petersburg Filial of IZMIRAN P.O. Box 123 184 200 Apatity, Russia
Klein, Ulf	University of Bremen Institute of Environmental Physics P.O. Box 330440 D-28334 Bremen, Germany ulf@atm.physik.uni-bremen.de
König-Langlo, Gert	Alfred-Wegener-Institute for Polar and Marine Research (AWI), P.O. Box 120 161 D-27570 Bremerhaven, Germany gkoenig@awi-bremerhaven.de

Koppman, Ralf	Forshungszentrum Jülich (FZJ) P.O. Box 1913 D-52425 Jülich, Germany r.koppman@kfa-juelich.de
Krognes, Terje	Norwegian Institute for Air Research (NILU) P.O. Box 100 N-2007 Kjeller, Norway Terje.Krognes@nilu.no
Langendörfer, Uwe	University of Heidelberg Institute for Environmental Physics Im Neuenheimer Feld 366 D-69120 Heidelberg, Germany la@uphys1.uphys.uni-heidelberg.de
Stoltz Larsen, Elisabeth	Norwegian Polar Institute (NP), P.O. Box 505 N-9170 Longyearbyen, Norway esl@lby.npolar.no
Leck, Caroline	Stockholms University Department of Meteorology S-10691 Stockholm, Sweden lina@misu.su.se
Lehrer, Eckard	University of Heidelberg Institute for Environmental Physics Im Neuenheimer Feld 366 D-69120 Heidelberg, Germany le@uphys1.uphys.uni-heidelberg.de
Martinez-Walter, Monika	Max-Planck-Institut für Chemie (MPI) P.O. Box 3060 D-55020 Mainz, Germany martinez@diane.mpch-mainz.mpg.de
Nielsen, Claus	University of Oslo Department of Chemistry P.O. Box 1033, Blindern N-0315 Oslo, Norway c.j.nielsen@kjemi.uio.no

Notholt, Justus	Alfred-Wegener-Institute for Polar and Marine Research (AWI) Research Department Potsdam P.O. Box 60 01 49 D-14473 Potsdam, Germany jnotholt@awi-potsdam.de
Ørbæk, Jon Børre	Norwegian Polar Institute (NP) P.O. Box 5072, Majorstua N-0301 Oslo, Norway jonbo@npolar.no
Perner, Dieter	Max-Planck-Institut für Chemie (MPI) P.O.Box 3060 D-55020 Mainz, Germany dip@mpch-mainz.mpg. de
Platt, Ulrich	University of Heidelberg Institute for Environmental Physics Im Neuenheimer Feld 366 D-69120 Heidelberg, Germany pl@uphys1.uphys.uni-heidelberg.de
Prestrud, Pål	Norwegian Polar Institute (NP) P.O. Box 5072, Majorstua N-0301 Oslo, Norway pal.prestrud@npolar.no
Radionov, Vladimir F.	Arctic and Antarctic Research Institute (AARI) Bering Street 38 199 226 St. Petersburg, Russia aaricoop@aari.nw.ru
Rognerud, Bjørg	University of Oslo Geophysical Institute P.O. Box 1022 N-0315 Oslo, Norway bjorg.rognerud@geofysikk.uio.no
Schlabach, Martin	Norwegian Institute for Air Research (NILU), P.O. Box 100 N-2007 Kjeller, Norway Martin.Schlabach@nilu.no

Schrems, Otto	Alfred-Wegener-Institute for Polar and Marine Research (AWI) P.O. Box 120161 D-27515 Bremerhaven, Germany otto_schrems@awi-bremerhaven.de
Seiler, Thomas	Alfred-Wegner-Institut for Polar and Marine Research (AWI) Koldewey-Station N-9173 Ny-Ålesund, Norway seiler@awi-koldewey.no
Shumilov, Oleg I.	High-Latitude Geophysical Laboratory St. Petersburg Filial of IZMIRAN P.O. Box 123 184 200 Apatity, Russia
Solberg, Sverre	Norwegian Institute for Air Research (NILU) P.O. Box 100 N-2007 Kjeller, Norway Sverre.Solberg@nilu.no
Sorteberg, Asgeir	University of Bergen Geophysical Institute Allégaten 70 N-5007 Bergen, Norway asgeir@gfi.uib.no
Stordal, Frode	Norwegian Institute for Air Research (NILU) P.O. Box 100 N-2007 Kjeller, Norway Frode.Stordal@nilu.no
Tüg, Helmut	Alfred-Wegener-Institute for Polar and Marine Research (AWI), P.O.Box 120 161 D-27570 Bremerhaven, Germany htueg@awi-bremerhaven.de
Vike, Eli	Norwegian Pollution Control Authority (SFT) P.O. Box 8100 Dep. 0032 Oslo, Norway Eli.Vike@sftospost.md.dep.telemax.no

von der Gathen, Peter	Alfred-Wegener-Institute for Polar and Marine Research (AWI) Research Department Potsdam P.O. Box 60 01 49 D-14473 Potsdam, Germany gathen@awi-potsdam.de
Wada, Makoto	National Institute of Polar Research (NIPR), 9-10, Kaga 1-Chome, Itabashi-ku 173 Tokyo, Japan wada@nipr.ac.jp
Wasseng, Jan Henrik	Norwegian Institute for Air Research (NILU) P.O. Box 100 N-2007 Kjeller, Norway Jan.Henrik.Wasseng@nilu.no
Windstad, Hilmar	Kings Bay Kull Compani A/S N-9173 Ny-Ålesund, Norway

Norwegian Institute for Air Research (NILU)
P.O. Box 100, N-2007 Kjeller – Norway

REPORT SERIES SCIENTIFIC REPORT	REPORT NO. OR 19/97	ISBN 82-425-0866-6 ISSN 0807-7207	
DATE 7/4-97	SIGN.	NO. OF PAGES 220	PRICE NOK 250,-

TITLE Atmospheric Research in Ny-Ålesund 9.-11. April 1997	PROJECT LEADER Inga Fløisand NILU PROJECT NO. O-1900
AUTHOR(S) Edited by Inga Fløisand, Hartwig Gernandt, Elisabeth Stoltz Larsen, Frode Stordal, Makoto Wada	CLASSIFICATION * A CONTRACT REF.

REPORT PREPARED FOR:
Ny-Ålesund Science Managers Committee

ABSTRACT
This report includs abstracts from papers presentet at the NySMAC-meeting on "Atmospheric Research in Ny-Ålesund"

NORWEGIAN TITLE
Atmosfæreforskning i Ny-Ålesund

KEYWORDS		
Atmospheric research	Ny-Ålesund	international collaboration

ABSTRACT (in Norwegian)